THE HONG KONG
POLYTECHNIC UNIVERSITY
香港理工大學
Pao Yue-kong Library
包玉剛圖書館

Copyright Undertaking

This thesis is protected by copyright, with all rights reserved.

By reading and using the thesis, the reader understands and agrees to the following terms:

1. The reader will abide by the rules and legal ordinances governing copyright regarding the use of the thesis.
2. The reader will use the thesis for the purpose of research or private study only and not for distribution or further reproduction or any other purpose.
3. The reader agrees to indemnify and hold the University harmless from and against any loss, damage, cost, liability or expenses arising from copyright infringement or unauthorized usage.

IMPORTANT

If you have reasons to believe that any materials in this thesis are deemed not suitable to be distributed in this form, or a copyright owner having difficulty with the material being included in our database, please contact lbsys@polyu.edu.hk providing details. The Library will look into your claim and consider taking remedial action upon receipt of the written requests.

Pao Yue-kong Library, The Hong Kong Polytechnic University, Hung Hom, Kowloon, Hong Kong

http://www.lib.polyu.edu.hk

MODELING TRAVELERS' SAFETY BEHAVIORS IN ROAD NETWORKS: INTEGRATING CRASH RISK MODELS, GAME THEORY, AND EQUILIBRIUM ANALYSIS

UMER MANSOOR

PhD

The Hong Kong Polytechnic University

2025

The Hong Kong Polytechnic University

Department of Civil and Environmental Engineering

Modeling Travelers' Safety Behaviors In Road Networks: Integrating Crash Risk Models, Game Theory, And Equilibrium Analysis

UMER MANSOOR

PhD

A thesis submitted in partial fulfilment of the requirements for the degree of Doctor of Philosophy

June 2025

CERTIFICATE OF ORIGINALITY

I hereby declare that this thesis entitled “Modeling Travelers' Safety Behaviors in Road Networks: Integrating Crash Risk Models, Game Theory, and Equilibrium Analysis” is my own work and that, to the best of my knowledge and belief, it reproduces no material previously published or written, nor material that has been accepted for the award of any other degree or diploma, except where due acknowledgement has been made in the text.

Signed. _____

Umer Mansoor

DEDICATION

I dedicate this thesis to Allah the Almighty, my parents, my wife, and my son.

ABSTRACT

Globally, road crashes are a leading cause of fatalities and serious injuries, placing a significant burden on healthcare systems and resulting in substantial economic and social losses. These challenges highlight the critical importance of road network safety planning and policy-making. Road crashes result from a complex interplay of factors, including road design, environmental conditions, vehicle characteristics, and human behavior. Among these, human behavior is the most significant contributor, accounting for 90% of all crashes. Conventional safety planning relies on historical data-based crash prediction models to minimize crash-related costs. While such approaches are helpful in pinpointing factors affecting crash frequency/severity and locating high-risk areas, they fail to incorporate travelers' safety behaviors, preferences, and network-wide interactions, limiting their ability to resolve safety issues proactively. To address these limitations, this thesis proposes integrating safety models with game theory and network equilibrium approaches, enabling the explicit modeling of traveler behaviors and interactions within transportation systems. Such integration can address several key challenges in the field and contribute to developing proactive improvement strategies and policies.

First, this thesis examines crash severity prediction modeling techniques, which rely on two main methodological approaches: (a) statistical models and (b) machine learning (ML) models. These approaches aim not only to improve predictive accuracy but also to offer a better understanding of the factors influencing severity. Although ML models often deliver superior or comparable predictive performance relative to statistical models, limited research has explored whether the contributing factors identified by these two approaches are consistent, particularly in the context of vulnerable road users in developing countries. To address these gaps, this thesis utilizes motorcycle crash data

from Pakistan. It employs a Shapley value-based cooperative game theory approach to interpret the outputs of ML models in crash severity analysis. The results are compared with those derived from traditional statistical models, revealing that user behavior (e.g., distracted riding) is the most significant factor affecting crash severity. Moreover, the contributing factors identified by ML models align closely with those derived from statistical models, thus enhancing confidence in the interpretability of ML models for transportation safety analysis. These findings strengthen our comprehension of ML applications in safety research and support their use in formulating effective safety policies.

Second, this thesis highlights the need for effective screening methods that proactively identify and rank critical links by safety importance, a crucial step for prioritizing interventions and improving overall network safety. Current approaches, such as crash prediction models, identify critical links by analyzing relationships between variables (e.g., roadway characteristics, traffic flow) and safety metrics like crash frequency and severity. However, these methods are limited in evaluating how disruptions on one or more links (e.g., crashes) impact overall network safety due to travelers' rerouting behavior and often ignore network-wide interactions. This thesis addresses these limitations by developing a framework that integrates transportation safety analysis and network equilibrium analysis using a Shapley value-based cooperative game theory approach, where links are treated as players to account for collaborative interactions. A flow-dependent safety evaluation metric, which assesses safety based on varying traffic conditions, is used to calculate the Shapley value. This value represents the average marginal contribution of links to network safety, considering all possible combinations of links known as link coalitions. The results demonstrate that the Shapley value comprehensively captures safety contributions, identifying links connecting multiple

origin-destination pairs as having higher safety importance due to greater interactions. This approach provides planners with a valuable tool to identify safety-critical links, enabling improvements in network safety during the planning stage.

Third, this thesis emphasizes the importance of enhancing the widely used four-step transportation planning model, which is primarily mobility-based and often overlooks travelers' safety preferences and behaviors. This model involves several key decisions travelers' make, such as whether to travel (trip generation), where to go (trip distribution), which mode of transport to use (modal split) and which route to take (traffic assignment). Car ownership and car type choice are integral to the trip generation and modal split, as they influence the number of trips generated and the modes of transport selected. Given the critical role safety plays in these decisions, as highlighted by numerous empirical studies, it is essential to integrate safety considerations into the transportation planning process. This need is further amplified by the rise of new technologies like autonomous vehicles (AVs), which introduce additional safety and security concerns. To address this, this thesis considers travelers' safety behaviors across various stages of transportation planning using network equilibrium approaches. Specifically, it employs a discrete-choice modeling-based equilibrium analysis framework to examine joint car ownership and car type choice behaviors. It incorporates safety and security risk concerns for both conventional and autonomous vehicles. The findings indicate that safety preferences significantly influence car ownership and car type decisions. Moreover, reductions in travelers' risk perceptions toward AVs lead to significant increases in AV adoption, highlighting the critical role of public trust in transitioning to AV-dominated markets.

Additionally, travelers' heterogeneous safety preferences are incorporated into route choice and traffic assignment (TA) models, exploring aspects such as safety-conscious

route choice sets, safety reliability requirements, and travelers' heterogeneous value of safety. The results demonstrate that equilibrium flow patterns derived from these models differ from those of conventional mobility-based models, with highly safety-conscious travelers' prioritizing safer routes, even at the cost of longer travel times. These models can serve as a foundation for safety-conscious planning, enabling planners to develop targeted safety improvement policies informed by travelers' safety behaviors, rather than relying solely on historical crash data or past experiences.

In summary, this thesis contributes to transportation network safety and planning by integrating safety models, cooperative game theory, and network equilibrium approaches, offering insights into theory and practice. First, it enhances the interpretability of ML-based crash prediction models through the Shapley value, comparing the consistency of crash contributing factors with traditional models and translating these insights into policy recommendations. Second, it develops a transportation network safety analysis framework for identifying the safety critical links, enabling proactive improvements in network safety during the planning stage. Finally, the thesis considers travelers' safety behaviors in car ownership, car type choice, and traffic assignment, shifting from reactive to proactive, behavior-aware strategies. Together, these enhancements provide new insights into network safety, policy development, and safety-conscious transportation planning, offering practical strategies for improving overall network safety.

LIST OF PUBLICATIONS

JOURNAL PAPERS

Mansoor, U., Jamal, A., Su, J., Sze, N. N., & Chen, A*. (2023). Investigating the risk factors of motorcycle crash injury severity in Pakistan: Insights and policy recommendations. Transport Policy, 139, 21-38. (*Chapter 3 in the thesis*)

Mansoor, U., Chen, A*. (2025). Safety-based vulnerability assessment for identifying critical road links: A cooperative game theory approach. Under second review with IEEE Transactions on Intelligent Transportation Systems (*Chapter 4 in the thesis*).

Mansoor, U., Gu, Y., Chen, A*. (2025). Modeling travelers' joint car ownership and car type choice behavior: The role of autonomous vehicle safety-security perceptions. Under second review with Travel Behaviour and Society (*Chapter 5 in the thesis*).

Mansoor, U., Li, Z., Chen, A*. (2025). Modeling safety reliability and unreliability in a mean-excess network equilibrium framework: Heterogeneous users with safety-conscious route choice sets. Under second review with Transportation Research Part C (*Chapter 6 in the thesis*).

Mansoor, U., Li, Z., Chen, A*. (2025). Trade-off between travel time and safety: Modeling travelers' heterogeneous preferences in traffic assignment. Under second review with Transportation Research Part E (*Chapter 7 in the thesis*).

CONFERENCE PAPERS

Mansoor, U., Li, G., and Chen, A*. (2021). A safety-based N-path user equilibrium model. The 25th International Conference of Hong Kong Society for Transportation Studies, 9-10 December 2021, Hong Kong.

Mansoor, U., Li, Z., Li, G., and Chen, A*. (2022). Modeling travelers' heterogenous value of safety in the continuous multiclass traffic assignment problem. The 26th International Conference of Hong Kong Society for Transportation Studies, 12-13 December 2022, Hong Kong.

Mansoor, U., Chan, HY., Su, J., & Chen, A*. (2023). Exploring pedestrian network choice behavior between at-grade and bridge networks in Hong Kong using machine learning with SHAP approach. The 3rd International Conference on Urban Informatics, 20-23 August 2023, Hong Kong (Best presentation award).

Mansoor, U., Gu, Y., Li, G., & Chen, A*. (2024). A joint car ownership and mode choice equilibrium model incorporating autonomous vehicle risk perceptions. 103rd Transportation Research Board (TRB) Annual Meeting, 7-11 January 2024, USA (No. TRBAM-24-05679).

Mansoor, U., Li, G., & Chen, A*. (2024). A bi-objective, multi-class traffic assignment model considering reliability and unreliability of safety and travel time: An α-reliable mean-excess modeling approach. 103rd Transportation Research Board (TRB) Annual Meeting, 7-11 January 2024, USA (No. TRBAM-24-05678).

Mansoor, U., Li, Z., Li, G., and Chen, A*. (2024). A continuous bi-criteria traffic assignment model with safety consideration. The 28th International Conference of Hong Kong Society for Transportation Studies, 9-10 December 2024, Hong Kong.

Mansoor, U., Chen, A*. (2025). Proactive road network safety evaluation using game theory for resource prioritization. Under review in the 3rd PolyU Research Student Conference (PRSC), 2-4 July 2025, Hong Kong.

ACKNOWLEDGEMENTS

First and foremost, I am most grateful to Allah the Almighty for granting me the knowledge, strength, and ability to embark on this research work. I thank the Department of Civil & Environmental Engineering (CEE), the Research Institute for Sustainable Urban Development (RISUD) at The Hong Kong Polytechnic University, and the Hong Kong Ph.D. Fellowship Scheme for their support of this PhD research.

I would like to sincerely thank my Chief Supervisor, Professor Anthony Chen, for his unwavering support, insightful guidance, and remarkable patience throughout my PhD journey. His deep expertise, thoughtful mentorship, and kindness have greatly enriched my academic and personal growth. I am truly grateful for the encouragement and opportunities he has provided and the inspiration he has given me to pursue excellence in my research.

Thanks also to my co-supervisors, Professor Tony Sze and Professor Edward Chung, for their guidance and support.

Many thanks are also extended to the past and present members of Hong Kong Polytechnic University transportation groups for their cooperation in the past years.

Above all, my deepest gratitude goes to my parents for their sacrifices and for always believing in me. To my wife, I am thankful for her patience, love, and unwavering support throughout this journey. To my son, whose presence has been a constant source of joy and inspiration, I owe endless motivation. Finally, to my brother, I am grateful for his encouragement and steadfast support during my PhD studies

TABLE OF CONTENTS

ABSTRACT ..... **v**
LIST OF PUBLICATIONS ..... **ix**
ACKNOWLEDGEMENTS ..... **xi**
TABLE OF CONTENTS ..... **xii**
LIST OF FIGURES ..... **xviii**
LIST OF TABLES ..... **xx**
LIST OF ABBREVIATIONS ..... **xxi**
CHAPTER 1 Introduction **1**
1.1 Background 1
1.2 Motivation and research gaps 4
1.3 Research objectives and contributions 7
1.4 Research significance 9
1.5 Thesis Organization 10
CHAPTER 2 Literature Review **14**
2.1 Overview 14
2.2 Transportation safety analysis using crash prediction models 15
2.2.1 Statistical models for motorcycle crash severity analysis 15
2.2.2 Machine learning models for motorcycle crash severity analysis 16
2.2.3 Influencing factors to motorcycle crash severity 18
2.2.4 Road network safety screening 19
2.3 Shapley value-based cooperative game theory in transportation 20
2.3.1 Shapley value in transportation safety analysis 20
2.3.2 Shapley value in transportation network analysis 21
2.4 Travelers' safety behaviors and preferences in travel choices 23
2.4.1 Vehicle choices in the era of autonomous vehicles 23
2.4.1.1 Travelers risk perceptions and vehicle choice 23
2.4.1.2 Equilibrium modeling framework and users' joint choice behavior 25
2.4.2 Travelers' heterogeneous safety preferences in route choice 26
2.4.2.1 Travelers' heterogeneous value of safety 26
2.4.2.2 Safety in traffic assignment for users with heterogeneous preferences 29

2.4.2.3 Modeling travelers' heterogeneity in bicriteria traffic assignment 32

2.5 Knowledge gaps 33

PART I. Crash factors investigation and network safety evaluation 36

CHAPTER 3 Analyzing crash injury severity: Consistency analysis between statistical and interpretable machine learning models 37

3.1 Motivation 37

3.2 Data 39

3.3 Methods 42

3.3.1 Multinomial logit model 42

3.3.2 Naïve bayes classifier 43

3.3.3 Gradient boosted decision trees 44

3.3.4 Random forest 45

3.3.5 SHAP method based on Shapley value 47

3.3.6 Performance metrics 47

3.4 Results and discussions 49

3.4.1 Model performance 49

3.4.2 Consistency analysis of risk factors between statistical and ML models 52

3.4.3 Discussion of risk factors 58

3.5 Policy recommendations 61

3.5.1 Implications for human factors 61

3.5.2 Implications of vehicular and environmental factors 63

3.6 Conclusions 64

CHAPTER 4 A cooperative game theory framework for proactive identification of safety-critical road links 66

4.1 Motivation 66

4.1.1 Contributions 69

4.2 Methodology 70

4.2.1 Notations 70

4.2.2 Study framework 71

4.2.3 Flow-dependent safety evaluation metric 71

4.2.4 The cooperative game 74

4.2.4.1 Shapley value of a cooperative game 75
4.2.4.2 Utility function of a cooperative game in transportation network 75
4.2.5 An illustrative example for a single O-D pair without congestion effect 76
4.2.5.1 Illustration of utility function and utility calculation 77
4.2.5.2 Shapley value vs marginal contribution for links 79
4.2.6 Transportation network cooperative game based on user equilibrium 80
4.2.6.1 User equilibrium formulation for cooperative game 80
4.3 Numerical experiments 81
4.3.1 Experiment settings for multiple O-D pairs in UE traffic assignment 81
4.3.2 Numerical results and discussions 82
4.3.2.1 Shapley value calculation for flow-dependent safety evaluation metric 82
4.3.2.2 Link safety contribution: Single vs multiple O-D pairs 86
4.3.2.3 Effect of congestion level on the Shapley value 87
4.3.2.4 Marginal contribution vs the Shapley value at different congestion levels 89
4.3.3 Recommendations 90
4.4 Conclusions 91
4.4.1 Summary 91
4.4.2 Practical implications 91

PART II. Modeling safety behaviors in transportation planning models 93

CHAPTER 5 Modeling safety and security concerns of AVs in joint car ownership and car type choice 94

5.1 Motivation 94
5.1.1 Contributions 96
5.2 Methodology 97
5.2.1 Joint car ownership and car type choice equilibrium framework 97
5.2.2 Assumptions. 98
5.2.3 Notations 98
5.2.4 Modeling travelers' risk perceptions 99
5.2.4.1 Safety Modeling 100
5.2.4.2 Security Modeling 103
5.2.4.3 Range anxiety for electric vehicles 105
5.2.5 Travel cost functions 106

5.2.5.1 Human-driven vehicle 106
5.2.5.2 Autonomous vehicle 107
5.2.5.3 Public transport 108
5.2.6 Structure of joint car ownership and car type model 108
5.2.6.1 Dogit and nested logit models used in joint choice structure 110
5.3 Model formulation 112
5.4 Numerical experiments 118
5.4.1 Single OD pair example. 118
5.4.1.1 Experiment setting 118
5.4.1.2 Effect of considering car type similarity 120
5.4.1.3 Effect of captivity parameter on car ownership 121
5.4.1.4 Effect of the perceived crash risk parameter of AVs on joint choice 122
5.4.1.5 Effect of the perceived security risk parameter of AVs on joint choice 123
5.4.2 Case study with multiple origin-destination pairs 125
5.4.2.1 Experiment setting 125
5.4.2.2 The effects of travelers' risk perceptions on market share. 126
5.4.2.3 Effect of the technological improvements on EV market share 127
5.4.2.4 The effects of network congestion levels on market share. 128
5.5 Implications for policy and practice 129
5.5.1 Effect of risk perceptions on AV adoption 129
5.5.2 Technological advancements and EV adoption 130
5.5.3 Consideration of captive travelers in transportation planning 130
5.5.4 Policy and planning recommendations 131
5.6 Conclusions 131

CHAPTER 6 Modeling safety variability in a mean-excess network equilibrium framework for users with heterogeneous preferences 133
6.1 Motivation 133
6.1.1 Contributions 135
6.2 Methodology 136
6.2.1 Notation 136
6.2.2 Study framework 137
6.2.3 Safety level of a route based on roadway characteristics 138

6.2.3.1 Definition of different criteria 138
6.2.3.2 Quantification of route safety score 139
6.2.3.3 Safety-conscious route choice sets 140
6.2.4 Safety of a route based on traffic conditions 142
6.2.4.1 Crash risk cost distribution 143
6.2.4.2 Definition of mean excess crash risk cost 146
6.2.4.3 Derivation of mean excess crash risk cost 150
6.2.5 UE formulation considering safety-conscious route choice sets 151
6.2.6 Solution algorithm 154
6.3 Numerical experiments 155
6.3.1 A small network: Single class travelers to compare different TA models 155
6.3.2 A small network: Multiclass travelers with heterogeneous safety concerns 157
6.3.2.1 Equilibrium flows for travelers with heterogeneous safety concerns (Case 1) 159
6.3.2.2 Effect of different route choice sets (Cases 2-3) 160
6.3.2.3 Expected travel time versus METT time in generalized cost (Case 4) 163
6.3.3 Real world case study: Winnipeg Network 164
6.3.3.1 Equilibrium results for travelers with heterogenous safety concerns 165
6.4 Practical implications 168
6.5 Conclusions 169

CHAPTER 7 Trade-off between travel time and safety: Modeling heterogeneous preferences in traffic assignment 170
7.1 Motivation 170
7.1.1 Contributions 173
7.2 Methodology 174
7.2.1 Notations 174
7.2.2 Modeling route safety 175
7.2.2.1 Definition of different criteria 176
7.2.2.2 Quantification of risk score of a route 179
7.2.3 Efficient frontier for time-safety trade-off 181
7.2.4 An illustrative example: Discrete vs continuous VoS distributions 182
7.2.5 Continuous VoS for time-safety trade-off 185
7.2.6 Continuous bicriteria traffic assignment formulation 188

7.2.7 Solution algorithm 192
7.3 Numerical experiments 193
7.3.1 A small network 193
7.3.1.1 Calculation of risk score for each route 194
7.3.1.2 Routes choices and equilibrium flows for heterogenous users 195
7.3.1.3 Effect of the degree of users' safety heterogeneity on route choice 196
7.3.1.4 Comparison of flows between discrete and continuous VoS distributions 197
7.3.2 Real world case study: Winnipeg network 198
7.3.2.1 Equilibrium flows and route choices for heterogeneous users 200
7.3.2.2 Reasonableness check of the model 202
7.4 Implications for policy and practice 204
7.4.1 Applicability in autonomous vehicle futures 205
7.5 Conclusions 206
CHAPTER 8 Conclusion and recommendations 207
8.1 Introduction 207
8.2 Summary of findings 207
8.3 Summary of research contributions 211
8.3.1 Consistency of risk factors between statistical and interpretable ML models 211
8.3.2 Framework for identification of safety-critical road links 211
8.3.3 A joint car ownership and car type equilibrium choice model 212
8.3.4 Modeling safety variability preferences and safety-conscious choice sets 212
8.3.5 Model time-safety trade-off by proposing travelers' value of safety 213
8.4 Research Limitations 214
8.5 Future research directions 215
REFERENCES 218
APPENDIX 235

LIST OF FIGURES

Figure 1.1. An integrated approach to safety-conscious transportation planning 3
Figure 1.2. Proactive approaches to road network safety 6
Figure 1.3. Modeling features, methodological tools, outcomes, and implications for each objective 9
Figure 1.4. Thesis structure 10
Figure 2.1. Structure of the literature review 14
Figure 3.1. Study area location 40
Figure 3.2. Illustration of a random forest classifier 46
Figure 3.3. Interpretations of the RF model using the SHAP method for minor injury crash 53
Figure 3.4. Interpretations of the RF model using the SHAP method for severe injury crash 54
Figure 3.5. Interpretations of the RF model using the SHAP method for fatal injury crash 55
Figure 4.1. Illustration of link and route safety due to user interactions under link disruptions 68
Figure 4.2. Framework of the methodology used for identifying safety-critical links 71
Figure 4.3. Road safety as a complex interplay of different factors. 72
Figure 4.4: Illustrative network with two routes 77
Figure 4.5. Graphical illustrations of utility and MC calculations for a small network 78
Figure 4.6. Comparison of link safety contribution between Shapley value and MC 79
Figure 4.7. A transportation network with two O-D pairs, five routes, and five links 82
Figure 4.8. Calculation of TNCF for different coalitions in the cooperative game 83
Figure 4.9. Shapley value of links in the cooperative game based on UE principle 85
Figure 4.10. Comparison of link safety contribution between single vs multiple O-D pairs 86
Figure 4.11. Graphical representation of Shapley values at varying congestion levels 88
Figure 4.12. Comparison of MC and Shapley value of link k at different congestion levels 89
Figure 4.13. Comparison of the safety-critical links between MC and Shapley value 90
Figure 5.1. Framework for modeling joint car ownership and car type equilibrium choices 97
Figure 5.2. Perceived crash risk of AVs and HVs as a function of safety level and exposure 102
Figure 5.3. Illustration of relationship between AV security risk penetration rate 104
Figure 5.4. Illustration of factors affecting range anxiety 105
Figure 5.5. Structure of joint car ownership and car type choice model 109
Figure 5.6. Dogit and nested logit models based on the joint model's structure 111
Figure 5.7. Equivalent MP formulation for the joint model 112
Figure 5.8. Effect of considering car type similarity on demand in each nest. 121
Figure 5.9. Effect of captivity parameter on car ownership demand 122
Figure 5.10. Effect of crash risk perception parameter (γAV) of AV on market share 123
Figure 5.11. Effect of security risk perception parameter of AV (αAV) on market share 124
Figure 5.12. Study area in Singapore with multiple OD pairs (Noruzoliaee et al., 2018) 125
Figure 5.13. Effect of risk perceptions on market share 127
Figure 5.14. Effect of technological improvements on EV market share 128
Figure 5.15. The effects of congestion level on market share 129

Figure 6.1. Illustration of the methodological framework 137
Figure 6.2. Methodology for calculating safety level of routes and safety-conscious choice sets. 142
Figure 6.3. Crash risk cost (safety) of a route based on traffic conditions 143
Figure 6.4. Illustration of link and route CRC distribution for a small network. 145
Figure 6.5. Illustration of the mean excess crash risk cost 149
Figure 6.6. An overview of the two-stage algorithm 154
Figure 6.7. A small network comprising five links and four routes 155
Figure 6.8. Equilibrium path flow patterns for different traffic assignment models 156
Figure 6.9. Illustration of unsafety scores for each criterion and total safety score for routes 159
Figure 6.10. Comparison of results for three cases with different route choice sets for TC_2 162
Figure 6.11. Routes in TC2's choice set at varying safety levels and their generalized costs 162
Figure 6.12. Winnipeg network showing the road functional class 164
Figure 6.13. Illustration of link flow pattern 166
Figure 6.14. Equilibrium results for multiclass travelers on OD pair (92,4) 166
Figure 6.15. Equilibrium results for multiclass travelers on OD pair (79,103) 167
Figure 6.16. Sensitivity analysis for route flows at different demand levels for OD 79-103 167
Figure 7.1. Continuous VoS distribution to represent heterogenous safety preferences 172
Figure 7.2: Methodology for calculating the safety level of routes based on different criteria 180
Figure 7.3. Efficient routes and efficient frontier for time-safety trade-off 182
Figure 7.4. An illustrative example comparing the discrete vs continuous VoS 184
Figure 7.5. Illustration of (a) efficient frontier of time-safety trade-off, (b) PDF of VoS 188
Figure 7.6. Mathematical programming formulation 189
Figure 7.7. An overview of the two-stage solution algorithm 192
Figure 7.8. A small network example 193
Figure 7.9. Illustration of risk score of routes for each criterion 194
Figure 7.10. Illustration of route flows and VoS boundaries in traffic assignment 195
Figure 7.11. Effect of VoS range on route choice behavior 196
Figure 7.12. Comparison of flows between discrete and continuous VoS distributions 198
Figure 7.13. Winnipeg network showing the road functional class 199
Figure 7.14. Efficient routes and route flows for heterogeneous users in OD pair (31,3) 200
Figure 7.15. Efficient routes and route flows for heterogeneous users in OD pair (91,102) 201
Figure 7.16. Convergence performance of the algorithm on the Winnipeg network 202
Figure 7.17. Reasonableness check using GPS trajectories for OD pair (31–3) 203
Figure 7.18. Reasonableness check using GPS trajectories for OD pair (91–102) 203

LIST OF TABLES

Table 2.1. Travelers' safety and security concerns on AV adoption. 24
Table 3.1. Descriptive statistics of variables used in the study. 42
Table 3.2. Confusion matrix 48
Table 3.3. Summary of classification performance of models 50
Table 3.4. Comparison of performance results with previous studies 51
Table 3.5. Parameter estimation results for the multinomial logit (MNL) models 56
Table 3.6. Consistency analysis of risk factors between the MNL and RF models 57
Table 4.1. Notations 70
Table 4.2. Shapley value calculation for link b 79
Table 4.3. Input parameters for the network 82
Table 4.4. Calculation of Shapley value for link i 84
Table 4.5. Calculation of the Shapley value for all links 85
Table 5.1. Notations 99
Table 5.2. Default model parameters for the base scenario 120
Table 5.3. Effect of considering car type similarity on the equilibrium demand. 121
Table 5.4. Effect of perceived crash risk cost parameter on modal demand 122
Table 5.5. Effect of security risk perception parameter on car type demand 124
Table 5.6. Input data for each OD pair 126
Table 6.1. Notations 136
Table 6.2. Link characteristics for a small network 156
Table 6.3. Cases considered in numerical experiments 157
Table 6.4. Normalized scores for each route 158
Table 6.5. Weighted normalized scores for each route 158
Table 6.6. Equilibrium flow of the multiclass travelers for case 1 $(\Theta req, TC2 = 0\%)$ 160
Table 6.7. Equilibrium flow of the multiclass travelers for case 2 $(\Theta req, TC2 = 40\%)$. 161
Table 6.8. Equilibrium flow of the multiclass travelers for case 3 $(\Theta req, TC2 = 60\%)$. 161
Table 6.9. Equilibrium flow of the multiclass travelers for case 4. 164
Table 7.1. Notations 174
Table 7.2. Normalized scores for each route 180
Table 7.3. Weighted normalized scores for each route 180
Table 7.4. Route characteristics of a small network 194
Table 7.5. Details of VoS and demands for three classes. 197

LIST OF ABBREVIATIONS

CPM	Crash prediction model
ML	Machine learning
SPF	Safety performance function
MNL	Multinomial logit
RF	Random forest
GBT	Gradient boosted trees
NB	Naïve bayes
SHAP	Shapley additive explanations
O-D	Origin-destination
IIA	Independence of irrelevant alternatives
IID	Independent and identically distributed
MC	Marginal contribution
UE	User equilibrium
SUE	Stochastic user equilibrium
SO	System optimal
TA	Traffic assignment
METE	Mean excess traffic equilibrium
C-BiTA	Continuous bicriteria traffic assignment

CHAPTER 1 Introduction

1.1 Background

Road crashes are among the leading causes of fatalities and serious injuries globally, contributing to immense economic and social losses while placing significant pressure on healthcare systems. In 2021, an estimated 1.19 million individuals died as a result of road crashes, making these incidents the foremost cause of mortality for children and young people aged 5 to 29 and the twelfth leading cause of death overall (WHO, 2023). The situation is especially severe in low-income nations, where the likelihood of dying in a road crash is three times greater than in high-income countries, even though these regions possess less than 1% of the world's vehicles. Vulnerable road users, such as motorcyclists and pedestrians, are disproportionately affected, representing 30% and 21% of global road fatalities, respectively (WHO, 2023). Recognizing the urgency of these challenges, the 2030 Agenda for Sustainable Development[1] emphasizes road safety as a vital component of creating inclusive, safe, resilient, and sustainable cities. Similarly, the Decade of Action for Road Safety 2020–2030[2], declared by the UN General Assembly in 2020 to save millions of lives, underscores the need for proactive road safety planning and evidence-based policy-making.

Road crashes result from a complex interplay of factors, including roadway characteristics, environmental conditions, vehicle features, and user behavior (Damani & Vedagiri, 2021; Sze & Wong, 2007; Wong et al., 2007). Among these, user behavior stands out as the most significant contributor, accounting for approximately 90% of all crashes (NHTSA, 2008). While roadway and environmental factors also play a role,

[1] https://unctad.org/publication/road-safety-considerations-support-2030-agenda-sustainable-development
[2] Decade of Action for Road Safety 2021-2030

improving road safety requires a deeper understanding of user behavior. Crash prediction models (CPMs) are widely used to identify crash-contributing factors (Mannering et al., 2020). These models rely on historical crash data to estimate crash frequency and severity and to identify high-risk locations in a road network.

Two main types of CPMs are commonly employed: traditional statistical models (Quddus et al., 2002; Shankar & Mannering, 1996) and modern machine learning (ML) models (Abdel-Aty & Abdelwahab, 2004; Rezapour et al., 2021). With the growth of big data, ML models have gained popularity due to their advanced ability to make accurate predictions. However, while ML models excel in predictive accuracy, they are often criticized for their black-box nature, as they lack interpretability regarding how variables influence outcomes (Rudin, 2019). In contrast, although traditional statistical models rely on assumptions, such as specific statistical distributions, they offer the advantage of interpretability by quantifying the effects of variables through coefficients and elasticities. To improve the transparency of ML models, researchers have developed interpretable ML techniques, such as SHAP (Shapley additive explanations), which is grounded in the Shapley value from cooperative game theory (Lundberg & Lee, 2017; Shapley, 1953).

Although these approaches have proven helpful in reducing crash-related costs, a shift toward proactive, safety-conscious planning is essential to address safety issues more effectively. Unlike conventional techniques, which assess safety only after the planning process is complete, safety-conscious planning integrates safety considerations during the process itself. For instance, macroscopic CPMs evaluate network safety by using zonal-level variables such as trip generation variables, socio-economic factors, and land use (Abdel-Aty et al., 2013; Cai et al., 2019; Lovegrove & Sayed, 2006). These models

help planners optimize population densities and employment intensities to achieve desired safety outcomes.

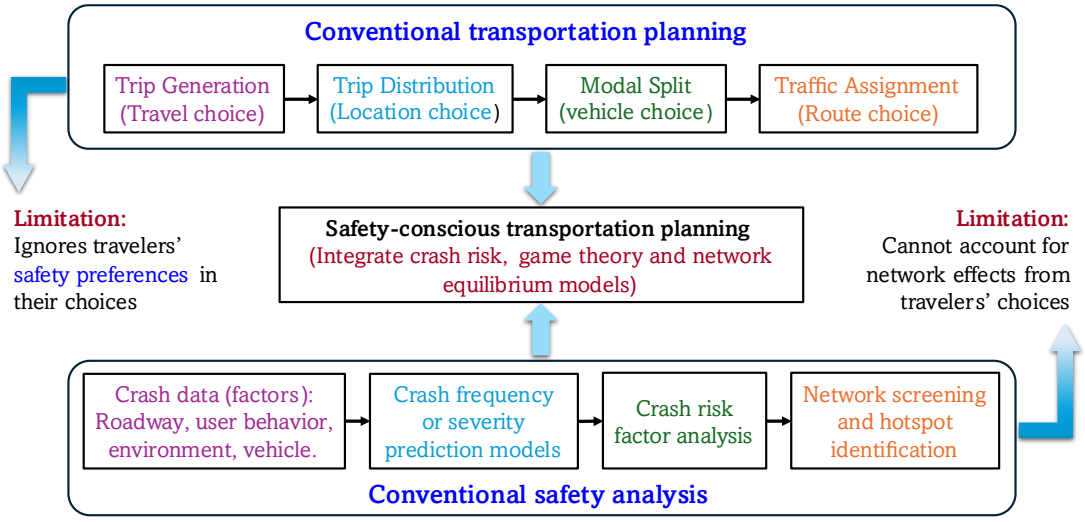

Figure 1.1. An integrated approach to safety-conscious transportation planning

However, crash data-based approaches have key limitations. They fail to account for user behaviors and preferences, such as how individuals with varying safety preferences make travel choices such as vehicle type, and route choices, and how these choices impact overall network safety. Conventional safety analysis treats traffic flow as exogenous, overlooking the endogenous effects of user decisions and their network-wide impacts. To comprehensively evaluate the interplay between traveler behavior and network safety, it is essential to explicitly incorporate safety preferences and behaviors into transportation planning, specifically within the four steps of trip generation, trip distribution, mode choice, and traffic assignment. Despite advancements, challenges remain, including limited data and the lack of models that capture both network-wide effects and user behavior. Addressing these challenges is crucial for comprehensive transportation network safety analysis and achieving meaningful improvements in road safety outcomes. This thesis proposes integrating crash risk models with cooperative game theory and equilibrium analysis to capture the effects of travelers' safety

behaviors, preferences, and network interactions. Such integration supports the development of proactive, behaviorally informed safety strategies and policies. Figure 1.1 illustrates how incorporating crash risk models, game theory, and network equilibrium approaches can model travelers' safety preferences within the planning process, while also highlighting the limitations of current methods.

1.2 Motivation and research gaps

A comprehensive transportation network safety analysis must overcome several critical challenges to ensure the development of safe and reliable systems. This thesis is motivated by the following key research gaps:

First, crash severity prediction studies rely on two primary methodological approaches: (a) statistical models and (b) machine learning (ML) models. These approaches aim to improve predictive accuracy and offer insights into the factors contributing to crash severity. While comparative studies have shown that ML models often outperform or at least match the predictive performance of statistical models (Rezapour et al., 2021; Wahab & Jiang, 2019a), there has been no systematic investigation into whether the contributing factors identified by these two approaches are consistent, particularly in the context of vulnerable users for developing countries. Recently, interpretable ML techniques, such as SHAP analysis based on cooperative game theory, have been used to explore contributing factors. Comparing the consistency of crash severity risk factors between statistical and ML models is crucial for instilling confidence in ML-based approaches among transportation safety practitioners and policymakers. However, no study has systematically examined this consistency. Addressing this gap will provide valuable insights and foster greater trust in ML models.

Second, effective screening methods that proactively identify and rank critical links by safety importance are crucial for prioritizing interventions and improving overall network safety. Current approaches, including crash prediction models, typically identify critical links by analyzing relationships between independent variables (e.g., roadway characteristics and traffic flow) and safety performance metrics like crash frequency and severity (Stipancic et al., 2019; Yasmin & Eluru, 2018). However, these methods are limited in their ability to assess the contribution of individual links to the overall network safety performance. Moreover, these approaches evaluate links in isolation and fail to account for network-wide interactions (Liu et al., 2017). For example, disruptions on one or more links (e.g., due to crashes) can alter traffic flow and safety conditions on neighboring links due to travelers' rerouting behavior, potentially affecting the entire network (Zhang et al., 2023). To comprehensively evaluate a link's contribution to network safety, it is necessary to consider its average contribution across all possible disruption scenarios, including the ripple effects on other links. Conventional approaches cannot capture these cooperative link interactions or endogenous traffic flow effects as they treat traffic flow as an exogenous input rather than an endogenous outcome influenced by driver rerouting behavior. To address these limitations, crash risk models can be integrated with network equilibrium and game theory (e.g., the Shapley value) approaches, enabling the proactive identification of safety-critical links during transportation planning, while accounting for network-wide interactions.

Third, the conventional four-step transportation planning process is primarily mobility-based and often overlooks travelers' safety preferences and behaviors. This model involves several key decisions travelers make, such as whether to travel (trip generation), where to go (trip distribution), which mode of transport to use (modal

split), and which route to take (traffic assignment) (Ortúzar & Willumsen, 2011). Car ownership and car type choice are integral to the trip generation and modal split, as they influence the number of trips generated and the modes of transport selected (Chu, 2016). As highlighted by numerous empirical studies, safety plays a pivotal role in shaping these decisions (Rizzi & Ortúzar, 2003; Yannis et al., 2005). However, existing planning models do not explicitly incorporate these safety preferences, limiting their ability to capture how individual choices at different planning stages ultimately affect system-wide safety. This gap is especially significant with emerging technologies like autonomous vehicles, which raise new safety and security concerns (Bansal & Kockelman, 2017; Hulse et al., 2018). Addressing this requires explicitly incorporating travelers' safety behaviors and preferences into the planning process. Integrating safety models within a network equilibrium framework enables modeling of decisions such as car ownership, car type choice, and route choice under safety concerns. This proactive approach embeds safety into the planning process, not just as a reactive response to crash data but as a core objective, allowing for safer, behaviorally-informed transportation network planning. Based on the discussion in this section, Figure 1.2 illustrates the three key motivations of this thesis, highlighting the shift toward more proactive approaches to road network safety.

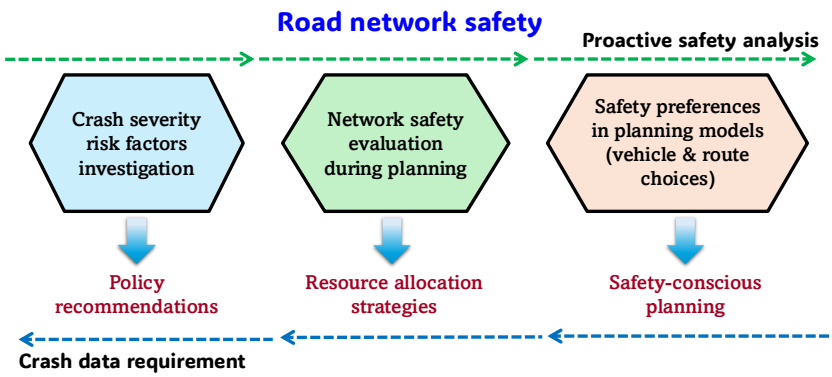

Figure 1.2. Proactive approaches to road network safety

1.3 Research objectives and contributions

In light of the above discussion and literature gaps, this thesis aims to enhance the understanding of road network safety by integrating crash risk models, game theory and network equilibrium models. The key objectives and contributions are:

I. Analyze the consistency of crash severity risk factors between statistical and interpretable ML models for vulnerable road users.

This objective compares the crash severity risk factors between traditional statistical and modern ML models using SHAP analysis (based on the Shapley value) to provide actionable insights for policymakers.

II. Develop a proactive framework for identifying the safety-critical links in a road network during the planning stage.

This objective advances the network screening analysis by proposing a framework that identifies the most safety-critical links, i.e., those that contribute the most to network safety. By integrating safety analysis with network equilibrium analysis and game theory, it captures the effect of travelers rerouting behaviors under link disruptions while also accounting for the cooperative interactions between links in a transportation network.

III. Develop joint car ownership and car type equilibrium choice model incorporating travelers' perceptions of safety and security.

This objective aims to incorporate the travelers' safety and security perceptions in the car ownership and car type choice stage of the planning model. It explicitly develops an equilibrium analysis framework to model the joint car ownership and car type choice decisions based on endogenous travel disutility, considering the specific characteristics

of each car type. It explicitly considers travelers' risk perceptions related to safety (crash risk) and security issues of AVs, as well as the range anxiety associated with EVs, within the joint choice equilibrium model.

IV. Propose a traffic assignment framework for modeling travelers' safety reliability and unreliability preferences along with safety-conscious route choice sets.

This objective advances safety-conscious planning by incorporating travelers' safety behaviors and preferences within a network equilibrium framework. It models the travelers' heterogeneous preferences for reliability and unreliability of safety variability and considers safety-conscious route choice sets for each user class. It divides the population into discrete classes. Thus, users within each class have heterogenous safety reliability requirements as well as their own route choice set. This objective aims to explore the network flow patterns of heterogeneous users.

V. Develop a traffic assignment framework for modeling the travelers' trade-off between travel time and safety by incorporating their heterogeneous safety preferences.

This objective focuses on modeling the trade-off between travel time and safety for travelers with heterogeneous safety preferences. The value of safety (VoS) is proposed to model travelers' heterogeneous safety preferences. The proposed model can endogenously determine the number of user classes and their travel patterns in a network by incorporating VoS as a continuous variable.

Figure 1.3 summarizes each objective, highlighting the features being modeled, the models being used, and their outcomes and implications. This visual overview provides a clear roadmap of how the study's objectives are interconnected and contribute to the overall research framework.

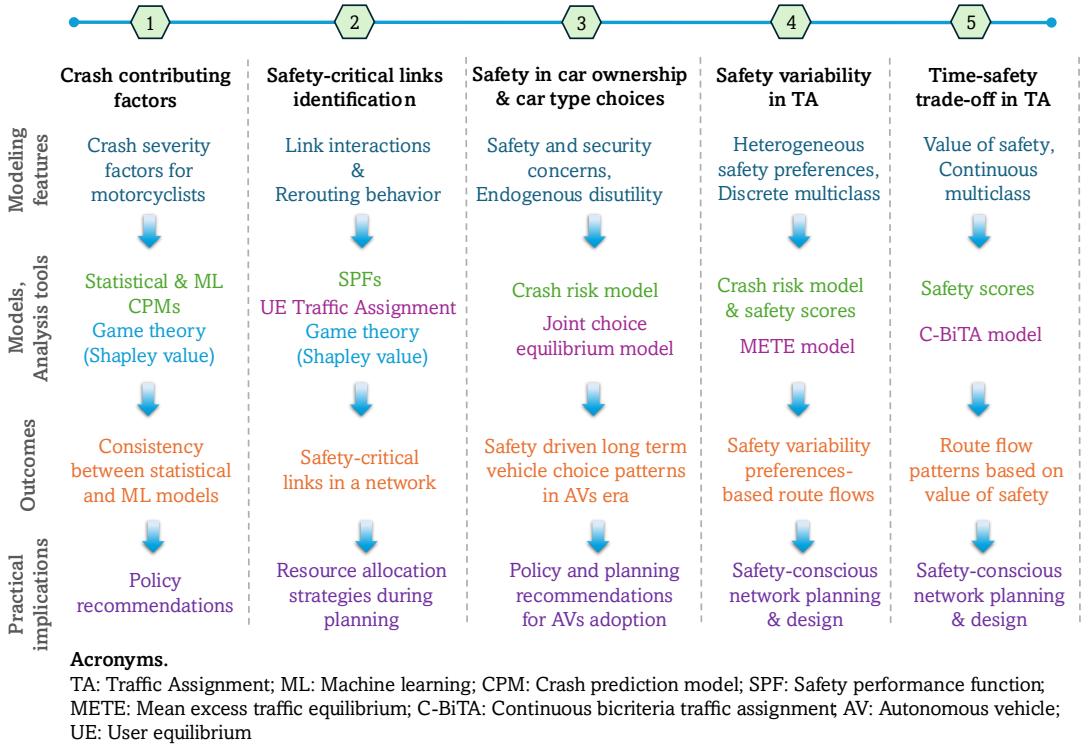

Figure 1.3. Modeling features, methodological tools, outcomes, and implications for each objective

1.4 Research significance

This thesis contributes to transportation network safety and planning by integrating crash risk models, cooperative game theory, and network equilibrium approaches. By highlighting the consistency of crash severity risk factors between statistical and ML models, it enhances the confidence of researchers and safety planners in using the ML models for policy-making and improvement strategies for network safety. Based on the identified factors, it provides policy recommendations for improving the safety of motorcyclists in a developing country. Moreover, it provides a framework for proactively recognizing the safety-critical links in a transportation network that can be used for investment strategies during the planning stage.

It most importantly advances safety-conscious transportation planning by integrating travelers' safety preferences and behaviors into car ownership, route choice, and traffic

assignment models. It enables planners to anticipate how travel patterns may shift as safety becomes a more prominent consideration in the era of emerging technologies. By providing tools to design safer transportation networks and develop targeted safety improvement policies based on traveler behavior, rather than relying solely on historical crash data or past experiences, this work has the potential to transform transportation planning. It ensures the development of safer, more reliable transportation networks by prioritizing safety alongside mobility.

1.5 Thesis Organization

This thesis is organized into eight chapters and two parts. The thesis structure is presented in Figure 1.4.

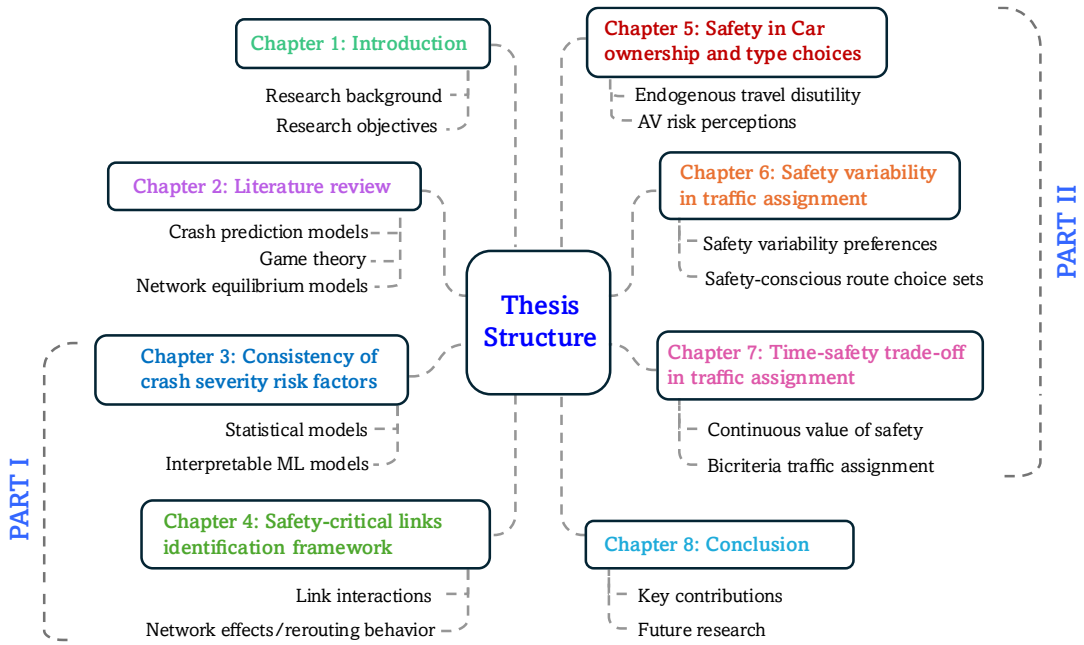

Figure 1.4. Thesis structure

Chapter 1 presents the research problem and details the objectives of the study. Chapter 2 presents a comprehensive literature review. Part I, which focuses on crash severity factors investigation and network safety evaluation, consists of Chapters 3 and 4. Chapter 3 analyzes crash severity risk factors using crash prediction models. Chapter 4

develops a proactive tool for evaluating road network safety. Part II, which focuses on incorporating travelers' safety behaviors and preferences into the planning process, with particular emphasis on car ownership choices and traffic assignment, consists of Chapters 5 to 7. The detailed content of each chapter is described below:

Chapter 1 introduces the research background, establishing the context for this thesis. It then presents the motivation for the study and identifies specific research gaps addressed in this work. The chapter clearly states the research objectives and outlines the key contributions of the thesis, followed by a discussion of its overall significance. Finally, it concludes with an overview of the thesis structure, briefly outlining each subsequent chapter.

Chapter 2 presents a comprehensive literature review relevant to the research objectives of this thesis. It first examines existing crash severity prediction models and network screening approaches. The chapter then reviews the Shapley value-based game theoretical methods for transportation safety and network analysis. Finally, it explores travelers' safety behaviors and preferences in the planning process, focusing on car ownership, car type selection, and route choice.

Chapter 3 addresses the first research objective by assessing the consistency of crash severity risk factors identified by statistical and machine learning models. The Shapley value method from cooperative game theory is used to interpret the machine learning models' results. Using crash data for vulnerable road users from a developing country, this chapter also provides policy recommendations aimed at enhancing road safety.

Chapter 4 addresses the second research objective by developing a tool for proactively identifying safety-critical links within a road network during the planning stage. This chapter integrates transportation safety analysis (traditionally conducted without

considering network effects), and transportation network analysis (typically performed without accounting for safety impacts) using a Shapley value-based cooperative game theory approach. Combining these methodologies, the analysis incorporates travelers' rerouting behaviors and cooperative interactions among network links under all possible disruption scenarios, thereby comprehensively identifying the most safety-critical links.

Chapter 5 addresses the third research objective by proposing an equilibrium framework for jointly modeling car ownership and car type choice decisions, incorporating endogenous travel disutility and the specific characteristics of each car type. The model explicitly accounts for travelers' perceptions of safety and security regarding autonomous vehicles. Specifically, a dogit model is adopted to model the car ownership choice by considering captive travelers, and a nested logit (NL) model is adopted to model the car type choice by accounting for similarities among different car types based on their associated risk perceptions. This framework supports evaluating and developing safety-conscious transportation policies by integrating travelers' risk perceptions and demand-dependent disutility into long-term decision-making.

Chapter 6 addresses the fourth research objective by modeling travelers' heterogeneous safety preferences in the traffic assignment model. It introduces an integrated network equilibrium framework that models safety-conscious class-specific route choice sets while simultaneously incorporating travelers' concerns about the reliability and unreliability of safety and travel time. The route choice set for each class is defined based on their safety score requirements, with the score of each route quantified by its roadway characteristics. The users are divided into two discrete classes. The safety variability concerns for heterogeneous travelers are modeled using the α-reliable mean-excess concept, and a crash risk cost distribution represents their

safety variability concerns. The proposed framework enables transportation planners to consider the impact of evolving travel behaviors on demand trends.

Chapter 7 addresses the fifth research objective by modeling the time-safety trade-off in traffic assignment for travelers with heterogeneous safety preferences. It introduces the concept of the value of safety (VoS) as a continuous variable, enabling a nuanced representation of individual safety preferences rather than grouping travelers into discrete classes. A bicriteria traffic assignment model incorporating the continuous VoS distribution determines route flows between OD pairs based on travel time and safety considerations. This framework provides a foundation for safety-conscious planning, allowing transportation planners to develop targeted safety improvement policies informed by travelers' safety behaviors.

Chapter 8 summarizes the thesis's primary contributions and outlines prospects for further research.

CHAPTER 2 Literature Review

2.1 Overview

The primary objective of this thesis is to enhance transportation network safety analysis by integrating crash risk models, game theory and equilibrium analysis. This chapter reviews the literature on transportation safety analysis from several perspectives. Figure 2.1 provides an overview of different sections related to each objective.

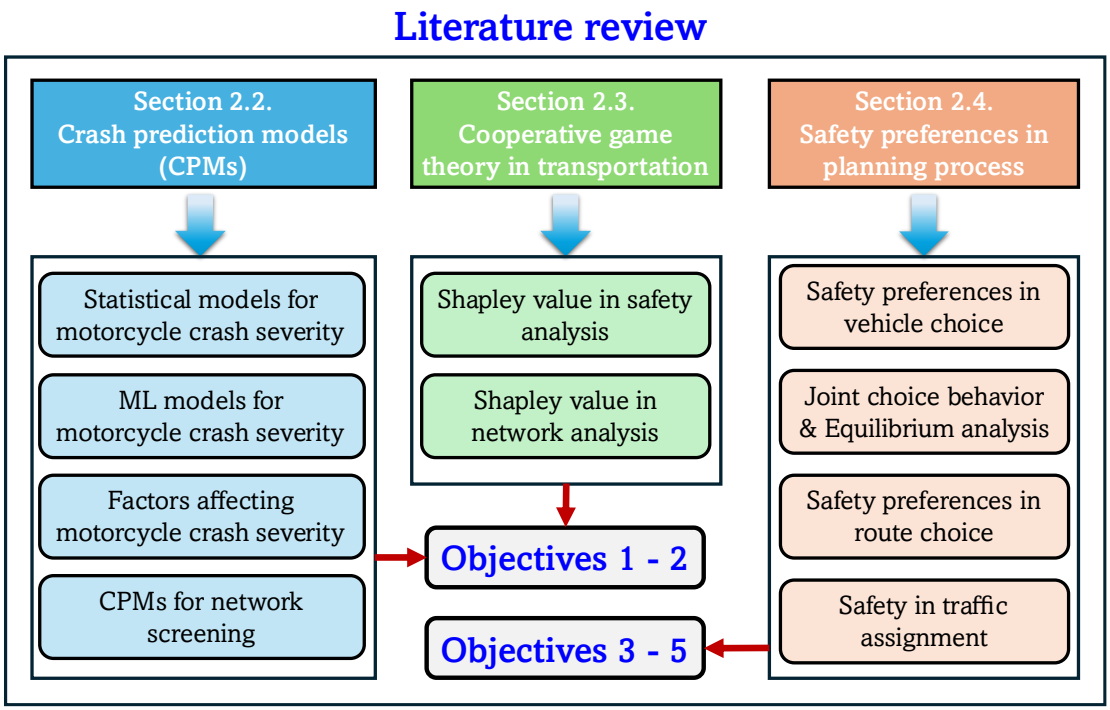

Figure 2.1. Structure of the literature review

Section 2.2 examines: (a) crash severity prediction modeling techniques using motorcycle crash data, (b) factors influencing crash severity for motorcyclists, and (c) crash prediction-based road network screening techniques. **Section 2.3** explores the application of cooperative game theory, particularly the Shapley value, in the context of (a) transportation network safety analysis and (b) transportation network analysis more broadly. **Section 2.4** reviews the influence of travelers' safety and security perceptions on (a) their vehicle choices in the era of autonomous vehicles and (b) their

route choices and traffic assignment models. This structured approach ensures a thorough examination of the key areas relevant to transportation network safety analysis by identifying the knowledge gaps in Section 2.5.

2.2 Transportation safety analysis using crash prediction models

2.2.1 Statistical models for motorcycle crash severity analysis

Statistical models such as the multinomial logit (MNL) model (Shankar & Mannering, 1996; Wahab & Jiang, 2019b), the ordered logit model (O'donnell & Connor, 1996; Pour-Rouholamin et al., 2017), and the ordered probit model (Li et al., 2021; Zeng et al., 2022) have been widely used for modeling motorcycle crash injury severity. Shankar and Mannering (1996) used the MNL model to investigate the factors contributing to motorcycle crash injury severity. Quddus et al. (2002) used the ordered probit model to account for the ordinal nature of motorcycle crash severity outcomes. In more recent studies, Rahman et al. (2021) used the binary logit model, whereas Schneider and Savolainen (2011) used the MNL model and the ordered probit model to study the crash injury severity levels of motorcycle crashes. These models have shown promising performance in investigating the contributing factors.

However, these models are not without limitations. They assume that estimated parameters are fixed and do not vary across observations, which might not entirely reflect the real world. Due to unobserved factors (not collected in the data, such as driver aggression), the effects of an observed variable might be different across different individuals instead of fixed effects over the population. Ignoring the unobserved factors may result in biased parameter estimates (termed unobserved heterogeneity) (Pervez et al., 2021). Several kinds of random parameter models have been introduced to address these concerns, including the mixed or random parameter

logit/probit model (Islam et al., 2014; Pervez et al., 2021), and the latent class model with random parameters (Shaheed & Gkritza, 2014). Kitali et al. (2020) analyzed the injury severity of motorcycle crashes in Dar es Salaam, Tanzania, using the Bayesian Dirichlet-MNL model and four years of data (2013–2016). This model accounts for unobserved heterogeneity by including a Dirichlet random effect parameter. Similarly, Cunto and Ferreira (2017) adopted mixed-ordered response models to investigate the factors influencing motorcycle crash injury severity in the urban streets of Fortaleza, Brazil. Specifically, they estimated conventional and mixed-ordered logit models using 8 years of crash data (2004–2011). Farid and Ksaibati (2021) extended the random parameter logit model by considering interaction effects and revealed several unobserved effects and interaction effects pertaining to motorcycle crash injury severity.

2.2.2 Machine learning models for motorcycle crash severity analysis

Although the statistical models introduced in Section 2.2.1 can be easily interpreted, the performance of these models in terms of prediction accuracy may not be the best as they cannot capture the complex relationships between dependent variables and a large number of predictors. In recent years, ML methods have emerged as promising alternatives that address the significant limitations of statistical models. Unlike traditional statistical methods, ML models do not rely on strong assumptions as needed in statistical models (such as the IID assumption of MNL model) and can better deal with complex nonlinear relationship between dependent and independent variables (Li et al., 2012). ML models such as artificial neural networks, support vector machines (SVM), decision tree (DT), the random forest (RF), and the *k*-nearest neighbors (KNN) have been applied to analyze crash injury severity (Mansoor et al., 2020; Silva et al., 2020). Abdel-Aty and Abdelwahab (2004) compared ML and parametric models for

crash severity prediction and suggested that the former performed better than the latter with higher prediction accuracy. Rezapour et al. (2021) applied four methods (RF, support-vector machine, logistic regression, and multivariate adaptive regression) to predict the motorcycle crash injury severity for ten years of data (2008–2017) from Wyoming, United States. The results showed that the RF model outperformed other models with an overall accuracy of 76%. In another study, Rezapour et al. (2020b) modeled motorcycle crash injury severity with several deep neural network models, such as a deep belief network, a multilayer neural network, a standard recurrent neural network (RNN), and a single-layer neural network. Their empirical results showed that the RNN achieved the best classification performance with an accuracy rate of 71%. Ijaz et al. (2021) also compared the performance of various ML classifiers (the RF, the DT, and decision jungles) in a crash injury severity study of three-wheeled motorized rickshaws in Islamabad, Pakistan. They found that the decision jungle model, with an overall accuracy of approximately 84%, outperformed the other models.

Despite the better performance of ML models in prediction accuracy, the applications of these methods have often been criticized for poor interpretability power. Decision-makers might prefer models that are easy to interpret and can explicitly support their policy-making decisions. Concerning this, researchers have recently tried to improve the interpretability power of ML models using various techniques such as partial dependence plots and feature ranking techniques for traffic volume prediction, road crash studies, and mode choice studies (Ozonder & Miller, 2021; Zhang et al., 2020b). One recent and novel technique introduced by Lundberg and Lee (2017) is the SHAP method, grounded in the Shapley value technique from cooperative game theory, which helps interpret the results of ML models in traffic crash studies (Tahfim & Yan, 2021; Yang et al., 2021). The SHAP method provides interpretations for each variable similar

to what conventional statistical models offer. Ma et al. (2021) developed a deep learning-based predictive model by employing the boosting ML model (CatBoost) and SHAP method to identify the significant risk factors of injury. Another study used the boosting-based ensemble ML models combined with the SHAP method to explore the significant crash risk factors (Dong et al., 2022). Though the interpretability of ML methods on crash severity analysis has been carried out, no study has ever paid attention to the consistency of the results from ML methods and statistical models. The SHAP technique provides research opportunities to intuitively interpret ML on crash severity analysis. It can also help to explore the consistency of significant risk factors, i.e., whether the identified risk factors between the two methods are similar and to what extent.

2.2.3 Influencing factors to motorcycle crash severity

Many researchers have studied the injury severity of motorcycle crashes and listed several possible factors contributing to human injuries. The potential risk factors for the injury severity of a crash can be grouped into four categories, i.e., the attributes of the road user, traffic characteristics, roadway features, and environmental attributes (Damani & Vedagiri, 2021; Das et al., 2025; Sze & Wong, 2007; Wong et al., 2007). The age and sex of a motorcyclist are examined to influence the severity of a motorcycle crash (Haque et al., 2009; Jafari et al., 2025). Other factors related to drivers, including in-experienced driving, risky behavior, low helmet use, inadequate driving training, recklessness, and risky behaviors such as overspeeding and red-light violations, are more likely to result in a more severe injury (Cheng et al., 2017; Jamson & Chorlton, 2009; Savolainen & Mannering, 2007; Shankar & Mannering, 1996). Traffic characteristics, e.g., heavy traffic volume, significantly increase the risk of serious injury (Haque & Chin, 2010; Pai & Saleh, 2007). The severity of injuries to

motorcyclists in crashes is also affected by motorcycle engine size (Quddus et al., 2002) and crash characteristics such as collision types and collision objects (Anvari et al., 2017). Roadway and environment characteristics such as highway functional class, intersection configuration, configuration of roadside fixed objects, highway alignment type (curved or straight), lane width, shoulder width, longitudinal slopes, surface condition, visibility levels at horizontal/vertical curves, weather and lighting conditions have been examined to have impacts on the injury severity of motorcyclists (Manan et al., 2018; Quddus et al., 2002; Robbins & Fotios, 2020; Savolainen & Mannering, 2007; Sivasankaran et al., 2021).

2.2.4 Road network safety screening

Road network safety screening is a critical step in safety analysis, which aims to evaluate network safety performance and identify critical links or sections (Bonera et al., 2024). The network safety performance evaluation approaches fall into two categories: reactive approaches, which analyze historical crash data, and proactive approaches, which employ crash prediction modeling (CPMs) techniques (Stipancic et al., 2019; Wang et al., 2011). CPMs predict crash frequency and severity to assess the importance of specific network components. CPMs have gained prominence in transportation safety research by establishing relationships between predictors (e.g., traffic flow and road geometry) and safety performance metrics. Recent advancements in literature have introduced simultaneous crash frequency-severity modeling, which integrates crash frequency and severity into a unified framework to evaluate the overall safety performance of links (Miranda-Moreno et al., 2009; Yasmin & Eluru, 2018). Unlike independent models that assess the criticality of links using separate analyses for crash frequency or severity, joint models estimate both metrics simultaneously using specialized model structures.

While conventional approaches effectively identify critical links based on crash frequency or severity, they cannot evaluate the contribution of a link to overall network safety. Furthermore, these approaches assess links individually, overlooking the interactions across the entire network (Kweon & Lim, 2014). For instance, these methods do not consider how a disruption (e.g., a traffic crash) on a specific link might influence the safety of other links or the entire network due to changing flow patterns caused by traffic diversions and rerouting. Such flow changes can be modeled using a network equilibrium framework (Sheffi, 1985), which predicts how travelers adjust their routes in response to disruptions. Additionally, since links in a transportation network are part of an interconnected system, comprehensively evaluating the contribution of each link to overall network safety requires assessing its impact across all possible scenarios where one or more links may be disrupted, resulting in different link coalitions (Zhao et al., 2023). To address this issue, the Shapley value offers a powerful solution, as it quantifies the average marginal contribution of links across all possible link coalitions (Shapley, 1953). By combining Shapley value analysis with network equilibrium and transportation safety assessments, achieving a more comprehensive understanding of safety-critical links within a transportation network is possible.

2.3 Shapley value-based cooperative game theory in transportation

2.3.1 Shapley value in transportation safety analysis

Over the past decade, the rise of ML models in transportation safety analysis has highlighted the relevance of Shapley value as a key method for interpreting these models. Initially, ML models were primarily employed to predict crash frequency and severity; however, their inherent complexity and black-box nature raised concerns regarding interpretability. Addressing these limitations, Lundberg and Lee (2017)

highlighted the usefulness of Shapley value in interpreting the output of ML models initially applied in the medical field. This breakthrough laid the foundation for widespread adoption across various research domains, including transportation safety (Kashifi, 2024; Kong et al., 2022; Mansoor et al., 2023).

In crash prediction modeling, the Shapley value has become an essential tool for interpreting complex ML and deep learning models by quantifying each feature's contribution to the predicted output while considering feature interactions. In this approach, the independent variables (features) act as players in a cooperative game, and the average marginal effect of each variable on the output is analyzed. For example, recent research has used the Shapley value to rank the critical variables in crash prediction models and study their effects on crash frequency and severity, bridging the gap between complex predictive models and their practical implications (Kashifi, 2024; Mansoor et al., 2023; Yang et al., 2021).

As evident from the literature, most applications of the Shapley value in transportation safety have been limited to assessing the importance of variables in crash prediction models. The application of this technique to evaluate the significance of transportation network components, specifically from a safety perspective, is unexplored. There remains a gap in understanding how links contribute to overall network safety, considering traffic interactions and congestion effects that influence safety across interconnected links. Ranking links using the Shapley value, which provides a holistic evaluation of link importance, can enable transportation safety planners to prioritize critical links for improvements during the planning stage.

2.3.2 Shapley value in transportation network analysis

Although the Shapley value has been rarely utilized in transportation network analysis, recently few researchers have applied this methodology to measure the importance of

network components, particularly nodes, in terms of connectivity (Gnecco et al., 2021, 2022; Hadas et al., 2017). Traditionally, the importance of nodes within a transportation network has been studied using classical centrality measures such as degree, closeness, and betweenness. While these measures offer valuable insights, they suffer from an intrinsic limitation as they only focus on the individual contribution of components to network performance, which can overlook cooperative interactions and congestion effects. In contrast, the Shapley value, rooted in cooperative game theory, provides a more refined interpretation by assuming that nodes in a network are players that do not act individually but as members of groups of nodes (Hadas et al., 2017). This approach enables the evaluation of node importance not only by its individual utility but also as an average contribution of various node coalitions. The utility function in these studies has generally been defined based on the network topology describing the effectiveness of cooperative strategies for capturing network interactions. However, the utility function defined in these studies does not consider congestion on a road network (i.e., flow-dependent link performance function).

To evaluate the importance of links using the Shapley value, few studies defined a utility function based on appropriate congestion measures (Passacantando et al., 2021a). The utility function was solved to identify important links based on the principles of user equilibrium (UE) and system optimal (SO) traffic assignment models. Their results demonstrated that the Shapley value could effectively highlight the links with the highest influence on network efficiency. Moreover, based on the flow-dependent utility measure, the classical Braess paradox was studied from a game-theoretic perspective. (Passacantando et al., 2021a, 2021b). The results show that using the Shapley value, which captures the average marginal contribution by considering all possible link coalitions, offers a more comprehensive understanding of the Braess

paradox compared to analyzing the marginal contribution of individual links in isolation. Zhao et al. (2023) used the Shapley value to identify critical links and distribute network traffic using a UE traffic assignment model with emission constraints. Other researchers explored its use in pre-disaster network investment strategy in a bi-level optimization framework (Niu et al., 2023; Zhang et al., 2023).

While these studies have used the Shapley value to evaluate the importance of network components with topological and flow-dependent utility measures, the criticality of these components from a transportation safety perspective remains largely underexplored. This research gap provides an interesting avenue to apply the Shapley value for evaluating network safety in the context of transportation safety analysis. Given its extensive use in interpreting ML models for crash prediction, applying the Shapley value for transportation network safety analysis could advance the understanding of safety-critical network components.

2.4 Travelers' safety behaviors and preferences in travel choices

2.4.1 Vehicle choices in the era of autonomous vehicles

2.4.1.1 Travelers risk perceptions and vehicle choice

An increasing number of empirical studies have explored how travelers' perceptions of safety and security risks influence their willingness to adopt AVs. For example, a cross-national survey conducted in several countries found that a significant proportion of respondents were concerned about the security risks associated with AVs, including fears of technological failures and cyber-attacks (Schoettle & Sivak, 2014). Similarly, Jardim et al. (2013) reported that security concerns influenced 82% of participants' decisions regarding AV adoption. Consistent with these findings, Nazari et al. (2018) found that individuals with heightened security concerns were less likely to adopt AVs.

Conversely, travelers who perceive AVs as safer regarding crash risk are more inclined to adopt them (Bansal & Kockelman, 2017; Hulse et al., 2018). As the perception of improved safety continues to grow, AV market share is likely to increase (Jabbari et al., 2022). Therefore, both risk perceptions, encompassing concerns about crash risk and security, emerge as pivotal factors in forecasting the intent to adopt AVs (Moody et al., 2020). Moreover, travelers' perceptions of different categories of AVs also influence their vehicle choice, especially when deciding between electric vehicles (EVs) and gasoline vehicles (GVs). For instance, individuals who experience range anxiety are less likely to purchase or adopt EVs and may instead prefer gasoline-powered AVs (Berkeley et al., 2018; Valeri & Danielis, 2015). Table 2.1 summarizes some of the empirical research highlighting the effect of various safety and security concerns in the adoption of AVs.

Table 2.1. Travelers' safety and security concerns on AV adoption.

Reference	Variable	Findings
(Bansal & Kockelman, 2017; Haboucha et al., 2017; Hulse et al., 2018)	Perceived safety improvement	Those who perceive AVs as safer are more inclined to adopt or purchase them.
(Choi & Ji, 2015; Nazari et al., 2018)	Perceived risk and security concerns	People with higher security concerns are less willing to adopt or buy AVs.
(Bansal & Kockelman, 2017; Sheela & Mannering, 2020)	Previous crash experience	People with prior crash experiences are more likely to use or purchase AVs.
(Berkeley et al., 2018; Valeri & Danielis, 2015)	Range anxiety (specific to EVs)	People with range anxiety are less willing to purchase EVs.

Although these studies highlight the significant impact of travelers' risk perceptions on AV adoption, most rely on stated choice surveys (Gkartzonikas & Gkritza, 2019; Haboucha et al., 2017; Jabbari et al., 2022) and microscopic traffic simulations (Arvin et al., 2020; Papadoulis et al., 2019). However, there is still a gap in the literature regarding the equilibrium analysis of how AV risk perceptions influence travelers' joint car ownership and car type choice behaviors. Existing empirical studies typically

forecast AV adoption based on exogenous (demand-independent) travel disutility using multinomial logit or more advanced mixed logit models. However, in reality, travel disutility is often demand-dependent, influenced by factors such as in-vehicle congestion and demand-driven crash risk costs (Kingsbury, 2016; Ma & Zhang, 2019). This recognition motivates the need for equilibrium-based approaches that can explicitly incorporate travelers' risk perceptions and endogenous disutility into joint car ownership and vehicle type choice decisions.

2.4.1.2 Equilibrium modeling framework and users' joint choice behavior

The equilibrium modeling framework has been widely adopted to study the travelers' joint choices in the context of AVs, including decisions related to vehicle selection, mode of transport, and route choice based on a choice model that considers the endogenous travel disutility dependent on the travel demand (Bagloee et al., 2017; Bahat & Bekhor, 2016; Wang et al., 2020b; Xie & Liu, 2022). For instance, Bagloee et al. (2017) modeled the users' choice between AVs and HVs using a logit model. In this model, AVs follow the SO principle for route choice, whereas HVs adhere to the UE principle. Wang et al. (2020b) extended this approach by examining combined mode and route choices across three mode options: HVs, firm-operated AVs, and government-operated AVs. An MNL model was used for mode choice, while HV route choices were determined using stochastic user equilibrium (SUE), government-operated AVs followed the SO principle, and firm-operated AVs adhered to the Cournot-Nash (CN). Similarly, Zhang et al. (2020a) used a nested logit (NL) model to describe travelers' joint vehicle and route choices between HVs and AVs. At the same time, other studies, such as those by Chen et al. (2019) and (Noruzoliaee et al., 2018), adopted an MNL model for vehicle choice and the UE principle for route choice.

While the studies above mainly focused on modeling travelers' vehicle choices with a single type of AV, Xie and Liu (2022) examined the travelers' joint vehicle and route preferences by considering AVs with varying automation levels. A joint NL-MNL model was adopted for the joint vehicle and route choice. Similarly, Jiang and Xie (2014) explored travelers' combined mode and route choices between electric vehicles (EVs) and gasoline vehicles (GVs), particularly addressing the issue of 'range anxiety' that affects EV adoption (Jiang et al., 2014). Another critical aspect of vehicle choice is the consideration of captive travelers who cannot afford or access all the modes. In the equilibrium framework, few researchers have adopted the dogit model, initially proposed by Gaundry and Dagenais (1979), to model captive travelers in mode choice (Wang et al., 2020a; Wang et al., 2024).

The above studies clearly underscore the importance of modeling joint decisions in the context of AVs, but they have primarily concentrated on route and mode dimensions. To date, no study has examined travelers' joint car ownership and vehicle type choices within an equilibrium framework, despite empirical evidence highlighting the interdependent nature of these decisions (Belgiawan et al., 2017; Kim et al., 2020). This omission is particularly critical in the era of AVs, where ownership and type selection are closely linked to long-term planning and risk perceptions. Addressing this gap enables equilibrium analysis to move beyond short-term route or mode choices, providing deeper insights into how travelers' joint decisions on ownership and vehicle type evolve under endogenous travel disutility and AV-related risks.

2.4.2 Travelers' heterogeneous safety preferences in route choice

2.4.2.1 Travelers' heterogeneous value of safety

Understanding how travelers value safety is vital for incorporating safety-oriented behaviors in transportation planning. Various methods have been employed to capture

the heterogeneity in travelers' safety preferences. One widely used concept in economics is the value of statistical life (VSL), which reflects the monetary value individuals assign to reducing the probability of serious injury or fatality. VSL provides critical insights into how travelers perceive and prioritize safety (Jones-Lee et al., 1985; Machina & Viscusi, 2013). Typically, two approaches are adopted to obtain empirical estimates: (1) revealed preferences (RP), based on observed behaviors, and (2) stated preferences (SP), which gather data from hypothetical scenarios (Jones-Lee et al., 1985).

In the transportation domain, studies have primarily focused on users' willingness to pay (WTP) for a unit reduction in crash risk as a way to analyze their heterogeneous safety preferences (Hensher et al., 2009; Mon et al., 2019; van Wee & Rietveld, 2013). A traveler's WTP, which reflects their individual risk preferences, governs their decision-making regarding safety. Studies show that individuals with cautious driving habits or those who prefer lower speeds are willing to pay more to reduce crash risks than those who prioritize speed (Antoniou, 2014; Mon et al., 2019). Furthermore, a positive relationship between income level and WTP has been identified, with wealthier individuals typically placing a higher monetary value on safety (Andersson & Treich, 2011; Mon et al., 2019).

Beyond monetary terms, travelers also trade between safety and travel time when selecting routes. Research using SP surveys reveals that travelers' exhibit heterogeneous safety preferences when choosing between faster or safer routes (Antoniou, 2014; Noland, 2013). Those willing to accept longer travel times to travel on safer routes demonstrate greater safety concerns (Rizzi & Ortúzar, 2003; Yannis et al., 2005). For example, Yannis et al. (2005) found that 60% of drivers are willing to accept 18 minutes of additional travel time to substantially reduce crash risk, while

others opted for shorter additional time, illustrating the heterogeneity in safety preferences.

To formalize these diverse safety preferences, travelers' VoS can be employed, as it can be inferred from their willingness to accept additional travel time in exchange for enhanced safety (Rizzi & Ortúzar, 2003; Yannis et al., 2005). In essence, travelers who accept a higher additional trip time to lower their crash risk have a higher VoS, and vice versa. Since VoS varies across individuals, it is treated as a traveler-specific and randomly distributed value. This variability gives rise to multiple user classes with distinct safety preferences.

A key challenge, however, lies in determining how many discrete user classes should be defined to effectively capture heterogeneity in users' route choice preferences. For example, users with similar and identifiable preference can be grouped together into discrete classes e.g., young and old (Deery, 1999; Machin & Sankey, 2008), male and female (Granié et al., 2025), etc. However, for more abstract characteristics like VoS, discretization approach suffers from arbitrary choices in both group threshold and group numbers resulting in discretization error, undermining its effectiveness in capturing user heterogeneity. For example, consider a population with VoS values ranging from 0 to 1. If discretized into two classes, low safety-conscious (0–0.5) and high safety-conscious (0.5–1.0), a traveler with a VoS of 0.45 would be treated the same as one with 0.05, and differently from one with 0.55, despite the latter being closer in preference. Within each class, assigning a representative average VoS (e.g., 0.25 for the low safety-conscious group) may force the users to choose the same route, even though their true preferences may imply different route choices. Given the potential bias introduced by such discretization and the difficulty of predetermining thresholds

and class numbers, continuous distributions provide a more natural and theoretically sound approach to modeling user heterogeneity (Antoniou, 2014; Ghoul et al., 2023).

2.4.2.2 Safety in traffic assignment for users with heterogeneous preferences

A few researchers have modeled travelers' safety concerns in the traffic assignment model. For example, Ma and Zhang (2019) modeled travelers' expected safety by adopting crash risk as a proxy. The crash risk was quantified using the safety performance functions (SPFs) developed for highways and freeways. It was noticed that the link flow patterns resulting from safety-oriented route choice decisions differed from those based on travel. However, this research did not simultaneously model travelers' time and safety concerns in the TA. Similarly, Sharifi and Shabaniverki (2016) incorporated the effect of mean crash delays on route choice behavior when modeling expected safety. The generalized link cost was obtained by adding the mean crash delay to the travel time function. The impact of opposing traffic on crash risk was modeled by assuming symmetric link interactions. Zhu et al. (2009) proposed a reliability-based SUE model to examine how turn delay uncertainties affect route choice behavior at signalized intersections. This model was used to identify optimal cycle times for both crash reduction and effective travel time reduction at these intersections.

Furthermore, Huang et al. (2020) extended expected safety cost models by considering the safety variability (reliability) in the route choice for users with heterogenous crash risk aversions (low and high-risk-averse users). Crash risk cost (CRC) distribution was used to model route safety variability. The concept of effective CRC, which is defined as the mean CRC plus an additional CRC margin, was proposed. This concept was inspired by the travel time budget (TTB) traffic equilibrium model. The TTB model considers travel time reliability, ensuring on-time arrival at a specified confidence level

α (Lo et al., 2006; Shao et al., 2006; Xu et al., 2018a). Similarly, an effective CRC accounts for safety reliability, ensuring a safe arrival at the prespecified confidence level α. However, in terms of travel time variability, Chen and Zhou (2010) explained that the sole consideration of TTB as a risk measure in the network equilibrium approach might not be adequate as it could result in overwhelming high trip times for travelers (unreliability aspect of travel time variability). Thus, they proposed the mean excess traffic equilibrium (METE) model, which considers both the reliability (acceptable travel time) and unreliability of travel time variability, i.e., trips longer than expected (worst scenarios) are considered unreliable or unacceptable.

In the same essence as TTB, effective CRC, which only considers the safety reliability aspect, may not sufficiently describe travelers' risk preferences. Research has demonstrated that losses linked to the worst-case scenarios of alternatives significantly impact decision-making (Yamai & Yoshiba, 2002). When the travelers' main aim is to maximize their trip safety, they are likely to incorporate the unreliability of safety variability in their route choices. For instance, travelers tend to avoid routes with a higher likelihood of fatal crashes, i.e., routes with an extremely high crash risk cost. This is particularly relevant in cases involving collisions with heavy vehicles (Anderson & Hernandez, 2017; Behnood & Mannering, 2019) or a crash on undivided roads (Kadeha et al., 2021; Kidando et al., 2019), which are known to often result in severe injuries or fatalities. As such, travelers are expected to account for these risks based on their travel experiences. Therefore, incorporating both the reliability and unreliability aspects of safety variability into the network equilibrium model is more appropriate to better reflect travelers' safety concerns. Han et al. (2023) addressed this by proposing a speed-route joint choice model that integrates both reliability and unreliability of safety variability into the generalized travel cost, alongside expected travel time. However,

while their model accounts for safety variability, travelers' concerns about travel time variability have also been shown to influence travelers' decisions. Thus, considering both safety and travel time variabilities in the network equilibrium model can capture more comprehensive user behavior.

Furthermore, the above studies modeling travelers' safety concerns in the traffic assignment models assume that travelers are willing to choose from all available routes between an OD pair (Han et al., 2023; Huang et al., 2020). However, more safety-conscious travelers may limit their choice set by excluding routes with higher safety risks based on intrinsic roadway properties, such as road classification, intersection density, and travel distance (Dijkstra, 2013; Dijkstra et al., 2007). Li and Huang (2019) proposed different perceived route choice sets for travelers with varying safety preferences, using an exogenously given route safety index. While this approach reflects meaningful progress, it does not consider a route's safety level derived directly from roadway characteristics, which may provide a more appropriate representation. A similar concept of a class-specific route choice set was introduced by Lin and Leong (2014), stating that the users select from a limited subset of routes rather than all the available routes. However, their study did not specifically address safety concerns, and the route choice set was exogenously defined.

Additionally, while Huang et al. (2020) and Han et al. (2023) modeled users' heterogeneity regarding the trade-off between expected safety and safety reliability, the heterogeneity in the time-safety trade-off was not explicitly addressed. This leaves a critical gap in understanding how travelers with varying safety preferences trade travel time with safety. Moreover, representing users with only two discrete classes (e.g., high and low risk-averse) may oversimplify the diversity in safety-related behavior, as each user possesses a unique risk preference that may not fit neatly into two classes.

2.4.2.3 Modeling travelers' heterogeneity in bicriteria traffic assignment

The bicriteria multiclass traffic assignment problem is well-studied in modeling the trade-off between travel time and toll by defining a value of time (VoT) parameter. To account for the user heterogeneity of VoT, two approaches have been mainly used: (a) model discrete set of VoT for several user classes (Nagurney, 2000; Nagurney & Dong, 2002; Yang & Huang, 2004) and (b) model VoT as a continuous variable across the whole population, allowing for a more refined representation of the population (Dial, 1996; Leurent, 1993; Marcotte, 1998; Xu et al., 2023). The first approach divides the support of VoT into discrete intervals, with each interval representing a distinct user class. However, this method has several limitations. First, while each user class theoretically corresponds to a continuous range of VoT, it has to be represented by a single or average value from the range. Such an assumption tends to produce estimates with large errors. Second, discretization introduces computational difficulties. Although finer discretization may improve accuracy, it also significantly increases computational costs. To overcome these limitations, researchers have proposed using a continuous distribution of VoT, leading to a continuous bicriteria traffic assignment model (Leurent, 1993; Marcotte, 1998).

While the heterogeneity of VoT has been extensively studied in both discrete and continuous forms to model the time-toll trade-off, the heterogeneity of VoS for modeling the time-safety trade-off has received little attention. Although the former is important in policymaking and congestion pricing (Meng & Liu, 2011), the latter also holds significant importance in reducing the burden of crash costs on society (Forkenbrock & Foster, 1997). A few researchers modeled users' heterogeneous safety concerns in terms of the crash risk cost variability by dividing the users into discrete classes (high and low-risk averse) based on their safety reliability requirements (Han et

al., 2023; Huang et al., 2020). However, dividing users into two classes may not replicate the actual travel behavior of users since VoS is a traveler-specific value that follows a continuous distribution. Therefore, a more accurate representation of traveler behavior requires modeling VoS as a continuous variable, capturing the unique safety concerns of each traveler.

2.5 Knowledge gaps

This chapter reviews the literature on crash prediction models, game theory applications in transportation (with a focus on the Shapley value), and travelers' safety behaviors in vehicle and route choices, all with the aim of enhancing road network safety. The objective is to advance understanding of how these areas contribute to improving road network safety. Based on this review, several research gaps have been identified and are outlined below.

- Studies comparing statistical and ML models for crash severity analysis have focused on prediction accuracy. While the Shapley value has been applied to interpret machine learning outputs and address their black-box nature, little attention has been given to the consistency of risk factors identified by both modeling approaches. For transportation safety practitioners and planners, understanding contributing factors is as critical as predictive accuracy, yet this consistency remains unexplored. These gaps are addressed in **Chapter 3**.
- Conventional safety analysis approaches, such as crash prediction models, identify critical links in a road network based on crash frequency or severity but fail to evaluate the safety contribution of each link to the overall network safety. These approaches overlook cooperative interactions among links and the influence of routing behaviors under link disruptions. Although the Shapley value has been used

to assess link importance by considering link interactions, its application in evaluating link criticality from a safety perspective is still lacking. These gaps are addressed in **Chapter 4**.

- Recent empirical studies emphasize the interdependent nature of car ownership and car type decisions, highlighting the need to model them jointly. Most vehicle choice studies rely on stated choice surveys and microscopic traffic simulations, typically forecasting AV adoption through multinomial or mixed logit models based on exogenous assumptions of travel disutility. However, travel disutility is inherently demand-dependent, shaped by congestion and crash risk factors. Moreover, critical considerations like crash risk and security concerns, which significantly influence AV adoption (see Table 2.1), are rarely integrated into joint car ownership and car type models. This gap underscores the importance of developing equilibrium-based approaches that account for travelers' AV risk perceptions and how these perceptions shape their joint decisions under demand-dependent conditions. These gaps are addressed in **Chapter 5**.
- In traffic assignment models, travelers' safety preferences are often incorporated using traffic conditions such as speed or flow, while the influence of roadway characteristics is frequently overlooked. Although safety and travel time variability have been studied individually, their combined effect within network equilibrium models has received limited attention. Additionally, most models assume a complete route choice set for all users, disregarding the fact that travelers with different levels of safety awareness may have different route choice sets. These gaps are addressed in **Chapter 6**.
- While some studies have addressed user heterogeneity in the trade-off between expected safety and safety reliability, they have not explicitly examined

heterogeneity in the time-safety trade-off, such as travelers' decisions between the safest and the fastest routes. These studies often categorize users into two discrete classes; however, this binary classification oversimplifies the variation in safety-related behavior. In reality, each traveler has a unique risk preference that may not align with predefined categories. To more accurately reflect this diversity, the value of safety (VoS) should be modeled as a continuous variable, allowing for a more nuanced representation of individual safety concerns in the time-safety trade-off. These gaps are addressed in **Chapter 7**.

PART I. Crash factors investigation and network safety evaluation

Part I investigates the crash severity risk factors for motorcyclists, compares the consistency of identified factors between statistical and ML models and provides a proactive framework for identification of safety-critical road links using crash risk models, game theory and network equilibrium models.

CHAPTER 3 Analyzing crash injury severity: Consistency analysis between statistical and interpretable machine learning models

3.1 Motivation

Road crashes result in numerous fatalities and injuries each year. Among these fatalities, motorcyclists accounted for a major part (30%) of the fatalities (WHO, 2023), as they are particularly vulnerable in crash events due to limited protection (Elliot et al., 2003). The situation is more severe in developing countries with more challenges in road safety improvement. Pakistan is a developing country that suffers tremendous economic and life losses from road crashes. The fatality rate (road deaths per 10 thousand registered vehicles) in Pakistan is among the highest in the world, with more than 27 thousand people dying of crashes every year while the number of crashes is continuously increasing. The death rate in crashes in Pakistan is 14.2 per 100,000 population annually, among which more than 50% of crashes involve motorcyclists (Ahmed, 2007). Especially motorcycle crashes in the Rawalpindi district have increased by 137% over the past decade (Rescue 1122, 2016). On the other hand, motorcycles and autorickshaws constitute 61% of the registered vehicles (PBS, 2015) in the whole country. Motorcycle registrations have witnessed an annual increase of 20%, especially since 2008, along with the considerable growth of registered vehicles in Pakistan (MOC, 2018). In the meantime, only 7% of motorcyclists involved in crashes were found wearing a helmet (Shamim et al., 2011). Due to fast motorcycle growth without equivalent improvement in infrastructure, lack of law enforcement, and inadequate safety awareness, motorcycle crashes have been an outstanding problem to address for road safety improvement in Pakistan (Pervez et al., 2021; Waseem et al.,

2019). Toward this end, it is vital to identify the potential risk factors resulting in motorcycle crashes and the consequent severity levels for effective countermeasures.

Statistical models such as the multinomial logit (MNL) model, the ordered logit model, and the ordered probit model have been most commonly used to identify the factors contributing to crash injury severity (Jafari et al., 2025; O'donnell & Connor, 1996; Quddus et al., 2002; Shankar & Mannering, 1996). These models are easy to interpret because the associations between the independent variables (potential risk factors) and the response variable (severity levels of crashes) are explicitly formulated. However, these explicit formulations limit statistical models on specific assumptions, e.g., independently and identically distributed (IID) assumptions for the MNL model. If model assumptions about the distributions of variables are violated, the models may generate incorrect parameter estimates, which may lead to wrong implications for policy-making (Delen et al., 2006).

To overcome these strict assumptions of statistical models, another stream of methodological approaches, the machine learning methods, have caught the attention of scholars for crash severity prediction (Abdel-Aty & Abdelwahab, 2004; Rezapour et al., 2021). Most of these methods can account for the complex nonlinear relationships between dependent and independent variables and perform better than statistical models in prediction performance. Nevertheless, ML methods have been criticized as "black boxes" with weak interpretability power because they are incapable of interpreting the relationship between dependent and independent variables with explicit parameters (Rudin, 2019). Recently, some interpretable techniques for ML methods, such as partial dependence plots, feature importance (Ozonder & Miller, 2021; Zhao et al., 2020), and Shapley Additive explanations (SHAP) summary plots have been developed to show nonlinear relationships between the dependent variable and contributing factors. Few

recent studies have explored the interpretability of these techniques in the area of crash severity analysis (Dong et al., 2022; Ma et al., 2021).

Moreover, as ML methods and statistical models work with different mechanisms, one concern should be raised: whether the risk factors identified from the two streams of models are consistent and to what extent. Since the interpretation of contributing factors is of key interest to transportation safety practitioners and planners, the consistency of risk factors can significantly increase their confidence in adopting ML methods for policymaking. However, to our knowledge, no study has been carried out to investigate the consistency of crash severity risk factors obtained from the two kinds of models. Towards this gap in the literature, this study attempted to answer the following question: ***Are statistical and interpretable ML models consistent in identifying risk factors contributing to crash injury severity?*** Thus, using the motorcycle crash data in Pakistan, the consistency of risk factors contributing to the motorcycle crash injury severity is well studied in this Chapter.

3.2 Data

The study focuses on the city of Rawalpindi in Pakistan, which shares a border with the federal capital, Islamabad. The topography and the neighboring locations of the city are presented in Figure 3.1. Rawalpindi is the country's fourth-largest city, with a population of 5.40 million (PBS, 2017). The main transport modes in the city are private cars, taxis, bus rapid transit, suzuki vans, rickshaws, and motorcycles (Adeel et al., 2016; Starkey et al., 2021). Due to Pakistan's inadequate public transportation system, the motorcycle is an essential mode of transportation in the country.

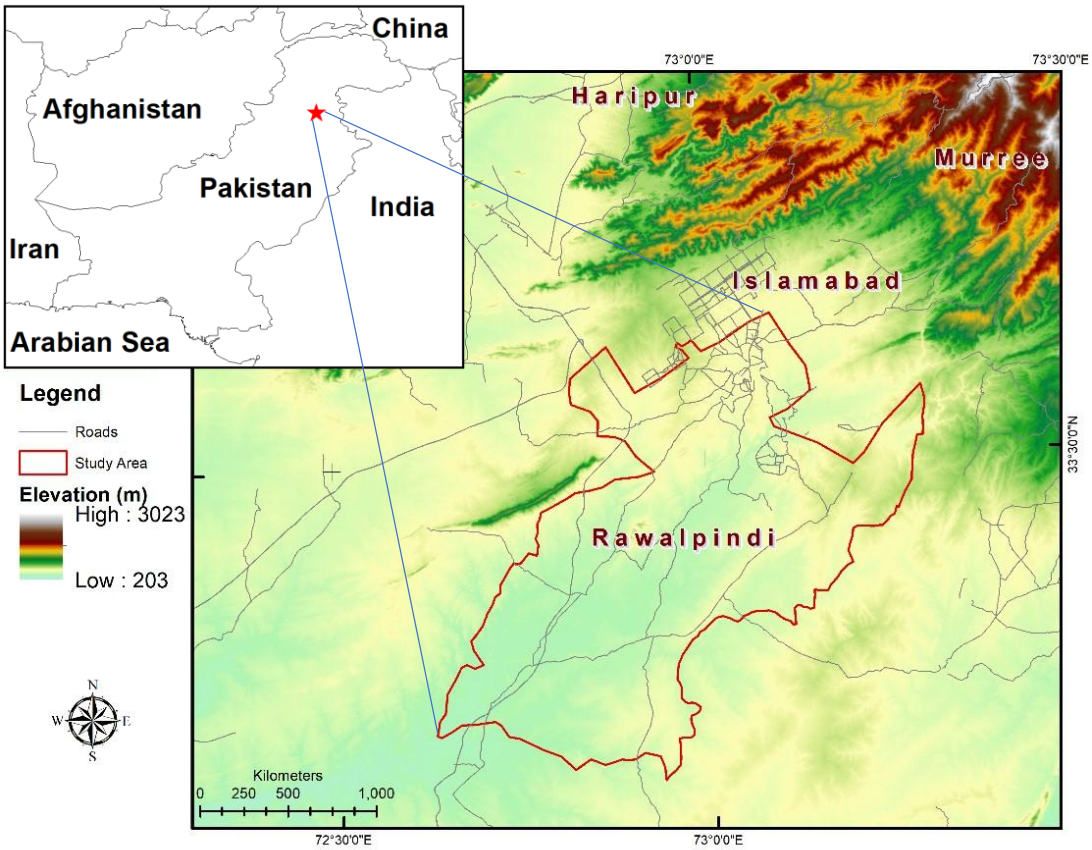

Figure 3.1. Study area location

One year of crash data for the city from January 2019 to December 2019 was obtained from the emergency response unit, Rescue 1122, which keeps a record of all emergency responses in Punjab. The motorcycle crash dataset was obtained in the Excel spreadsheet format. The dataset was cleaned and preprocessed using the SPSS software before conducting crash severity analysis. Incomplete data, such as data missing information about crash variables, data with incorrect codes, data with inconsistent names, and data with unrealistic values, were deleted from the dataset. Table 3.1 presents the final list of crash variables and their description. The dataset recorded every emergency response, among which 9,465 records were motorcycle crashes. The crash injury severity of motorcyclists was categorized into four groups: (I) no injury, (II) minor injury (crashes in which the victims suffered only minor cuts and abrasions), (III) severe injury (crashes in which at least one person was seriously injured and admitted

to hospital with, for example, a head, neck, or spinal injury, or excessive bleeding), and (IV) fatal injury (crashes in which at least one of the injured persons died the same day). The dataset contained several categorical variables (two or more categories) related to humans, the environment, and vehicles, and the summary statistics are presented in Table 3.1. Out of the 9,465 motorcycle crashes, 5.6%, 65.6%, 15.7%, and 13.1% were involved in no-injury, minor injury, severe injury, and fatal injury crashes, respectively. Underreporting of the no-injury crashes is observed in our data, which is a more pronounced and unavoidable issue in developing countries (Wahab & Jiang, 2019b; Waseem et al., 2019). The primary reason is the poor system of reporting and recording crash data due to a lack of resources. To overcome this issue, immediate measures are required to improve the reporting and recording of crash data in Pakistan (Ahmed et al., 2016).

Furthermore, the frequency of crashes was almost equally distributed between peak and off-peak periods. The frequency was highest during summer (35.9%), weekdays (72%), and sunny weather conditions (62.4%). More crashes occurred during the daytime (72%) compared to nighttime (28%). The dataset demarcates the day and night as; day (06:01 am to 07:00 pm) and night (07:01 pm to 06:00 am). Most motorcyclists involved in crashes were male (87.9%), which can be explained by the societal and cultural restrictions that make it difficult for a female to ride a motorcycle in Pakistan. Over 34.1% of the crashes involved young riders (aged 21–30). The majority of crashes were single motorcycle crashes (30.6%) that occurred due to motorcycles slipping on the road. The statistics also showed that speeding (78%) and distractions (22%) while driving were the leading causes of motorcycle crashes. Roads with a speed limit of 60km/h witnessed the highest number of crashes (72.6%).

Table 3.1. Descriptive statistics of variables used in the study.

Feature	Categories	Frequency	Percentage
Crash injury severity	No Injury	530	5.6
	Minor Injury	6,209	65.6
	Severe Injury	1,486	15.7
	Fatal Injury	1,240	13.1
Period of the day	Off-Peak	4,780	50.5
	Peak	4,685	49.5
Lighting conditions	Day	6,818	72.1
	Night	2,647	27.9
Day of the week	Weekday	6,815	72.0
	Weekend	2,650	28.0
Season	Summer	3,398	35.9
	Winter	2,821	29.8
	Spring	1,533	16.2
	Autumn	1,713	18.1
Gender	Female	1,174	12.4
	Male	8,291	87.6
Age group	≤20 years	2,470	26.1
	21–30 years	3,228	34.1
	31–40 years	1,704	18.0
	41–50 years	1,003	10.6
	>50 years	1,060	11.2
Vehicle involved	Collision with truck/van	1611	17.0
	Collision with moving car	1658	17.5
	Collision with pedestrian	1028	10.8
	Single motorcycle slipped	2898	30.6
	Collision between two motorcycles	1684	17.7
	Others	586	6.1
Weather condition	Cloudy	1,306	13.8
	Sunny	5906	62.4
	Rainy	2253	23.4
Motorcyclist behavior	Distractions	2,082	22.0
	Speeding	7,383	78.0
Speed limit	≤50 km/h	1,420	15.0
	60 km/h	6,872	72.6
	≥70 km/h	1,174	12.4

3.3 Methods

This section introduces the methodologies of several models applied in the study, including the MNL model and three ML models, i.e., the naïve Bayes model, a gradient-boosted trees model, and the RF model.

3.3.1 Multinomial logit model

The MNL model was selected as a baseline model due to its simplicity in terms of estimation and interpretation (Washington et al., 2003). It is a conventional unordered

discrete outcome model that accounts for more than two outcomes regardless of their orders. The MNL model is used to explore the relationship between the explanatory variables and the severity levels of motorcycle crash injury. The probability of a motorcycle crash injury's severity level lies between zero and one, which relies on the latent utility of alternative outcomes. The latent utility, S_{in}, of the crash injury severity level *i* of a motorcyclist, *n,* consists of two components, the deterministic term and the error term, given in Equation (3.1):

$$S_{in} = \beta_i X_{in} + \varepsilon_{in} \tag{3.1}$$

where X_{in} is the predictor vector (such as the driver, the environment, and the roadway characteristics), and β_i is the vector of parameters to be estimated. ε_{in} is the error term that accounts for effects from unobserved factors. The error term is assumed to be independently and identically distributed as Gumbel distribution, which results in the closed form probability in Equation (3.2) (Manski & McFadden, 1981):

$$P_n(i) = \frac{EXP[\beta_i X_{in}]}{\sum_i EXP[\beta_i X_{in}]} \tag{3.2}$$

The coefficients β_i are estimated with the maximum likelihood estimation method. The log-likelihood function is given by Equation (3.3) (Washington et al., 2003):

$$LL = \sum_{i=1}^{N} \left(\sum_{i=1}^{N} \delta_{in} \left[\beta_i X_{in} - LN \sum_{\forall I} EXP(\beta_I X_{In}) \right] \right) \tag{3.3}$$

where, δ_{in} is defined as being equal to 1 if the observed discrete outcome for observation *n* is *i* and zero otherwise, *N* is the total number of observations.

3.3.2 Naïve bayes classifier

The Naïve Bayes algorithm is a supervised ML algorithm frequently used as a linear classifier for classification problems. The Naïve Bayes classifier is based on the Bayes

theorem under the assumption of conditional independence among the dataset's features. Sometimes, the independent features assumption is violated; however, the naïve Bayes algorithm performs well under unrealistic assumptions, especially with a small sample size (Domingos & Pazzani, 1997). For a classification problem, assume Y is to be classified, and X is a set of attributes $X = (X_1, X_2, \ldots, X_n)$. Based on the Bayes theorem, the predicted probability of class variable $Y = y_i$ conditioned on x can be expressed as (Equation (3.4)):

$$P(Y = y_i|X) = \frac{P(X = x = (x_1, x_2, \ldots, x_n)|Y = y_i)P(Y = y_i)}{P(X = x = (x_1, x_2, \ldots, x_n))} \tag{3.4}$$

Naïve Bayes algorithm is fast, easy to implement, accurate, and robust and has been used as a classifier in many applications (Kazmierska & Malicki, 2008).

3.3.3 Gradient boosted decision trees

The gradient boosting decision trees (GBDT) improve a simple Decision tree (DT) model using a stochastic boosting approach (Friedman, 2002). Boosting is a general approach that tries to improve the accuracy of any learning algorithm by fitting a series of models. In the GBDT model, DT is a basic model considered a weak learner. The main motivation is to combine several weak learners to produce an improved ensemble model. Assuming g(x) as an approximation function of the dependent variable y, it can be expressed as: $g(x) = \sum_{n=1}^{N} \alpha_n f_n(x)$, where $f_n(x)$ are basic functions termed as weak learners. The loss function is expressed as, $L(y, g(x)) = \log(1 + e^{-yg(x)})$ The additive model is developed in a greedy fashion.

$$g_n(x) = g_{n-1}(x) + \alpha_n f_n(x) \tag{3.5}$$

The newly added tree f_n minimizes loss L based on the previous ensemble $g_{n-1}(x)$.

$$f_n = \arg_h min \sum_{i=1}^{m} L(y_i, g_{n-1}(x_i) + f(x_i)) \tag{3.6}$$

GBDT solves this minimization problem numerically using the steepest descent.

$$g_n(x) = g_{n-1}(x) - \alpha_n \sum_{i=1}^{m} \nabla_g L(y_i, g_{n-1}(x_i)) \tag{3.7}$$

Where the step length α_n is determined using the step search.

$$\alpha_n = \arg_h min \sum_{i=1}^{m} L(y_i, g_{m-1}(x_i) - \alpha \left(\frac{\partial L(y_i, g_{m-1}(x_i))}{\partial g_{m-1}(x_i)} \right) \tag{3.8}$$

GBDT model has several advantages over a simple DT model; it is robust, can manage a large amount of data, and is resistant to overfitting and outliers (Hastie et al., 2009).

3.3.4 Random forest

The RF algorithm is an ensemble learning algorithm based on a decision tree model Breiman (2001). It uses a bootstrap sampling approach to generate *k* training data subsets from the original training data, and then *k* trees are trained based on these subsets. A random forest is developed by assembling these decision trees. The RF algorithm overcomes the overfitting issue of the DT model. Each DT in the RF algorithm performs a prediction on the testing dataset, and the final classification result is obtained from the majority voting of these trees, as illustrated in Figure 3.2.

To initialize the RF algorithm, two important parameters must be decided: the number of trees (N) to be grown and the number of variables selected at each split (*m*). *N* bootstrap samples are selected from the training dataset, whereas the remaining dataset (denoted the out-of-bag data) is used to test the prediction error. After growing *N* trees for *m* random features selected for each tree, the outcome for new data is predicted

based on the outcome prediction of N trees. The original training dataset can be written as follows (Chen et al., 2016):

$$S = [(x_i, y_j), i = 1,2, \ldots\ldots, N, j = 1,2, \ldots\ldots, M]] \tag{3.9}$$

where x is a sample and y is a feature variable of S. There are N samples and M features in each sample of the original training dataset.

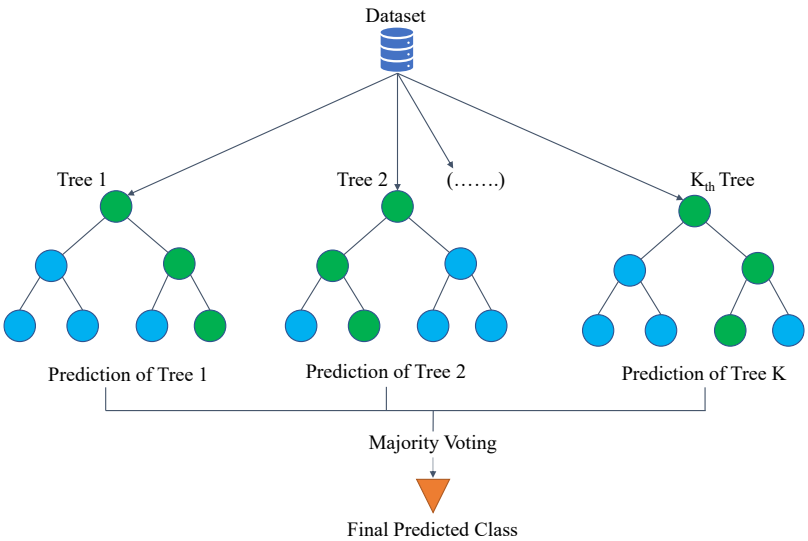

Figure 3.2. Illustration of a random forest classifier

The stepwise procedure for selecting bootstrap samples and generating the RF model from a set of trees is as follows:

$$S_{Train} = [S_1, S_2, \ldots\ldots, S_K] \tag{3.10}$$

Here, $S_{Train;}$ contains the subset of k bootstrap training samples. Thus, k trees are generated from these k samples. These k trees are then collected as an RF model, as follows:

$$H(X, O_j) = \sum_{i=1}^{k} h_i(x, O_j), (j = 1,2, \ldots\ldots, m) \tag{3.11}$$

where X is the input feature vector from the training data, $h_i(x, O_j)$ is a meta-DT classifier, and O_j is an IID-distributed vector determining the growth process of the tree.

3.3.5 SHAP method based on Shapley value

The SHAP method, introduced by Lundberg and Lee (2017), leverages Shapley values from cooperative game theory to interpret the predictions of machine learning models. Shapley values provide a systematic way to quantify the contribution of each variable to the model's output (Shapley, 1953). First, the SHAP method builds a model based on all input variables, followed by a model without the variable of interest to explore the effect of its absence on model performance. The SHAP value of a variable is defined as its average marginal contribution to the prediction of the outcome. The SHAP value of the variable is calculated using Equation (3.12) (Shapley, 1953):

$$\phi_i(X, f) = \sum_{S \subseteq X} \left(\left(f(x_S) - f(x_{S \setminus \{i\}}) \right) \times \frac{(|S|-1)!(|X|-|S|)!}{X!} \right) \tag{3.12}$$

where ϕ_i is the SHAP value of a variable; X represents all variables; S is the subset of all variables; and x_S denotes the values of the variables in S. To study the effects of the feature of interest, a model $f(x_S)$ is trained with the variable of interest, and another model $f(x_{S \setminus \{i\}})$ is trained, excluding the variable of interest. The predictions from the two models are then compared with the current output, represented as $\left(f(x_S) - f(x_{S \setminus \{i\}})\right)$. Since a variable of interest also depends on other variables in the model, the differences are calculated for all possible subsets (Lundberg & Lee, 2017).

3.3.6 Performance metrics

The most widely used metrics for comparing the predictive performance of models for classification problems are accuracy, precision, recall, and F_1 score. These metrics have been mostly adopted by many studies focusing on traffic crash severity prediction (Dong et al., 2022; Ijaz et al., 2021; Zhang et al., 2018). These metrics are calculated from the confusion matrix (CM). A sample of CM is shown in Table 3.2. A column in CM represents the predicted class instances, a row denotes actual class instances, and

the correct predictions are represented by the diagonal elements. The true positives (TP) and true negatives (TN) are instances that are correctly classified by the model. A false positive (FP) means an instance which is incorrectly classified as positive when it is negative. On the other hand, a false negative (FN) is when an instance is incorrectly classified as negative when it is positive (Shalev-Shwartz & Ben-David, 2014).

Table 3.2. Confusion matrix

		Predicted class	
	Total instances	Positive	Negative
Actual class	Positive	True Positive (TP)	False Negative (FN)
	Negative	False Positive (FP)	True Negative (TN)

The formulas to calculate performance metrics are shown in Equations (3.13)-(3.16). Accuracy is defined as the proportion of correctly classified crashes. Since we know that crash datasets are often imbalanced in terms of crash distribution by severity class, thus relying simply on accuracy to analyze the model's performance might not be conclusive. Therefore, for a deeper understanding of the model's performance for each severity class, it is important to explore other metrics such as recall, precision, and F_1 score. Recall measures the completeness of a model, and precision represents its exactness. A low recall value means many false negatives, while a low precision value denotes many false positives. Precision and recall can be combined to obtain one measure in terms of F_1 score.

Accuracy: The proportion of the total number of instances that are classified correctly (Equation (3.13)):

$$Accuracy = \frac{TP+TN}{TP+TN+FP+FN} \tag{3.13}$$

Recall: The number of positive instances that are classified correctly, given in Equation (3.14):

$$Recall\ (R) = \frac{TP}{TP+FN} \tag{3.14}$$

Precision: The proportion of predicted positive cases that were correct (Equation (3.15)).

$$Precision\ (P) = \frac{TP}{TP+FP} \tag{3.15}$$

F_1-Score: The harmonic mean of the precision (*P*) and recall (*R*). The F_1 score ranges from 0-1, where 1 indicates the best model and 0 represents the worst model. The F_1 score is calculated using Equation (3.16):

$$F_1 = \frac{2\times(R\times P)}{R+P} \tag{3.16}$$

3.4 Results and discussions

The dependent variable in this study was the motorcycle crash severity, divided into four levels (no injury, minor injury, severe injury, and fatal injury). To evaluate the accuracy of the developed ML models, a 10-fold cross-validation technique was adopted. This process of cross-validation minimizes the bias related to the random selection of training and validation sets. Moreover, the results of the ML models were interpreted using the SHAP method. The predictive performance of the adopted models and the consistency of crash risk factors identified by the MNL and the ML models are explored in this section.

3.4.1 Model performance

Knowing a model's predictive performance for each severity class is fundamental for efficiently prioritizing and selecting appropriate treatment measures under time and budget constraints. The predictive performance results (accuracy and F_1-score) of the four classification models are shown in Table 3.3.

Table 3.3. Summary of classification performance of models

Classification Model	Severity class	Recall	Precision	F_1	Accuracy (%)
Multinomial logit	No injury	0.528	0.600	0.562	86.1
	Minor Injury	0.956	0.864	0.908	
	Severe injury	0.568	0.925	0.704	
	Fatal injury	0.876	0.894	0.885	
Gradient boosted trees	No injury	0.440	0.627	0.517	85.6
	Minor Injury	0.953	0.873	0.911	
	Severe injury	0.631	0.815	0.711	
	Fatal injury	0.819	0.874	0.845	
Naïve bayes	No injury	0.474	0.661	0.552	85.7
	Minor Injury	0.951	0.865	0.906	
	Severe injury	0.565	0.899	0.694	
	Fatal injury	0.901	0.841	0.870	
Random forest	No injury	0.472	0.668	0.553	86.7
	Minor Injury	0.959	0.870	0.913	
	Severe injury	0.621	0.893	0.732	
	Fatal injury	0.874	0.889	0.881	

F_1-score reports the classification performance of the model for each severity class. As is evident from the F_1-score, all models perform well in predicting minor-injury and fatal-injury motorcycle crashes and exhibit average predictive performance for predicting severe-injury motorcycle crashes (F_1-score is approximately 0.7 for each model). In contrast, no-injury motorcycle crashes are predicted with an F_1-score ranging from 0.51 to 0.56. The low predictive performance for this injury severity category may be attributable to the dataset's small number of no-injury observations. All of the models gave acceptable results of the proposed classification evaluation metrics in terms of overall model performance. The RF model outperforms the other models with a prediction accuracy of 86.7%, followed by the MNL model (86.1%), the naïve Bayes (NB) model (85.7%), and the gradient boosted trees (GBT) model (85.6%). In this study, the MNL model performs better than the two ML models (i.e., NB and GBT). Literature suggests that different models may respond differently to different datasets. No single model is universally the best-performing model for all datasets (Shalev-Shwartz & Ben-David, 2014). Previous studies conducted on modeling traffic crash severity have confirmed that the performance of statistical models can be comparable

and even better than a few ML models depending on the dataset (Mahmud et al., 2024; Rezapour et al., 2020a; Zhang et al., 2018).

Table 3.4. Comparison of performance results with previous studies

Reference	Data/Severity Classes	Models used (Accuracy)	Best model (Accuracy)
Wahab and Jiang (2019a)	Motorcycle crash data from Ghana/ 4 classes	Random forest (73.91%) Instance-based learning with parameter k (73.71%) J48 decision tree classifier (73.64%) Multinomial logistic regression (52.04%)	Random forest (73.91%)
Rezapour et al. (2020a)	Motorcycle crash data from Wyoming/ 2 classes	Binary logistic regression (69%) Decision tree (68%)	Binary logistic regression (69%)
Rezapour et al. (2021)	Motorcycle crash data from Wyoming/ 2 classes	Multivariate adaptive regression splines (73%) Support vector machine (74%) Binary logistic regression (74%) Random forest (76%)	Random forest (76%)
Zhang et al. (2021)	USA motorcycle crash data from National highway traffic safety administration (NHTSA)/ 3 classes	Bayesian network model (64.57%) Multinomial logit model (65.97%)	Multinomial logit model (65.97%)
This study	Motorcycle crash data from Pakistan/4	Multinomial logit model (86.1%) Gradient boosted trees (85.6%) Naïve bayes (85.7%) Random forest (86.7%)	Random forest (86.7%)

Previous studies conducted on motorcycle crash injury severity have compared the predictive performance of statistical and ML models. Few studies are compared in Table 3.4, and it can be seen that the results of different studies may not be consistent due to their distinct databases. Nevertheless, few similarities can be noticed with our study; the random forest is the best-performing model in most of the studies. Literature indicates that the RF model has been found to be the best-performing model in 70% of the times that it was applied (Santos et al., 2022). Furthermore, statistical models show comparable performance to ML models in most studies.

3.4.2 Consistency analysis of risk factors between statistical and ML models

This section investigates the consistency of risk factors identified from the statistical model and best-performing machine learning model (RF model). The influential risk factors in the RF model identified with the SHAP method and MNL model are presented in Figure 3.3 to Figure 3.5 and Table 3.5, respectively.

Figure 3.3 to Figure 3.5 show the important features contributing to a motorcycle crash injury severity ranked by their importance in the RF model. Only the features with a feature importance value greater than 0.01 are illustrated. Besides simply showing the importance of predictors, the SHAP method provides detailed statistics on how each predictor contributes to a model with SHAP value and direction of association. The variable importance is illustrated in SHAP feature importance plots (Figure 3.3a, Figure 3.4a, Figure 3.5a), while the variable's direction of association with the dependent variable can be explained from the SHAP summary plots (Figure 3.3b, Figure 3.4b, Figure 3.5b). The SHAP summary plot's horizontal axis indicates the variables' impact on the severity level (either positive or negative). The color bar on the right-hand side shows the values of the variables (red color stands for a large value, while blue color stands for a small value). In Figure 3.3(b), Figure 3.4(b), and Figure 3.5(b), red dots capture the effect of the presence of a specific variable category on the dependent variable, while blue dots show the effect of the absence of that category. For example, from Figure 3.4(b), we notice that red dots for the variable "*female*" (presence of female rider in the crash event) have a positive SHAP value, indicating a positive effect on the severe injury crash. In contrast, blue dots (absence of female rider in the crash event) show a negative effect. Each point in the summary plot denotes a crash in the test data set. The clustering of the several dots in the SHAP summary plot indicates the same value for overlapping cases. A higher SHAP value means a higher effect of the variable

on the severity level and vice versa. Table 3.5 presents the estimated parameters for the MNL model. The estimated parameter of each variable reflects the variable's effect on a specific injury severity class compared to the no-injury class (baseline category).

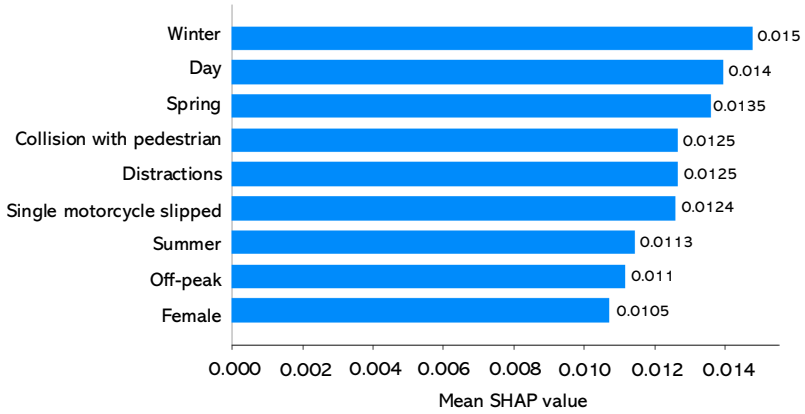

(a) SHAP feature importance for minor injury crash

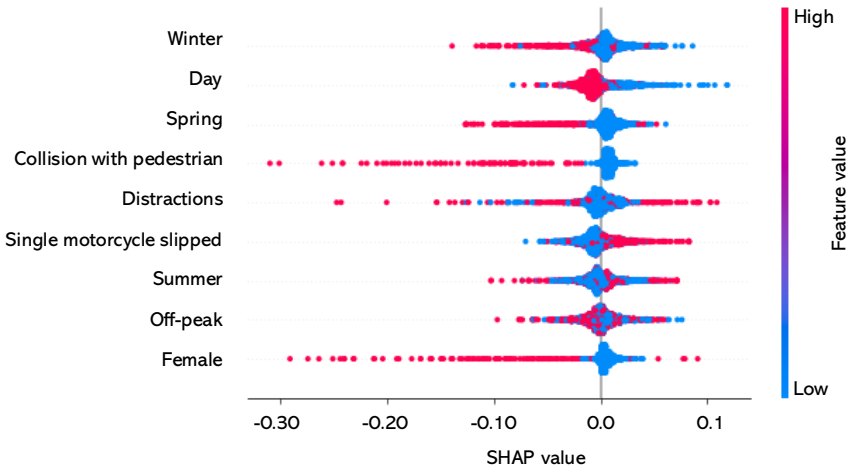

(b) SHAP summary plot for minor injury crash

Figure 3.3. Interpretations of the RF model using the SHAP method for minor injury crash

From Figure 3.5(a & b), we notice that influencing factors such as distractions (SHAP importance: +0.130), collisions with pedestrians/trucks (SHAP importance: +0.076/+0.012), and the female motorcyclists involved in motorcycle crashes (SHAP importance: +0.023) significantly increase the chance of crashes resulting in fatalities. In the meantime, teenage motorcyclists (aged <=20) (SHAP importance: +0.044), female motorcyclists (SHAP importance: +0.125), and collisions with trucks (SHAP importance: +0.024) are significant positive contributors to severe injury (Figure 3.4 (a

& b)). On the other hand, factors such as winter season (SHAP importance: -0.044) and mid-age group (aged 21-30) riders (SHAP importance: -0.041) would decrease the chance of crashes resulting in fatalities.

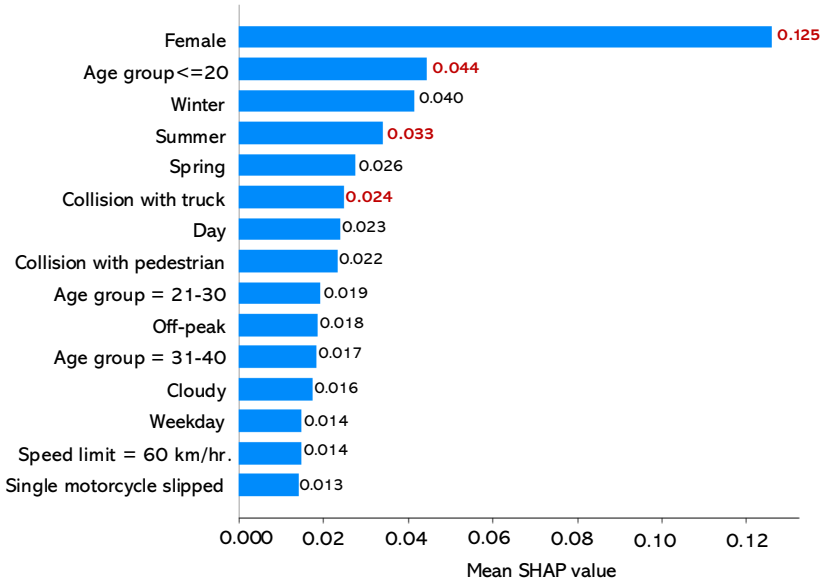

(a) SHAP feature importance for severe injury crash

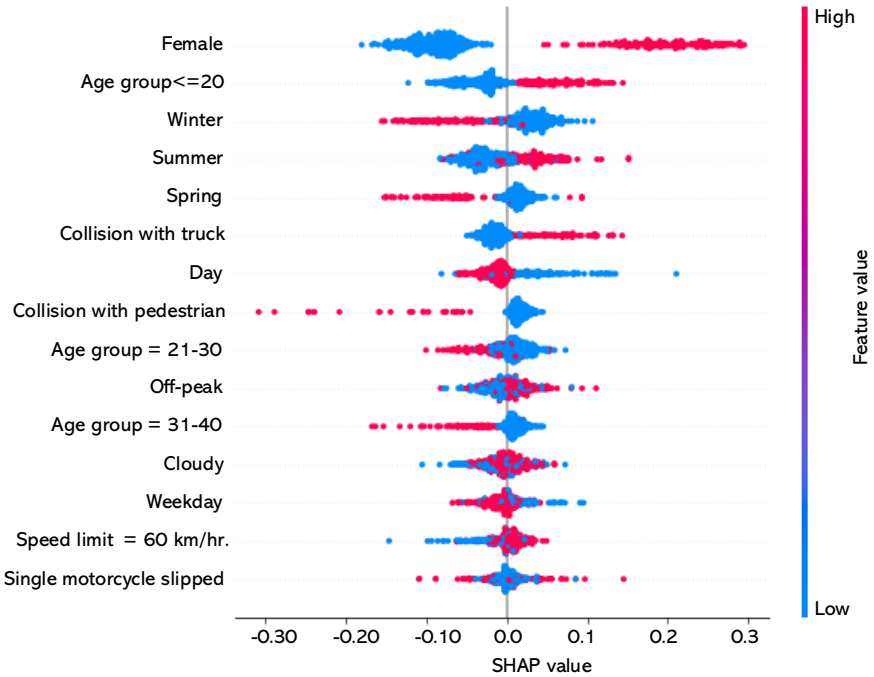

(b) SHAP summary plot for severe injury crash

Figure 3.4. Interpretations of the RF model using the SHAP method for severe injury crash

The factors that reduce the likelihood of severe injury crashes include winter season (SHAP importance: -0.040), daytime (SHAP importance: -0.023), etc. These findings

for intuitively interpreting the effects of risk factors on crash injury severity level are consistent with those inferred from the traditional statistical MNL model in Table 3.5.

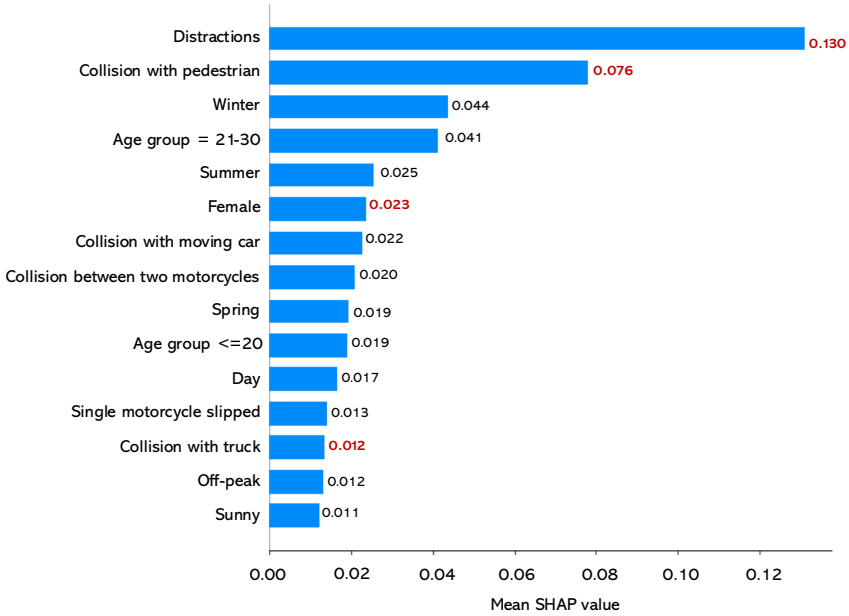

(a) SHAP feature importance for fatal injury crash

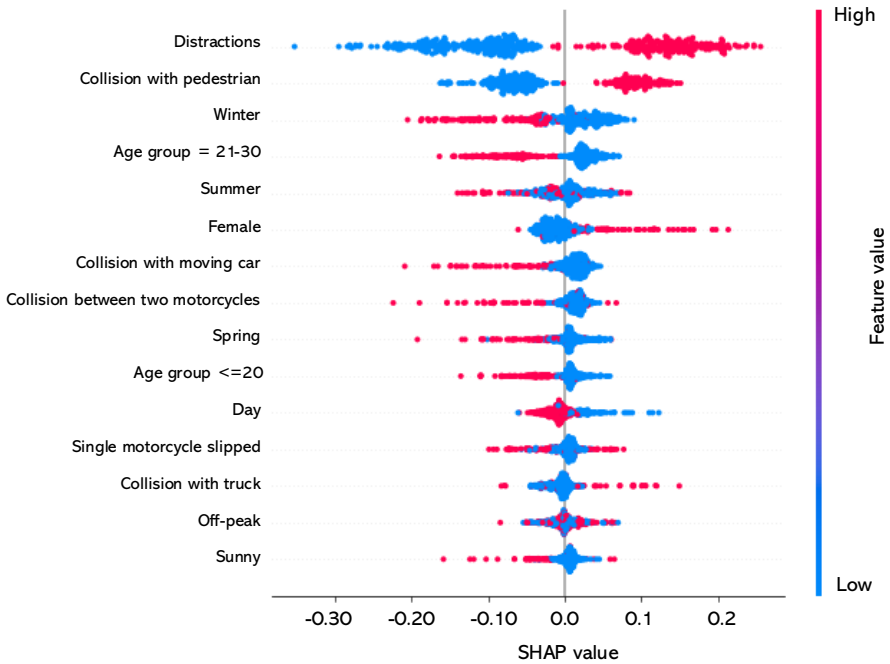

(b) SHAP summary plot for fatal injury crash

Figure 3.5. Interpretations of the RF model using the SHAP method for fatal injury crash

The fitted MNL model results reveal that the significant factors contributing to a severe injury or fatal crash are distractions while riding (odds ratio of 1.437 for severe injury

and 5.926 for fatality), collision with a truck (odds ratio of 1.785 for severe injury and 1.620 for fatality), collision with pedestrian (odds ratios of 3.280 for fatality), and female motorcyclist (odds ratio of 6.464 for severe injury and 1.207 for fatality). Similar results of variable interpretation are obtained when SHAP is applied to the GBT model (see Appendix A).

Table 3.5. Parameter estimation results for the multinomial logit (MNL) models

Variables	Minor Injury			Severe Injury			Fatal Injury		
	Coeff.	**Odds Ratio**	**Std. err**	**Coeff.**	**Odds Ratio**	**Std. err**	**Coeff.**	**Odds Ratio**	**Std. err**
Intercept	3.27***	---	---	0.644*	---	---	1.88***	---	---
Lighting Condition									
Day	-0.429***	0.650	0.107	-0.432*	0.694	0.127	-0.484***	0.615	0.130
Night (control)									
Weather									
Cloudy	-0.309**	0.733	0.139	-0.528***	0.589	0.176	-0.303*	0.738	0.174
Rainy (control)									
Season									
Winter	-0.838***	0.432	0.151	-0.906***	0.404	0.180	-1.385***	0.250	0.179
Summer	-0.423***	0.654	0.153	---	---	---	-0.869**	0.419	0.180
Spring	-1.029***	0.357	0.161	-0.898***	0.407	0.195	-1.088***	0.336	0.193
Autumn (control)									
Gender									
Female	-0.902***	0.405	0.140	**1.86*****	**6.464**	0.145	**0.188*****	**1.207**	0.154
Male (Control)									
Age group									
Age (≤20 yr)	---	---	---	**0.600*****	**1.823**	0.196	-1.307***	0.270	0.186
Age (21–30 yr)	---	---	---	---	---	---	-1.564***	0.209	0.179
Age (31–40 yr)	---	---	---	---	---	---	-1.101**	0.332	0.195
Age >50 years (control)									
Vehicle/Object Involved									
Collision with truck/van	0.385*	1.469	0.209	**0.579****	**1.785**	0.245	**0.482****	**1.620**	0.266
Collision with pedestrian	-1.331***	0.264	0.222	---	---	---	**1.187*****	**3.280**	0.254
Others (control)									
Motorcyclist Behavior									
Distractions	0.464*	1.591	0.137	**0.363****	**1.437**	0.163	**1.779*****	**5.926**	0.153
Speeding (control)									
Speed Limit									
60 km/h.	---	---	---	0.305*	1.357	0.165	---	---	---
≥70 km/h (control)									

Notes: *, **, and *** represent statistical significance at 10%, 5%, and 1% levels, respectively. ---: Insignificant

The detailed comparison of the findings between statistical and ML models on interpreting the effects of risk factors on motorcycle crash severity is summarized in

Table 3.6. It can be seen that the SHAP method performs well in identifying the effective factors in the ML model (specifically the RF model here). It is worth noting that the significant variables identified in the MNL model are found to influence motorcycle crash severity in the same direction as the RF model. Thus, it can be concluded that the influential risk factors identified by the MNL and ML models are consistent to a greater extent. The bold and highlighted text in Table 3.6 indicates the influencing factors contributing to severe injury and fatal injury crashes. Furthermore, the consistency analysis of risk factors between MNL and GBT models is provided in Appendix A (Table A1). The results in Table A1 are consistent with Table 3.6 to a large extent. This confirms that the results of the SHAP method obtained from different ML models are consistent.

Table 3.6. Consistency analysis of risk factors between the MNL and RF models

Variables	**Minor Injury**		**Severe Injury**		**Fatal Injury**	
	MNL	RF (SHAP)	MNL	RF (SHAP)	MNL	RF (SHAP)
Lighting Condition						
Day	-0.429***	-(0.014)	-0.432*	-(0.023)	-0.484***	-(0.017)
Weather						
Cloudy	-0.309**	IS	-0.528***	IS	-0.303*	IS
Season						
Winter	-0.838***	-(0.015)	-0.906***	-(0.040)	-1.385***	-(0.044)
Summer	-0.423***	-(0.0113)	IS	**+(0.033)**	-0.869**	-(0.025)
Spring	-1.029***	-(0.0135)	-0.898***	-(0.026)	-1.088***	-(0.019)
Gender						
Female	-0.902***	-(0.0105)	**+1.86*****	**+(0.125)**	**+0.188*****	**+(0.023)**
Age group						
Age (≤20 yr)	IS	IS	**+0.600*****	**+(0.044)**	-1.307***	-(0.019)
Age (21–30 yr)	IS	IS	IS	-(0.019)	-1.564***	-(0.041)
Age (31–40 yr)	IS	IS	IS	-(0.017)	-1.101**	IS
Vehicle/Object Involved						
Collision with truck/van	+0.385*	IS	**+0.579****	**+(0.024)**	**+0.482****	**+(0.012)**
Collision with pedestrian	-1.331***	-(0.0125)	IS	-(0.022)	**+1.187*****	**+(0.076)**
Motorcyclist Behavior						
Distractions	+0.464*	+(0.0125)	**+0.363****	IS	**+1.779*****	**+(0.130)**
Speed Limit						
60 km/h.	IS	IS	**+0.305***	**+(0.014)**	IS	IS

Notes: *, **, and *** represent statistical significance at 10%, 5%, and 1% levels, respectively. +: Positive effect, -: Negative effect IS: insignificant; numbers in parentheses indicate SHAP feature importance; numbers without parenthesis are MNL coefficients.

3.4.3 Discussion of risk factors

Though the statistical model (MNL) and machine learning model (RF) work under different mechanisms, the risk factors identified by these model streams have been revealed to be highly consistent. This section carries out discussion on the risk factors identified by the two models.

According to the consistency analysis in Table 3.6, distraction while riding a motorcycle was the most significant factor contributing to the crash fatality. Riders need to be highly aware of the road environment while riding a two-wheeler, and even a tiny distraction, such as mobile phone use, can lead to irretrievable catastrophes (Nguyen-Phuoc et al., 2019). In Pakistan, where heterogeneous and non-lane disciplined conditions exist, distractions are a significant threat, as in many developing countries (Gupta et al., 2022). Distracted motorcyclists are more likely to collide with another vehicle or slip on the road (Jones et al., 2013; Wundersitz, 2019). The consequences of a crash for a motorcyclist in Pakistan are much worse than for a car driver due to inadequate protection during a crash event (Waseem et al., 2019).

The vehicle type involved in a crash also influences the severity levels of casualties in a motorcycle crash (Table 3.6). It is found that collisions with a pedestrian or a truck increase the chances of a fatal crash. Both pedestrians and motorcyclists are vulnerable road users, and even a minor collision can result in a severe or fatal injury. Also, violations of traffic rules, such as red-light running, are typical safety issues in Pakistan (Pervez et al., 2021), and such behavior increases the probability of motorcycle-pedestrian crashes at the crossings, leading to pedestrian-related fatalities. Previous studies have obtained similar results for motorcycle crashes involving pedestrians (Agyemang et al., 2021; Kashani et al., 2020). Similarly, the probability of a fatality is higher in a motorcycle crash involving heavy vehicles (Savolainen & Mannering, 2007;

Wahab & Jiang, 2019b). Due to the lack of dedicated motorcycle lanes in Pakistan, motorcyclists share the same roadway with heavy vehicles (Waseem et al., 2019). Motorcyclists are often unnoticed by truck drivers, and even a minor collision can cause fatality or severe injury to a motorcyclist. Besides, the difference in momentum between a truck and a motorcycle leads to higher chances of severe crashes. Previous studies have reported similar results for motorcycle crashes involving heavy vehicles (Savolainen & Mannering, 2007; Wahab & Jiang, 2019b). Thus, adequate protection, such as wearing a helmet while riding a motorcycle, is vital (Savolainen & Mannering, 2007; Shaheed & Gkritza, 2014). However, the low level of helmet use in Pakistan increases the chances of head and facial injuries, which cause severe injury or fatality more easily. It was reported that only 34% of motorcyclists wear a helmet in Pakistan, and only 6% wear it correctly (MOC, 2018). Furthermore, only 7% of motorcyclists involved in crashes were found to have been wearing a helmet (Shamim et al., 2011). The use of a helmet is even worse for pillion riders (only 4% of the whole population) (MOC, 2018).

Results also suggest that females in Pakistan are more prone to fatal injury or severe injury crashes than males. Other than the general reasons reported in other countries, the wearing habits of females in Pakistan might also be attributed to severe injury and fatality (Khan et al., 2015). The cultural milieu in Pakistan encourages females to ride as pillion passengers rather than riders. Females usually wear loose dresses (long shirts over trousers with an overcoat) that can easily be entangled in a motorcycle's rear wheel or chain. The case will increase the chance of causing the crash incident and hinder the female motorcyclists or passengers from taking preventive action. Furthermore, the results indicate that teenage motorcyclists (age ≤ 20) are prone to severe injury crashes. The reason can be their inexperience and rash riding behavior (Bjørnskau et al., 2012;

Pervez et al., 2021). Many teenagers in Pakistan ride motorcycles without acquiring a license (the minimum age for obtaining a license is 18 years), leading to their high level of involvement in severe injury crashes (Pervez et al., 2021). Despite being more susceptible to severe injury crashes due to their rash riding behavior, teenage motorcyclists (age≤20) have a lower probability of being involved in fatal injury crashes compared to older motorcyclists (age>50) (Geedipally et al., 2011). This may be because younger motorcyclists tend to have stronger bodies, which can better withstand the impact of a crash. Conversely, older motorcyclists often experience physiological changes in their bodies with age, such as a decrease in bone strength and elasticity of the chest wall, which may make them more vulnerable to fatal injuries (Islam & Mannering, 2006; Pai & Saleh, 2007). Furthermore, roads with posted speed limits of 60 km/h increase the probability of severe injury crashes. This result is consistent with previous studies, that found a positive effect of speeding on severe injury (Savolainen & Mannering, 2007).

Some factors were negatively related to the crash severity or fatality. For example, fatal injury crashes were less likely to occur during the daytime and in cloudy weather conditions. Previous studies reported similar results, indicating that crashes occurring during the day and in cloudy weather conditions are less associated with fatal injuries (Geedipally et al., 2011; Wahab & Jiang, 2019b). It can be inferred that clear roadway delineation and clear visibility strategies such as adequate street lighting help reduce fatal crashes. The reduced incidence of fatal crashes in cloudy weather can be explained by cautious behavior in such conditions (Clarke et al., 2007; Jones et al., 2013). Moreover, the summer season was found to be associated with an increased risk of severe injury crashes as revealed by the SHAP method. This may be due to the extreme temperatures in the region, which can discourage motorcyclists from wearing helmets

due to thermal discomfort, thereby increasing the likelihood of severe injury crashes (Shaheed & Gkritza, 2014). However, fatal injury crashes were found to be less likely to occur during the summer, winter, and spring seasons. Previous studies have found mixed results regarding the effect of season on crash severity. For example, some studies have found a positive association between severe injury crashes and the summer season (Pai & Saleh, 2007), while others have found that the winter season is positively associated with severe injury crashes and negatively associated with fatal injury crashes (Sivasankaran et al., 2021).

3.5 Policy recommendations

With the identified potential risk factors that result in economic losses and human suffering in a motorcycle crash in Pakistan, government agencies need to improve road safety and create a safer driving environment. Practical policy implications and effective countermeasure suggestions will help managers and decision-makers to make appropriate decisions. Subject to the significant risk factors identified in the current study, we discuss possible suggestions or countermeasures for road safety improvement.

3.5.1 Implications for human factors

This study found that distractions while riding were the most significant cause of fatal injury motorcycle crashes. Crashes resulting from distracted driving are usually more severe than cautious driving (Chen & Lym, 2021). On the other hand, distracted driving and violation of traffic safety regulations on highways turned out to be common cases in Pakistan (Pervez et al., 2021). Thus, state authorities must strengthen compliance with the traffic laws devised for distracted driving. Educating the public and increasing drivers' awareness about the dangers of distracted driving can help improve adherence to traffic rules (Lim & Chi, 2013). Teenage motorcyclists (under 20) were revealed to

be one of the major contributors to severe injury crashes, which may be because they are inexperienced, often drive carelessly, too fast, and violate traffic regulations (Elvik, 2010). In addition, the licensing system in Pakistan is poor. Several drivers in Pakistan have never passed a driving test or acquired a driving license (Batool & Carsten, 2017). The situation adds to unsafe driving practices. Changes to this situation must be made from the driver's perspective. Thus, formal training must be provided to teenage motorcyclists before granting them a license. Furthermore, appropriate educational programs for teenagers can help raise their safety awareness and safe driving habits (Guria & Leung, 2004). Therefore, road safety education shall be included in the curriculum of primary education to encourage good driving habits at a young age (Haque et al., 2013). This study also uncovered an obvious gender effect on the injury severity of motorcycle crashes: females had a higher probability of getting involved in a crash with severe injury or fatality injuries. Thus, the government must educate females to wrap their loose dresses around themselves while riding a motorcycle. In addition, as pillion passengers in Pakistan often do not wear a helmet (MOC, 2018), education on the proper wearing of helmets for both motorcyclists and pillion passengers should be enhanced (Kanitpong et al., 2008). Towards this end, the community participation approach, in which people are the driving force behind community safety, can help increase helmet use by creating safety knowledge and awareness among the riders. The success of community participation is advocated in three districts of Thailand, where a 13.23% increase in helmet use was observed (Ratanavaraha & Jomnonkwao, 2013). Besides, appropriate and effective law enforcement shall also be implemented to make it compulsory for pillion passengers to wear a helmet.

3.5.2 Implications of vehicular and environmental factors

Motorcycle crashes involving pedestrians and heavy vehicles were more likely to result in fatal crashes. Both pedestrians and motorcyclists are vulnerable road users; thus, a minor collision can result in severe injury or fatality (Kashani et al., 2020). In this regard, we recommend improving sidewalk fences, reducing speed limits, installing frequent speed humps, and fixing retroreflective safety devices on roads in high-volume pedestrian areas. Moreover, appropriate placements of signboards and advertisements can be enhanced to raise the awareness of motorcyclists to ride more cautiously than expected in areas with high pedestrian volumes (Haque et al., 2013; Mfinanga, 2014). Safety education should be improved for motorcyclists and pedestrians (Agyemang et al., 2021).

Given the fact that heavy vehicles play a critical role in causing severe and fatal injuries, actions are needed to reduce the consequences of motorcycle crashes involving heavy vehicles. Heavy vehicle drivers should be educated to pay more attention to the road environment and keep concertation with the presence of motorcyclists on roadways. Furthermore, restrictions on heavy vehicles on highways in remote areas can also be implemented to improve management. Such a strategy can eliminate the interaction between motorcycles and heavy vehicles (Chang et al., 2019). One another effective way will be segregating motorcyclists and heavy vehicles by providing dedicated motorcycle lanes (Cherry & Adelakun, 2012). In Malaysia, segregating motorcyclists from mixed traffic has substantially reduced motorcycle-related fatalities (Radin Umar, 2006). However, the provision of dedicated motorcycle lanes is at the cost of other vehicles' space; thus, an in-depth assessment of traffic congestion in the area is required (Chang et al., 2019).

Furthermore, roadway delineation, streetlight provision during the night to improve visibility, and timely roadway maintenance (Zimmerman et al., 2015) would enhance the safety of motorcyclists in Pakistan. In addition, educating motorcyclists about the factors contributing to crash injury severity (Salvarani et al., 2009) and enforcing the traffic regulations on motorcycle registration and the driving license procedure may also help reduce the severity of injuries and deaths associated with motorcycle crashes (Haque et al., 2013). These recommendations may also be helpful for other developing countries with similar traffic, environmental, and roadway conditions.

3.6 Conclusions

This Chapter investigates motorcycle crash injury severity using statistical and machine learning models. The contributions of the study are four-fold. First, a comparison of the model performance between statistical and ML models for crash severity analysis has been carried out with multiple evaluation metrics such as accuracy and F1 score. The overall predictive accuracies of injury severity obtained from the methods were above 85.5%, indicating the effectiveness and robustness of the models. Among these models, the RF model, with an average accuracy of 86.7%, outperformed the other models; the MNL model was the second best-performing model, with an overall accuracy of 86.1%. Second, the SHAP analysis method has been applied to derive the risk factors affecting the crash severity outcome. Distractions while riding, collisions with a pedestrian, collisions with a heavy vehicle, and female riders were found to be the most significant variables contributing to motorcycle crash fatality. Third, an explicit comparison of the consistency of identified risk factors between machine learning methods and statistical models has been performed. The risk factors captured from the RF model with the help of the SHAP method are examined to be highly consistent with the MNL model. The finding revealed that though the statistical models and ML methods follow two streams

of methodologies on prediction, the identified risk factors are reasonably consistent to a greater extent. Finally, according to the findings of the crash severity study in the case of Pakistan, we have suggested appropriate policies and countermeasures to reduce motorcycle crash injuries. The study of the consistency between the two streams of methodologies will provide decision-makers with key insights that will help them initiate clear remedial measures to promote the safety of motorcyclists and pillion passengers in Pakistan.

CHAPTER 4 A cooperative game theory framework for proactive identification of safety-critical road links

4.1 Motivation

Network-wide vulnerability assessment of road links from a safety perspective can support the proactive identification of critical links. This assessment focuses on how network safety performance may degrade under disruptions such as traffic crashes or natural disasters (Kurmankhojayev et al., 2024). In this context, a link is considered safety-critical if its removal significantly reduces overall network safety. Identifying such links enables agencies to prioritize safety interventions and allocate resources more effectively during transportation planning (Bonera et al., 2024). Conventional network safety approaches typically identify critical links by exploring relationships between independent variables (e.g., roadway characteristics and traffic flow) and safety performance metrics such as crash frequency and severity (Bonera et al., 2022; Bonera et al., 2024; Mansoor et al., 2020). However, assessing link importance through a network vulnerability perspective, specifically by examining how much each link contributes to overall network safety, adds a valuable and unexplored dimension. This new perspective shifts the focus from evaluating the local impacts of traffic crashes on individual links to assessing each link's contribution to overall network-wide safety.

Safety of a link is a flow-dependent quantity that changes with changes in traffic conditions. While a link's safety contribution depends on its attributes and traffic conditions, it is also shaped by the interacting traffic conditions across neighboring links and routes serving various origin–destination (O–D) pairs (Liu et al., 2017; Lv et al., 2015). For instance, a crash on one link may reroute traffic through alternative routes, altering flows and crash risks across the neighboring links and the broader

network (Zhao et al., 2023). Conventional safety models treat traffic flow as exogenous, limiting their ability to capture these cascading effects driven by driver rerouting behavior. A network equilibrium framework that models route choices in response to disruptions can be integrated with conventional models to address this limitation.

To describe this traffic influence, we use traffic interactions to explain how neighbouring links connecting routes between different O-D pairs affect each other's safety conditions due to vehicle movements, illustrated in Figure 4.1(a-c). This traffic influence extends beyond upstream or downstream links, including all links that flow into or out of a specific link (Liu et al., 2017). For example, in Figure 4.1(a), four routes connect two O-D pairs (1-4 and 2-4). O-D pair 1-4 has two routes that share a common link (1-2), and congestion on this shared link impacts the safety conditions of downstream links connecting both O-D pairs. Furthermore, these downstream links can also mutually influence each other's safety. The safety of route 1 and route 3 depends on traffic interactions among local roads, whereas interactions between a local road and a highway influence the safety of route 2 and route 4. Additionally, as shown in Figure 4.1(b), when link (2-3) is disrupted, traffic from route 1 and route 3 diverts to route 2 and route 4, respectively, influencing the safety conditions of the links along these routes. Conversely, in Figure 4.1(c), disruption on the link (2-4) leads to traffic redistribution, affecting the safety conditions of links along routes 1 and 3. Moreover, the disruption of link (2-3) renders link (3-4) inaccessible for travel. These examples highlight that a comprehensive safety assessment of links in a road network must account for traffic interactions across all O-D pairs and routes under all possible disruption scenarios.

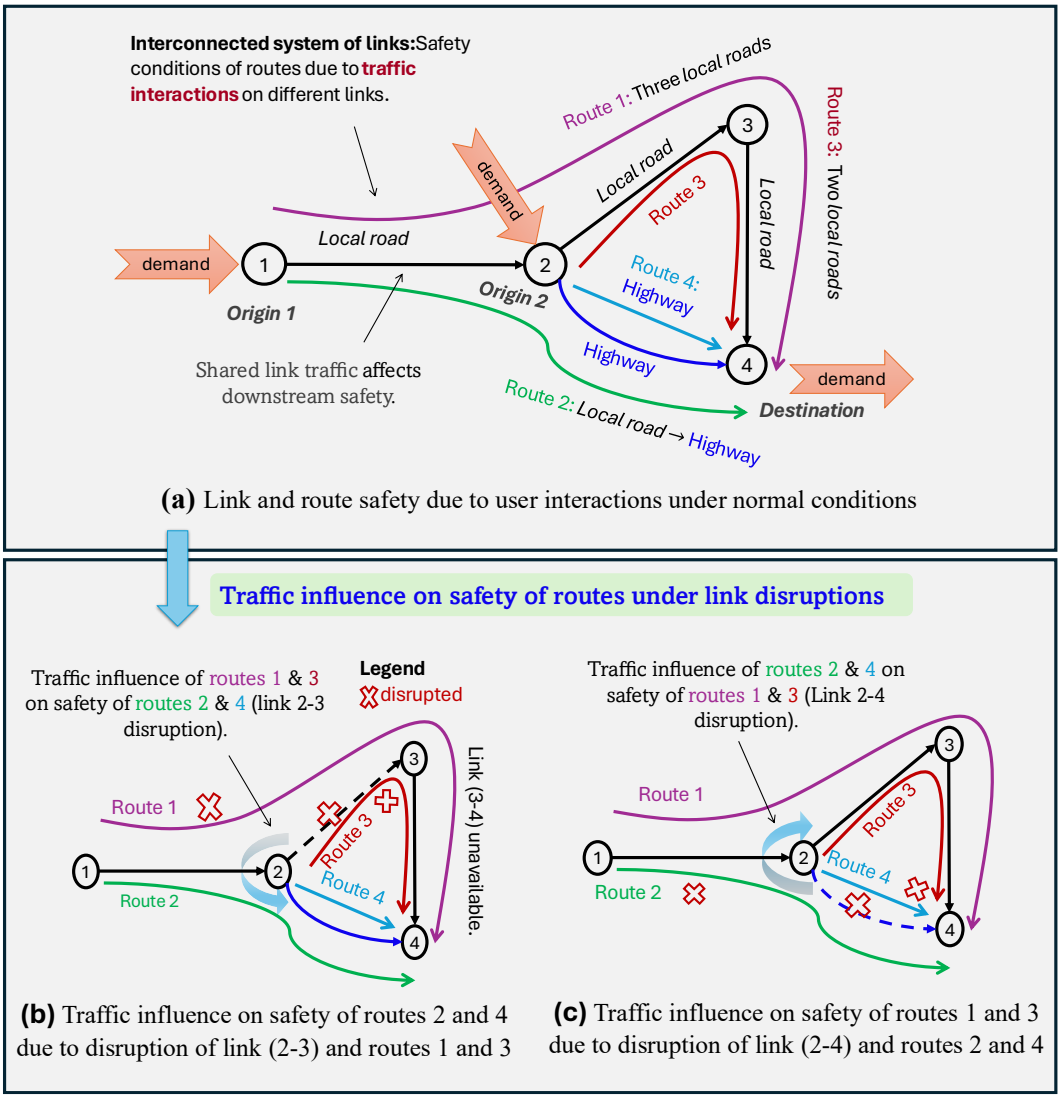

Figure 4.1. Illustration of link and route safety due to user interactions under link disruptions

Conventionally, the contribution of each link to network safety can be determined based on its marginal safety contribution. Marginal contribution (MC) can be determined by evaluating changes in network safety when a specific link is removed. However, such an approach has limitations as it evaluates links in isolations and overlooks the broader context of links cooperative interactions (Gnecco et al., 2021; Hadas et al., 2017). In reality, multiple links may be disrupted simultaneously, or a disruption in a single link can affect many others due to the network topology (Gu et al., 2023). For example, as shown in Figure 4.1(b), a disruption on link (2-3) also renders link (3-4) unavailable for travel. Therefore, to effectively evaluate the importance of each link, it is essential to

account for all potential scenarios where one or more links may be disrupted and measure the average effect of each on overall network safety. This perspective recognizes that links do not function in isolation but as part of an interconnected system, working collaboratively with other links to serve road users from different O-D pairs (Zhao et al., 2023).

To address this complexity, we employ cooperative game theory, treating links as players that cooperate with each other to enhance overall network safety. In this framework, the Shapley value, a game-theoretic concept, assigns costs or benefits to each link based on its marginal contribution across all possible coalitions. A coalition in a cooperative game represents a subset of players (in this case, links) that work together to improve their collective benefits. By considering every coalition, the Shapley value provides a fair and comprehensive way to measure the safety contribution of each link (Shapley, 1953). The utility function of the cooperative game is expressed in terms of a flow-dependent safety evaluation metric, quantified using link flow patterns from the traffic assignment model (see Section 4.2.6). This cooperative game theory–based, vulnerability-oriented view of safety highlights links whose systemic importance may be overlooked by more static or link-isolated assessments. It offers planning-stage insights that support proactive interventions for enhancing the safety of these critical links.

4.1.1 Contributions

This Chapter develops a framework that identifies the safety-critical links by integrating transportation safety analysis without network effect and transportation network analysis without safety effect via the Shapley value from a cooperative game-theoretic approach. It identifies the safety-critical links by considering cooperative interactions among different links. The utility function of the cooperative game is expressed using

a flow-dependent safety evaluation metric, quantified by solving the UE traffic assignment problem for all possible coalitions of links in the game. The Shapley value of each link is then calculated to determine its safety importance. In summary, this Chapter provides the following contributions:

a) From the theoretical side, this Chapter develops a transportation network safety analysis framework by integrating transportation safety analysis without network effect and transportation network analysis without safety effect via the Shapley value from a cooperative game-theoretic approach. Accounting for cooperative interactions of links using a flow-dependent safety-evaluation metric enhances theoretical understanding of transportation network safety.

b) From a practical perspective, this approach offers transportation safety planners a useful transportation network safety analysis framework to identify the most safety-critical links for investment strategy at the planning stage.

4.2 Methodology

This section explains the methodology for calculating the link's contribution to the transportation network safety.

4.2.1 Notations

All the notations used in this Chapter are listed in Table 4.1.

Table 4.1. Notations

Symbol	Description
Sets:	
N	set of nodes
M	set of links/players (m)
I	set of origins (i)
J	set of destinations (j)
W	set of O-D pairs (w).
P_w	set of routes between O-D pair w
S	coalition in a cooperative game

Ω	coalitions that can serve the complete network demand
Ω_{min}	minimally connected coalitions
Variables	
f_p^w	flow on route p of O-D pair w
x_m	flow on link m
ϕ_m	Shapley value of link m
Functions	
$t_m(x_m)$	travel time of link m
$r_m(x_m)$	crash rate on link m
$U(S)$	utility of a coalition S in a cooperative game

4.2.2 Study framework

Figure 4.2 presents the framework of this study. The Shapley value is utilized to evaluate the contribution of each link to network safety.

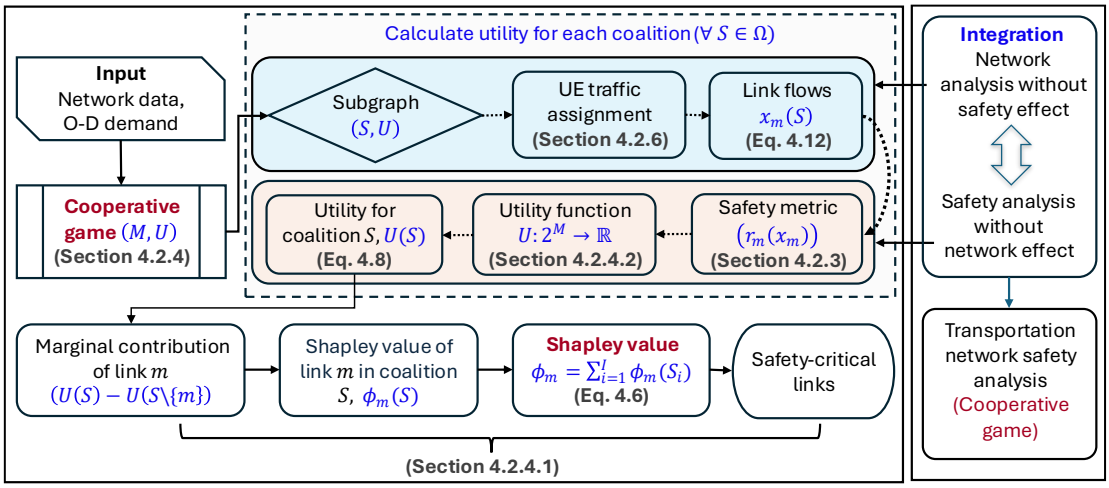

Figure 4.2. Framework of the methodology used for identifying safety-critical links

4.2.3 Flow-dependent safety evaluation metric

In this section, we introduce the safety evaluation metric for quantifying total network crash frequency ($TNCF$), which will be used to calculate the utility of each link in the cooperative game (explained in Section 4.2.4). Traffic crashes on a road network result from a complex interplay of factors, including roadway geometry, environmental conditions, driver behavior, and traffic characteristics, as illustrated in Figure 4.3 (Mansoor et al., 2023).

Safety performance functions (SPFs) are analytical tools developed using road network crash data to estimate crash frequency based on roadway type, crash severity, and crash type. They are estimated using negative binomial regression models and used to identify high-risk locations to support safety interventions. The Highway Safety Manual (HSM) provides a set of SPFs developed for various road types under base conditions i.e., the specified lane width, shoulder width, shoulder type, road hazard rating, passing lanes, and speed limit etc. Adjustments for deviations from these base conditions can be made using crash modification factors (CMFs), which scale the SPF outputs to reflect specific roadway or environmental changes (Al-Ahmadi et al., 2021). Jurisdictional agencies may choose to develop their own SPFs or calibrate existing ones, such as those provided in the HSM, to better reflect local conditions. While developing localized SPFs offers improved accuracy by capturing region-specific crash characteristics, it requires additional effort in terms of data collection and model calibration (Kweon & Lim, 2014).

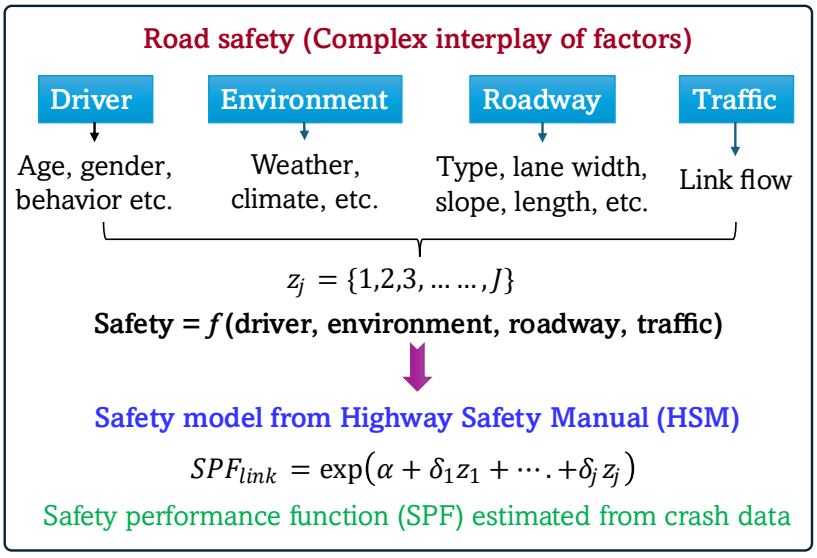

Figure 4.3. Road safety as a complex interplay of different factors.

Based on the safety model illustrated in Figure 4.3, the SPF in Equation (4.1) predicts the annual number of crashes (F_m) on a given link. In Equation (4.1), z_j represents the

independent variables associated with roadway characteristics, environmental factors, traffic conditions and driver characteristics etc. α and δ are the calibrated parameters typically estimated using Maximum Likelihood Estimation (MLE). The values of the calibrated parameters may vary for different road types, such as local roads and highways (Kweon & Lim, 2014).

$$F_m = \exp\left(\alpha + \sum_{j=1}^{J} \delta_j z_j\right) \tag{4.1}$$

SPF can be written as a function of exposure measures, which are the traffic flow (x_m) and link length (L_m), assuming that the links are in accordance with the base conditions of HSM, as shown in Equation (4.2) (Al-Ahmadi et al., 2021). It quantifies the average hourly number of crashes on link m per year. Similar SPFs have been applied in transport network design problems (Lin & Wei, 2019) and traffic assignment problems (Ma & Zhang, 2019) to evaluate the network safety.

$$F_m = \exp(\alpha + \delta \ln(x_m) + \ln L_m) \tag{4.2}$$

Since the traffic crash data includes various other variables, the calibrated parameters implicitly account for these factors within the functional form presented in Equation (4.2). If certain links do not conform to base conditions, deviations can be addressed by multiplying Equation (4.2) by the product of crash modification factors (CMFs), as shown in Equation (4.3).

$$F_m = \exp(\alpha + \delta \ln(x_m) + \ln L_m) \times \prod_{k=1}^{K} CMF_k \tag{4.3}$$

The crash rate (r_m) for each traveler, interpreted as the crash probability (or "normalized frequency" per unit of exposure e.g., vehicles) (Bonera et al., 2024), is calculated by dividing the number of crashes by the traffic flow (x_m) on the link. In

other words, Equation (4.3) is divided by x_m, as shown in Equation (4.4) (Ma & Zhang, 2019).

$$r_m = e^{\xi} x_m^{\delta-1} L_m \tag{4.4}$$

Using Equation (4.5), $TNCF$ is calculated by aggregating the crashes on links with nonzero flow (x_m), determined by solving the traffic assignment model (explained in Section 4.2.6).

$$TNCF = \sum_{m \in M} r_m . x_m \tag{4.5}$$

This approach excludes links with zero flow from the $TNCF$ calculation, ensuring accuracy and generalizability to different functional forms of SPFs. While Equation (4.4) could aggregate crashes across all links, it does not exclude zero-flow links, which may lead to overestimation of the $TNCF$, especially when using SPFs that include additive flow-independent terms. Equation (4.5), by contrast, avoids this issue and provides a more robust and adaptable method for calculating the $TNCF$ using the link flows from the traffic assignment model.

4.2.4 The cooperative game

In the cooperative game, players unite to form sub-coalitions and grand coalition. Sub-coalitions (S) contain a few players, while grand coalition (M) contains all the players. A pair define a cooperative game (M, U), where $M = (1,2,3, \ldots\ldots, m)$ is the set of players (links in this study) and $U: 2^{\mathrm{M}} \rightarrow \mathbb{R}$ is a utility function with $U(\emptyset) = 0$, i.e., the utility of an empty coalition has a zero value, and 2^m is the set of all possible subsets of M. For any subset $S \subseteq M$, $U(S)$ represents the utility of coalition S achieved by players in S without the help of remaining players in $M \backslash S$. $U(M)$ is the utility of the grand coalition, i.e., the utility achieved by all the players in the coalition. In

cooperative games, a medium of exchange (e.g., money) is freely movable between players and is quantifiable. As explained in the section below, the Shapley value can divide the utility among players in a cooperative game fairly.

4.2.4.1 Shapley value of a cooperative game

The Shapley value, introduced by Shapley (1953), is a method used in cooperative game theory to distribute the total payoff among players fairly. It considers each player's contribution to different coalitions and calculates their fair share. Since some players may contribute more to the final value, it is important to ensure that players are rewarded fairly. The Shapley value ϕ_i for each player i is calculated using Equation (4.6) (Narayanam & Narahari, 2010):

$$\phi_i(M,U) = \sum_{S \subseteq M} \left(\underbrace{(U(S) - U(S \backslash \{i\})}_{Marginal\ contribution} \times \underbrace{\frac{(|S|-1)!\,(|M|-|S|)!}{M!}}_{Weight} \right), \quad \forall\, i \in M \qquad (4.6)$$

where $U(S) - U(S \backslash \{i\})$ is the marginal contribution (MC) of player i to the coalition S. Hence, the Shapley value represents the average marginal contribution of each player across all possible coalitions, considering every possible order in which players can join the grand coalition, starting from an empty set. In this Chapter, each network link is treated as a player that cooperates/interacts with other links. To evaluate the contribution of each link to network safety, this Chapter utilizes the Shapley value. A higher Shapley value of a link indicates its greater contribution to network safety.

4.2.4.2 Utility function of a cooperative game in transportation network

This section defines the utility function of a cooperative game for a transportation network, $G(N, M)$, where N and M are, respectively, the sets of nodes and links. Let $w \in W$ denote the sets of origin-destination pairs such that each O-D is connected by a set of routes P_w. We define Ω as the set of coalitions $\Omega \subset S$ such that for each O-D pair

$w \in W$, there exists at least one route in $G(S)$ connecting w. A subset of these coalitions $\Omega_{min} \subset \Omega$, is defined as the set of minimally connected coalitions, the ones for which the removal of any one player makes the resulting coalition not belong to Ω, i.e., no single route exists between O-D pair w. Based on the definition of $TNCF$ in Section 4.2.3, the $TNCF(S)$ for coalition S can be calculated using Equation (4.7), where $r_m(S)$ and $x_m(S)$ denote the crash rate and traffic flow on link m in coalition S, respectively.

$$TNCF(S) = \sum_{m \in M} r_m(S).x_m(S) \tag{4.7}$$

The utility function $U(S)$ is defined in Equation (4.8):

$$U(S) = \begin{cases} \left(\max_{S' \in \Omega_{min}} TNCF(S')\right) - TNCF(S) & \forall\, S \in \Omega, \\ 0 & \forall\, S \notin \Omega \end{cases} \tag{4.8}$$

The interpretation of the utility function, $U(S)$, is that when the whole demand between an O-D pair w is served i.e., at least one route exists ($S \in \Omega$), the utility represents the savings in number of crashes (reduction in $TNCF$) with respect to the maximum number of crashes (maximum $TNCF$) for all minimally connected coalitions, $\Omega_{min} \subset \Omega$; otherwise, if the whole demand is not served ($S \notin \Omega$), the utility is zero. In Equation (4.8), the $TNCF$ for each coalition is subtracted from the maximum $TNCF$ of the minimally connected coalitions, in order to convert the disutility (crash frequency) into utility (savings in number of crashes).

4.2.5 An illustrative example for a single O-D pair without congestion effect

A small network with graphical illustrations is presented to provide detailed interpretations of the cooperative game, utility function and the Shapley value. Figure 4.4 shows a network with a single O-D pair (1,4) comprising of 4 links (a, b, c, d) and 2 routes (P_1, P_2).

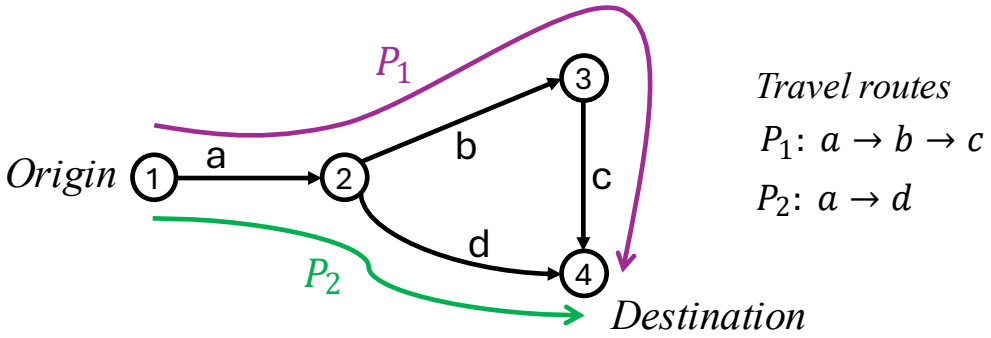

Figure 4.4: Illustrative network with two routes

4.2.5.1 Illustration of utility function and utility calculation

For illustration purposes, $TNCF$ is assumed to be exogenously provided in Figure 4.5(a-h). However, in practice, this depends on the traffic flow, as explained in Section 4.2.3. In Figure 4.5, $TNCF(S)$ represents the $TNCF$ for any coalition $S \subseteq M$, $TNCF(M)$ represents the $TNCF$ for grand coalition (M), while $TNCF(S')$ represents the $TNCF$ for any minimally connected coalition (S'). Figure 4.5(a-b) illustrate the minimally connected coalitions along with their $TNCF(S')$, as described in the utility function (Equation (4.8)). Figure 4.5(a) has the maximum $TNCF(S')$ between the two minimally connected coalitions i.e., $TNCF(S') = 0.445$. Similarly, Figure 4.5(c-d) depict coalitions with zero utility i.e. those for which there in no available route to serve the O-D demand (Equation (4.8)). These coalitions are excluded from the calculations. Figure 4.5(e) depicts the grand coalition containing all links having $TNCF(M) = 0.268$. Figure 4.5(f-h) show the $TNCF(S)$ for coalitions with at least one inactive link and at least one available route from origin to destination. Additionally, Figure 4.5(i) shows the utility calculations for some coalitions while Figure 4.5(j) illustrates the MC of each link solely to the grand coalition (MC is used in Equation(4.6) to calculate Shapley value). Figure 4.5(j) also illustrates each link percent contribution to network safety, based on their MC.

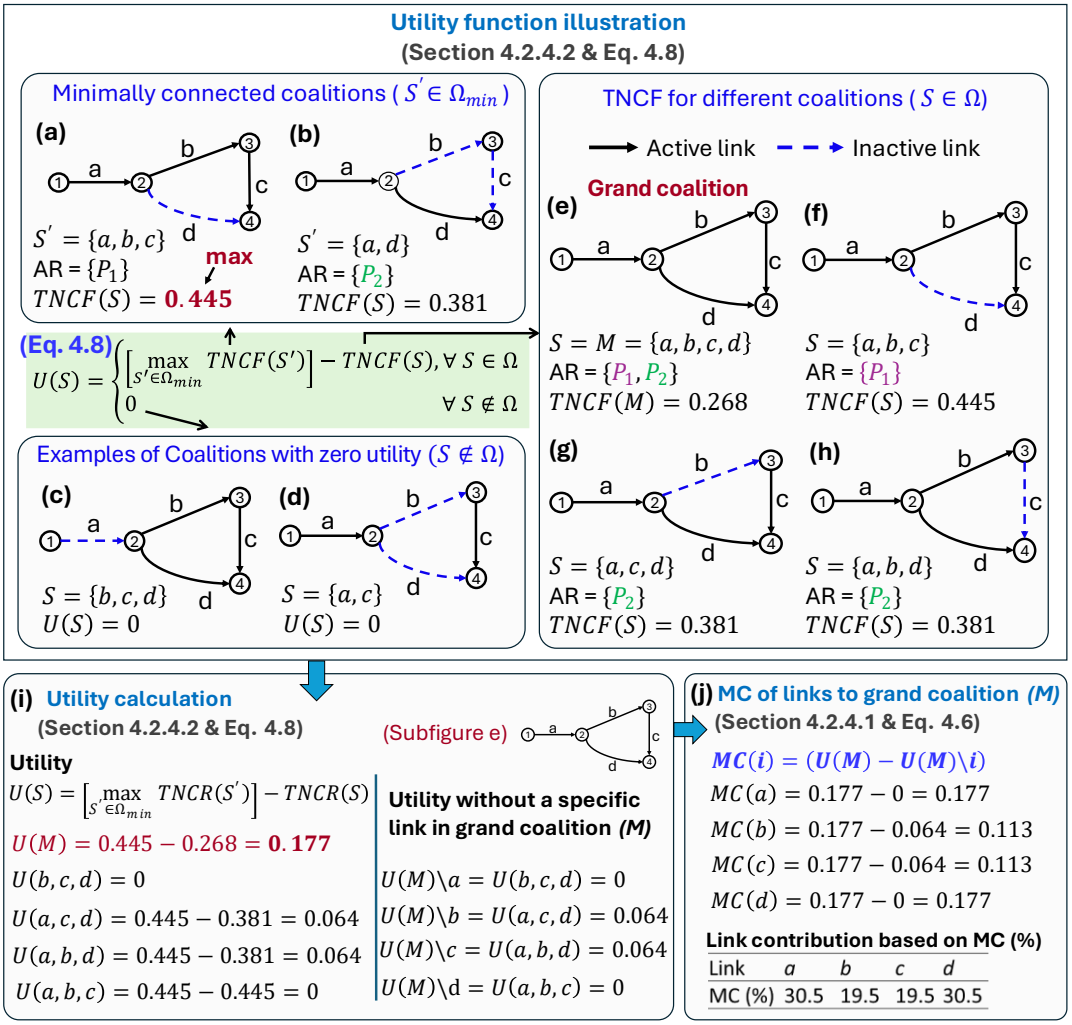

Notes: AR stands for available routes in each coalition *(S)*, *M* represents grand coalition of links.

Figure 4.5. Graphical illustrations of utility and MC calculations for a small network

Using the data from Figure 4.5 and the process outlined in Figure 4.5 and Equation (4.8), Table 4.2 presents the Shapley value calculation for the link b. The effect of link b in all the possible coalitions is evaluated to determine the final Shapley value, $\phi_b = \sum_{i=1}^{I} \phi_b(S_i)$. Importantly, we use the utility function definition to focus on five specific coalitions, rather than analyzing the entire set of 16 possible coalitions (since, $2^4 = 16$). Coalitions shown in Figure 4.5 (c-d), which have a utility of zero, are excluded from the analysis. This selective approach reduces the computational burden, making it more practical for solving real-world transportation network problems.

Table 4.2. Shapley value calculation for link b

S	$TNCF(S)$	$U(S)$	$U(S)\backslash b$	MC	ω	$\phi_b(S)$
a, b, c, d	0.268	0.177	0.064	0.113	0.25	0.028
a, b, c	0.445	0	0	0	0.08	0
a, b, d	0.381	0.064	0.064	0	0.08	0
a, c, d	0.381	0.064	0.064	0	0.08	0
a, d	0.381	0.064	0.064	0	0.08	0
						$\phi_b = 0.028$

Notes: $MC = (U(S) - U(S)\backslash b)$, and $\omega = \frac{(|S|-1)!(|M|-|S|)!}{M!}$

4.2.5.2 Shapley value vs marginal contribution for links

This section compares the link safety contribution between Shapley value and MC (Figure 4.6).

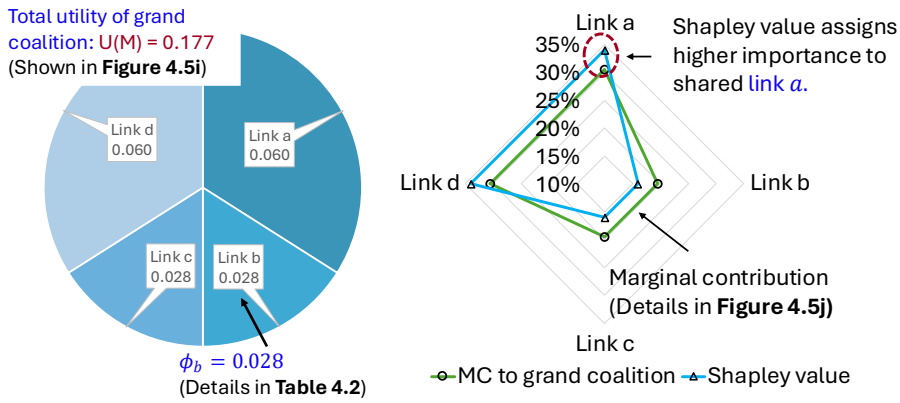

(a) Shapley value for each link **(b)** Shapley value vs MC

Figure 4.6. Comparison of link safety contribution between Shapley value and MC

Figure 4.6(a) shows the Shapley value for each link, where the total utility for the grand coalition ($U(M) = 0.177$ from Figure 4.5(i)) is fairly distributed among players i.e., $\sum_{i=1}^{M} \phi_i = 0.177$. Figure 4.6(b) compares the link safety contribution based on the Shapley value versus the MC to grand coalition only. The Shapley value assigns a comparatively higher safety contribution to shared link a and link d. This indicates that when cooperative interactions are comprehensively considered between links in the Shapley value calculation, the contributions of links a and d to the overall network safety are relatively higher. This conclusion will be further explored in Section 4.3 to

demonstrate why the Shapley value is a better metric for evaluating link safety contribution than MC.

4.2.6 Transportation network cooperative game based on user equilibrium

4.2.6.1 User equilibrium formulation for cooperative game

Consider a directed network $G(N, M)$, where q_w is defined as the user demand between an O-D pair w. The non-negative flow on a route $p \in P_w$ is represented by f_p^w. The flow on link m is represented by x_m. We denote $t_m(x_m)$ as travel time on links m. δ_m^p is the route link incidence matrix whose elements are defined as $\delta_m^p := 1$, if link m belongs to route p, and 0; otherwise. Finally, the cost for route $p \in P_w$, denoted as by $c_p^w(f_p^w)$, is defined as the sum of the costs on all links comprising the route between the O-D pair w. A route flow pattern is feasible if it satisfies the demands, i.e., $\sum_{p \in P_w} f_p = q_w, \forall w \in W$ as well as the non-negativity condition.

We assume that the drivers have perfect knowledge of the travel costs on the network and choose the route according the Wardrop's first principle, i.e., "no user can unilaterally change his/her travel cost by shifting to another route" (Sheffi, 1985). At equilibrium, for any coalition $S \in \Omega$, a feasible route flow pattern can be defined as (Tan et al., 2024):

Definition 1: Equilibrium route flow pattern. A feasible route flow pattern $(f_p^w, \forall p \in P_w, w \in W)$ satisfies the following conditions at equilibrium (Equation (4.9)).

$$c_p^w(f_p^w) \begin{cases} = \mu_w(S) & \text{if } f_p^w(S) \geq 0, \\ \geq \mu_w(S) & \text{if } f_p^w(S) = 0, \end{cases} \quad \forall p \in P_w, w \in W \tag{4.9}$$

where $\mu_w(S)$ is the minimum cost route at equilibrium for O-D pair w for each coalition S. The following mathematical program can be solved for finding the equilibrium route flow pattern $f_p^w(S)$ for any coalition S.

$$min\ Z(x(S)) = \sum_{m \in M} \int_{0}^{x_m(S)} t_m(w)dw \tag{4.10}$$

subject to.

$$\sum_{p \in P_w} f_p^w(S) = q_w\ , \forall w \in W \tag{4.11}$$

$$x_m(S) = \sum_{w \in W} \sum_{p \in P_w} f_p^w(S)\delta_m^p\ \ \forall m \in M \tag{4.12}$$

$$f_p^w(S) \geq 0, \forall p \in P_w, w \in W \tag{4.13}$$

where Equation (4.10) is the objective function of coalition S represented by the well-known Beckmann's transformation. The flow conservation constraints, definitional constraints and non-negativity constraints are given in Equations (4.11), (4.12), and (4.13), respectively. The convex programming formulation in Equations (4.10)- (4.13) has a unique link flow pattern if the link costs are monotonically increasing function of link flows; however, there could be multiple equilibrium route flow patterns (Sheffi, 1985).

4.3 Numerical experiments

4.3.1 Experiment settings for multiple O-D pairs in UE traffic assignment

Consider the cooperative game (M, U) for a transportation network in shown in Figure 4.7, which consists of five links, $M = \{i, j, k, l, m\}$. There are two O-D pairs, where O-D pair 1-4 is connected by three routes while O-D pair 2-4 is connected by 2 routes. The demand between both the O-D pairs is 3 vehicles/hour (vph) i.e., $q_{14} = 3\ vph$ and $q_{24} = 3\ vph$. Table 4.3 presents the input parameters for this case study including the link travel time functions, link lengths, and the parameters of the safety performance function. All links are assumed to be of the same type; therefore, the parameters (α and

δ) for the safety performance function in Equation (4.4) are set equal for all the links according to Kweon and Lim (2014).

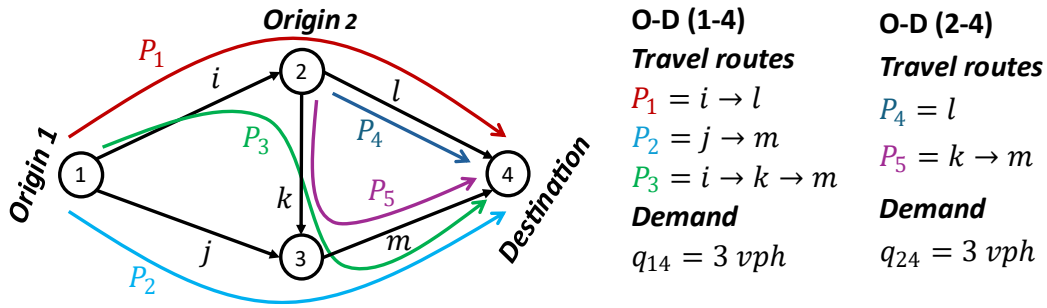

Figure 4.7. A transportation network with two O-D pairs, five routes, and five links

Table 4.3. Input parameters for the network

Link	$t_m(x_m)$	L_m	ξ	δ
i	$10x_i$	1	-7.05	2.0
j	$50 + x_j$	1	-7.05	2.0
k	$10 + x_k$	0.5	-7.05	2.0
l	$50 + x_l$	1	-7.05	2.0
m	$10x_m$	1	-7.05	2.0

We use the input parameters from Table 4.3 and link flows from the UE traffic assignment model to quantify $TNCF(S)$ for each coalition S. The computed $TNCF$ values for each coalition are shown in Figure 4.8. These values are then used to calculate the Shapley values.

4.3.2 Numerical results and discussions

In this section, we present the calculation of the Shapley value for a flow-dependent safety evaluation metric within a UE traffic assignment model. We provide the comparison of Shapley values when considering both single and multiple O-D pairs. We then explore the effect of varying congestion levels on the Shapley value.

4.3.2.1 Shapley value calculation for flow-dependent safety evaluation metric

This section shows the detailed process of the Shapley value calculation in the traffic assignment model using graphical illustrations (Figure 4.8).

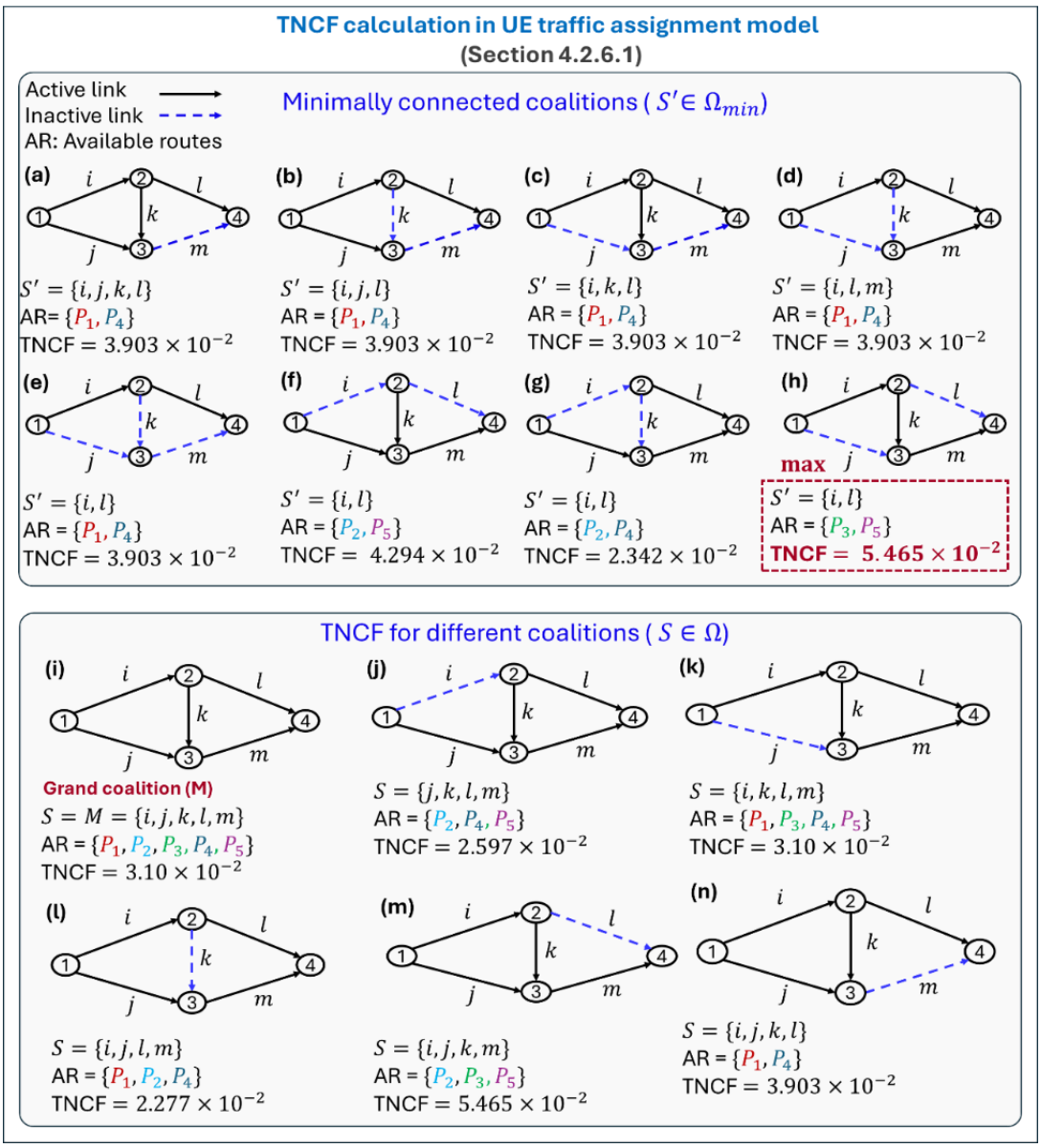

Figure 4.8. Calculation of TNCF for different coalitions in the cooperative game

The $TNCF(S)$ is calculated using Equation (4.7), after solving the optimization model in Equations (4.10)- (4.13) for each coalition S, as shown in Figure 4.8. Figure 4.8(a-h) depict the minimally connected coalitions and their $TNCF(S')$ where the coalition in Figure 4.8(h) has the maximum $TNCF(S')$ (i.e., $TNCF(S')$= 5.465×10^{-2}). Figure 4.8(i) presents the *TNCF (M)* for grand coalition (M), where all five routes are available ($TNCF(M) = 3.10 \times 10^{-2}$). Figure 4.8(j-n) illustrate the $TNCF(S)$ for scenarios where one link from the grand coalition is inactive. These scenarios are used to calculate

the MC of each link to the grand coalition within the utility function. Additionally, Figure 4.8 provides information about the available routes (AR) for each coalition.

Based on the *TNCF* for different coalitions shown in Figure 4.8, the calculation of the Shapley value for link i is detailed in Table 4.4. It does not show coalitions $S \notin \Omega$, as their utility and MC are zero. Table 4.5 shows the Shapley value calculations for all the links.

Table 4.4. Calculation of Shapley value for link i

Coalition	$TNCF(S)$	$U(S)$	$U(S)\backslash i$	MC	ω	$\phi_i(S)$
i,j,k,l,m	0.031	0.024	0.029	-0.0050	0.200	-0.0010
i,j,k,l	0.039	0.016	0.	0.0156	0.050	0.0008
i,j,k,m	0.055	0.000	0.012	-0.0117	0.050	-0.0006
i,j,l,m	0.023	0.032	0.031	0.0006	0.050	0
i,j,l	0.039	0.016	0	0.0156	0.033	0.0005
i,k,l,m	0.031	0.024	0	0.0236	0.050	0.0012
i,k,l	0.039	0.016	0	0.0156	0.033	0.0005
i,k,m	0.055	0.000	0	0	0.033	0
i,l,m	0.039	0.016	0	0.0156	0.033	0.0005
i,l	0.039	0.016	0	0.0156	0.050	0.0008
j,k,l,m	0.026	0.029	0.029	0	0.050	0
j,k,m	0.043	0.012	0.012	0	0.033	0
j,l,m	0.023	0.031	0.031	0	0.033	0
						$\phi_i = 0.00275$

Notes: $MC = (U(S) - U(S)\backslash i)$, and $\omega = \frac{(|S|-1)!(|M|-|S|)!}{M!}$

Figure 4.9(a) illustrates the Shapley values for all links, where a total utility of $U(M) = 23.64 \times 10^{-3}$ is divided among the links. Link l has the highest Shapley value, indicating it is the most safety-critical link, and the network would be most affected if this link were disrupted. Conversely, link k is colored red due to its negative Shapley value ($\phi_k = -0.979 \times 10^{-3}$), which can be interpreted as the negative contribution of the link to overall network safety. This implies that the presence of this link adversely affects network safety, and its removal would improve it.

Table 4.5. Calculation of the Shapley value for all links

Coalition	$TNCF(S)$	$U(S)$	Shapley value for coalition S, $\phi_a(S)$				
			i	j	k	l	m
i,j,k,l,m	0.031	0.024	-0.0010	0	-0.0016	0.0047	0.0016
i,j,k,l	0.039	0.016	0.0008	0	0	0.0008	0
i,j,k,m	0.055	0	-0.0006	0	0	0	0
i,j,l,m	0.023	0.032	0	0.0008	0	0.0016	0.0008
i,j,l	0.039	0.016	0.0005	0	0	0.0005	0
i,k,l,m	0.031	0.024	0.0012	0	0.0004	0.0012	0.0004
i,k,l	0.039	0.016	0.0005	0	0	0.0005	0
i,k,m	0.055	0	0	0	0	0	0
i,l,m	0.039	0.016	0.0005	0	0	0.0005	0
i,l	0.039	0.016	0.0008	0	0	0.0008	0
j,k,l,m	0.026	0.029	0	0.0014	-0.0001	0.0008	0.0014
j,k,m	0.043	0.012	0	0.0004	0.0004	0	0.0004
j,l,m	0.023	0.031	0	0.0010	0	0.0010	0.0010
		ϕ_a	0.00275	0.00368	-0.00098	0.01252	0.00569

However, the decision to remove such a link depends on several factors. For instance, the link may serve as the only connection between two points in the network or may become useful during disruptions on surrounding links, as it could provide a rerouting option for travelers. Identifying such links at the planning stage, however, can help transportation planners proactively address potential safety challenges.

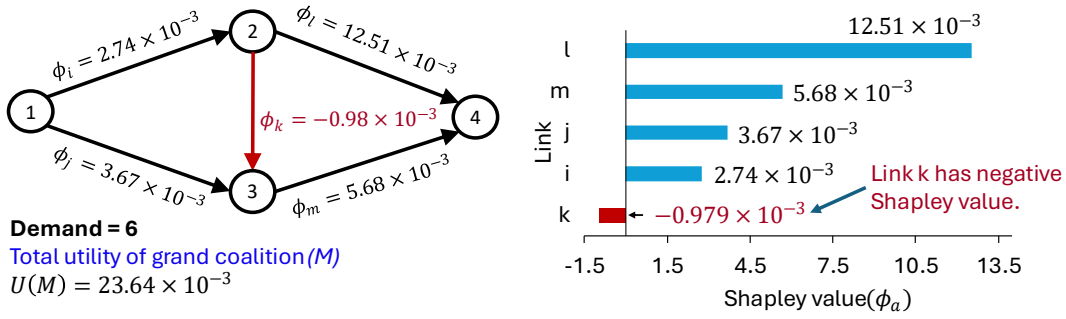

(a) Graphical illustration of link Shapley value **(b)** Links ranked by Shapley values

Figure 4.9. Shapley value of links in the cooperative game based on UE principle

For example, planners could implement strategies to control or limit traffic flow on these links under normal conditions to mitigate their adverse effects on network safety. This phenomenon is similar to the Braess paradox in traffic assignment; however, it

represents a cooperative version that arises by considering all link coalitions when evaluating overall network safety using the Shapley value. The links are ranked by their importance in Figure 4.9(b).

4.3.2.2 Link safety contribution: Single vs multiple O-D pairs

This section compares the safety contribution of links (represented by the Shapley value) for single versus multiple O-D pairs in the network (Figure 4.10). For the single O-D pair case, all demand ($d = 6vph$) is assumed to flow exclusively between O-D pair 1-4.

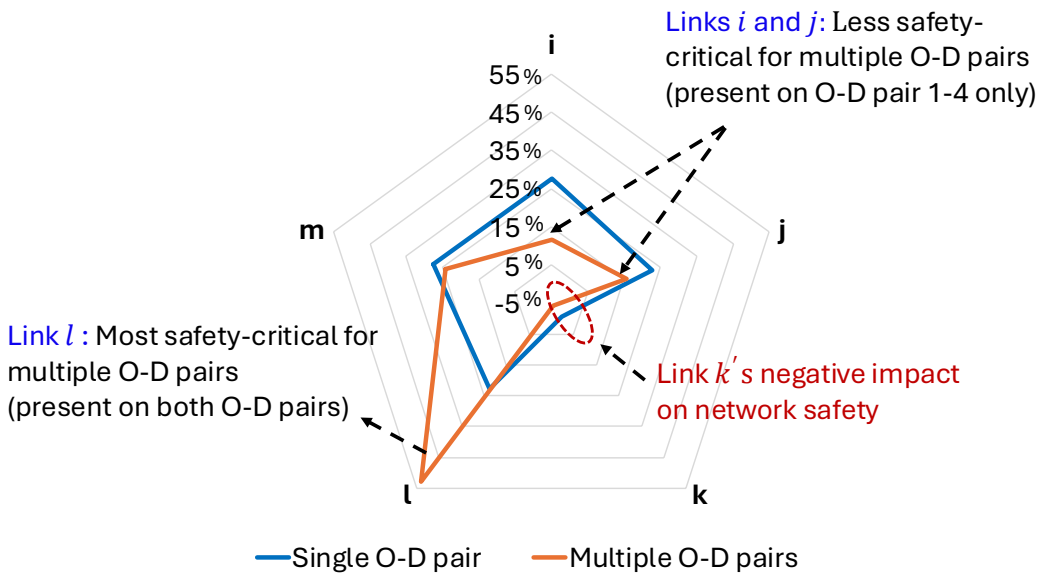

Figure 4.10. Comparison of link safety contribution between single vs multiple O-D pairs

The comparison in Figure 4.10 highlights the differences in link safety contributions between the two cases. Links i and j that have comparable safety contributions to links l and m in the single O-D pair case. In fact, links i and m are symmetric, as are links j and l, meaning they have the same Shapley values under this case. However, in the multiple O-D pairs case, significant differences emerge. This is because links i and j only serve users traveling between O-D pair 1-4, resulting in a lower safety contribution. The removal of such a link only affects users from a single O-D pair. In

contrast, links l and m serve users from both O-D pairs, leading to a higher contribution to network safety. In the event of the disruption of a shared link between two O-D pairs, the impact on network safety will be higher. Figure 4.10 further shows that link l is the most safety-critical with the highest Shapley value and the disruption on such a link can make network safety worse. Additionally, the negative impact of the presence of link k on network safety is higher in the multiple O-D pairs case compared to the single O-D pair case.

4.3.2.3 Effect of congestion level on the Shapley value

In this section, we compare the Shapley values for links at different congestion levels by increasing the demand (d), as illustrated in Figure 4.11(a-d). At a lower congestion level, the Shapley value for link k is negative ($\phi_k = -0.979 \times 10^{-3}$ at $d = 6$). However, as congestion levels increase, the Shapley value for link k becomes positive ($\phi_k = 1.15 \times 10^{-3}$ at $d = 8$, and $\phi_k = 4.16 \times 10^{-3}$ at $d = 10$). This occurs because, at lower congestion levels, most of the flow is allocated to routes 3 and 5 (containing link k), due to their lower free-flow travel times. However, these routes have a higher $TNCF$ compared to the other routes, resulting in a negative MC of link k to the grand coalition, as shown in Figure 4.12(a).

As routes 3 and 5 become congested, flow shifts to routes 1, 2, and 4, which have lower travel times. Consequently, the MC of link k to the grand coalition becomes less negative or even positive, leading to a positive Shapley value. The MCs of link k are illustrated in Figure 4.12(a). It is noteworthy that while the MC of link k is negative at $d = 8$, its Shapley value is positive. This is because the Shapley value represents the average MC across all coalitions, resulting in an overall positive value. Moreover, the MC of link k is positive at $d = 10$.

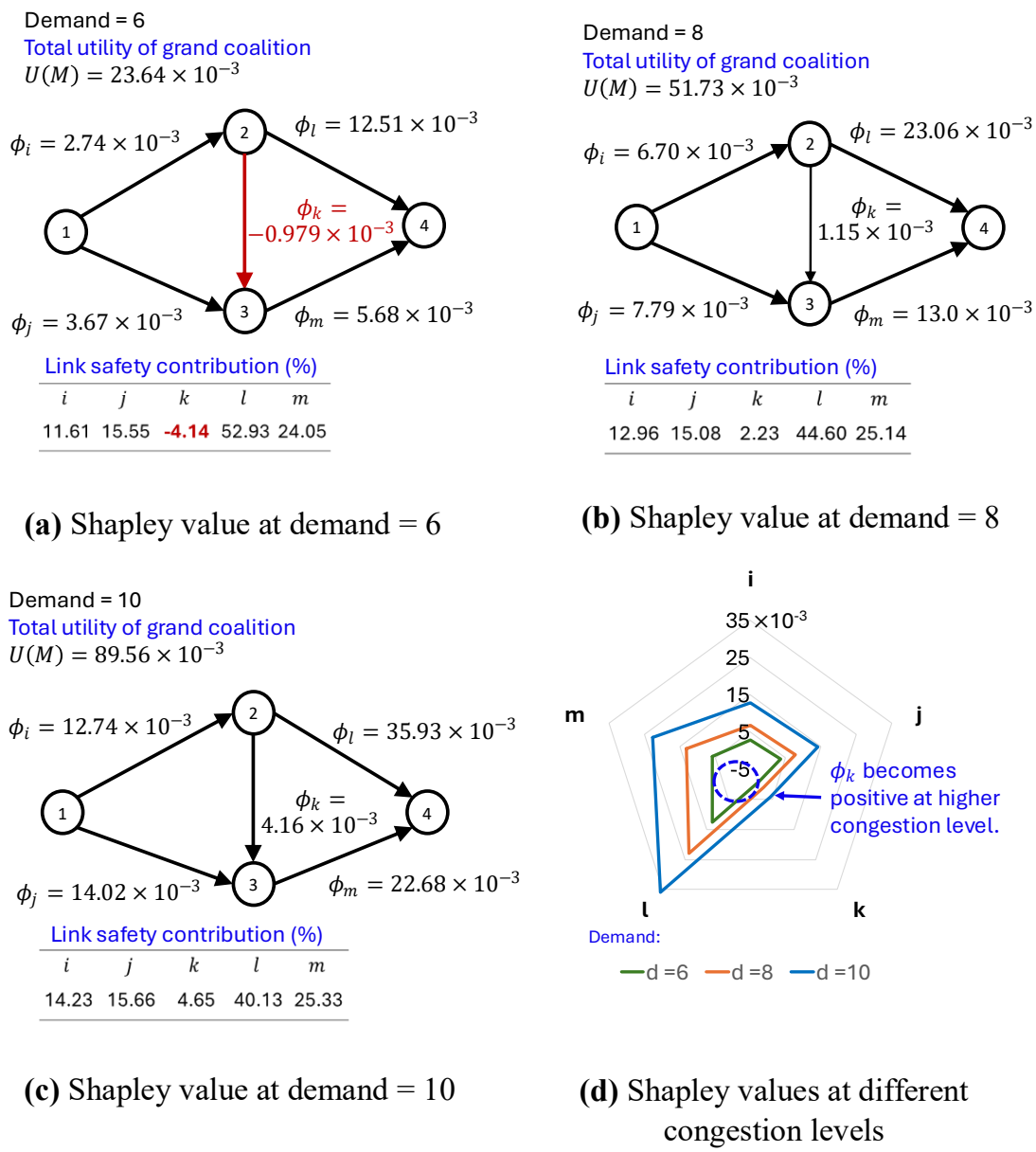

(a) Shapley value at demand = 6

(b) Shapley value at demand = 8

(c) Shapley value at demand = 10

(d) Shapley values at different congestion levels

Figure 4.11. Graphical representation of Shapley values at varying congestion levels

Furthermore, Figure 4.12(b) compares the percentage safety contribution of link k between the Shapley value and the MC to the grand coalition only. In Figure 4.12(b), red text indicates a negative contribution of link k to network safety. A significant difference is seen between the Shapley value and the marginal contribution. This highlights that the Shapley value provides a more comprehensive and complete assessment by considering all possible coalitions.

d	$U(M)$	$U(M)\backslash k$	$MC(k)$
6.0	23.6×10^{-3}	31.9×10^{-3}	-8.3×10^{-3}
8.0	51.7×10^{-3}	56.6×10^{-3}	-4.9×10^{-3}
10.0	89.6×10^{-3}	88.5×10^{-3}	1.1×10^{-3}

Notes: $MC(k) = (U(M) - U(M)\backslash k), M = \{I, j, k, l, m\}$

(a) MC of link k to grand coalition (M)

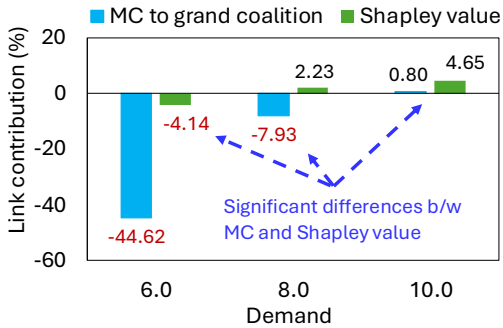

(b) MC vs Shapley value for link k

Figure 4.12. Comparison of MC and Shapley value of link k at different congestion levels

4.3.2.4 Marginal contribution vs the Shapley value at different congestion levels

This section demonstrates why the Shapley value is a more suitable metric to identify the safety-critical links compared to the MC calculated solely for the grand coalition. In Figure 4.13(a), the MC is determined for a single scenario, specifically the removal of a link from the grand coalition only. We notice that the MC for links i and k is negative at lower congestion levels (d = 6 and 8), indicating their negative impact on the network safety.

Conversely, Figure 4.13(b) shows that the Shapley value reveals a positive contribution of link i to network safety across all congestion levels. This is because the Shapley value represents the average MC by considering all possible scenarios, including all coalitions. According to Figure 4.13(b), only link k exhibits a negative impact on network safety. This demonstrates that relying solely on MC can misidentify important links as having a negative impact, whereas the Shapley value provides a more comprehensive assessment by accounting for link interactions across all scenarios.

While the order of link importance remains the same when using MC and the Shapley value, the distinction lies in how a link's contribution is interpreted, either positively or negatively. This has practical implications because interpreting a link's contribution to network safety positively, even if small, is fundamentally different from interpreting it

negatively. A negative contribution indicates that flow on the link adversely affects network safety, and overall network safety would be higher without any flow on this link. Therefore, the Shapley value offers a more holistic and accurate approach for identifying critical links, enabling more effective network safety management.

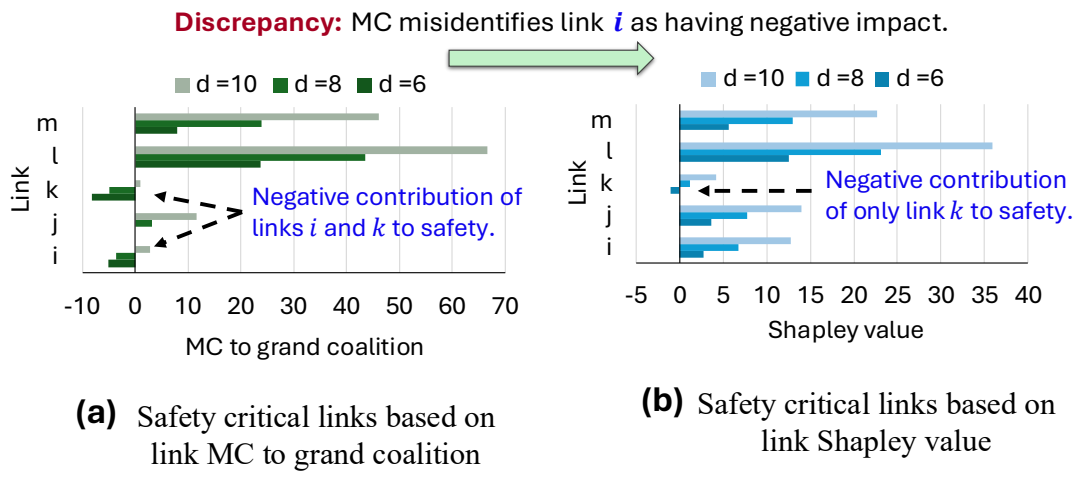

(a) Safety critical links based on link MC to grand coalition

(b) Safety critical links based on link Shapley value

Figure 4.13. Comparison of the safety-critical links between MC and Shapley value

4.3.3 Recommendations

This Chapter offers several recommendations for enhancing overall network safety. Priority should be given to links that contribute the most to network safety, specifically those with the highest Shapley values. For instance, greater investment should be directed toward improving the design and infrastructure of these critical links. In the event of a crash on such links, road authorities must act swiftly to clear the road, as disruptions can significantly compromise network safety. Additionally, links with negative safety contributions (negative Shapley values) should be improved in terms of design, or traffic on these links should be minimized, especially if they are essential, such as being the only connection between two points. Links that connect multiple origin-destination pairs should be prioritized, as disruptions to these can affect a larger number of people. Finally, traffic management policies should be applied to links that deteriorate network safety, such as reducing traffic by incentivizing alternative routes.

4.4 Conclusions

4.4.1 Summary

In this Chapter, we propose a framework to evaluate transportation network safety by determining safety-critical links, those that contribute most to network safety. A cooperative game theoretic approach was employed where links in a road network act as players forming coalitions among each other. The utility function of the cooperative game was quantified in the UE traffic assignment model using a flow-dependent safety evaluation metric. The solution of cooperative game is obtained using Shapley value, which calculates the average MC of links to all possible coalitions.

Numerical experiments illustrate the interpretations of the Shapley value, offering several insights: (1) Significant differences are observed between a link's percent contribution to network safety when using the Shapley value compared to its MC to the grand coalition alone; (2) a link's Shapley value can be negative, indicating its adverse contribution to network safety; (3) the congestion level in a network affects the Shapley value for some links, which may shift from negative to positive at higher congestion levels, thereby highlighting the link's benefits under increased demand; (4) The safety contribution of a link that receives traffic flow from multiple O-D pairs is higher compared to those receiving flow from a single O-D pair.

4.4.2 Practical implications

This theoretical framework has the following implications:

a) Transportation planners can use the framework to identify the most safety-critical links at the planning stage. This information can help prioritize resources for links that have the greatest potential to improve overall network safety.
b) Planners can proactively address safety issues before they occur by utilizing this Shapley value-based framework. This minimizes the likelihood of costly reactive

measures to improve safety in the future (e.g., retrofitting existing links after crashes occur).

c) The framework can be adopted to quantify the safety impact of future traffic scenarios, such as population growth, infrastructure development, and changes in origin-destination demand.

d) The framework can be integrated with real-world crash and traffic data to develop validated tools for transportation safety planning, allowing for reliable and evidence-based decision-making.

PART II. Modeling safety behaviors in transportation planning models

Part II advances transportation planning models by incorporating travelers' safety behaviors and preferences with a specific focus on car ownership choice, car type choice and traffic assignment.

CHAPTER 5 Modeling safety and security concerns of AVs in joint car ownership and car type choice

5.1 Motivation

Information concerning car ownership and car type choice holds significant importance in transportation planning and policymaking, drawing attention from government organizations, environmental agencies, public transportation operators, and car manufacturers. As the primary determinant of individual travel decisions , car ownership has long been a critical factor in travel demand models (Chu, 2016). Extensive research exists on the factors that influence car ownership and the choice of car, encompassing socio-demographics, income, and various other determinants (Haque et al., 2019; Hess et al., 2012; Manski & Sherman, 1980; Papu Carrone et al., 2021). Additionally, the importance of travelers' attitudes and preferences has been increasingly recognized as a key determinant of both car ownership and car type decisions (Belgiawan et al., 2014; Kim et al., 2020). Traditionally, these decisions have been modeled separately, often leading to incomplete insights into the interdependence that exists between car ownership and car type choices.

Recent empirical studies have highlighted the interdependent nature of car ownership and car type choices, advocating for these decisions to be modeled jointly (Belgiawan et al., 2017; Kim et al., 2020). This integrated approach provides a more comprehensive understanding of consumer behavior, as car type preferences can serve as valuable indicators of overall car ownership tendencies. The advent of autonomous vehicles (AVs) is expected to further complicate these decisions, as AVs introduce a range of benefits and risks that are likely to reshape car ownership and car type preferences in the future, impacting the overall transportation planning process (Jabbari et al., 2022).

AVs offer substantial advantages over human-driven vehicles (HVs), including significant reductions in crash risk (enhanced safety), reduced traffic congestion, increased accessibility for disabled and elderly individuals, and a notable decrease in environmental pollution (Fagnant & Kockelman, 2015). These benefits are expected to exert a profound influence on travel demand patterns, potentially leading to shifts in both car ownership and car type choices. Among these benefits of AVs, safety improvements stand out as particularly influential. AVs have the potential to significantly reduce human errors, which account for approximately 90% of road fatalities and injuries in HVs (Hussain et al., 2021; NHTSA, 2008). This capability to enhance safety is expected to be a key factor driving consumer adoption of AVs (Wadud, 2017). AVs operate without human input, avoiding issues such as fatigue, distraction, and inconsistent driving behaviors, and strictly adhering to traffic regulations. Consequently, the introduction of AVs is expected to curtail accidents stemming from human errors (Litman, 2017; Morando et al., 2018).

However, despite these long-term benefits, the widespread adoption of AVs faces significant barriers. One of the most prominent concerns among the public is the security of AVs, particularly regarding the protection of personal data, including location and other sensitive information (Anderson et al., 2014; Panagiotopoulos & Dimitrakopoulos, 2018). Apprehensions related to cybersecurity risks, such as vulnerability to hacking and data privacy concerns, contribute to a lack of trust in this technology. Since travelers' perceptions of risk, encompassing both safety and security, differ from those associated with conventional vehicles, it becomes imperative to account for these factors when modeling the joint car ownership and car type choices within a multimodal network where conventional and autonomous vehicles coexist.

This Chapter aims to present a behaviorally informed theoretical framework that models the joint decisions of car ownership and car type choice, utilizing discrete choice models within an equilibrium framework. By focusing on the evolving risk perceptions associated with AVs, this study seeks to provide valuable insights into how these perceptions may shape future patterns of car ownership and vehicle selection. Understanding these mechanisms is crucial for effective transportation planning and policy-making, as it enables policymakers to anticipate shifts in travel behavior and design strategies that prioritize safety, efficiency, and sustainability in the era of AVs.

5.1.1 Contributions

This Chapter makes a preliminary effort to model travelers' risk perceptions of different car types in joint car ownership and car type choice within multimodal transportation networks, using the random utility theory. Specifically, a dogit model is adopted to model the car ownership choice by considering captive travelers, and a nested logit (NL) model is adopted to model the car type choice by accounting for similarities among different car types based on their associated risk perceptions. The proposed model can endogenously determine car ownership and car type demand. The following contributions are made in this Chapter.

a) An equilibrium analysis framework is proposed to model the joint car ownership and car type choice decisions based on endogenous travel disutility, considering the specific characteristics of each car type.

b) Travelers' risk perceptions related to safety (crash risk) and security issues of AVs, as well as the range anxiety associated with EVs, are explicitly incorporated within the joint choice equilibrium model. This explicit focus provides insights into how these factors influence long-term decisions, including car ownership and car type preferences, which are often overlooked in existing models.

c) By incorporating travelers' risk perceptions and demand-dependent disutility into long-term decision-making, the model provides a foundation for evaluating and developing safety-conscious transportation policies. The findings can guide policymakers in designing strategies to promote safer vehicle adoption (e.g., autonomous and electric vehicles) while addressing travelers' safety concerns.

5.2 Methodology

5.2.1 Joint car ownership and car type choice equilibrium framework

This section introduces the conceptual framework employed in this study in Figure 5.1.

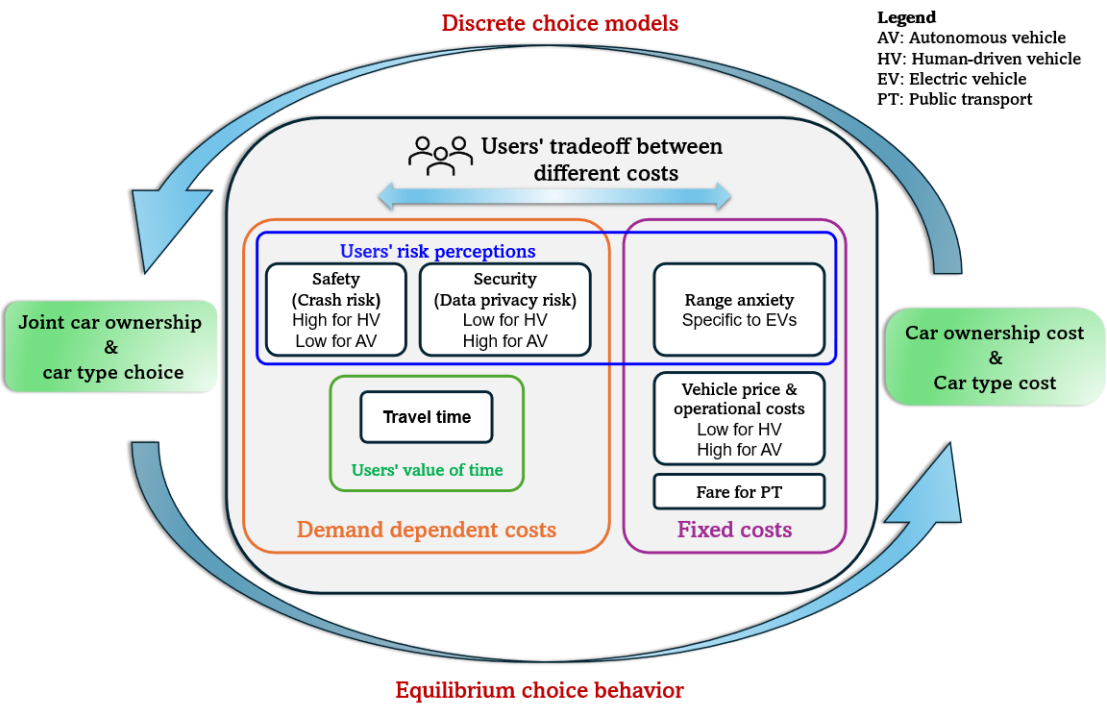

Figure 5.1. Framework for modeling joint car ownership and car type equilibrium choices

Discrete choice models are utilised to analyze joint car ownership and car type choices within an equilibrium context. Individuals weigh various cost factors such as safety, travel time, and vehicle price when deciding on car ownership and type. Notably, users' risk perceptions, particularly safety and security in the context of AVs, are explicitly modeled given their significance. The equilibrium model projects the demand for

diverse car types by factoring in a range of demand-dependent and fixed costs, as shown in Figure 5.1.

5.2.2 Assumptions.

Assumption 1: This study examines four types of private vehicles: gasoline human vehicles (GHV), electric human vehicles (EHV), gasoline autonomous vehicles (GAV), and electric autonomous vehicles (EAV), in addition to public transportation (PT). It is assumed that individuals who choose to own a car will select from these options, while those who do not own a car will use public transportation.

Assumption 2: To fully leverage the technological benefits of AVs in improving traffic safety and efficiency, the generalized travel cost for AVs is considered a function of the total demand for AVs only (i.e.,$q_{av}^{ij} = q_{gav}^{ij} + q_{eav}^{ij}$). Similarly, the generalized travel cost for HVs depends on the aggregate demand for HVs (i.e., $q_{hv}^{ij} = q_{ghv}^{ij} + q_{ehv}^{ij}$) (Lamotte et al., 2017; Wang et al., 2020b).

Assumption 3: The generalized travel costs of private cars (both AVs and HVs) are continuous and monotonically increasing functions of car type demand. Drivers of private vehicles have demand-dependent travel times and crash risk costs (Kingsbury, 2016; Ma & Zhang, 2019). The security risks associated with AVs are influenced by their penetration rate (Giannaros et al., 2023), while trip's distance-based costs and operational costs for different car types are considered fixed (Noruzoliaee et al., 2018; Xie & Liu, 2022). The disutility from crowding for PT passengers is a function of in-vehicle travel time and number of passengers, with in-vehicle travel time, walking time, and waiting time held constant (Gu & Chen, 2023).

5.2.3 Notations

The notations used in this Chapter are tabulated below.

Table 5.1. Notations

Sets	
IJ	Set of OD pairs.
U^{ij}	Set of car ownership indexes between OD pair *ij*.
E_u^{ij}	Set of types of cars (upper level) for car ownership *U* between OD pair *ij*.
M_{ue}^{ij}	Set of types of cars (lower level) for car ownership *U* between OD pair *ij*.
Functions	
$g_{uem}^{ij}(q_m^{ij})$	Generalized travel cost of car type *m* in nest *e* and car ownership nest *u* between OD *ij*.
$r_m^{ij}(q_m^{ij})$	Perceived crash risk of car type *m* between OD *ij*.
$S_m^{ij}(q_m^{ij})$	Perceived security risk of car type *m* between OD *ij*.
$g(q_{PT}^{ij})$	In-vehicle crowding discomfort for public transport between OD *ij*.
Decision variables	
q_u^{ij}	Demand for car ownership between OD *ij* (persons)
q_{uem}^{ij}	Demand of car type *m* in nest *e* and car ownership nest *u* between OD *ij*.
Inputs and Parameters for OD pair	
β_u^{ij}	Dispersion parameter for car ownership *u* between OD *ij*.
β_e^{ij}	Dispersion parameter for car type nest *e* between OD *ij*.
β_{em}^{ij}	Dispersion parameter for car type *m* under nest *e* between OD *ij*.
γ_m^{ij}	Crash risk perception parameter for car type *m* between OD *ij*.
α_m^{ij}	Security risk perception parameter for car type *m* between OD *ij*.
ψ_{uem}^{ij}	Constant attractiveness of car type m between OD *ij* between OD *ij*.
q^{ij}	Number of travelers between OD pair *ij*
$t_{wk,PT}^{ij}$	Walking time for public transport between OD *ij*.
$t_{wt,PT}^{ij}$	Waiting time for public transport between OD *ij*.
f_{PT}^{ij}	Fare for public transport between OD *ij*.
Global parameters	
VoT	Value of time
VoS	Value of safety
θ_{sr}	Cost converting factor for security risk
θ_{RA}	Cost converting factor for range anxiety

5.2.4 Modeling travelers' risk perceptions

This section models travelers' risk perceptions, including crash risk, cybersecurity, and range anxiety, to assess their effects on joint car ownership and type choices. Crash risk (for HVs and AVs) depends on traffic flow; cybersecurity concerns (for AVs) are linked

to AV penetration rates; and range anxiety (for EVs) is based on the relationship between daily VKT and EV battery range.

5.2.4.1 Safety Modeling

Safety is modeled based on the perceived crash risk associated with a specific mode of travel. Crash risk is commonly used to evaluate the safety level of links by incorporating exposure measures. A driver's risk of crash involvement is influenced by the safety level of the facility, which is typically estimated using crash counts or, in some cases, traffic conflict counts alongside exposure measures such as traffic flow or vehicle kilometers traveled. The fundamental relationship between crash risk, safety level, and exposure is expressed in Equation (5.1) (Chatterjee & and McDonald, 1999; Lord, 2002):

$$\text{Crash risk} = \frac{\text{Safety level}}{\text{Exposure}} \tag{5.1}$$

Equation (5.2) can be formulated to estimate a user's risk of being involved in a traffic crash, given a specific level of exposure. This represents the probability that a driver would experience a crash on a road segment characterized by a particular safety performance function (SPF) and exposure level. The SPF is a tool to estimate the expected number of crashes on a road segment per unit of time based on key factors such as traffic flow, segment length, and other relevant variables (Kweon & Lim, 2014).

$$\text{Crash risk} = \frac{\text{SPF}}{\text{Flow}} \tag{5.2}$$

Thus, the crash risk in Equation (5.2) can be estimated by dividing the expected number of crashes per unit of time by the traffic flow (exposure).

The relationship between flow and crash risk is inherently complex. Increased traffic flow can have varying impacts on different crash types and their severity. For example, researchers found traffic flow to be positively associated with multiple-vehicle crashes

while negatively associated with single-vehicle crashes (Elvik et al., 2009; Høye & Hesjevoll, 2020). Wang et al. (2013) have identified a positive relationship between traffic flow and crash severity, which could be attributed to the higher speed variance among vehicles in dense traffic conditions. Similarly, Christoforou et al. (2011) found that rear-end crashes are more frequent in high-traffic flow scenarios due to the increased interaction and conflict between vehicles. For the sake of modeling convenience and to ensure the convexity of the mathematical program (introduced in Section 3), we assume a monotonically increasing relationship between traffic flow and traveler's crash risk perception similar to previous studies (Kingsbury, 2016; Ma & Zhang, 2019). While assuming crash risk increases monotonically with flow ensures convexity and unique equilibria, real-world relationships could be more complex or non-monotone, especially under congested conditions, where drivers adapt by slowing down. These limitations highlight the trade-off between analytical solvability and realism: while simplifying to monotonicity enables efficient computation for planning applications, it could incur some behavioral limitations. Using the SPFs developed by Kweon and Lim (2014) for various road types, which are based on a negative binomial function, the SPF can be expressed in Equation (5.3):

$$F_a^{ij} = e^{\xi}(q_a^{ij})^{\delta} L_a^{ij}, \tag{5.3}$$

where, F_a^{ij} represents the total number of crashes on link a between OD pair ij, ξ is the intercept, δ is the slope coefficient, q_a^{ij} is the traffic demand (flow) on link a, and L_a^{ij} is the distance between an OD-pair ij. The crash risk r_a^{ij} can be determined by inputting Equation (5.3) into Equation (5.2) (Kingsbury, 2016; Ma & Zhang, 2019).

$$r_a^{ij} = e^{\xi}(q_a^{ij})^{\delta-1} L_a^{ij} \tag{5.4}$$

However, research suggests that the crash risk of AVs and users' safety perception of AVs may differ from that of HVs. An improvement in users' safety perception of AVs is likely to increase their market share (Bansal & Kockelman, 2017; Jabbari et al., 2022). To capture the effect of users' safety perception across car types, we adjust the crash risk in Equation 4 by introducing a crash risk perception parameter, γ_m, specific to each car type m, as shown in Equation (5.5). The parameter, γ_{av}, can be interpreted as the perceived crash risk level of AVs relative to HVs by setting $\gamma_{HV} = 1$. For example, if $\gamma_{AV} = 0.1$, AVs are perceived 90% safer than HVs, defined as AV safety effectiveness by Sohrabi et al. (2021).

$$r_{a,m}^{ij} = \gamma_m^{ij}\left(e^{\xi}\left(q_a^{ij}\right)^{\delta-1} L_a^{ij}\right) \tag{5.5}$$

Figure 5.2 depicts the relationship between perceived crash risk and traffic flow according to Equation (5.5).

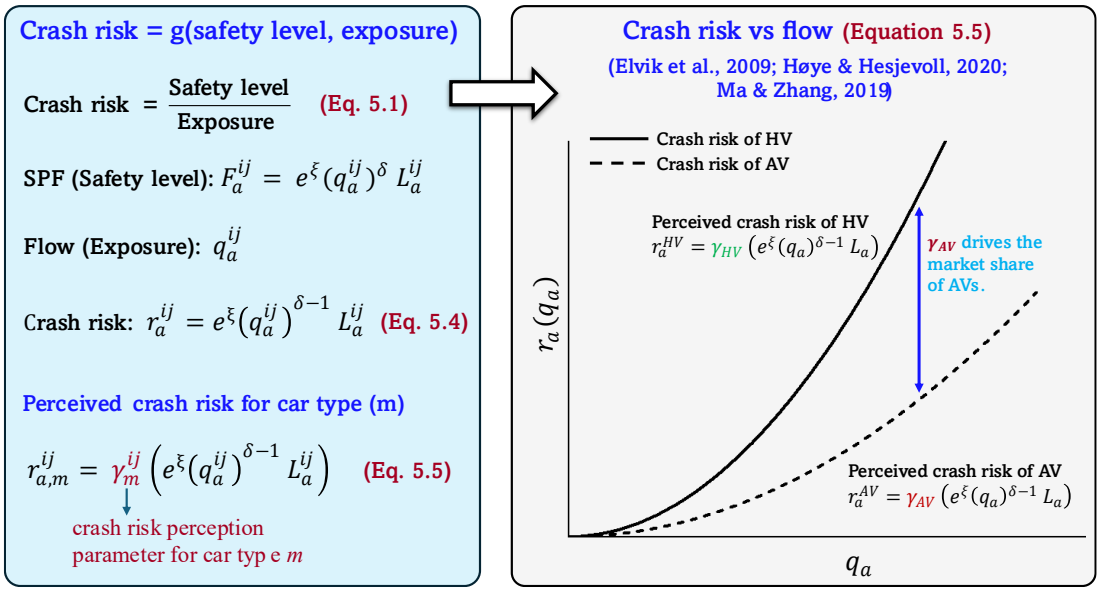

Figure 5.2. Perceived crash risk of AVs and HVs as a function of safety level and exposure

In this model, travelers' subjective safety perception is formed as a cognitive response to the objective safety risk of the roadway. The objective risk r_a serves as the universal stimulus, derived from the empirically calibrated crash risk function. Travelers then

process this stimulus through a perceptual lens, modeled by the parameter γ_m, which is specific to their vehicle type m. This yields their perceived crash risk ($r_{a,m}^{ij}$), which is the direct input to their decision-making process. This approach ensures that perception is theoretically grounded in objective reality while allowing for subjective variations across car types.

5.2.4.2 Security Modeling

Unlike HVs, which are primarily exposed to physical security risks only (such as physical crime), AVs have raised additional concerns among many people due to potential privacy and cybersecurity issues. These concerns encompass a broad spectrum, including susceptibility to hacking, protection of user data, and potential system failures (Bansal & Kockelman, 2017; Kockelman et al., 2016). AVs interact with each other, roadside units, and mobile devices via wireless communication channels to enable various Vehicle-to-Everything (V2X) applications, including vehicle-to-vehicle (V2V) and vehicle-to-infrastructure (V2I) communications. However, the integration of these diverse wireless technologies also makes AVs vulnerable to cyber-attacks (Parkinson et al., 2017; Petit & Shladover, 2015).

As the penetration rate of AVs increases, so does the number of potential targets for cyber-attacks, thereby heightening security risks that could disrupt large portions of the transportation network (Dong et al., 2020). Therefore, in this study, the security risk associated with AVs is assumed to depend on the AV penetration rate (Dong et al., 2020; Giannaros et al., 2023). Such an assumption has been employed in other equilibrium modeling contexts involving autonomous vehicles (AVs). For example, Xie and Liu (2022) used it to represent the relationship between market penetration and AV information quality, assuming that information quality improves as the penetration rate increases, thereby reducing users' perception errors in route choice decisions.

Moreover, their perceptions of security risks influence user acceptance and adoption of AVs (Bansal & Kockelman, 2017; Kenesei et al., 2022). To model users' security risk perceptions, we introduce a parameter, α_m, that adjusts the security risk of each vehicle type based on the traveler's perception parameter, as outlined in Equation (5.6):

$$S_m^{ij}(q_m) = \alpha_m^{ij}.sr_m^{ij} \quad \forall ij \in IJ, m \in M \tag{5.6}$$

where S_m^{ij} represents the perceived security risk for vehicle type m between OD-pair ij, sr_m denotes the inherent security risk associated with vehicle type m. The parameter, α_m^{ij}, represents the user's risk perception parameter for each car type m.

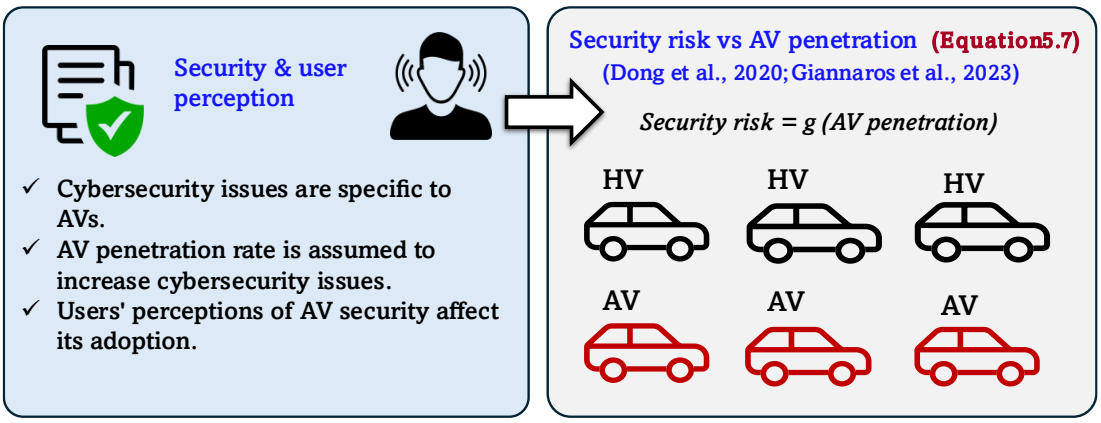

Figure 5.3. Illustration of relationship between AV security risk penetration rate

In the case of AVs, the security risk, sr_{av}^{ij}, which depends on the AV penetration rate (Dong et al., 2020; Giannaros et al., 2023) is given in Equation (5.7). A similar function was used by Xie and Liu (2022) to model the AV information quality.

$$sr_{av}^{ij}(q_{av}) = g\left(\frac{q_{av}^{ij}}{q_{ij}}\right) \quad \forall ij \in IJ \tag{5.7}$$

where $g\left(\frac{q_{av}^{ij}}{q_{ij}}\right)$ reflects the increasing security risk associated with a higher penetration rate of AVs. The security risk for HVs is assumed to be constant. Given the additional cybersecurity challenges associated with AVs, it is reasonable to assume that both the

security risks and user perceptions of these risks are higher for AVs compared to HVs (Choi & Ji, 2015; Nazari et al., 2018). Figure 5.3 illustrates the relationship between AV penetration rate and its security risk.

5.2.4.3 Range anxiety for electric vehicles

Range anxiety (RA) denotes the fear or stress experienced by individuals when they are concerned about the possibility of becoming stranded due to the limited battery capacity of an electric vehicle (EV). This anxiety is particularly relevant in a TA problem with distance constraints, where it arises from a lack of adequate charging infrastructure and unexpectedly limited battery range (Xie et al., 2019). Currently, EV charging stations' availability significantly lags behind gasoline stations, leading travelers to prefer charging their vehicles primarily at home or the workplace (Alberini & Santoboni, 2025; Jiang & Xie, 2014; Jiang et al., 2014). Travelers typically expect that a fully charged battery should provide sufficient range for typical trips. However, certain situations, such as the need for multiple trips on a single charge or starting with a partially charged battery, can trigger RA.

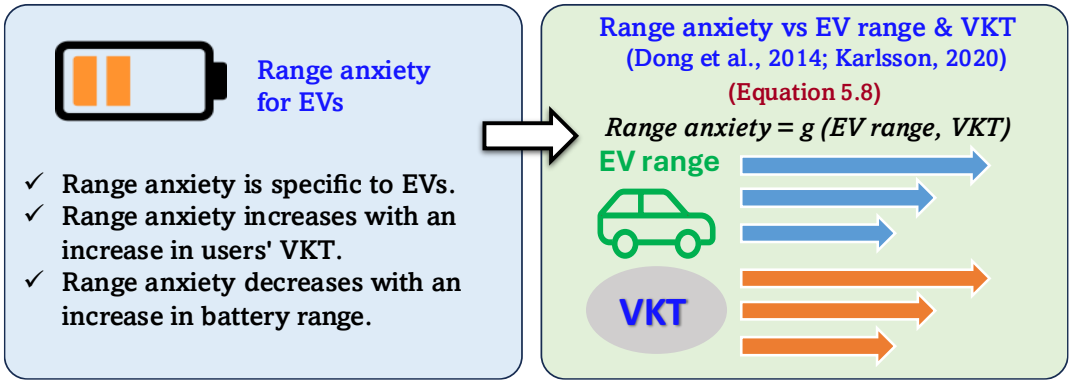

Figure 5.4. Illustration of factors affecting range anxiety

The RA for EVs can be linked to drivers' average daily vehicle kilometers traveled (VKT) and the range limit of an EV (Dong et al., 2014). In this Chapter, RA for EVs is modeled as a function of the ratio between drivers' average daily vehicle kilometers

traveled (VKT) and the EV's range. This formulation operationalizes the empirical finding that potential owners' assessment of an EV's range sufficiency for their regular travel patterns is a key purchase determinant (Dong et al., 2014; Karlsson, 2020; She et al., 2017). Figure 5.4 illustrates the relationship between range anxiety, battery range and driver's VKT.

The ratio reflects the potential for range anxiety, with higher values indicating greater concern. Similar to Karlsson (2020), we assume home charging only, thus the home-to-home vehicle kilometers traveled (VKT_{hth}^{ij}) is considered. The range anxiety is expressed in Equation (5.8).

$$RA_{ev}^{ij} = \left(\frac{VKT_{hth}^{ij}}{R_{ev}}\right)^{\omega} \qquad \forall ij \in IJ \tag{5.8}$$

where, RA_{ev}^{ij} is the range anxiety, R_{ev} is the maximum range of EV, VKT_{hth}^{ij} is the average daily home-to-home VKT between OD pair ij, and ω is a parameter to control the curvature of the function. According to Equation (5.8), range anxiety decreases as the EV range increases. Moreover, technological advancements, particularly improvements in battery technology, are expected to reduce the sensitivity of travelers to range anxiety (Zhou et al., 2023).

5.2.5 Travel cost functions

5.2.5.1 Human-driven vehicle

The generalized cost of human vehicle trips for car type m, $g_{m,hv}^{ij}$, between an OD pair ij is defined in Equation (5.9).

$$\begin{aligned} g_{m,hv}^{ij} = FC_{m,hv}^{ij} + OC_{m,hv}^{ij} + \left(t_{m,hv}^{ij}(q_{hv}^{ij})\right).VoT_{hv} + \left(r_{m,hv}^{ij}(q_{hv}^{ij})\right).VoS \\ + \left(S_{m,hv}^{ij}\right).\theta_{sr} + \left(RA_{m,hv}^{ij}\right).\theta_{RA} \quad \forall ij \in IJ, m \in M_{hv} \end{aligned} \tag{5.9}$$

where $FC_{m,hv}^{ij}$, is the fixed cost of a trip between an OD-pair ij, converted from the purchase price of car type m, P_m. The second term, $OC_{m,hv}^{ij}$, is the operational cost of a trip between OD-pair ij. $t_{m,hv}^{ij}$, and $r_{m,hv}^{ij}$ denote the demand-dependent in-vehicle travel time, and the crash risk of car type m between an OD-pair ij. q_{hv}^{ij} denotes the composite demand of HVs. $S_{m,hv}^{ij}$ is the fixed security risk of car type m between an OD-pair ij. $RA_{m,hv}^{ij}$ denotes the range anxiety for EHVs.

$$FC_m^{ij} = \frac{b_1}{b_2 b_3} P_m L^{ij} \qquad \forall, m \in M, ij \in IJ \tag{5.10}$$

$$OC_m^{ij} = \left(h_{fuel}^m + h_{ins}^m + h_{oth}^m\right) L^{ij} \quad \forall, m \in M, ij \in IJ \tag{5.11}$$

FC_m^{ij} and OC_m^{ij} are calculated using Equations (5.10)-(5.11), respectively following Noruzoliaee et al. (2018) and Xie and Liu (2022). In Equation (5.10), L^{ij} is the distance between an OD-pair ij, P_m is the purchase price of vehicle type m. b_1 is the scaling factor on vehicle price to capture other overhead costs, b_2 is the average vehicle lifetime in years, and b_3 is the average annual mileage (in km). OC_m^{ij}, which is calculated using Equation (5.11), consists of the fuel cost (h_{fuel}^m), insurance cost (h_{ins}^m) and other costs, h_{oth}^m (maintenance, parking, etc.).

5.2.5.2 Autonomous vehicle

The generalized cost of autonomous vehicle trips for car type m, $g_{m,av}^{ij}$, between an OD-pair ij includes the fixed cost, the operational cost, in-vehicle travel time, the crash risk cost, the security risk cost, and the range anxiety cost expressed in Equation (5.12).

$$\begin{aligned} g_{m,av}^{ij} = FC_{m,av}^{ij} + OC_{m,av}^{ij} + \left(t_{m,av}^{ij}(q_{av}^{ij})\right).VoT_{av} + \left(r_{m,av}^{ij}(q_{av}^{ij})\right).VoS \\ + \left(sr_{m,av}^{ij}(q_{av}^{ij})\right).\theta_{sr} + \left(RA_{m,av}^{ij}\right).\theta_{RA} \quad \forall ij \in IJ, m \in M_{av} \end{aligned} \tag{5.12}$$

where $FC_{m,av}^{ij}$ is the fixed cost calculated using Equation (5.10) and $OC_{m,av}^{ij}$ is the operational cost, which is calculated using Equation (5.11). $t_{m,av}^{ij}, r_{m,av}^{ij}, s_{gav}^{ij}$ denote the demand dependent in-vehicle travel time, crash risk, and security risk between OD-pair ij. q_{av}^{ij} denotes the composite demand of autonomous vehicles. $RA_{m,av}^{ij}$ denotes the range anxiety for EAVs.

5.2.5.3 Public transport

The cost of PT includes the crowding discomfort dependent on the PT demand, fixed travel time, walking, waiting time, and the fare (Gu & Chen, 2023). Crash risk is less of a concern for public transport (Truong & Currie, 2019). The generalized travel cost of the PT between an OD pair ij is given in Equation (5.13).

$$g_{PT}^{ij} = \left(t_{wk,PT}^{ij} + t_{wt,PT}^{ij}\right).VoT + \left(g\left(q_{PT}^{ij}\right).t_{iv,PT}^{ij}\right) + f_{PT}^{ij} \tag{5.13}$$

where $g\left(q_{PT}^{ij}\right).t_{iv,PT}^{ij}$ is the in-vehicle crowding discomfort, $t_{wk,PT}^{ij}$ and $t_{wt,PT}^{ij}$ are the waiting and walking times and f_{PT}^{ij} represents the fare for PT.

5.2.6 Structure of joint car ownership and car type model

This section presents the structure of a joint car ownership and car type choice model, illustrated in Figure 5.5, that accounts for the characteristics of each car type, especially the travelers' safety and security perceptions discussed in Section 5.2.4.

To account for the travelers who cannot afford a car i.e., those who are captive to public transport, the proposed structure represents the OD demand by two groups of travelers: (1) captive travelers, and (2) choice travelers who can choose from the complete choice set consisting of private cars (GHV, EHV, GAV, EAV) and public transport (PT). The dogit model is used to model the choice behavior of captive and choice travelers at the

car ownership choice level (upper level) while a nested logit model is adopted to model the choice behavior of travelers at the car type choice level (lower level).

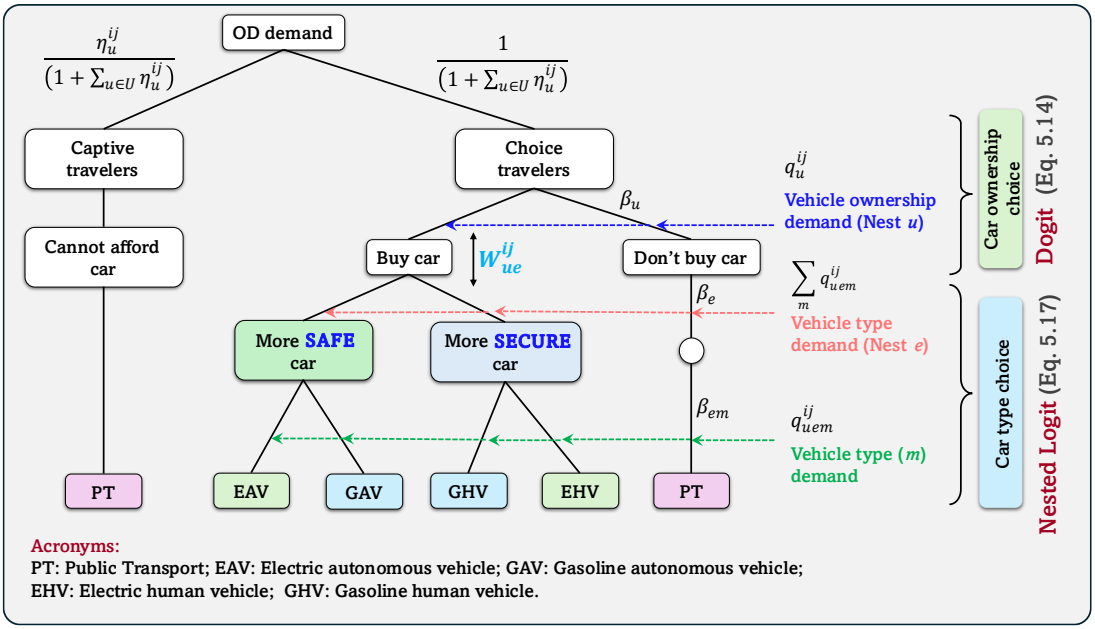

Figure 5.5. Structure of joint car ownership and car type choice model

As discussed, AVs may be safer regarding crash risk; however, additional security concerns are associated with AVs. Thus, the two types of AVs (EAV and GAV) are combined under a single nest i.e., a "***more safe car***" nest while the two types of HVs (GHV and EHV) are combined under a "***more secure car***" nest. Dividing alternatives into nests based on "safety" (AVs) versus "security" (HVs) was not arbitrary but was motivated by a body of empirical evidence suggesting these are primary, distinct factors influencing AV adoption. studies consistently show that perceived safety benefits (e.g., crash avoidance) are a major driver for AV adoption (Bansal & Kockelman, 2017; Hulse et al., 2018; Jabbari et al., 2022), while cybersecurity and privacy concerns are significant barriers (Jardim et al., 2013; Nazari et al., 2018). This structure directly captures this fundamental behavioral trade-off. Moreover, this nested structure has the ability to better capture the similarity among different car types under the same nest.

Moreover, the proportion of captive travelers, $\frac{\eta_u^{ij}}{\left(1+\sum_{u\in U}\eta_u^{ij}\right)}$, and that of choice travelers, $\frac{1}{\left(1+\sum_{u\in U}\eta_u^{ij}\right)}$, are derived based on the dogit model.

5.2.6.1 Dogit and nested logit models used in joint choice structure

The dogit and nested logit models used in the proposed joint choice structure in Figure 5.5 are explained in this section. The traveler's choice at car ownership and car type choice level are modeled using the dogit (Gaundry & Dagenais, 1979) and nested logit (NL) models (Ben-Akiva & Lerman, 1985), respectively. Figure 5.6 illustrates the two models based on the joint model's structure.

The dogit model proposed by Gaundry and Dagenais (1979) dodges the IIA property of the logit model by incorporating the behavior of captive travelers i.e., those who cannot afford to buy a car (Wang et al., 2024), as shown in Equation (5.14). The first term in Equation (5.14) denotes the share of travelers captive to one mode (in this case PT). The second term represents the share of travelers who can choose any mode m (car or PT), which is the product of the proportion of all choice travelers and the logit probability of choosing mode m.

$$P_u^{ij} = \underbrace{\frac{\eta_u^{ij}}{\left(1+\sum_{u\in U}\eta_u^{ij}\right)}}_{\text{captive share}} + \underbrace{\frac{1}{\left(1+\sum_{u\in U}\eta_u^{ij}\right)}}_{\text{choice share}} \cdot \underbrace{\frac{e^{\beta_u W_{ue}^{ij}}}{\sum_{u\in U_{ij}} e^{\beta_u W_{ue}^{ij}}}}_{\text{logit probability}} \tag{5.14}$$

In Equation (5.14), P_u^{ij} is the dogit probability, η_u^{ij} is the captivity parameter at the car ownership level to incorporate the share of captive travelers. β_u is the dispersion parameter for car ownership choice u, and W_{ue}^{ij} is the expected perceived cost of the nested logit model.

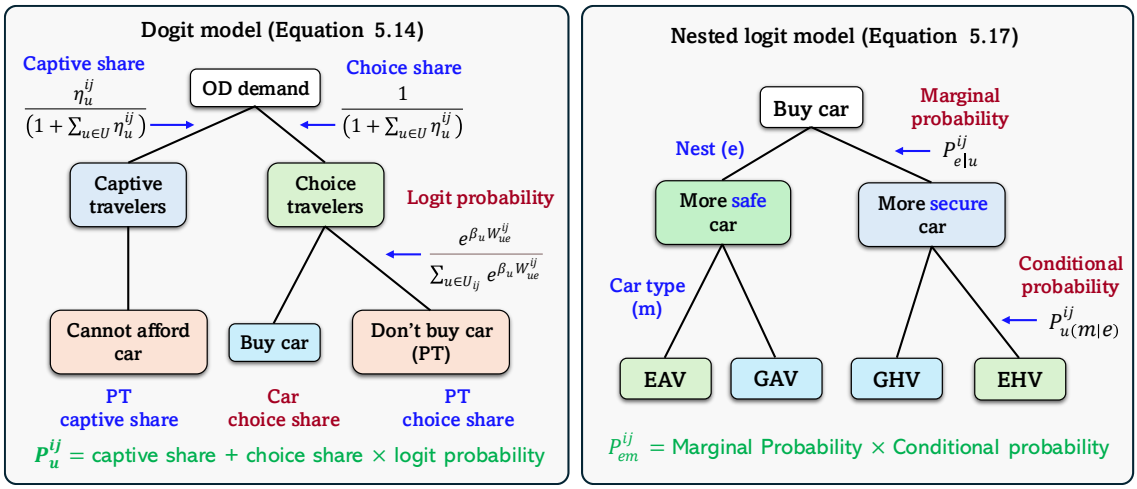

Figure 5.6. Dogit and nested logit models based on the joint model's structure

The NL model in Equation (5.17) relaxes the independence assumption embedded in the logit model to capture the mode/car type similarity (Ben-Akiva & Lerman, 1985). Instead of having a single-level tree structure, the NL model captures the car type similarity using a two-level tree structure. The car type similarity can be modeled by placing similar cars under the same nest, such as the cars with the same safety levels may be correlated.

$$P_{e|u}^{ij} = \frac{\sum_{m\in M_{ijue}} e^{-\beta_e c_{uem}^{ij}}}{\sum_{e\in E_{iju}} \sum_{m\in M_{ijue}} e^{-\beta_e c_{uem}^{ij}}} \tag{5.15}$$

$$P_{u(m|e)}^{ij} = \frac{e^{-\beta_{em} c_{uem}^{ij}}}{\sum_{m\in M_{ijue}} e^{-\beta_{em} c_{uem}^{ij}}} \tag{5.16}$$

$$P_{em}^{ij} = P_{u(m|e)}^{ij} . P_{e|u}^{ij} = \frac{e^{-\beta_{em} c_{uem}^{ij}}}{\sum_{m\in M_{ijue}} e^{-\beta_{em} c_{uem}^{ij}}} . \frac{\sum_{m\in M_{ijue}} e^{-\beta_e c_{uem}^{ij}}}{\sum_{e\in E_{iju}} \sum_{m\in M_{ijue}} e^{-\beta_e c_{uem}^{ij}}} \tag{5.17}$$

Equations (5.15) & (5.16) are the marginal and conditional probabilities for the two-level structure of the NL model. $P_{u(m|e)}^{ij}$ represents the conditional probability for car type m and $P_{e|u}^{ij}$ represents the marginal probability of car type nest e. P_{em}^{ij} represents the NL choice probability which is the product of the conditional and marginal choice

probabilities. β_e represents the dispersion parameter for the car type nest e and β_{em} represents the dispersion parameters for car type m in nest e. c_{uem}^{ij} is the generalized cost for car type m in nest e.

5.3 Model formulation.

This section presents the equivalent mathematical programming (MP) formulation of joint car ownership and car type choice equilibrium model for the proposed structure in Figure 5.5. The dogit probability expression (Equation (5.14)), which accounts for captive travelers, and the nested logit probability expression (Equation (5.17)), which captures car type similarities, are adopted to get the equivalent MP formulation of joint choice equilibrium model. The model formulation is given in Figure 5.7.

Objective function:

$$min\, Z(q_u^{ij}, q_{uem}^{ij}) = \sum_{ij\in IJ}\sum_{u\in U_{ij}}\sum_{e\in E_{iju}}\sum_{m\in M_{ijue}}\int_0^{q_{uem}^{ij}} g_{uem}^{ij}(w)dw$$

(Z_1) Beckmann's transformation (Congestion effect).

$$+\sum_{ij\in IJ}\sum_{u\in U_{ij}}\sum_{e\in E_{iju}}\sum_{m\in M_{ijue}}\frac{1}{\beta_{em}}q_{uem}^{ij}(lnq_{uem}^{ij}-1)$$

(Z_2) Entropy term for conditional probability of NL model for car type choice.

$$+\sum_{ij\in IJ}\sum_{u\in U_{ij}}\sum_{e\in E_{iju}}\left(\frac{1}{\beta_e}-\frac{1}{\beta_{em}}\right)\left(\sum_{m\in M_{ijue}}q_{uem}^{ij}\right)\left(ln\sum_{m\in M_{ijue}}q_{uem}^{ij}-1\right)$$

(Z_3) Entropy term for marginal probability of NL model for car type choice.

$$+\sum_{ij\in IJ}\sum_{u\in U_{ij}}\sum_{e\in E_{iju}}\sum_{m\in M_{ijue}}\psi_{uem}^{ij}q_{uem}^{ij}$$

(Z_4) Exogenous attractiveness.

$$+\sum_{ij\in IJ}\left(\frac{1}{\beta_u}-\frac{1}{\beta_e}\right)q_{u_1}^{ij}(lnq_{u_1}^{ij}-1)$$

(Z_5) Entropy term of dogit car ownership choice.

$$+\sum_{ij\in IJ}\left(\frac{1}{\beta_u}-\frac{1}{\beta_e}\right)\left(q_{u_2}^{ij}-\frac{q^{ij}\eta_{u_2}^{ij}}{1+\eta_{u_2}^{ij}}\right)\left(ln\left(q_{u_2}^{ij}-\frac{q^{ij}\eta_{u_2}^{ij}}{1+\eta_{u_2}^{ij}}\right)-1\right)$$

(Z_6) Entropy term of dogit PT choice for captive & non-captive travelers.

Subject to: (Constraints)

$$\sum_{e\in E_{iju}}\sum_{m\in M_{ijue}}q_{uem}^{ij}=q_u^{ij}\quad \forall\, u\in U_{ij}, ij\in IJ$$

(Constraint 1) Conservation constraint at car type choice level.

$$\sum_{u\in U_{ij}}q_u^{ij}=q^{ij}\quad \forall\, ij\in IJ$$

(Constraint 2) Conservation constraint at car ownership choice level.

$$q_u^{ij}\geq 0, q_{uem}^{ij}\geq 0\quad \forall m\in M_{ijue}, e\in E_{iju}, u\in U_{ij}, ij\in IJ$$

(Constraint 3) Non-negativity constraints.

Figure 5.7. Equivalent MP formulation for the joint model

The objective function in Figure 5.7 gives the equilibrium solution of car ownership choice and car type choice for the joint dogit-NL model. q_u^{ij} is the car ownership demand between OD pair ij, q_{uem}^{ij} is the demand of car type m in mode nest e. Z_1 is the well-known Beckmann's transformation for UE where, g_{uem}^{ij} is the generalized cost consisting of fixed and operational costs, travel time cost, crash risk cost, and security risk cost. Z_2 and Z_3 are conditional and marginal entropy terms for the car type choice NL two-level probability structure. Z_4 is the exogenous modal attractiveness term. Z_5 and Z_6 are the entropy terms for car ownership choice. Z_5 accounts for the choice behavior of travelers who buy a car. Since no captivity is considered for the car owners, Z_5 only shows the choice passengers while Z_6 accounts for the dogit based choice behavior of captive travelers and choice travelers for the public transport nest. The first two constraints in Figure 5.7 (green box) are conservation constraints while the third constraint represents the non-negativity constraint. The above MP formulation in Figure 5.7 can be solved using algorithms developed for convex optimization (Gu & Chen, 2023).

Proposition 1. The MP formulation in Figure 5.7 gives the car ownership solution of the dogit model and the car type choice solution of the NL model based on the expected perceived generalized cost.

Proof of proposition 1.

The Lagrangian of the equivalent minimization problem w.r.t the equality constraints can be formulated as:

$$L = Z + \sum_{ij \in IJ} \sum_{u \in U_{ij}} \phi_u^{ij} \left(q_u^{ij} - \sum_{e \in E_{iju}} \sum_{m \in M_{ijue}} q_{uem}^{ij} \right) + \sum_{ij \in IJ} \lambda^{ij} \left(q^{ij} - \sum_{u \in U_{ij}} q_u^{ij} \right) \qquad (5.18)$$

Where ϕ_u^{ij}, and λ^{ij} are the dual variables associated with the conservation constraints in Figure 5.7.

(1) Given that the Lagrangian L has to be minimized w.r.t to the positive car type demand, the following conditions shall hold w.r.t car type demand.

$$\frac{\partial L}{\partial q_{uem}^{ij}} = 0 \quad \Rightarrow \quad g_{uem}^{ij} + \left(\frac{1}{\beta_e} - \frac{1}{\beta_{em}}\right) \ln \sum_{m \in M_{ijue}} q_{uem}^{ij} + \frac{1}{\beta_{em}} \ln q_{uem}^{ij} - \phi_u^{ij} - \psi_{uem}^{ij} = 0 \tag{5.19}$$

Let's take,

$$g_{uem}^{ij} - \psi_{uem}^{ij} = c_{uem}^{ij} \tag{5.20}$$

$$c_{uem}^{ij} + \left(\frac{1}{\beta_e} - \frac{1}{\beta_{em}}\right) \ln \sum_{m \in M_{ijue}} q_{uem}^{ij} + \frac{1}{\beta_{em}} \ln q_{uem}^{ij} - \phi_u^{ij} = 0 \tag{5.21}$$

Rearranging the above Equation gives.

$$(q_{uem}^{ij})^{\frac{1}{\beta_{em}}} \left(\sum_{m \in M_{ijue}} q_{uem}^{ij} \right)^{\left(\frac{1}{\beta_e} - \frac{1}{\beta_{em}}\right)} = e^{\left(\phi_u^{ij} - c_{uem}^{ij}\right)} \tag{5.22}$$

Summing over all m gives.

$$\left(\sum_{m \in M_{ijue}} q_{uem}^{ij} \right)^{\frac{1}{\beta_e}} = \sum_{m \in M_{ijue}} e^{\left(\phi_u^{ij} - c_{uem}^{ij}\right)} \tag{5.23}$$

$$\left(\sum_{m \in M_{ijue}} q_{uem}^{ij} \right)^{\frac{1}{\beta_e}} = \sum_{m \in M_{ijue}} e^{\left(\phi_u^{ij} - c_{uem}^{ij}\right)} \tag{5.24}$$

$$\sum_{m \in M_{ijue}} q_{uem}^{ij} = \sum_{m \in M_{ijue}} e^{\beta_e\left(\phi_u^{ij} - c_{uem}^{ij}\right)} \tag{5.25}$$

Summing over all e gives.

$$\sum_{e\in E_{iju}}\sum_{m\in M_{ijue}} q_{uem}^{ij} = qc_u^{ij} = \sum_{e\in E_{iju}}\sum_{m\in M_{ijue}} e^{\beta_e\left(\phi_u^{ij}-c_{uem}^{ij}\right)} \tag{5.26}$$

Dividing Equation (5.25) by (5.26) gives the marginal probability of nest e.

$$\frac{\sum_{m\in M_{ijue}} q_{uem}^{ij}}{qc_u^{ij}} = P_{ue}^{ij} = \frac{\sum_{m\in M_{ijue}} e^{-\beta_e c_{uem}^{ij}}}{\sum_{e\in E_{iju}}\sum_{m\in M_{ijue}} e^{-\beta_e c_{uem}^{ij}}} \tag{5.27}$$

$$\frac{\sum_{m\in M_{ijue}} q_{uem}^{ij}}{qc_u^{ij}} = P_{ue}^{ij} = \frac{\sum_{m\in M_{ijue}} e^{-\beta_e (g_{uem}^{ij}-\psi_{uem}^{ij})}}{\sum_{e\in E_{iju}}\sum_{m\in M_{ijue}} e^{-\beta_e (g_{uem}^{ij}-\psi_{uem}^{ij})}} \tag{5.28}$$

Dividing Equation (5.22) by (5.23) gives the conditional probability.

$$\frac{q_{uem}^{ij}}{\sum_{m\in M_{ijue}} q_{uem}^{ij}} = P_{u(m|e)}^{ij} = \frac{e^{-\beta_{em} c_{uem}^{ij}}}{\sum_{m\in M_{ijue}} e^{-\beta_{em} c_{uem}^{ij}}} \tag{5.29}$$

$$\frac{q_{uem}^{ij}}{\sum_{m\in M_{ijue}} q_{uem}^{ij}} = P_{u(m|e)}^{ij} = \frac{e^{-\beta_{em} (g_{uem}^{ij}-\psi_{uem}^{ij})}}{\sum_{m\in M_{ijue}} e^{-\beta_{em} (g_{uem}^{ij}-\psi_{uem}^{ij})}} \tag{5.30}$$

Equations (5.28) and (5.30) and respectively correspond to the marginal and conditional NL probability expressions in Equations (5.15) and (5.16).

(2). Now we consider the car ownership choice. For convenience, first, we can write Z_5 and Z_6 as a single expression (Equation (5.31)) and then take the derivative.

$$\hat{Z}_5 = \sum_{ij\in IJ}\sum_{u\in U_{ij}} \left(\frac{1}{\beta_u}-\frac{1}{\beta_e}\right)\left(q_u^{ij} - \frac{q^{ij}\eta_u^{ij}}{1+\sum_{u\in U_{ij}}\eta_u^{ij}}\right)\left(ln\left(q_u^{ij} - \frac{q^{ij}\eta_u^{ij}}{1+\sum_{u\in U_{ij}}\eta_u^{ij}}\right) - 1\right) \tag{5.31}$$

$$\frac{\partial L}{\partial q_u^{ij}} = 0 \quad \Rightarrow \quad \left(\frac{1}{\beta_u}-\frac{1}{\beta_e}\right)\ln\left(q_u^{ij} - \frac{q^{ij}\eta_u^{ij}}{1+\sum_{u\in U_{ij}}\eta_u^{ij}}\right) + \phi_u^{ij} - \lambda^{ij} = 0 \tag{5.32}$$

We can replace the choice travelers in the above expression as: $qc_u^{ij} = \left(q_u^{ij} - \frac{q^{ij}\eta_u^{ij}}{1+\sum_{u\in U_{ij}}\eta_u^{ij}}\right)$

$$\left(\frac{1}{\beta_u} - \frac{1}{\beta_e}\right) \ln qc_u + \phi_u^{ij} - \lambda^{ij} = 0 \tag{5.33}$$

From Equation (5.26), ϕ_u^{ij} can be defined as.

$$\phi_u^{ij} = \frac{1}{\beta_e} \ln qc_u^{ij} - \frac{1}{\beta_e} \ln \sum_{e \in E_{iju}} \sum_{m \in M_{ijue}} e^{-\beta_e c_{uem}^{ij}} \tag{5.34}$$

The second term on the right-hand side is the NL expected perceived cost, W_{ue}^{ij}.

$$\phi_u^{ij} = \frac{1}{\beta_e} \ln qc_u^{ij} - W_{ue}^{ij} \tag{5.35}$$

Replacing ϕ_u^{ij} in Equation (5.36).

$$\left(\frac{1}{\beta_u} - \frac{1}{\beta_e}\right) \ln qc_u^{ij} + \frac{1}{\beta_e} \ln qc_u^{ij} - W_{ue}^{ij} - \lambda^{ij} = 0 \tag{5.36}$$

$$\frac{1}{\beta_u} \ln qc_u^{ij} - W_{ue}^{ij} - \lambda^{ij} = 0 \tag{5.37}$$

$$qc_u^{ij} = e^{\beta_u \left(W_{ue}^{ij} + \lambda^{ij}\right)} \tag{5.38}$$

Summing over all u gives.

$$\sum_{u \in U_{ij}} qc_u^{ij} = \sum_{u \in U_{ij}} e^{\beta_u \left(W_{ue}^{ij} + \lambda^{ij}\right)} \tag{5.39}$$

Dividing gives Equation (5.38) by (5.39) gives.

$$\frac{qc_u^{ij}}{\sum_{u \in U_{ij}} qc_u^{ij}} = \tilde{P}_{u|ij} = \frac{e^{\beta_u W_{ue}^{ij}}}{\sum_{u \in U_{ij}} e^{\beta_u W_{ue}^{ij}}} \tag{5.40}$$

Substituting $qc_u^{ij} = \left(q_u^{ij} - \frac{q^{ij}\eta_u^{ij}}{1 + \sum_{u \in U_{ij}} \eta_u^{ij}}\right)$ in the above expression.

$$\tilde{P}_{u|ij} = \frac{\left(q_u^{ij} - \frac{q^{ij}\eta_u^{ij}}{1+\sum_{u\in U_{ij}}\eta_u^{ij}}\right)}{\sum_{u\in U_{ij}}\left(q_u^{ij} - \frac{q^{ij}\eta_u^{ij}}{1+\sum_{u\in U_{ij}}\eta_u^{ij}}\right)} = \frac{\left(\frac{q_u^{ij}}{q^{ij}} - \frac{\eta_u^{ij}}{1+\sum_{u\in U_{ij}}\eta_u^{ij}}\right)}{\sum_{u\in U_{ij}} q_u^{ij} - \frac{q^{ij}\sum_{u\in U_{ij}}\eta_u^{ij}}{1+\sum_{u\in U_{ij}}\eta_u^{ij}}} \tag{5.41}$$

$$\tilde{P}_{u|ij} = \frac{\left(P_{u|ij} - \frac{\eta_u^{ij}}{1+\sum_{u\in U_{ij}}\eta_u^{ij}}\right)}{1 - \frac{\eta_u^{ij}}{1+\sum_{u\in U_{ij}}\eta_u^{ij}}} = \frac{\left(P_{u|ij} - \frac{\eta_u^{ij}}{1+\sum_{u\in U_{ij}}\eta_u^{ij}}\right)}{\frac{1}{1+\sum_{u\in U_{ij}}\eta_u^{ij}}} \tag{5.42}$$

Rearranging gives.

$$P_{u|ij} = \frac{\eta_u^{ij}}{1+\sum_{u\in U_{ij}}\eta_u^{ij}} + \frac{1}{1+\sum_{u\in U_{ij}}\eta_u^{ij}}.\tilde{P}_{u|ij} \tag{5.43}$$

$$P_{u|ij} = \frac{\eta_u^{ij}}{1+\sum_{u\in U_{ij}}\eta_u^{ij}} + \frac{1}{1+\sum_{u\in U_{ij}}\eta_u^{ij}}.\frac{e^{\beta_u W_{ue}^{ij}}}{\sum_{u\in U_{ij}} e^{\beta_u W_{ue}^{ij}}} \tag{5.44}$$

Equation (5.44) is exactly the dogit probability in Equation (5.14).

Proposition 2. If assumption A3 holds, the solution of the joint dogit-NL model is unique.

Proof of proposition 2.

The Hessian matrix of Z_1+Z_2+Z_3+Z_4 with respect to the car type demand can be expressed as:

$$\frac{\partial^2}{\partial q_{uem}^{ij}\partial q_{ust}^{ij}} = \begin{cases} \frac{\partial[g_{uem}^{ij}(q_{uem}^{ij})]}{\partial q_{ust}^{ij}} + \frac{1}{\beta_{em}}.\frac{\partial(\ln q_{uem}^{ij})}{\partial q_{ust}^{ij}} + \left(\frac{1}{\beta_e} - \frac{1}{\beta_{em}}\right).\frac{\partial(\ln\sum_{m\in M_{ijue}} q_{uem}^{ij})}{\partial q_{ust}^{ij}} > 0 & ; e = s, m = t \\ 0 & ; \quad otherwise \end{cases} \tag{5.45}$$

According to Assumption 3, the generalized travel cost is an increasing function of car type demand; thus, the first term in the equation is positive semi-definite. The second and third terms are positive when *e*=*s* and *m*=*t*, otherwise, they are zero. Positive semi-definite and positive definite matrices sum up to a positive definite matrix.

The Hessian matrix of Z_5 and Z_6, combined as a single term as shown in Equation (5.31), with respect to the car ownership demand variables can be expressed as:

$$\frac{\partial^2}{\partial q_u^{ij} \partial q_l^{ij}} = \begin{cases} \left(\frac{1}{\beta_u} - \frac{1}{\beta_e}\right) \cdot \frac{\partial \ln\left(q_u^{ij} - \frac{q^{ij}\eta_u^{ij}}{1 + \sum_{u \in U_{ij}} \eta_u^{ij}}\right)}{\partial q_l^{ij}} > 0 & ; u = l \\ 0 & ; \ otherwise \end{cases} \tag{5.46}$$

The above term is positive when *u*=*l*, otherwise, it is zero, which also implies the positive definite matrix. Therefore, the joint dogit-NL model has a unique solution. This completes the proof. □

5.4 Numerical experiments

This section applies the proposed model to illustrate its properties and examine joint equilibrium choice behavior using examples with single and multiple OD pairs. It first demonstrates how the model accounts for car type similarity and the impact of captive travelers on car ownership, then conducts sensitivity analysis to assess how different risk perception parameters affect equilibrium demand.

5.4.1 Single OD pair example.

5.4.1.1 Experiment setting

In this example, the proposed model investigates the joint equilibrium behavior of car ownership and car type choice among four private car types (GHV, EHV, GAV, EAV) and public transport (PT). The data used for this experiment is as follows:

$q_{ij} = 1000$ persons, $L = 20$ km, $t_{wk,PT} = 10$ min, $t_{wt,PT} = 5$ min, $t_{iv,PT} = 40$ min, $t_{iv,car} = 20$ min, $R_{eav} = 150$ km, $VKT_{hth}(2 \times L) = 40$ km, and public transport fare equals \$0.5/km. The in-vehicle travel time and the crash risk cost functions for the private car (AVs and HVs) are $t_{iv,m}(q_{car}) = t_{iv,car}.\left[1 + 0.15\left(\frac{q_{car}}{600}\right)^4\right]$ and $r_m^{ij} = \gamma_m(e^{-8.05}(q_{car}^{ij})^{\delta-1}\, L^{ij})$. The in-vehicle crowding discomfort cost for PT mode is $g(q_{PT}).\, t_{iv,PT} = t_{iv,PT}.\left[1 + 0.5\left(\frac{q_{PT}}{1000}\right)^2\right]$. The exogenous attraction is assumed to be the same for all the modes (i.e., $\psi_m^{ij} = 2$). The security risk of AV's vehicle class is assumed to be directly proportional to its market penetration, i.e., $sr_{m,av}^{ij} = 5\left(\frac{q_{AV}^{ij}}{q_{ij}}\right) + 0.5$. The security risk of AVs is assumed to be higher than that of HVs due to AVs' cybersecurity issues. Therefore the sr_{hv}^{ij} is set equal to 0.5. The captivity parameter for travelers who cannot afford a car is set equal to $\eta_{nocar} = 0.05$.

The data relating to fixed and operational costs of a vehicle is assumed similar to previous studies (Noruzoliaee et al., 2018; Singh et al., 2023; Xie & Liu, 2022). The vehicle purchase price of GHV is assumed to be \$14,775 while the purchase price of GAV is assumed to be \$10,000 higher than HVs i.e., \$24,775 (Xie & Liu, 2022). The prices of EHV and EAV are assumed to be slightly higher than those of GHV and GAV. Specifically, the price of an EHV is set at \$16,695 (calculated as $4\times(14{,}775)^{0.87}$), while the price of an EAV is \$26,598 (calculated as $4\times(24{,}775)^{0.87}$) (Singh et al., 2023). We assume the average lifespan of a vehicle to be equal to 10 years (b_2 = 10 years) and the overhead cost per vehicle equal to \$57,225, resulting in b_1 = 4.9 (57,225+14,475/14,475). Factor b_3 is assumed equal to 17500 km/year. The fuel cost and insurance cost of HV are set equal to \$0.102/km and \$0.8/km, respectively. The fuel cost of a AV is assumed to be 10% cheaper than the HV's fuel cost (Wadud, 2017).

The electricity cost for EVs is assumed to be \$0.04/km (Singh et al., 2023). For AVs, the Insurance companies provide a 20% discount (Palmer, 2015); therefore, a 20% reduction in the insurance cost of AVs is assumed compared to HVs. The VoT of driving HVs and AVs are set equal to \$0.298/min and \$0.176/min (41 % reduction compared to HVs, according to Kolarova et al. (2019)). Other running costs, such as maintenance, parking, etc., are assumed to be \$0.105/km for gasoline vehicles. Electric vehicles' maintenance costs are assumed to be reduced by 50% (i.e., at \$0.053/km) (Singh et al., 2023). The default model parameters for the base scenario are given in Table 5.2.

Table 5.2. Default model parameters for the base scenario

Parameter	Value	Parameter	Value
β_u	0.01	θ_{sr}	50
β_e	0.05	θ_{RA}	10
β_{em}	1	ω	2
γ_{HDV}	1	α_{AV}	0.1
γ_{AV}	0.1	α_{HDV}	0.1
VoS	100	η_{nocar}	0.05
δ	2		

5.4.1.2 Effect of considering car type similarity

This section investigates the effect of considering car type similarity among different car types in the nested structure. The car type demand obtained at different values of β_e/β_{em} are shown in Table 5.3 and Figure 5.8. A higher value of β_e/β_{em} indicates that car types within the same nest are less similar. Figure 5.8 shows that considering car type similarity significantly affects the estimated mode share for different nests. Without considering mode similarity, the estimated share of the HV collective mode (GHV and EHV) is lower and more share is allocated to the AV collective mode (GAV and EAV). Therefore, it is vital to consider car type mode similarity to achieve an unbiased estimate of the mode shares.

Table 5.3. Effect of considering car type similarity on the equilibrium demand.

β_e/β_{em}	HV collective mode		AV collective mode		PT
	GHV	EHV	GAV	EAV	
1	25.1	28.1	203.3	226.9	516.6
0.8	26.1	29.2	202.4	225.9	516.4
0.6	27.7	31.1	200.9	224.3	515.9
0.4	30.7	34.4	198.3	221.4	515.1
0.2	38.3	42.8	191.9	214.2	512.7
0.1	49.5	55.4	183.0	204.3	507.9
0.05	64.4	72.1	172.6	192.7	498.2
0.01	104.4	116.9	156.7	174.9	447.0

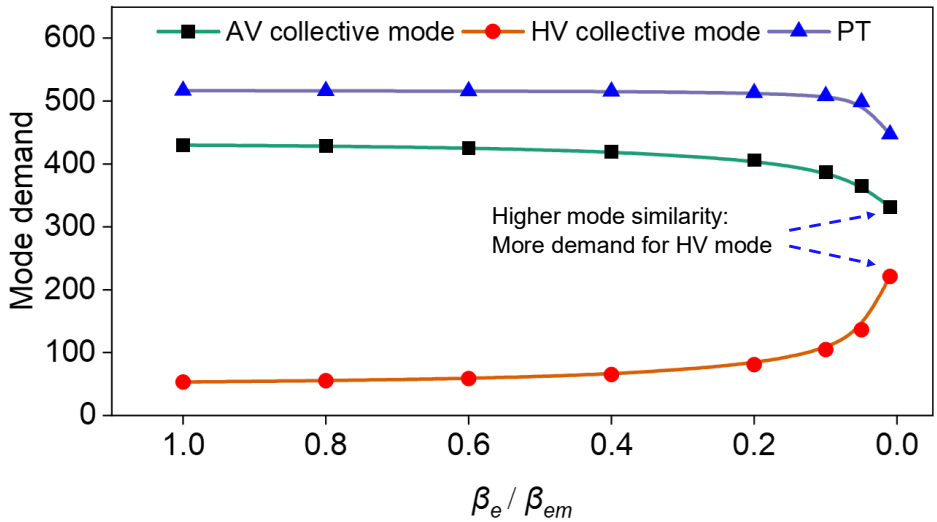

Figure 5.8. Effect of considering car type similarity on demand in each nest.

5.4.1.3 Effect of captivity parameter on car ownership

In this section, we examine how the captivity parameter in the dogit model affects car ownership demand. As previously discussed, not all travelers can afford to own a car, making them captive to public transport mode. Figure 5.9 illustrates that car ownership decreases as the captivity parameter increases, indicating that a higher proportion of travelers are reliant on public transport. These results underscore the significance of accounting for captive travelers in planning models; otherwise, car ownership demand may be overestimated.

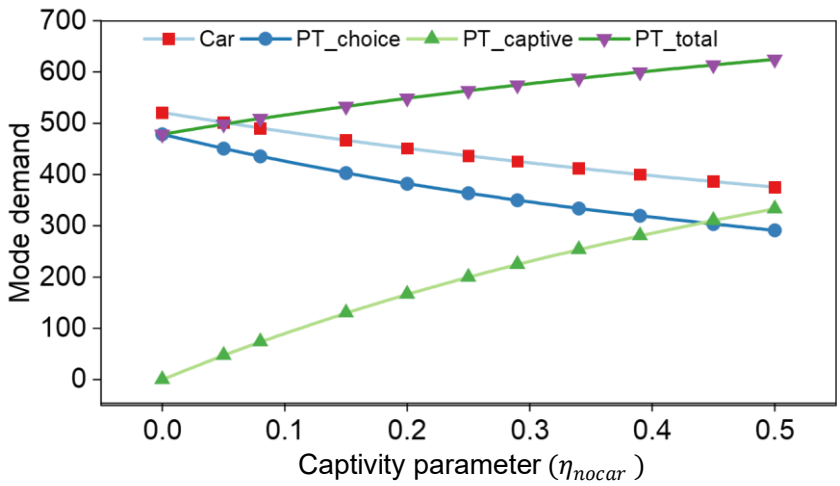

Figure 5.9. Effect of captivity parameter on car ownership demand

5.4.1.4 Effect of the perceived crash risk parameter of AVs on joint choice

This section investigates the impact of AVs' perceived crash risk parameter on joint choice behavior. As explained in Section 5.1, while AVs may reduce the crash risk, their adoption largely depends on the travelers' perceptions of their crash risk. A higher value of γ_{AV} indicates a higher perceived crash risk (lower perceived safety) of AVs, whereas a lower value indicates a lower perceived crash risk of AVs (higher perceived safety).

Table 5.4. Effect of perceived crash risk cost parameter on modal demand

γ_{AV}	HV collective mode		AV collective mode		PT
	GHV	EHV	GAV	EAV	
0.1	64.4	72.1	172.6	192.7	498.2
0.2	70.9	79.4	161.5	180.2	508.4
0.3	46.7	85.9	151.7	169.3	516.5
0.4	81.9	91.6	143.0	159.6	523.9
0.5	86.5	96.8	135.3	151.0	530.3
0.6	90.7	101.5	128.4	143.3	536.0
0.7	94.5	105.7	122.2	136.4	541.1
0.8	97.9	109.6	116.6	130.2	545.7
0.9	101.0	113.1	111.6	124.5	549.8
1	103.9	116.3	107.0	119.4	553.5

Table 5.4 and Figure 5.10(a) show estimated mode share for different modes at different values of γ_{AV}. At a higher value of γ_{AV}, less demand is allocated to the AV mode which

increases with the decrease of γ_{AV} leading to a reduction in demand for HVs and public transport. Similarly, Figure 5.10(b) shows that the car ownership demand is lower when γ_{AV} is high, but it increases as this parameter decreases. This suggests that when travelers perceive AVs as safer, more people are inclined to own an AV, which also leads to an increase in overall car ownership demand.

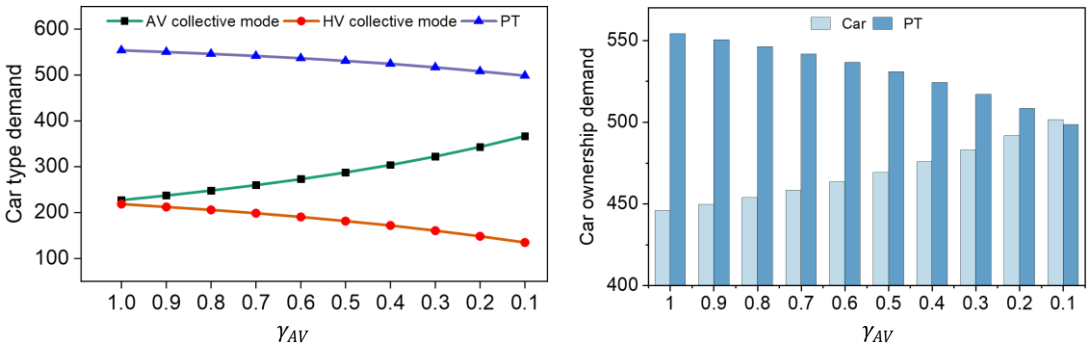

(a) Effect of AV's crash risk perception on car type demand

(b) Effect of AV's crash risk perception on car ownership demand

Figure 5.10. Effect of crash risk perception parameter (γ_{AV}) of AV on market share

These findings align with empirical studies, which indicate a shift from HV modes to AV modes as travelers' crash risk perceptions of AVs improve (Jabbari et al., 2022). Furthermore, the results highlight the importance of carefully calibrating or selecting the crash risk perception parameter to achieve accurate estimates of car type and car ownership demand in planning models.

5.4.1.5 Effect of the perceived security risk parameter of AVs on joint choice

As discussed in Section 5.1, users' perceptions of security, such as concerns about data privacy and system hacking, are crucial factors influencing the adoption of AVs. This section examines the impact of the security risk perception parameter, α_{AV}, on modal demand. A higher value of α_{AV} reflects a greater perceived security risk (less secure) for AVs, while a lower value indicates a lower perceived security risk (more secure).

The modal shares for different values of α_{AV} are presented in Table 5.5 and Figure 5.11(a).

Table 5.5. Effect of security risk perception parameter on car type demand

α_{AV}	Collective HV mode		Collective AV mode		PT
	GHV	EHV	GAV	EAV	
0.1	64.4	72.1	172.6	192.7	498.2
0.2	67.8	75.9	166.8	186.2	503.3
0.3	71.0	79.5	161.3	180.0	508.1
0.4	74.1	82.9	156.1	174.3	512.7
0.5	77.0	86.2	151.2	168.7	516.9
0.6	79.8	89.4	146.4	163.4	521.0
0.7	82.5	92.4	141.9	158.4	524.8
0.8	85.1	95.3	137.6	153.6	528.4
0.9	87.6	98.0	133.6	149.1	531.8
1	89.9	100.7	129.7	144.7	535.0

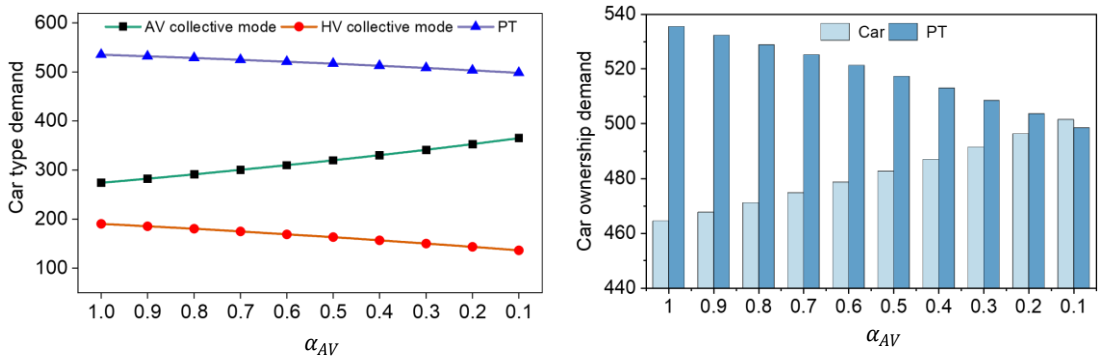

(a) Effect of AV's security risk perception on car type demand

(b) Effect of AV's security risk perception on car ownership demand

Figure 5.11. Effect of security risk perception parameter of AV (α_{AV}) on market share

When α_{AV} is higher, a smaller portion of demand is allocated to AVs due to heightened security concerns. Conversely, as this parameter decreases, demand shifts toward AVs from other modes, such as HVs and public transport. A similar pattern is observed for car ownership demand in Figure 5.11(b), where lower perceived security risks (lower α_{AV}) lead to higher AV ownership and, consequently, an increase in overall car ownership. Conversely, as α_{AV} increases, car ownership declines. Since cybersecurity concerns are unique to AVs, this factor significantly influences both AV ownership and overall car ownership decisions.

5.4.2 Case study with multiple origin-destination pairs

5.4.2.1 Experiment setting

This section applies the proposed model to a real-world case study in Singapore, shown in Figure 5.12 (adapted from Noruzoliaee et al. (2018)). The study area comprises five traffic analysis zones, resulting in 20 OD pairs.

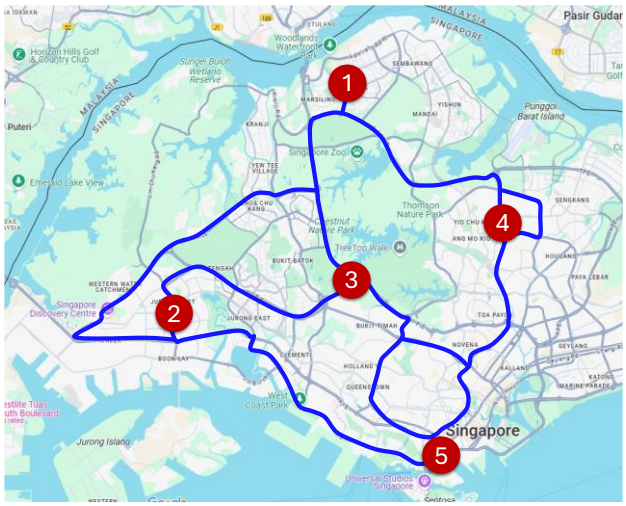

Figure 5.12. Study area in Singapore with multiple OD pairs (Noruzoliaee et al., 2018)

The attributes of all OD pairs, i.e., travel times, distances, and travel demands are detailed in Table 5.6. Other inputs and default parameters are consistent with those presented in Section 5.4.1. The in-vehicle travel times for a car is $t_{iv,m}(q_{car}) = t_{iv,car}.\left(1 + 0.15\left(\frac{q_{car}}{cap_{car}}\right)^4\right)$ and the discomfort cost for PT mode is $g(q_{PT}).t_{iv,PT} = t_{iv,PT}.\left(1 + 0.5\left(\frac{q_{PT}}{cap_{PT}}\right)^2\right)$. To explore the effect of EVs on environmental friendliness, the following expression in Equation (5.47) is adopted for calculating the CO emissions (Wallace et al., 1998). The PT mode is assumed to operate on electricity; therefore, its CO emissions are ignored, making cars the sole source of CO emissions in this analysis (Wang et al., 2020a).

$$E^{ij} = \sum_{m \in M_{ij}} q_m^{rs}.0.2038.t_m^{ij}.\exp(0.7962.L^{ij}/t_m^{ij}), \forall ij \in IJ \tag{5.47}$$

Table 5.6. Input data for each OD pair

OD	Demand (persons/h)	Distance (km)	Private car		Public transport	
			Travel time (min)	Capacity (vph)	Travel time (min)	Capacity (persons/h)
1↔2*	1745	21.2	21	2505	42	1745
1↔3	294	16.9	17	1670	34	294
1↔4	1833	11.7	14	2505	28	1833
1↔5	1272	27.0	34	1670	68	1272
2↔3	513	15.9	18	1670	36	513
2↔4	1278	26.5	31	1670	62	1278
2↔5	831	21.4	20	2505	40	831
3↔4	259	10.6	14	3340	28	259
3↔5	191	10.1	17	2505	34	191
4↔5	1421	12.9	15	2505	30	1421

1↔2* denotes both OD pairs 1→2 and 2→1.

5.4.2.2 The effects of travelers' risk perceptions on market share.

To assess how travelers' perceptions of crash risk and security risk of AVs affect their market share in a multi-OD case study, we performed a sensitivity analysis by adjusting the perception parameters for the AV mode across various O-D pairs.

In the first scenario, we analyzed the OD pairs originating from origin 3 (i.e., 3-1, 3-2, 3-4, and 3-5) by specifying different crash risk perception parameters (γ_{AV}) for these OD pairs while keeping other inputs fixed (Figure 5.13(a)). The analysis revealed that OD pairs with lower crash risk perceptions of AVs exhibited a higher market share for the AV mode. For example, Figure 5.13(a) shows that the OD pair 3-5, with γ_{AV} = 0.1, had the highest market share for AVs, while OD pair 3-1, with γ_{AV} = 1, had the lowest market share. This difference arises from travelers in OD pair 3-5 perceiving AVs as significantly safer than those in OD pair 3-1.

In the second scenario, we varied security risk perception parameter (α_{AV}) values for these OD pairs by keeping all other parameters fixed. A similar pattern emerged, as

shown in Figure 5.13(b). Travelers in OD pair 3-5, with $\alpha_{AV} = 0.1$, perceive AVs as more secure than travelers in other OD pairs, leading to the highest AV collective mode share, while OD pair 3-1 has the lowest market share. These results indicate that travelers' perceptions of both crash risk and security risk substantially influence AV adoption across OD pairs, consistent with the trends observed in the single OD-pair analysis.

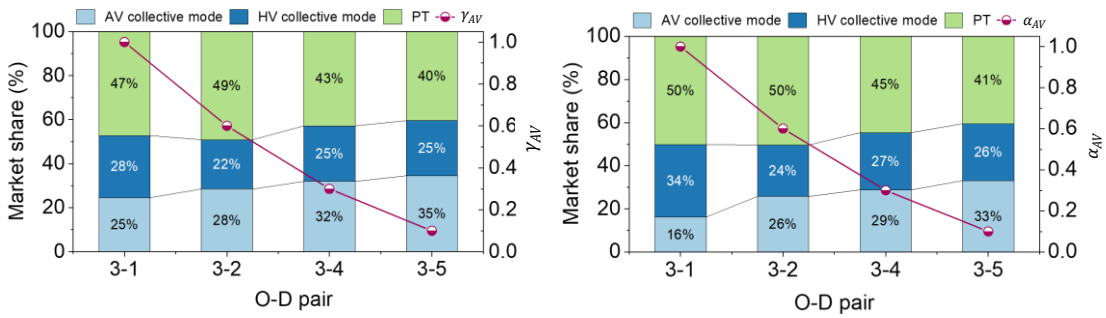

(a) Effect of AV's crash risk perception on market share

(b) Effect of AV's security risk perception on market share

Figure 5.13. Effect of risk perceptions on market share

5.4.2.3 Effect of the technological improvements on EV market share

In this section, we explore the impact of EV technological improvements on EV adoption. Technological improvements are considered through two key aspects: (a) reduction in EV price and (b) improvement in EV range. The results in Figure 5.14 (a and c) demonstrate that technological advancements prompt more travelers to shift from gasoline modes (GHV and GAV) to EV modes (EHV and EAV), aligning with findings from empirical studies (Zhou et al., 2023). The results also indicate that a reduction in EV price has a more pronounced effect on increasing EV market share compared to enhancements in EV range. Furthermore, these technological improvements lead to a substantial decrease in CO emissions, driven by the growing adoption of EVs as shown in Figure 5.14 (b and d).

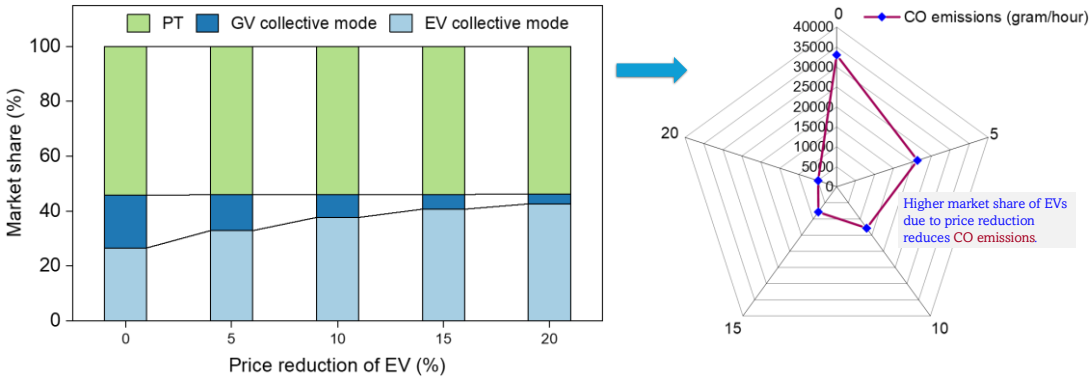

(a) Effect of EV price reduction on market share

(b) Reduction in CO emissions due to EV price reduction

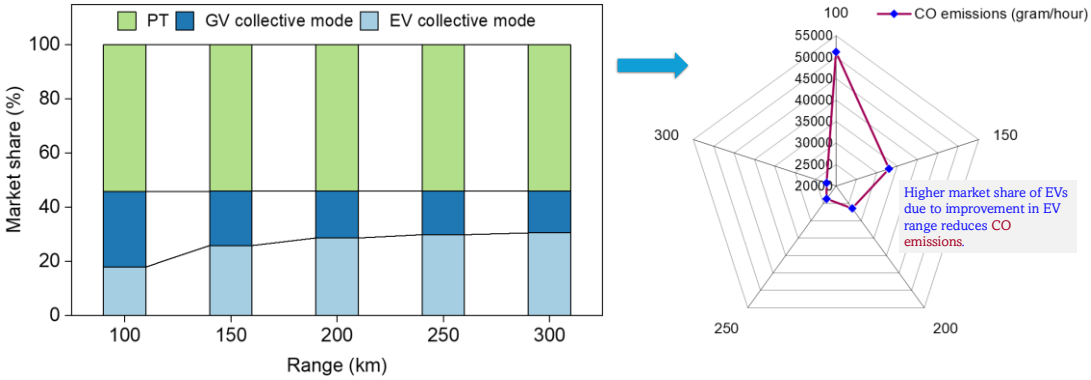

(c) Effect of EV range on market share

(d) Reduction in CO emissions due to EV range improvement

Figure 5.14. Effect of technological improvements on EV market share

5.4.2.4 The effects of network congestion levels on market share.

Travelers' joint car ownership and car type choices, as well as the subsequent market penetrations, may differ for different congestion levels on the road network due to travelers varying perceptions of the travel time, crash risk and security risk. This section investigates the effect of congestion level by changing the demand from 0.5 to 2.4 times that in the base scenario (Figure 5.15). It can be seen that the AV collective mode gets a higher market share as the congestion level increases while the HV collective mode loses market penetration to AV mode and PT. This is because the expected generalized travel cost increases with the rise in congestion level. However, due to the travelers lower VoT and lower crash risk perception for AVs, the travel cost of AV is less sensitive to the increase of travel time and crash risk cost compared to the HVs.

Consequently, the advantages of AVs, such as travel time savings and improved safety, become more pronounced under higher congestion. This increased market share of AVs is anticipated to alleviate traffic congestion and enhance overall travel safety.

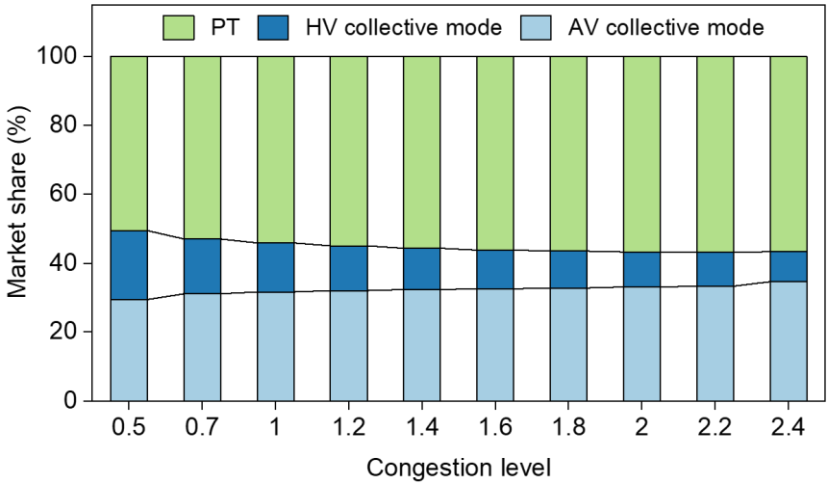

Figure 5.15. The effects of congestion level on market share

5.5 Implications for policy and practice

The proposed model offers several practical and policy implications that are pertinent to government bodies, transportation planning agencies, policymakers, and automobile manufacturers. By incorporating user behavior and the distinctive attributes of autonomous vehicles, the equilibrium joint choice model effectively predicts the market share of different car types and the overall demand for car ownership.

5.5.1 Effect of risk perceptions on AV adoption

By accounting for AVs' safety and security features, the model illustrates how travelers' perceptions of risk can influence their preference for autonomous vehicles. Empirical studies confirm that travelers' risk perceptions regarding crash risk and cybersecurity affect their preference for AVs (Choi & Ji, 2015; Haboucha et al., 2017). While AVs can potentially enhance travel safety by reducing traffic crashes, they also introduce cybersecurity risks (Kenesei et al., 2022; Kockelman et al., 2016). The findings

underscore the substantial impact of users' perceptions of crash and security risks on the adoption of AVs. Initially, despite the safety improvements AVs offer, adoption may be hindered by heightened user risk perceptions towards this new technology. Nevertheless, as users get accustomed to autonomous vehicles over time, concerns regarding safety and security are expected to diminish, prompting a transition from traditional HVs to AVs as users recognize the technology's benefits. Empirical results are in accordance with these conclusions, indicating that enhancements in travelers' risk perceptions of autonomous vehicles will elevate the market share of autonomous vehicles (Bansal & Kockelman, 2017; Hulse et al., 2018; Jabbari et al., 2022; Nazari et al., 2018).

5.5.2 Technological advancements and EV adoption

The model also examines how technological advancements affect the adoption of EVs. It explores two critical aspects: improvements in EV range and reductions in EV price. Research indicates that range anxiety significantly impacts individuals' willingness to adopt EVs (Berkeley et al., 2018; Valeri & Danielis, 2015). The findings of this study suggest that advancements in EV technology, including increased range and reduced prices, are likely to boost the market share of EVs. These results are supported by empirical evidence, which shows that as battery technology improves and prices decrease, EVs are expected to replace gasoline vehicles in the market increasingly (Berkeley et al., 2018; Zhou et al., 2023).

5.5.3 Consideration of captive travelers in transportation planning

The model also highlights the importance of accounting for captive travelers, those unable to afford a car and reliant on public transportation, in transportation planning (Chu, 2016). In practice, ignoring this critical aspect can result in overestimating the demand for car ownership, particularly in urban areas where substantial income

disparities exist. Assessing and fulfilling the needs of captive travelers through an accessible and affordable public transportation system is crucial for equitable and accurate transportation planning.

5.5.4 Policy and planning recommendations

a) *Enhanced safety and security measures:* Policymakers should prioritize strengthening cybersecurity measures and safety features to encourage AV adoption. Communicating openly about these advancements is crucial by giving thorough information, responding to public concerns, and providing frequent updates. Open communication between legislators and the public can alleviate fears and promote AV acceptance (Hamadneh et al., 2022). An effective transition to the adoption of AVs can significantly reduce road fatalities and overall crash risk costs (Fagnant & Kockelman, 2015; Kockelman et al., 2016).

b) *Incentives for EV Technological Advancements:* To accelerate the development and adoption of EVs, governments can offer a range of incentives and subsidies to manufacturers and consumers (Jenn et al., 2018). Making EVs more affordable can significantly boost demand, ultimately reducing pollution caused by gasoline vehicles.

c) *Public awareness campaigns:* Educational initiatives highlighting AVs and EVs' environmental and safety benefits can help increase adoption rates (Haboucha et al., 2017). Targeted campaigns addressing common concerns can also improve public perceptions and foster greater acceptance.

5.6 Conclusions

This Chapter presents a preliminary effort to model joint car ownership and car type decisions by incorporating users' risk perceptions of AVs within a discrete-choice-based equilibrium analysis framework. The model explicitly considers users' concerns

related to crash risk, security risk, and range anxiety in the joint choice framework. An equivalent MP formulation is provided, where a dogit model is employed to represent car ownership choice, and a nested logit model is used to capture car type choice, accounting for similarities among modes. The results from numerical experiments illustrate the impact of AV risk perceptions on the joint choice of car type and ownership. Specifically, the findings show that as travelers' risk perceptions of AVs decrease, the market share of AVs increases, leading to a corresponding rise in car ownership. Additionally, the experiments demonstrate that technological improvements in EVs, such as enhanced EV range and reduced prices, significantly drive a shift from gasoline vehicles to electric vehicles.

CHAPTER 6 Modeling safety variability in a mean-excess network equilibrium framework for users with heterogeneous preferences

6.1 Motivation

Transportation network safety is critical for planners designing safe and reliable systems. Safety-conscious planning involves embedding safety considerations into transportation planning to enhance system effectiveness. Traditionally, planners have relied on macro-level CPMs based on historical crash data to guide decisions about zonal development and achieve specific safety targets (Abdel-Aty et al., 2013; Li et al., 2013). While these models have proven useful, they fail to account for travelers' safety preferences and behaviors. This limitation prevents planners from fully understanding how individual route choices, shaped by safety concerns, influence traffic flow patterns and, ultimately, network-wide safety. Bridging this gap is essential for developing transportation networks that not only meet broader safety objectives but also reflect and accommodate real-world user behavior.

This consideration is especially crucial in traffic assignment, a key step in transportation planning, where different route choice criteria have been used to assign traffic on road networks, such as minimum travel time routes (Bellman, 1958; Gendreau et al., 2015), environment-friendly routes (Xu et al., 2015), and the most reliable routes (Xu et al., 2015). Empirical studies have also highlighted the importance of travel safety in travelers' route choice decisions (Abdel-Aty et al., 1995; Amirgholy et al., 2017; Yannis et al., 2005). Despite this evidence, little effort has been devoted to modeling safety, specifically crash risk, in traffic assignment models (Han et al., 2023; Huang et al., 2020; Ma & Zhang, 2019). As we move into an era of intelligent and connected

vehicles, the availability of real-time trip-related safety information highlights the need to incorporate safety considerations into traffic assignment models (Carmody & Sowers, 2019; Ghoul et al., 2023; Hoseinzadeh et al., 2020). Integrating safety into traffic assignment enhances safety-conscious planning by offering a behaviorally informed framework that explicitly incorporates travelers' safety behaviors and preferences as a core element of transportation planning.

Safety can be defined as the likelihood of a vehicle being involved in a crash while traveling within a road network (Chandra, 2014). The crash risk is influenced by various factors, such as roadway features, environmental conditions (e.g., weather), human behavior, and traffic conditions. Roadway characteristics such as functional class, intersection density, and geometric design are fixed and inherent to a specific location. In contrast, factors like weather, human behavior and traffic conditions are subject to change over time, inducing variability in the crash risk of a road site, which fluctuates around a mean crash risk value. This mean crash risk value represents the average safety condition of the road (Huang et al., 2020), while variability arises from uncertainties associated with changing traffic conditions, volatility in driving behavior (Wali et al., 2018; Wang et al., 2015), and environmental changes. Consequently, predicting the certainty of completing a trip safely is challenging, and a single deterministic value for trip safety may not be realistic. Although travelers may not know the absolute crash risk of a route, they may be familiar with the route's crash risk variability based on their daily traveling experiences. For example, travelers may know routes with a higher probability of severe crashes, such as those with more truck volume or high-speed vehicles (Kadeha et al., 2021; Kidando et al., 2019). Therefore, to ensure trip safety and avoid routes with higher probabilities of severe or fatal crashes (i.e., extremely high

crash costs), travelers are expected to consider the safety variability of a route in their habitual route choice process.

Moreover, empirical studies indicate that travelers on the road exhibit varying degrees of safety consciousness, leading to heterogeneous safety preferences (May et al., 2008). For example, younger drivers are likelier to operate vehicles at elevated speeds, underestimate the probability of crash involvement, and overestimate their driving capabilities. (Castellà & Pérez, 2004; Deery, 1999; Machin & Sankey, 2008; McKenna & Horswill, 2006). In contrast, older drivers tend to be more defensive and risk-averse (Simons-Morton et al., 2014). Incorporating these heterogeneous safety preferences into traffic assignment models is essential, particularly when addressing safety variability.

Additionally, travelers with higher safety preferences may not consider all available routes in their choice set, excluding those with higher predefined safety risks. These exclusions are often based on fixed roadway characteristics such as road functional classification (e.g., highway or local road), intersection density, and total travel distance (Dijkstra, 2013; Dijkstra et al., 2007). Consequently, each traveler class may have a distinct route choice set that is aligned with its safety preferences (Li & Huang, 2019). Therefore, this chapter aims to incorporate and explore the effect of travelers' heterogeneous safety preferences on their route choices and equilibrium flow patterns.

6.1.1 Contributions

This Chapter develops a comprehensive network equilibrium framework that considers roadway characteristics and traffic conditions to model travelers' safety concerns. The key contributions of this study are as follows.

a) The proposed framework models and analyzes the effect of safety-based class-specific route choice sets on equilibrium flow patterns, extending prior assumptions

of complete choice sets (Han et al., 2023; Huang et al., 2020). This accounts for heterogeneous travelers with varying degrees of safety consciousness.

b) The framework incorporates a traffic equilibrium model that simultaneously accounts for travelers' concerns related to both the reliability and unreliability of safety and travel time variabilities, considering traveler classes with heterogeneous safety reliability preferences. This integration builds on prior models of individual variability, including travel time variability (Chen & Zhou, 2010; Chen et al., 2011; Xu et al., 2018b) and safety variability (Han et al., 2023; Huang et al., 2020), to provide a unified approach that captures holistic traveler behavior under dual uncertainties.

6.2 Methodology

6.2.1 Notation

All the notations used in the Chapter are tabulated below unless otherwise specified.

Table 6.1. Notations

Symbol	Description
Sets:	
$G(N, A)$	a road network
N	set of nodes
A	set of links (a)
P	Set of routes (p)
W	set of origin destination pairs (w)
M	Set of traveler classes (m)
Parameters/inputs:	
$\Gamma/\overline{\Gamma}$	adjustment coefficients
$\omega/\overline{\omega}$	parameters of travelers' risk perceptions
t_a^0	free-flow travel time of link a
c_a	capacity of link a
q_w^m	travel demand between an O-D pair w for user class m
Variables	
$f_{p,m}^w$	traffic flow on route p between O-D pair w for traveler class m
x_a	flow of link a
Others	
t_a	mean travel time of link a
r_a	CRC distribution of link a
μ_a	average CRC of link a
σ_a	standard deviation of CRC on link a
$ls_{lr}^{p,w}$	length share of local road on route p between O-D pair w
$ls_{cr}^{p,w}$	length share of collector road on route p between O-D pair w

l_p^w	total length of route p between O-D pair w
$id_{p,w}$	intersection density on route p between O-D pair w
Θ_p^w	safety score of route p between O-D pair w
Θ_{req}^m	safety score requirement of traveler class m
r_p^w	CRC distribution of route p between O-D pair w
δ_a^p	route-link incidence parameter
μ_p^w	mean CRC of route p between O-D pair w
σ_p^w	standard deviation of CRC of route p between O-D pair w
$R_{p,m}^w$	effective CRC of route p between O-D pair w for class m
$G_{p,m}^w$	generalized travel cost of route p between O-D pair w
T_p^w	mean travel time of route p between O-D pair w for class m
$\widehat{\sigma_p^w}$	standard deviation of travel time of route p between O-D pair w
$\psi_{p,m}^w$	mean excess CRC of route p between O-D pair w for traveler class m
η_p^w	mean excess travel time of route p between O-D pair w

6.2.2 Study framework

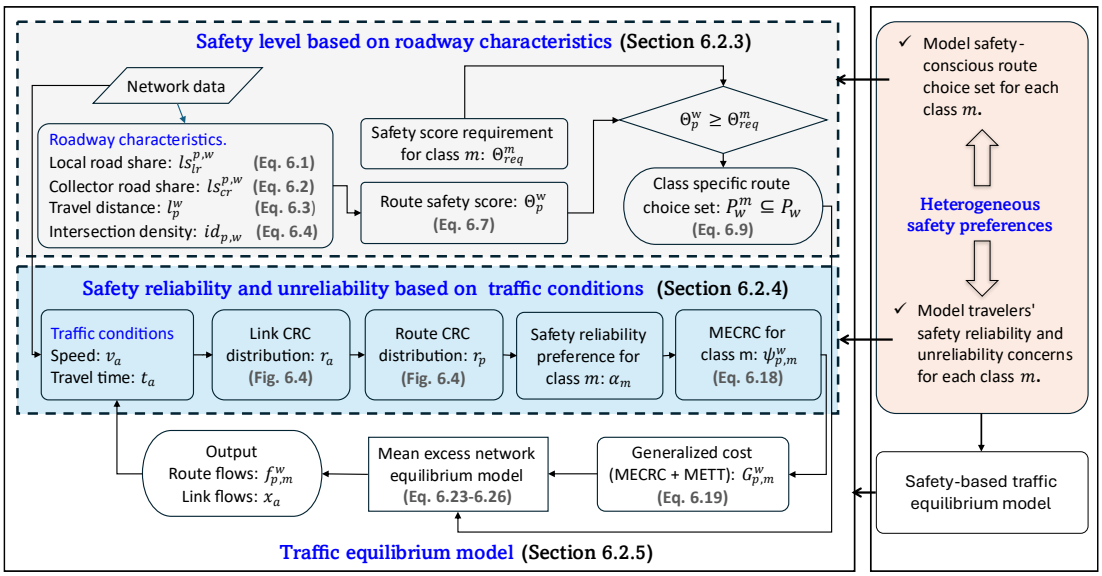

Figure 6.1. Illustration of the methodological framework

The framework of this study is illustrated in Figure 6.1. The class-specific route choice sets are determined based on the safety score of each route, as explained in Section 6.2.3. Travelers' concerns regarding the reliability and unreliability of safety variability are detailed in Section 6.2.4. Finally, travelers safety preferences are incorporated into the traffic equilibrium model in Section 6.2.5.

6.2.3 Safety level of a route based on roadway characteristics

Routes with varying roadway characteristics exhibit different levels of safety. Specifically, routes differ in terms of their functional classes, intersection density, and total travel distance, all of which influence travel safety. Below, we explain the procedure for computing the safety score of a route based on several criteria related to its fixed characteristics (Dijkstra, 2013; Dijkstra et al., 2007).

6.2.3.1 Definition of different criteria

i. Minimize the share of local roads on a route.

The major function of local roads is to provide direct access to residential and commercial areas. These have lower speed limits and are not meant for through-traffic. A greater proportion of local roads along a route can result in increased transitions between high-speed and low-speed roadway segments (Pervaz et al., 2024). Therefore, the proportion of this road type on a given route should be kept to a minimum. The percentage length share ($ls_{lr}^{p,w}$) of local roads on a route is calculated as the length of local roads ($l_{lr}^{p,w}$) to the total length (l_p^w) of a route p between OD pair w (Equation (6.1)) (Dijkstra, 2013).

$$ls_{lr}^{p,w} = \frac{l_{lr}^{p,w}}{l_p^w} \times 100\%, \qquad \forall p \in P_w, w \in W \tag{6.1}$$

ii. Minimize the share of collector roads on a route.

The collector roads have a higher crash risk than the highways and should be used as little as possible. Therefore, the length of collector roads on a route should be minimized (Dijkstra, 2013). The percentage length share ($ls_{cr}^{p,w}$) of collector roads on a route is calculated as the length of collector roads ($l_{cr}^{p,w}$) to the total length (l_p^w) of a route p between OD pair w (Equation (6.2)).

$$ls_{cr}^{p,w} = \frac{l_{cr}^{p,w}}{l_p^w} \times 100\%, \qquad \forall p \in P_w, w \in W \tag{6.2}$$

iii. Minimize the total travel distance on a route.

The travel distance on a route explains the exposure to crash risk, which is generally measured in terms of total vehicle kilometers traveled (VKT) (Amoh-Gyimah et al., 2017). The shorter the distance on a route, the lesser the exposure to crash risk. Therefore, a higher safety score requires the total distance traveled on a route to be kept to a minimum. It is calculated by adding the length of all the links passing through a route, as shown in Equation (6.3).

$$l_p^w = \sum_{a \in A} \delta_a^p l_a, \qquad \forall p \in P_w, w \in W \tag{6.3}$$

iv. Minimize the density of intersections on a route.

Intersections in a road network are hotspots for serious and fatal crashes (Alarifi et al., 2017). In the US, roughly one-quarter of deadly and one-half of serious crashes are attributed to intersections (FHWA, 2024). Thus, a route with a lower density of intersections will be safer than one with a higher density. To calculate the safety score for this criterion, the intersection density is calculated as the number of intersections (n_i^p) per kilometer on a route (Equation (6.4)).

$$id_{p,w} = \frac{n_i^{p,w}}{l_p^w}, \qquad \forall p \in P_w, w \in W \tag{6.4}$$

6.2.3.2 Quantification of route safety score

For each route, the safety score is quantified based on the above four criteria by using the network topology data and applying Equations (6.5) and (6.6). To compare the scores of different routes, min-max normalization is carried out for each criterion such that the best route is awarded a score of 0 while the worst route is awarded a score of 1. The normalized score for any other route is calculated by subtracting the minimum

criterion score from the score of the route in question and then dividing this value by the range between the maximum and minimum scores for that criterion as shown in Equation (6.5) (Dijkstra, 2013; Dijkstra et al., 2007).

$$score_c^{p,w} = \frac{y_c^{p,w} - \min_c\{y_c^{p,w}\}}{\max_c\{y_c^p\} - \min_c\{y_c^{p,w}\}}, \qquad \forall p \in P_w, w \in W \tag{6.5}$$

where $score_c^p$ is the normalized score for criterion c of route p and y_c^p is the score of a criterion c for route p. The total score is calculated by multiplying the normalized score by a weight factor and adding all the criteria to get the score indicating the unsafety level Equation (6.6).

$$US_p^w = \sum_{c=1}^{C} score_c^{p,w} \times \gamma_c, \qquad \forall p \in P_w, w \in W \tag{6.6}$$

where US_p is the unsafety score for route p, γ_c is the weight factor for the criterion c, and C is the number of total criteria. The weight factor γ_c, in the unsafety score calculation, are set equally across the criteria (e.g., $\gamma_c = \frac{1}{|C|}$, where $|C| = 5$ in our case, yielding $\gamma_c = 0.2$ per criterion) to ensure the aggregate unsafety score remains bounded between 0 and 1 following the established literature (Dijkstra, 2013; Dijkstra et al., 2007). The unsafety score is deducted from 1 and multiplied by 100 as expressed in Equation (6.7) to arrive at the per cent safety score.

$$\Theta_p^{\mathrm{w}} = \left(1 - US_p^w\right) \times 100\%, \qquad \forall p \in P_w, w \in W \tag{6.7}$$

where Θ_p^{w} is the safety score, which indicates the degree of safety for each route p.

6.2.3.3 Safety-conscious route choice sets

Travelers with varying safety requirements may have different route choice sets. Some travelers might exclude specific available routes from their choice set if the safety level

of those routes is less than their acceptable safety requirement. Generally, a more safety-conscious traveler will have a more limited route choice set than a less cautious traveler. This is because a more safety-conscious traveler may prefer a safer route, even if it is not the shortest option. Thus, users with heterogeneous safety requirements traveling between OD pair w can be divided into M classes, where each class has its own route choice set shown in Equation (6.8).

$$P_w^m \subseteq P_w, \qquad \forall\, w \in W, m \in M \tag{6.8}$$

Here P_w represents the entire route choice set while P_w^m is the route choice set for user class m between OD pair w.

Definition 1. A route $p \in P_w$ in OD pair $w \in W$ will be included in the route choice set P_w^m for user class m if its safety score is greater than the safety requirement of that user class (Equation (6.9)).

$$P_w^m = \{p \in P_w \mid \Theta_p^{\mathrm{w}} \geq \Theta_{req}^m\}, \qquad \forall\, w \in W, m \in M \tag{6.9}$$

where Θ_p^{w} is the safety score of a route p between OD pair w and Θ_{req}^m is the safety requirement of user class m. The safety requirement parameter Θ_{req}^m introduced to represent heterogeneous safety preferences across traveler classes. It serves as a minimum safety score for route inclusion in the choice set, analogous to risk thresholds used in prior studies (Li & Huang, 2019). While analyst-defined in this study, the parameter could be calibrated from empirical data in practice.

Figure 6.2 illustrates the methodology outlined in Section 6.2.3 for assessing the safety levels of routes with diverse characteristics. For demonstration purposes, two routes with distinct features are presented. The safety level of each route can be calculated based on Equation (6.7) using the criteria in Equations (6.1) – (6.4). The safety-

conscious route choice set for each user class can be determined based on their safety requirements, as shown in Equation (6.9).

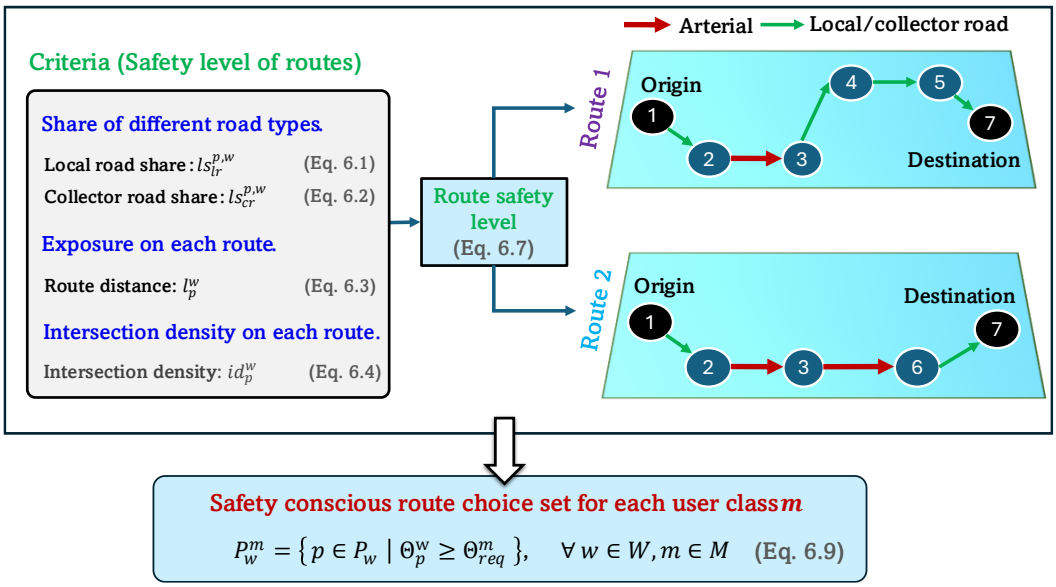

Figure 6.2. Methodology for calculating safety level of routes and safety-conscious choice sets.

6.2.4 Safety of a route based on traffic conditions

In this section, we introduce the safety of a route in relation to its traffic conditions (i.e., the travel speed and travel time). Safety of a transportation system is the product of crash risk per unit exposure and the number of exposure units occurring on the system during the specified time period as illustrated in Figure 6.3 (Chapman, 1973; Hauer, 1982). The travelers crash risk is affected by a number of factors such as traffic conditions, driver behavior and environmental characteristics (e.g., weather). Exposure is defined as some form of travel either by foot or vehicle. The exposure factors measure how exposed travelers are to risk such as traveling for longer time periods or longer distance could increase the likelihood of being involved in a dangerous situation. In transportation safety, travel time (Chipman et al., 1992), travel volume (Wong et al., 2007) and travel distance (Amoh-Gyimah et al., 2017) are often used as proxies for exposure. Here we define safety in terms of crash risk cost (CRC), which indicates the

level of crash risk in terms of the societal losses incurred due to crash occurrence and severity. In the next section, CRC distribution is introduced to consider the reliability and unreliability of safety variability.

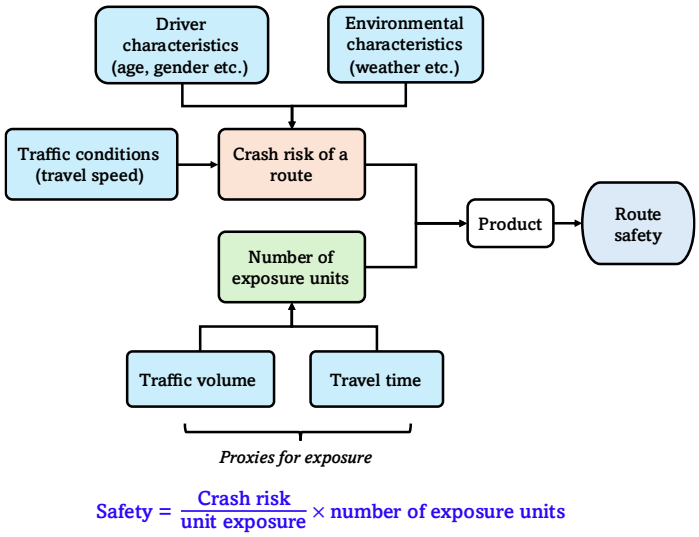

Figure 6.3. Crash risk cost (safety) of a route based on traffic conditions

6.2.4.1 Crash risk cost distribution

Each link in a road network has an average crash risk (average safety condition) due to its preexisting design features and traffic flow under specific conditions. The mean safety condition of a road link can be estimated by evaluating the environmental, roadway, and driving-related factors (Figure 6.4). However, travelers' crash risk on a road segment is random due to variability in the safety conditions. Accurately estimating the safety condition of a traveler traveling on a route may not be possible (Huang & Abdel-Aty, 2010; Mannering & Bhat, 2014). This study assumes that travelers have acquired knowledge regarding the distribution of safety variability, such as the CRC, on each segment of the road network. Travelers acquire this knowledge through accumulated long-term travel experiences, which they integrate into their decision-making processes, ultimately resulting in a habitual equilibrium flow pattern over time. Thus, in addition to the average safety condition of a road link, travelers also

consider the safety reliability (probability of a trip being safe more frequently) and unreliability (probability of significantly higher CRC) aspects of safety variability.

It is assumed that the CRC follows a statistical distribution, described by its mean and variance, which is termed the CRC distribution (Huang et al., 2020). The CRC distribution for a road link (r_a) is shown in Figure 6.4 (green box). μ_a is the mean of CRC distribution which corresponds to the safety aspects of road properties under specific driving conditions and σ^2 is the variance of CRC distribution, which represents the safety variability. The hypothetical link CRC distribution illustrated in Figure 6.4 serves as a theoretical model to capture the traveler's subjective perception of the mean safety and safety variability. Nonetheless, it is essential to validate the parameters of this distribution using empirical data to adopt it for different road types and traffic conditions.

The mean and variance of the CRC distribution are calculated using travel time (t_a) as an exposure indicator, which helps explain differences in crash risk associated with varying driving patterns. (Pei et al., 2012). Moreover, travel speed is one of the most significant factors influencing crash occurrence, crash severity, and, most importantly, traveler's safety perception, as evident from various empirical studies (Aljanahi et al., 1999; Elvik, 2002). The relationship between the traveler's perception of mean CRC (μ_a) and the average travel speed (v_a) is based on the crash risk model proposed by Elvik et al. (2004), shown in Figure 6.4 (green box). Similarly, the perceived CRC variance (σ^2) also depends on the average speed of the road segment, as shown in Figure 6.4 (green box) (Huang et al., 2020).

Based on the definition of link CRC distribution, the route CRC distribution ($\mathrm{r_p}$) can be obtained by summing the CRC variables of the corresponding links, as illustrated in

Figure 6.4 (orange box). Assuming that the link's CRC distribution is independent, bounded, and has a finite, non-zero variance, the central limit theorem indicates that the route CRC distribution converges to a normal distribution (Lo et al., 2006). Therefore, the mean (μ_p) and standard deviation (σ_p) of the route's CRC can be expressed as shown in Figure 6.4 (orange box).

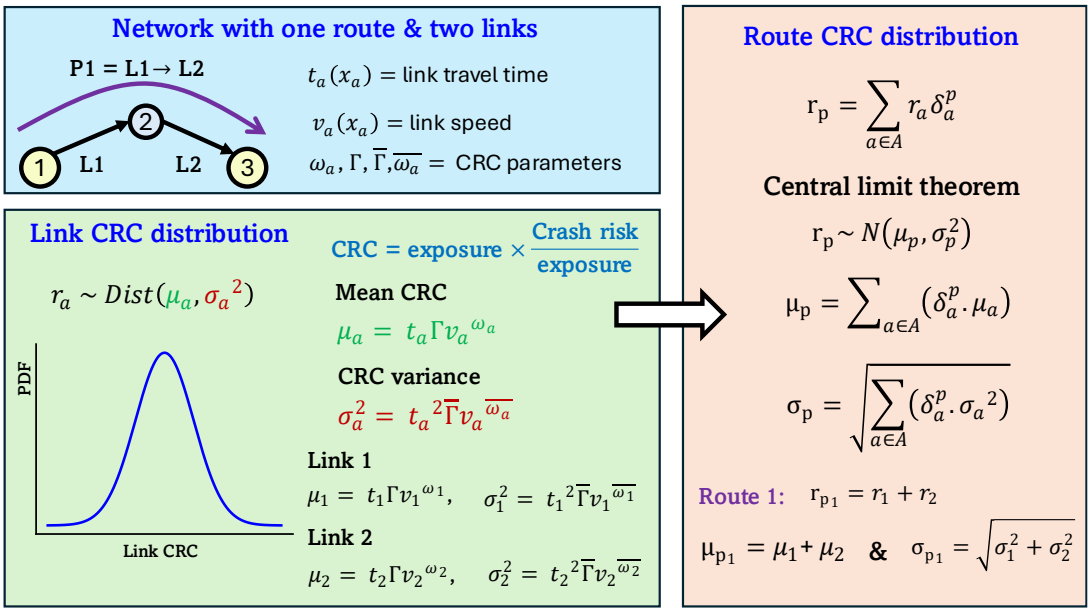

Figure 6.4. Illustration of link and route CRC distribution for a small network.

For modeling tractability and to highlight the core mechanisms of safety-oriented route choice with heterogeneous preferences, this study assumes independent link CRC distributions, allowing route CRC distributions to follow normal distribution via the central limit theorem. This mirrors common assumptions in travel time variability models (Chen & Zhou, 2010; Lam et al., 2008; Lo et al., 2006; Shao et al., 2006), despite empirical evidence of link correlations due to congestion propagation, shared infrastructure, or external factors such as weather (Liu et al., 2017; Prakash & Srinivasan, 2015; Srinivasan et al., 2014). While such correlations have been addressed in advanced equilibrium frameworks (Chen et al., 2020; Prakash et al., 2018), their incorporation here is left for future work to maintain focus on behavioral insights.

Additionally, a small network example with two links and one route, depicted in Figure 6.4 (blue box), demonstrates how the route CRC distribution is derived from the link CRC distributions, as shown in Figure 6.4 (orange box). In the next section, we explain the concept of mean excess crash risk cost (MECRC).

6.2.4.2 Definition of mean excess crash risk cost

Various aspects of the transportation system are unreliable: for example, whether an individual will be able to arrive at the destination on time, whether an individual will be able to get a seat on the bus, and whether an individual will be able to reach his destination safely (Bates et al., 2001). In theory, individual decision-making is governed by generalized cost, which is intrinsically linked to utility theory. Under uncertainty: an individual chooses an option, keeping in mind the probability of different outcomes, that has the highest value of expected utility (minimum cost) and minimum associated risk/uncertainty (developed from the basic theory proposed by Von Neumann and Morgenstern (1944)) (Bates et al., 2001). The mean represents the expected value of choice, and the variance defines the risk or uncertainty.

This study assumes that travelers have gained prior knowledge of the distribution of each alternative's safety variability (CRC variability) based on their past traveling experiences, which they incorporate into their route choice decisions. Travelers have different safety preferences, as some may be more concerned about their safety than others, judged by their driving behaviors (May et al., 2008). For instance, research has shown that older drivers tend to be more safety-conscious than younger drivers (Deery, 1999; McKenna & Horswill, 2006). By considering the safety reliability requirements, travelers select routes for which effective CRC guarantees a higher probability of safe arrival at a predefined confidence level α (Huang et al., 2020), as shown in Equations (6.10) and (6.11).

$$R_p^w(\alpha) = \min\left(R | Pr(S_p^w \leq R) \geq \alpha\right) \tag{6.10}$$

$$R_p^w = \mu_p^w + \phi(\alpha).\sigma_p^w \qquad \forall p \in P_w, w \in W \tag{6.11}$$

where R is the effective CRC required to ensure safe arrival at a confidence level α. $\phi(\alpha).\sigma_p$ is the extra CRC added to the mean CRC as CRC margin to ensure more frequent safe arrivals under the CRC reliability requirement at a predefined confidence level α. This concept is analogous to the travel time budget (Lo et al., 2006).

However, travelers with higher safety concerns also consider the consequences of excessively higher crash risk costs (i.e., the unreliability aspects of safety variability). If the consequences of traveling on a particular route result in a very high CRC, such as a traffic crash with a higher probability of severe injury or fatality, the route would be considered entirely unacceptable to the traveler. The CRC is associated with various factors, including driving conditions, roadway features, and human behavior. Driving conditions, such as heavy traffic and high travel speeds, can increase the risk of crashes, as can poorly designed roadway features, such as undivided highways or roads with poorly designed horizontal and vertical curves. Studies have shown that impact speed is directly related to crash severity (Hauer, 2009; Solomon, 1974), and heavy truck volume increases the probability of severe crashes (Behnood & Mannering, 2019). Additionally, traffic crashes on undivided highways have a higher likelihood of resulting in severe injury or fatality (Kadeha et al., 2021; Kidando et al., 2019). Thus, it is rational for travelers to select a route that ensures safety reliability (defined by effective CRC) more frequently while minimizing the expected unreliability aspect (i.e., unaccepted CRC beyond effective CRC). It means travelers ensure a safe trip more regularly at a specified confidence level α, and avoid the routes with a higher probability of fatal/severe crashes (unacceptable high CRC). This tradeoff between the

reliable and unreliable aspects of the safety variability can be modeled by adopting the METE model (Chen & Zhou, 2010; Chen et al., 2011; Xu et al., 2014). The mean excess crash risk cost (MECRC) is explained here.

The MECRC, $\psi_p^w(\alpha)$, for a route $p \in P^w$ between OD pair w at a specified confidence level α is equal to the conditional expectation of CRC exceeding the corresponding route's effective CRC $R_p^{rs}(\alpha)$ as shown in Equation (6.12).

$$\psi_p^w(\alpha) = E\left[S_p^w | S_p^w \geq R_p^w(\alpha)\right] \quad \forall p \in P_w, w \in W \tag{6.12}$$

where S_p^w is the random CRC on a route p between OD pair w, $E[.]$ is the expectation operator, and R_p^w is the effective CRC defined in Equation (6.11).

If the route CRC distribution $f(S_p^w)$ is known, the mean excess CRC (MECRC) definition in Equation (6.12) as a conditional expectation can be rewritten as:

$$\psi_p^w(\alpha) = E\left[S_p^w | S_p^w \geq R_p^w(\alpha)\right] = \int_{S_p^w \geq R_p^w(\alpha)} S_p^w \frac{f(S_p^w)}{\Pr(S_p^w \geq R_p^w)} d(S_p^w) \tag{6.13}$$

$$\psi_p^w(\alpha) = \frac{1}{1-\alpha} \int_{S_p^w \geq R_p^w(\alpha)} S_p^w f(S_p^w) d(S_p^w) \tag{6.14}$$

Equation (6.14) can be written as.

$$\psi_p^w(\alpha) = R_p^w(\alpha) + E\left(S_p^w - R_p^w(\alpha) | S_p^w \geq R_p^w(\alpha)\right) \tag{6.15}$$

The MECRC can be divided into two parts. The first part is precisely the effective CRC of route p, explaining the reliability aspect of the safety variability (more frequent safe arrivals) at a user-specified confidence level α. The second part is the "expected excess CRC (EECRC)" beyond the effective CRC, reflecting the unreliability aspect of safety variability (i.e., possible high-risk scenarios) in the distribution tail of $1-\alpha$. MECRC criterion based on the METE model incorporates safety variability's reliability and

unreliability aspects. In our model, both aspects are assumed to affect the traveler's decisions.

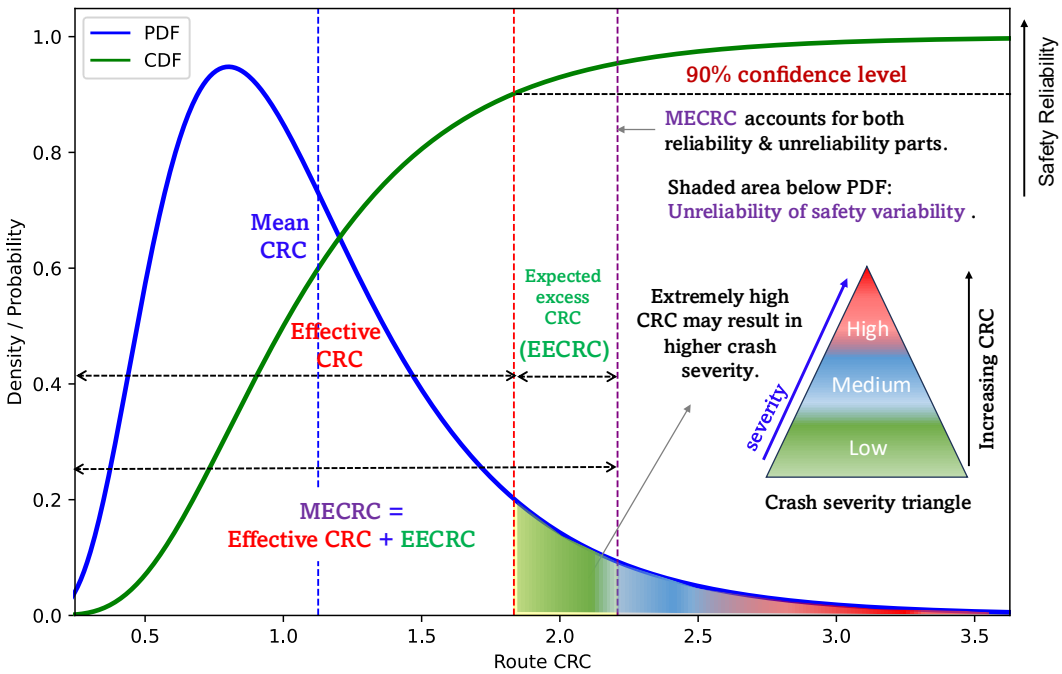

Figure 6.5. Illustration of the mean excess crash risk cost

To explain the concept of MECRC, Figure 6.5 illustrates a route's hypothetical CRC distribution, with both the probability density function (PDF represented by a blue line) and cumulative density function (CDF represented by a green line). At a specified confidence level α, effective CRC is defined as the minimum CRC threshold, calculated as the sum of mean CRC (MCRC) and buffer CRC (BCRC), that travelers are willing to accept such that the cumulative probability of the actual CRC being less than this limit is at least α. The tail (shaded area) of the distribution beyond the effective CRC represents all the possible high-risk scenarios (potential crashes) in which the actual CRC exceeds the effective CRC. When considering the unreliability aspect of safety variability, travelers may accept a higher CRC margin to increase their probability of safe arrival further

As illustrated in Figure 6.5, the effective CRC does not capture the magnitude of CRC associated with the most severe outcomes. It cannot differentiate between situations where the actual CRC slightly exceeds the effective CRC (indicating low-severity crashes) and those where it greatly exceeds (indicating high-severity crashes). Thus, while the effective CRC addresses the reliability aspect of safety variability at a specified confidence level α, the MECRC accounts for both the reliability (i.e., effective CRC required for safe arrival at a confidence level α) and the unreliability of safety variability (i.e., accounting for the worst crash severity levels). The MECRC, therefore, comprises both the effective CRC and the expected excess CRC beyond the effective CRC.

6.2.4.3 Derivation of mean excess crash risk cost

The link CRCs are assumed to be independent, similar to previous studies modeling safety variability Huang et al. (2020). Thus, according to the central limit theorem, the route CRC distribution follows a normal distribution, as shown in Figure 6.4. According to the definition of MECRC in Equation (6.12), the route MECRC can be expressed as follows:

$$\min \frac{1}{1-\alpha} \int_{R_p^w}^{\infty} S_p^w . \frac{1}{\sigma_p^w \sqrt{2\pi}} \exp\left(-\frac{\left(S_p^w - \mu_p^w\right)^2}{2\left(\sigma_p^w\right)^2}\right) d\left(S_p^w\right) \tag{6.16}$$

$$s.t \int_{-\infty}^{R_p^w} \frac{1}{\sigma_p^w \sqrt{2\pi}} \exp\left(-\frac{\left(S_p^w - \mu_p^w\right)^2}{2\left(\sigma_p^w\right)^2}\right) d\left(S_p^w\right) \geq \alpha, \tag{6.17}$$

where Equation (6.17) represents the crash risk cost reliability chance constraint. MECRC of route p can be represented as.

$$\psi_p^w = \mu_p^w + \frac{\sigma_P}{\sqrt{2\pi}(1-\alpha)} \exp\left(-\frac{\left(\phi^{-1}(\alpha)\right)^2}{2}\right) \tag{6.18}$$

While we rely on the independent assumption of link CRCs, they may not be independent due to the network topology or sources of uncertainty. Thus, link interactions should be considered in future research.

6.2.5 UE formulation considering safety-conscious route choice sets

In this section, we provide the UE formulation for the METE model, considering the travelers' travel time variability and safety variability concerns. In general, traveler classes are characterized by different levels of safety variability concerns and a corresponding confidence level α_m exist on the road network. Each class m has its own route choice set determined by its specific safety requirements, denoted as Θ_{req}^m, shown in Equation (6.9). Thus, the generalized cost for class m can be represented as:

$$G_{p,m}^w = \psi_{p,m}^w + \Lambda(\eta_p^w) \tag{6.19}$$

where $\psi_{p,m}^w$ is the MECRC for travelers of class m (Equation (6.20)).

$$\psi_{p,m}^w = \mu_p^w + \frac{\sigma_p^w}{\sqrt{2\pi}(1-\alpha_m)} \exp\left(-\frac{\left(\phi^{-1}(\alpha_m)\right)^2}{2}\right) \tag{6.20}$$

η_p^w is the travelers' METT and Λ is the cost-converting factor of travel time. METT is also assumed to follow normal distribution and can be expressed as follows (Chen & Zhou, 2010):

$$\eta_p^w = T_p^w + \frac{\widetilde{\sigma_p^w}}{\sqrt{2\pi}(1-\tilde{\alpha})} \exp\left(-\frac{\left(\phi^{-1}(\tilde{\alpha})\right)^2}{2}\right) \tag{6.21}$$

It is logical to assume that travelers of each class aim to minimize their generalized cost when traveling between OD pair w in an uncertain environment. Accordingly, the long-term habitual flow pattern can be reached, which is termed the multiclass mean excess traffic equilibrium (MC-METE) model. Let G represent the generalized cost vector

$\left(\ldots, G_{p,m}^{w}, \ldots\right)^{T}$, π_{m}^{w} represent the minimum generalized cost for traveler class m between an O-D pair w, i.e., $\pi_{m}^{w} = min\left(\sum_{m=1}^{M}\sum_{p\in P_w} G_{p,m}^{w}\right)$, and f denote the route-flow vector $\left(\ldots, f_{p,m}^{w}, \ldots\right)^{T}$. Thus, the equilibrium conditions can be stated as follows.

At the equilibrium state, for each traveler class, no individual traveler can reduce their generalized cost by unilaterally switching routes. This implies that all routes utilized between an OD pair w have equal and minimal generalized costs and that no unused route offers a lower generalized cost than those included in the choice set. The following conditions must be satisfied (Equation (6.22)).

$$G_{p,m}^{w}(f^{*}) - \pi_{m}^{w}\begin{cases} = 0 & \text{if } \left(f_{p,m}^{w}\right)^{*} > 0 \\ \geq 0 & \text{if } \left(f_{p,m}^{w}\right)^{*} = 0 \end{cases} \qquad \forall p \in P_{w}^{m}, \forall w \in W, \forall\, m \in M \tag{6.22}$$

Such an equilibrium state can be formulated as a variational inequality (VI) problem, in which the objective is to find a solution vector of route flows $f^{*} \in \Omega$, such that:

$$G(f^{*})^{T}(f - f^{*}) \geq 0, \qquad \forall f \in \Omega \tag{6.23}$$

where the following equations define the feasible set Ω:

$$\sum_{p\in P_{w}^{m}} f_{p,m}^{w} = q_{w}^{m}, \qquad \forall w \in W, \forall\, m \in M \tag{6.24}$$

$$x_{a} = \sum_{m\in M}\sum_{w\in W}\sum_{p\in P_{w}^{m}} f_{p,m}^{w}\delta_{a}^{p}, \qquad \forall a \in A \tag{6.25}$$

$$f_{p,m}^{w} \geq 0 \qquad \forall p \in P_{w}^{m}, \forall w \in W, \forall\, m \in M \tag{6.26}$$

where $f_{p,m}^{w}$ is the flow for traveler class m on route $p \in P_{w}^{m}$ connecting an OD pair w; $G_{p,m}^{w}$ is the generalized travel cost for traveler class m on route p connecting an OD pair w; q_{w}^{m} is the travel demand for traveler class m between an OD pair w; x_{a} is the link flow on the link a; δ_{a}^{p} denotes the link-route incidence indicator, which takes the

value of 1 if link a is included in route p connecting an OD pair w, and 0 otherwise. The conservation, definitional, and non-negative constraints are given in Equations (6.24), (6.25), and (6.26), respectively.

The subsequent two propositions demonstrate both the equivalence of the variational inequality (VI) formulation to the equilibrium condition and the existence of an equilibrium solution.

Proposition 1 (Equivalence). Suppose the route generalized cost function $\mathrm{G}(\mathrm{f})$, which comprises the sum of the METT and the MECRC cost functions for each route, is positive. Then, the solution to the VI formulation is equivalent to the equilibrium solution of the MC-METE model.

Proof. f^* is a solution of the VI problem if and only if it is a solution of the following linear program:

$$\min_{f \in \Omega} G(f^*)^T f \tag{6.27}$$

By examining the primal-dual optimality conditions of (6.27), we have.

$$f_{p,m}^{w*}\left(G_{p,m}^{w}(f^*) - \pi_m^w\right) = 0, \qquad \forall p \in P_w^m, \forall w \in W, \forall\, m \in M \tag{6.28}$$

$$G_{p,m}^{w}(f^*) - \pi_m^w \geq 0, \qquad \forall p \in P_w^m, \forall w \in W, \forall\, m \in M \tag{6.29}$$

It is evident that the MC-METE condition (6.22) is satisfied. This completes the proof. □

Proposition 2 (Existence). The proposed VI problem admits at least one solution, provided that the generalized travel cost on each route between O-D pair w for each class is positive and continuous with respect to its route flow.

Proof. Note that the feasible set Ω is nonempty, closed, and convex. Furthermore, the mapping $G(f)$ is positive and continuous with respect to f. Thus, the VI problem has at least one solution. This completes the proof. □

6.2.6 Solution algorithm

This section introduces the two-stage algorithm for solving the TA model (Figure 6.6).

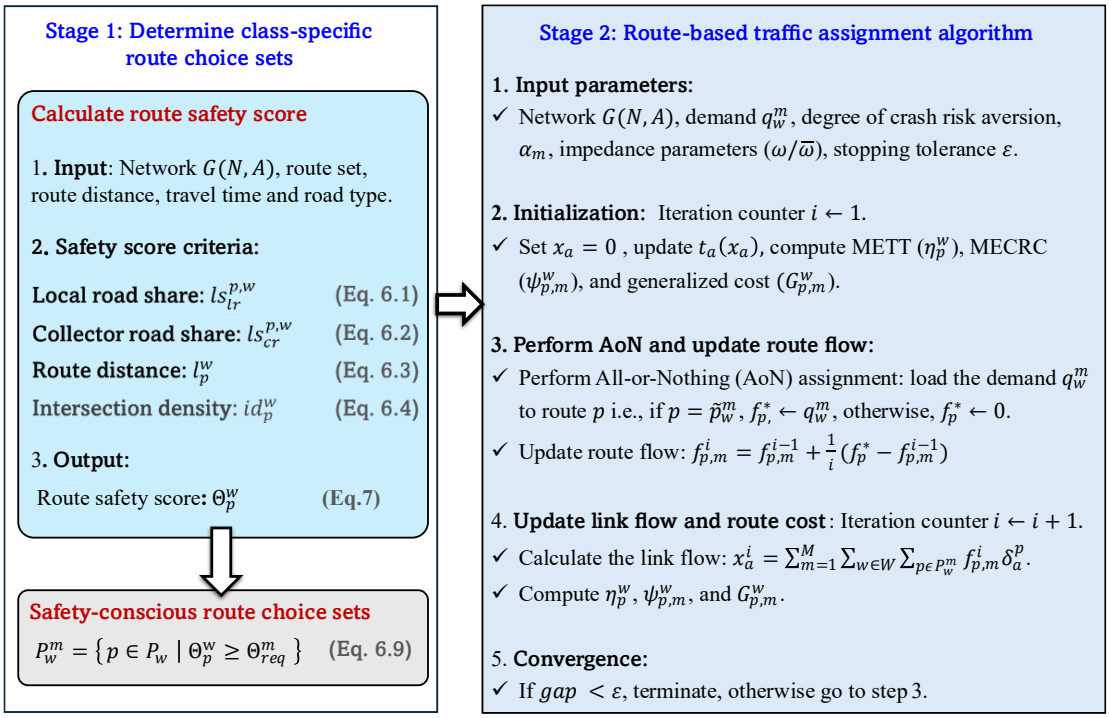

Figure 6.6. An overview of the two-stage algorithm

In Stage 1, safety scores for all routes in the given route set between each OD pair are calculated using the methodology in Section 6.2.3. These scores determine route choice sets for each class according to their safety score requirements. In Stage 2, the non-additive traffic assignment problem is solved using a route-based algorithm, as the route costs are non-additive with link costs and must be treated as route-specific (Lo & Chen, 2000). The method of successive averages (MSA) is used to iteratively update the step size and flow.

6.3 Numerical experiments

This section presents the results from two networks to demonstrate the properties and application of the model. First, we analyze a small network with two traveler classes to illustrate the safety-conscious route choice behavior. This is followed by examining a real-world network, specifically the Winnipeg network.

6.3.1 A small network: Single class travelers to compare different TA models

In this example, a small network consisting of 6 links and 4 routes is illustrated in Figure 6.7. The link free-flow travel time, link capacity, link length, variance of free-flow travel time, and travelers' risk perception of a link related to its features are shown in Table 6.2. The parameters used in the link performance and generalized cost functions are $\gamma = 0.15$, $\beta = 4.0$, and $\Lambda = 3.0$. The CRC and travel time for each link are assumed to follow a normal distribution to facilitate the use of analytical expressions for the MECRC and METT.

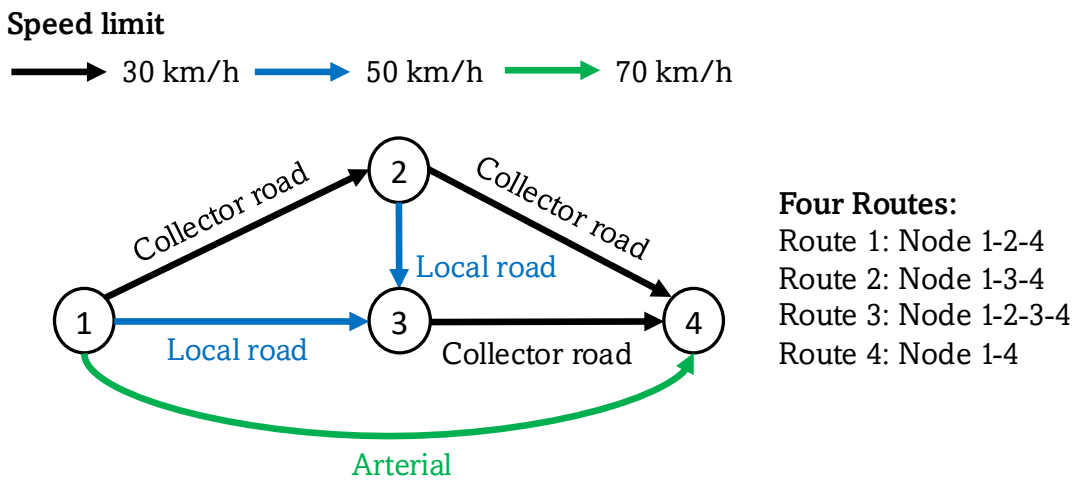

Figure 6.7. A small network comprising five links and four routes

The mean travel time is calculated using the BPR function provided in Equation (6.30).

$$t_a = t_a^0 \left(1 + 0.15 \left(\frac{x_a}{c_a}\right)^4\right) \tag{6.30}$$

Table 6.2. Link characteristics for a small network

Link	Type	t_a^0 (min)	C_a (pcu/h)	l (m)	$\widetilde{\sigma_a^2}$ (min)	ω_a	$\overline{\omega_a}$
1-2	Collector	1.4	921	1139	1.0	2.0	2.5
1-3	Local road	0.9	952	450	1.0	2.1	2.6
1-4	Arterial	2.6	1200	3014	1.0	2.0	2.5
2-3	Local road	1.2	921	600	1.0	2.0	2.5
2-4	Collector	1.1	952	944	1.0	2.0	2.5
3-4	Collector	1.0	1071	833	1.0	2.1	2.6

For the comparison between different traffic assignment models, we consider a single user class with the safety score requirement $\Theta_{req} = 0\%$, meaning all the routes are included in the choice set. The confidence levels for both the CRC distribution (α) and the travel time distribution ($\tilde{\alpha}$) are set equal to 0.9. The results are presented in Figure 6.8, which illustrates how equilibrium route flows change under different route choice criteria.

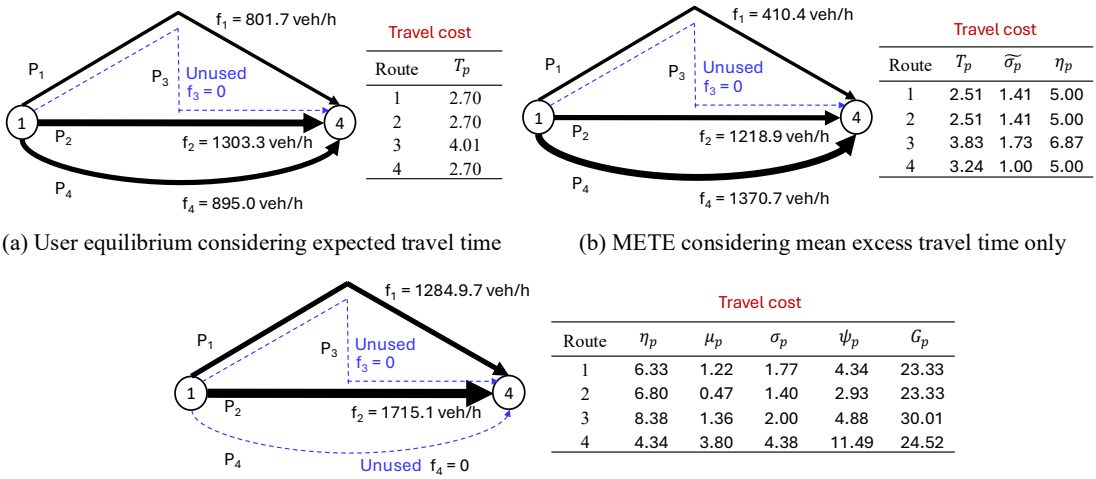

(a) User equilibrium considering expected travel time

(b) METE considering mean excess travel time only

(c) METE considering both mean excess travel time and mean excess CRC

Figure 6.8. Equilibrium path flow patterns for different traffic assignment models

In the UE case shown in Figure 6.8(a), the highest flow is noticed on route 2, followed by route 4. Figure 6.8(b) presents the METE model in which travelers consider mean excess travel time only; here, flows from routes 1 and 3 shift to route 4 due to its lowest

travel time variability, reflected in the lowest variance ($\widetilde{\sigma_4} = 1.0$). Figure 6.8(c) shows the METE model where travelers consider both mean excess travel time and mean excess CRC. In this case, route 4 attracts no flow because of its high safety variability ($\sigma_p = 4.38$), and the highest flow shifts to route 2, which has the lowest safety variance ($\sigma_p = 1.40$). This comparison demonstrates how equilibrium flow patterns differ depending on whether travelers account for expected travel time alone, travel time variability, or both travel time and safety variability in their generalized cost.

6.3.2 A small network: Multiclass travelers with heterogeneous safety concerns

To model travelers with heterogeneous safety concerns, we assume that the network in Figure 6.7 consists of two traveler classes (TC) in a multiclass mixed equilibrium model. The confidence level $\tilde{\alpha}$ for travel time distribution equals 0.9 for both the classes. TC_1 is low safety-conscious while TC_2 is high safety-conscious. We look into safety heterogeneity from two perspectives: (a) safety-conscious class-specific route sets by setting different Θ_{req}^{m} values and (b) heterogeneous safety variability preferences by setting different α_m values for the CRC distribution. Each class is assumed to have its own route choice set based on the safety score requirement (Θ_{req}^{m}) of each class (Table 6.3).

Table 6.3. Cases considered in numerical experiments

Case	Safety score requirement for each class		Generalized travel cost
	$\Theta_{req}^{TC_1}$	$\Theta_{req}^{TC_2}$	
1	0%	0%	METT and MECRC
2	0%	40%	METT and MECRC
3	0%	60%	METT and MECRC
4	0%	0%	ETT and MECRC

Note: MECRC stands for "mean excess crash risk cost"; ETT stands for "expected travel time"; and METT stands for "mean excess travel time"

The safety score requirement of TC_1 ($\Theta_{req}^{TC_1}$) is set to 0% in all cases, meaning that all routes are included in its choice set. On the other hand, TC_2, which is considered more

safety-conscious, has a different safety score requirement ($\Theta_{req}^{TC_2}$) for each case (Table 6.3). The confidence level α_m for the CRC distribution equals 0.5 for TC_1 while it is equal to 0.9 for TC_2, which means TC_2 is more concerned about CRC variability

Based on the network data, the safety score of each route is calculated in Table 6.4-Table 6.5, following the procedure explained in Section 6.2.3. We can see that the route with the highest safety score is route 4 while route 3 has the lowest safety score, as shown in Table 6.5.

Table 6.4. Normalized scores for each route

Criterion	Variable	Unit	Scores for each route				Normalized scores for each route			
			1	2	3	4	1	2	3	4
1	ls_{lr}	%	0.00	0.35	0.23	0.00	0.00	1.00	0.67	0.00
2	ls_{cr}	%	1.00	0.65	0.77	0.00	1.00	0.65	0.77	0.00
3	l	m	2083	1283	2572	3014	0.46	0.00	0.74	1.00
4	id	km^{-1}	1.44	2.34	1.56	0.66	0.46	1.00	0.53	0.00

Table 6.5. Weighted normalized scores for each route

Criterion	Variable	Unit	Weight	Weighted normalized scores for each route			
				1	2	3	4
1	ls_{lr}	%	0.25	0.00	0.25	0.17	0.00
2	ls_{cr}	%	0.25	0.25	0.16	0.19	0.00
3	l	m	0.25	0.12	0.00	0.19	0.25
4	id	km^{-1}	0.25	0.12	0.25	0.13	0.00
			US_p	0.48	0.66	0.68	0.25
			Θ_p	52%	34%	32%	75%

Figure 6.9 presents a comparison of the unsafety scores for each criterion and total safety score across three routes. Route 4 has the highest safety score ($\Theta_4 = 75\%$), as it has the lowest unsafety scores for three (i.e., ls_{lr}, ls_{cr} and id) out of four criteria. Routes 1 and 4 have safety scores greater than 50% while routes 2 and 3 have safety scores less than 50%.

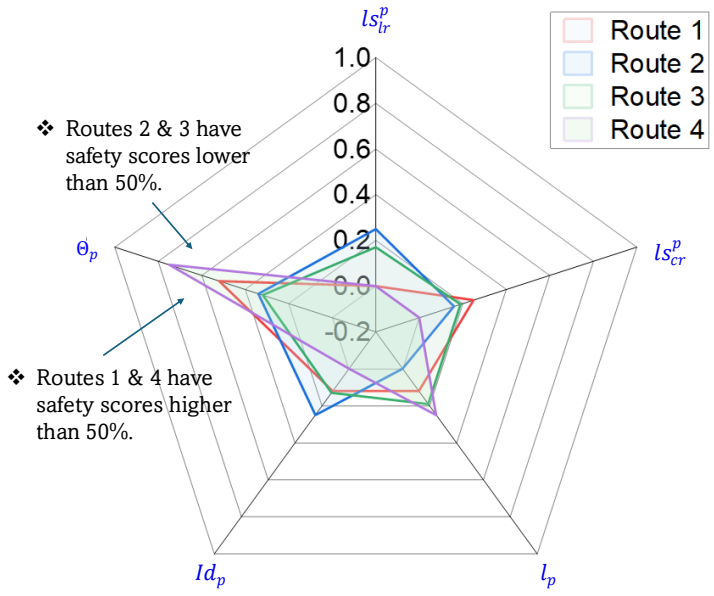

Figure 6.9. Illustration of unsafety scores for each criterion and total safety score for routes

6.3.2.1 Equilibrium flows for travelers with heterogeneous safety concerns (Case 1)

The results for the multiclass mixed equilibrium model for case 1 are presented in Table 6.6. In this case, all the routes are considered in the choice sets of both classes. Route 2 stands out as the safest option based on MECRC, exhibiting both the smallest mean CRC ($\mu_2 = 0.75$) and the lowest CRC variability ($\sigma_2 = 1.25$). It also has the lowest MECRC ($\psi_2 = 1.73$), while route 4 achieves the lowest METT ($\eta_4 = 4.34$) for both the traveler classes. For TC_1, which is low risk-averse, most of the flow is allocated to route 1, which has the second-lowest MECRC while a portion of flow is also assigned to route 2, which has the lowest MECRC, reflecting some preferences for safer routes. Additionally, some flow is also allocated to route 4 due to its lowest METT among all the routes, attributed to its minimal travel time variability. At equilibrium, it is observed that all the three used routes (routes 1,2, and 4) have the same generalized cost ensuring consistency with equilibrium conditions.

For the TC_2, which is high risk averse (higher concern for safety variability), all the flow is allocated to route 2, as it has the lowest MECRC and the smallest CRC

variability. No flow is observed on the other three routes. This result highlights that the high-risk averse travelers in TC_2 exclusively choose route 2, prioritizing its lowest MECRC and CRC variability while avoiding the other three routes with a higher CRC variability. These travelers aim to ensure a safe arrival and avoid routes with a higher likelihood of severe or fatal crashes.

Table 6.6. Equilibrium flow of the multiclass travelers for case 1 ($\Theta_{req,TC_2} = 0\%$)

Class	Route	η_p	μ_p	σ_p	ψ_p	G_p	f_p	Used route
TC_1	1	5.81	1.41	1.84	2.89	20.32	1136.96	✓
	2	6.20	0.75	1.25	1.73	20.32	96.75	✓
	3	7.83	1.69	1.95	3.24	26.73	0.00	×
	4	4.34	3.80	4.38	7.29	20.32	266.28	✓
TC_2	1	5.81	1.41	1.84	4.65	22.07	0.00	×
	2	6.20	0.75	1.25	2.94	21.53	1500.00	✓
	3	7.83	1.69	1.95	5.12	28.61	0.00	×
	4	4.34	3.80	4.38	11.49	24.52	0.00	×

Note: ✓ denotes used route, × denotes unused route.

6.3.2.2 Effect of different route choice sets (Cases 2-3)

This section presents the effect of different route choice sets on the route flows in a multiclass mixed equilibrium model for cases 2 and 3. For case 2, $\Theta_{req}^{TC_2}$ is equal to 40%, therefore, the routes with the safety score of less than 40% (calculated in Table 6.7) are not considered as part of the choice set by TC_2. Only routes 1 and 4 are considered in the choice set by TC_2 while TC_1 considers all the 4 routes. For TC_2 most of the flow is allocated to route 1 which has the lowest MECRC between the two considered routes while the flow of TC_1 is all allocated to route 2 with the lowest MECRC (Table 6.7). We also notice that the generalized cost for route 2 is lowest for TC_2, however no flow is allocated to this route as it is not considered as part of the choice set. This finding shows that a more safety conscious traveler class may be willing to travel on routes with a higher generalized cost if their safety scores are lower than the safety requirement of that class.

Table 6.7. Equilibrium flow of the multiclass travelers for case 2 ($\Theta_{req,TC_2} = 40\%$).

Class	Route	η_p	μ_p	σ_p	ψ_p	G_p	f_p	Used route
TC_1	1	6.78	1.09	1.72	2.47	22.81	0.00	×
	2	5.80	0.84	1.29	1.87	19.26	1500	✓
	3	8.23	1.58	1.91	3.10	27.79	0.00	×
	4	4.34	3.80	4.38	7.29	20.32	0.00	×
TC_2	1	6.78	1.09	1.72	4.16	24.50	1381.67	✓
	2	5.80	0.84	1.29	3.10	20.49	0.00	**NC**
	3	8.23	1.58	1.91	4.93	29.62	0.00	**NC**
	4	4.34	3.80	4.38	11.47	24.50	118.33	✓

Note: ✓ denotes used route, × denotes unused route, NC denotes "not considered" route.

Table 6.8 presents the case in which the safety requirement is equal to 60% for TC_2 thus only route 4 is considered as part of the choice set and all the flow is allocated to this route while ignoring the other 3 routes. This route has a higher generalized cost compared to routes 1 and 2, however those routes are not considered in the choice set due to their safety score being lower than the safety requirement of TC_2.

Table 6.8. Equilibrium flow of the multiclass travelers for case 3 ($\Theta_{req,TC_2} = 60\%$).

Class	Route	η_p	μ_p	σ_p	ψ_p	G_p	f_p	Used route
TC_1	1	4.99	1.87	1.98	3.45	18.41	93.68	✓
	2	5.48	0.93	1.32	1.98	18.41	1406.32	✓
	3	7.06	2.09	2.07	3.74	24.92	0.00	×
	4	5.29	2.78	4.05	6.01	21.88	0.00	×
TC_2	1	4.99	1.87	1.98	5.35	20.31	0.00	**NC**
	2	5.48	0.93	1.32	3.26	19.68	0.00	**NC**
	3	7.06	2.09	2.07	5.72	26.90	0.00	**NC**
	4	5.29	2.78	4.05	9.90	25.76	1500.00	✓

Note: ✓ denotes used route, × denotes unused route, NC denotes "not considered" route.

Figure 6.10 presents the comparison for the first three cases presented in Table 6.6 to Table 6.8. Figure 6.11 illustrates the number of routes considered in the choice of TC_2 under different safety score requirements ($\Theta_{req}^{TC_2}$). At a higher value of $\Theta_{req}^{TC_2}$, there are a smaller number of routes in the choice set, resulting in an overall increase in the network generalized travel cost.

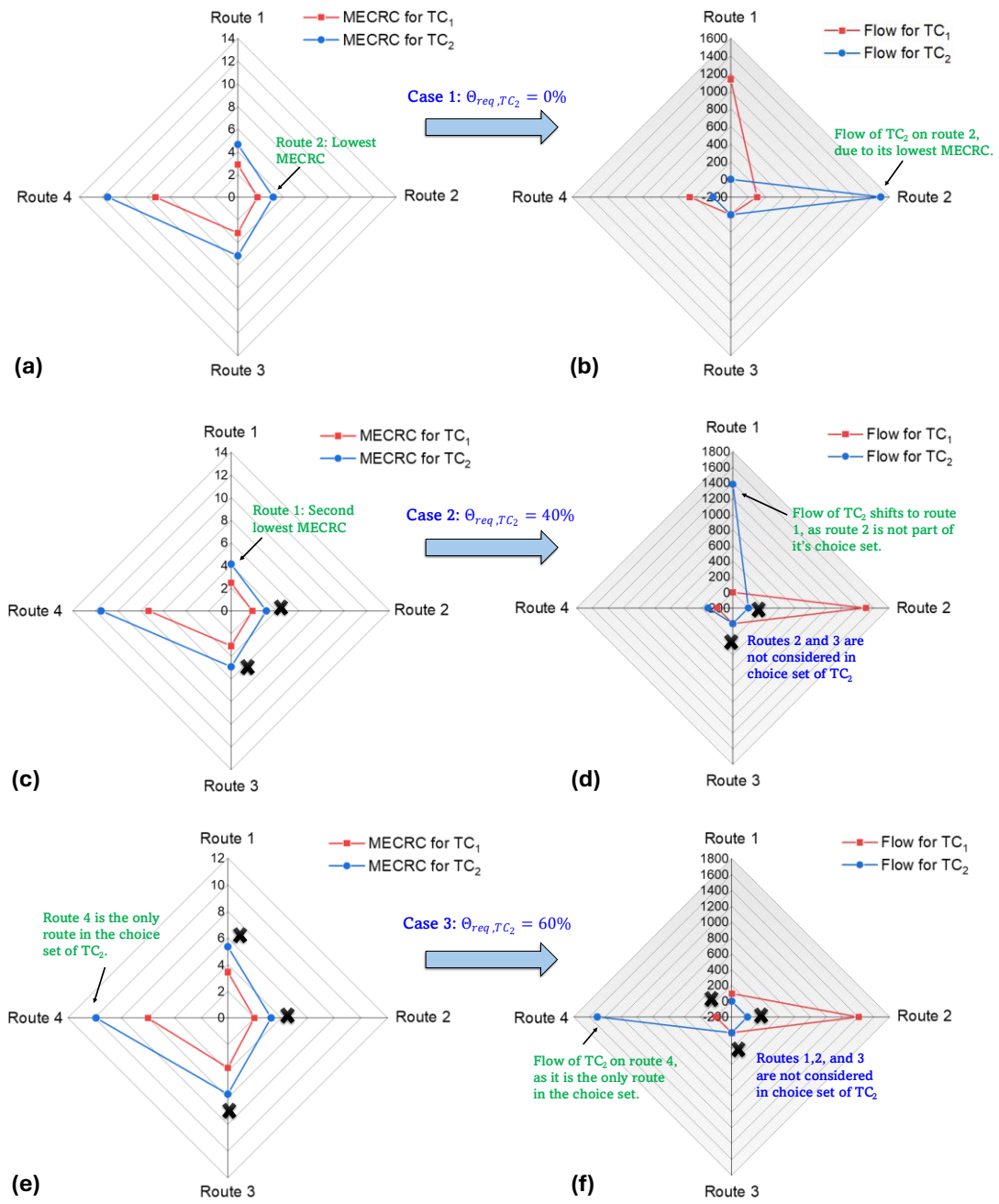

Figure 6.10. Comparison of results for three cases with different route choice sets for TC_2

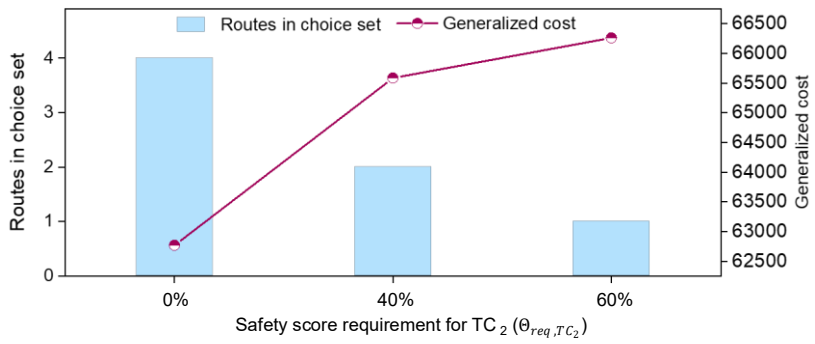

Figure 6.11. Routes in TC2's choice set at varying safety levels and their generalized costs

6.3.2.3 Expected travel time versus METT time in generalized cost (Case 4)

This section presents and compares the results for the case where the expected travel time is considered in the generalized cost instead of the METT. Differences in the flow patterns are observed between the two cases for TC_1. When the expected travel time is considered (Table 6.9), the flow is allocated exclusively to routes 1 and 2 for TC_1, as they have lower generalized costs. Both routes also exhibit the lowest MECRC compared to the other routes, even though their expected travel times are higher than that of route 4. In contrast, when travel time variability is considered in case 1 (Table 6.6), a portion of the flow is allocated to route 4. This is due to its lower travel time variability ($\widetilde{\sigma_4}$ =1.0), which results in the lowest METT among all routes, despite having the highest MECRC. Due to the consideration of travel time variability, travelers of class 1 also allocate some flow to route 4, as its generalized cost becomes equal to that of routes 1 and 2. This is because routes 1 and 2 have higher travel time variability, while route 4 offers lower variability, making it an attractive option despite its higher MECRC.

This finding demonstrates that equilibrium flow patterns vary depending on whether travelers consider expected travel time or METT along with MECRC when making route choice decisions. Incorporating both METT and MECRC in the generalized cost highlights the trade-offs between minimizing the travel time variability and CRC variability in travelers route choice. This finding demonstrates that equilibrium flow patterns vary depending on whether travelers consider expected travel time or METT along with MECRC when making route choice decisions. Incorporating both METT and MECRC in the generalized cost highlights the trade-offs between minimizing the travel time variability and CRC variability in travelers route choice.

Table 6.9. Equilibrium flow of the multiclass travelers for case 4.

Class	Route	T_p	μ_p	σ_p	ψ_p	G_p	f_p	Used route
TC_1	1	3.90	1.20	1.77	2.61	14.31	1298.69	✓
	2	4.23	0.65	1.20	1.61	14.31	201.31	✓
	3	5.33	1.50	1.88	3.00	19.00	0.00	×
	4	2.58	3.80	4.38	7.29	15.04	0.000	×
TC_2	1	3.90	1.20	1.77	4.31	16.01	0.00	×
	2	4.23	0.65	1.20	2.77	15.47	1500.00	✓
	3	5.33	1.50	1.88	4.81	20.81	0.00	×
	4	2.58	3.80	4.38	11.49	19.24	0.00	×

Note: ✓ denotes used route, × denotes unused route.

6.3.3 Real world case study: Winnipeg Network

Figure 6.12. Winnipeg network showing the road functional class

This section demonstrates the proposed model and solution procedure using the Winnipeg network (Figure 6.12), a real-scale network comprising 2,535 links and 4,345 OD pairs, with a total demand of 54,459 trips. The working route set for the network is adopted from Bekhor et al. (2008). In total, 174,491 routes are considered across all OD pairs, corresponding to an average of 40.1 routes for any OD pair. The maximum number of routes generated for any single OD pair is 50.

Since the original network does not include road functional class information, we utilized Google Maps to classify roads into two types: arterials and non-arterials

(collectors/local roads). Consequently, only three criteria are used to determine the safety score of each route. The variance-to-mean ratio of travel time is assumed to be equal to 0.3. The values of ω and $\overline{\omega}$ for all the links are set equivalent to 2.1 and 2.5, respectively. The adjustment coefficients used in the unit crash risk and safety reliability functions given in Equations 11 and 12 are taken as $\Gamma = 3 \times 10^{-4}$ and $\overline{\Gamma} = 7 \times 10^{-5}$ respectively.

The confidence level α_m for the CRC distribution equals 0.5 for TC_1 while it is equal to 0.95 for TC_2. The confidence level $\tilde{\alpha}$ for travel time distribution equals 0.9 for both the classes. Moreover, each class is assumed to have its own route choice set based on the safety score requirement ($\Theta_{req,m}$). Θ_{req,TC_1} and Θ_{req,TC_2} are set equal to 0% and 50% respectively, thus TC_2 only consider the routes with a safety score of greater than 50% in their choice set. The route-based traffic assignment algorithm is tested on a PC with intel(R) Core (TM) i7-10700 CPU 2.9 GHz and 16 GB RAM using the Windows 10 operating system. The stopping criteria are set equal to 1e-4.

6.3.3.1 Equilibrium results for travelers with heterogenous safety concerns

The aggregate link flows for the equilibrium model are presented in Figure 6.13, which highlights the distribution of flows across the network, with notably higher volumes observed in the CBD area. To further investigate the route choice behavior of heterogeneous travelers, we conducted a disaggregate analysis focusing on two high-demand OD pairs: (92, 4) and (79, 103). We consider two traveler classes, where TC_1 exhibits a lower crash risk aversion whereas TC_2 shows higher aversion to crash risk. Only the routes that are used by at least one of the two classes are shown for each OD pair.

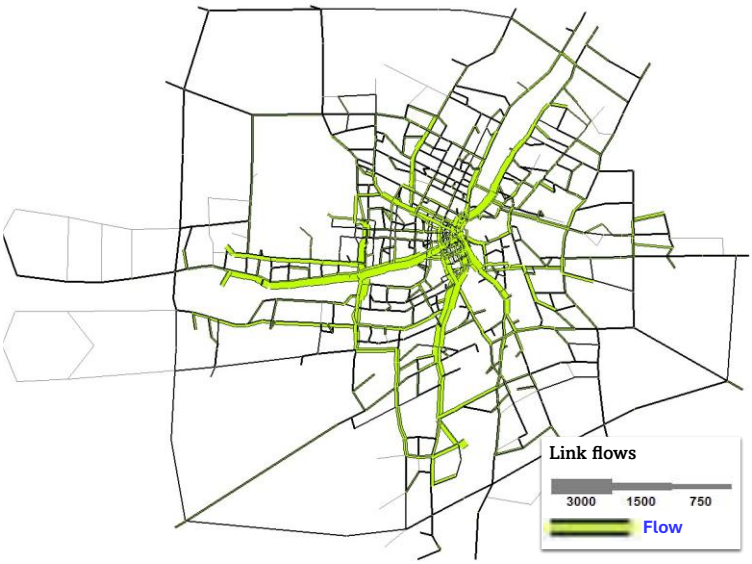

Figure 6.13. Illustration of link flow pattern

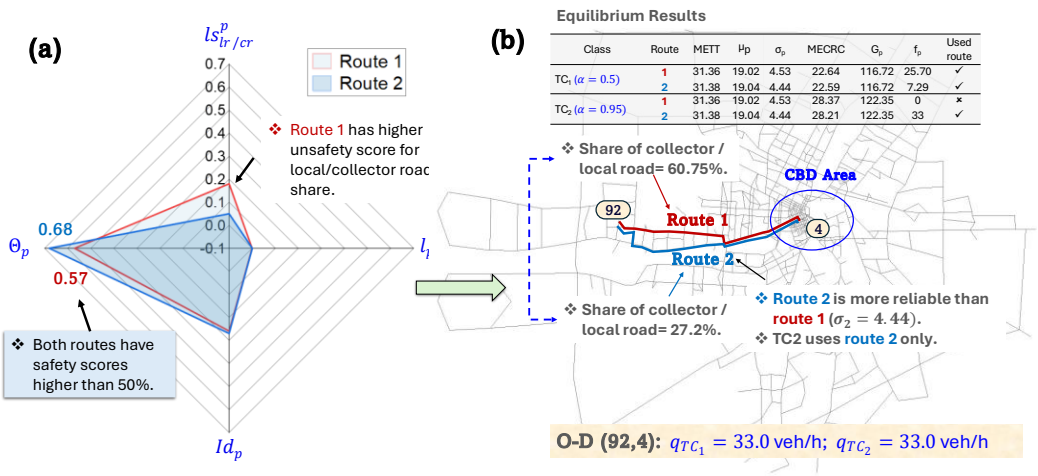

Class	Route	METT	μ_p	σ_p	MECRC	G_p	f_p	Used route
TC_1 ($\alpha = 0.5$)	1	31.36	19.02	4.53	22.64	116.72	25.70	✓
	2	31.38	19.04	4.44	22.59	116.72	7.29	✓
TC_2 ($\alpha = 0.95$)	1	31.36	19.02	4.53	28.37	122.35	0	×
	2	31.38	19.04	4.44	28.21	122.35	33	✓

Figure 6.14. Equilibrium results for multiclass travelers on OD pair (92,4)

For the OD pair (92,4), we see that the safety scores of both the routes (Figure 6.14a) are higher than 50% thus both the routes are part of the choice set for TC_2. Route 2 has a higher safety score ($\Theta_2 = 68\%$) than route 1 ($\Theta_1 = 57\%$) because it has a lower share of local/collector roads compared to route 1. Route 2 has a local/collector road share of 27.2% compared to 60.7% for route 1. From Figure 6.14b, we notice that TC_1 uses both routes 1 and 2, while TC_2, due to greater safety variability concerns, opts only for route 2. Route 2 has a lower safety variability ($\sigma_2 = 4.44$), resulting in a lower MECRC.

For OD pair (79,103), both routes have safety scores above 50% (Figure 6.15a), making them part of the choice set for both classes. However, as shown in Figure 6.15b, TC_2 exclusively uses route 1 due to its lower CRC variability and MECRC, reflecting higher risk aversion, while TC_1 utilizes both routes. These results highlight the model's applicability to real-scale networks.

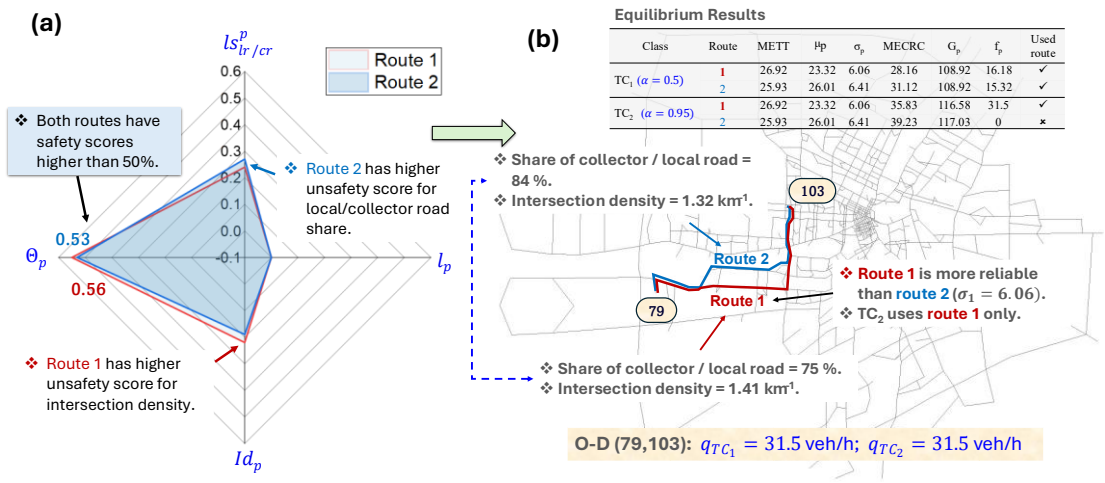

Figure 6.15. Equilibrium results for multiclass travelers on OD pair (79,103)

Figure 6.16 illustrates the sensitivity analysis of route flows across different demand levels for each traveler class.

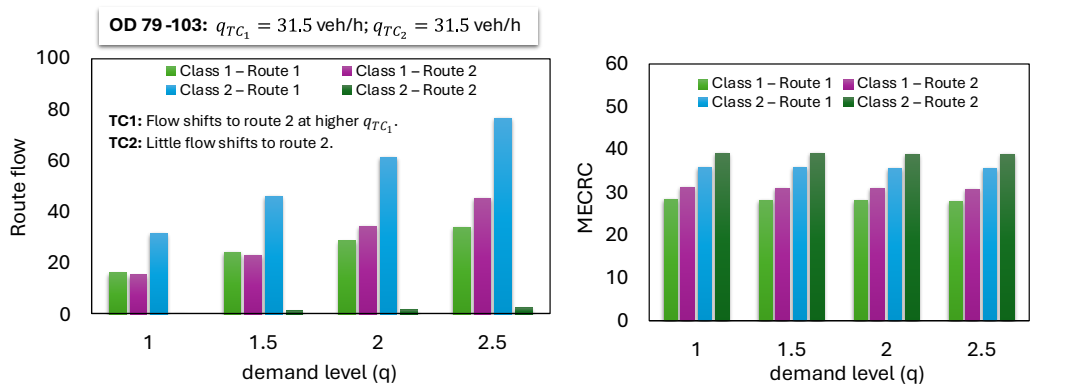

(a) Route flows pattern at different demand levels (b) Route MECRC at different demand levels

Figure 6.16. Sensitivity analysis for route flows at different demand levels for OD 79-103

From Figure 6.16(a), it can be observed that as demand increases, the flow for the low safety-conscious class (TC_1) progressively shifts toward Route 2. In contrast, Figure

6.16(b) shows that Route 2 is associated with a higher MECRC cost. Consequently, the high safety-conscious class (TC_2) allocates the majority of its flow to Route 1, with only a negligible proportion of users selecting Route 2. These results clearly highlight the influence of travelers' safety-consciousness on their route choice behavior under varying demand conditions.

6.4 Practical implications

By incorporating travelers' safety behavior in the network equilibrium model, the proposed TA model has significant potential for use by traffic planners, and policymakers for improving network safety. In the era of connected vehicles, route safety information will be disseminated to travelers, increasing its importance and demand in decision-making. The proposed model considers travelers' route choice behavior in light of crash risk and its consequences (i.e., the risk of fatal/severe crashes). It provides transportation planners with a means to account for the impact of changes in travel behavior on demand patterns arising from travelers' safety concerns. Furthermore, this model provides an opportunity to systematically evaluate the effect of proposed traffic safety countermeasures and regulations on the traffic flow. Possible changes in the flow pattern can be identified based on the estimates of travelers' responses to safety regulations. Thus, traffic planners and policymakers can develop safety improvement policies more systematically than relying on historical data and experience.

Furthermore, the model can be applied to design safety measures targeting the most vulnerable travelers' class. Empirical research suggests that travelers with heterogeneous safety preferences exist on road networks (May et al., 2008). Gong and Fan (2017) found that reckless driving or overspeeding significantly increases the chances of sustaining a fatal or severe injury. Similarly, distracted driving negatively

affects the driver's reaction towards an unsafe condition (Islam & Mannering, 2006). Thus, various countermeasures can be designed for routes accommodated by the vulnerable group of people to minimize the severity of crash effects. Several countermeasures have proven effective in increasing road safety, including legislation and enforcement (Gitelman et al., 2012), safety awareness campaigns (Hoekstra & Wegman, 2011), and traffic calming measures (e.g., provision of speed humps). Safety education programs can be initiated through media and traffic police to target a specific group, such as young drivers fond of reckless driving (Machin & Sankey, 2008).

6.5 Conclusions

In this Chapter, we propose a framework that integrates class-specific route choice sets while accounting for both the reliability and unreliability of the travelers' safety and travel time concerns within a network equilibrium model. The route choice set for each class is defined based on their safety score requirements, with the score of each route quantified by its roadway characteristics. Safety variability's reliability and unreliability aspects are modeled using the α-reliable mean-excess concept. The safety variability is modeled using a CRC distribution, and travelers are assumed to have prior knowledge of the distribution based on their long-term travel experience. The model is formulated as a VI problem. A two-stage non-additive route-based generalized cost, comprising METT and MECRC costs, is solved to reach a user equilibrium solution. The proposed framework demonstrates that travelers with higher safety-score requirements have a more limited route choice set. In contrast, those with higher safety variability concerns tend to select routes with a lower CRC variability. The proposed framework shows how safety concerns influence route choice and network equilibrium flow patterns.

CHAPTER 7 Trade-off between travel time and safety: Modeling heterogeneous preferences in traffic assignment

7.1 Motivation

Several empirical studies emphasize the critical role of safety in travelers' route choice decisions (Abdel-Aty et al., 1995; Amirgholy et al., 2017; Yannis et al., 2005). However, the integration of safety into traffic assignment, a key step in transportation planning, remains limited. With advancements in intelligent and connected vehicle technologies providing real-time safety information, incorporating safety alongside traditional criteria like travel time in traffic assignment models has become increasingly urgent (Ali et al., 2023; Ghoul et al., 2023; Hoseinzadeh et al., 2020). Addressing this research gap advances safety-conscious planning by bridging the gap between static, data-driven crash prediction models and a behaviorally informed framework that explicitly incorporates travelers' safety behaviors and preferences into route choice decisions, enriching the traditional traffic assignment process.

Every trip a traveler makes is associated with a certain degree of crash risk, highlighting the importance of incorporating individual safety preferences into planning models. Travelers accept this risk, more or less consciously, as part of their route choice. The crash risk is influenced by various factors, including roadway characteristics, human behavior, and prevailing traffic conditions. Since a traffic crash is an unwanted event, rational travelers are expected to trade between ***travel time*** and ***safety (crash risk)***, to minimize their overall travel cost (Intini et al., 2017; Noland, 2013). A critical consideration in modeling safety-aware route choice is the salience of safety information to individual travelers. While it is true that travelers are unlikely to possess

explicit, link-level knowledge of historical crash rates, which are rare events, a substantial body of research indicates that they infer safety based on readily observable network attributes. These attributes, such as road functional class, intersection density, and lane width, act as behavioral proxies for road safety (Dijkstra et al., 2007; Hao et al., 2025). Empirical evidence from revealed preference studies using trajectory data confirms that safety perceptions significantly influence actual route choices (Hao et al., 2025). Furthermore, stated preference experiments consistently demonstrate that many travelers are willing to accept increased travel times for safer routes (Rizzi & Ortúzar, 2003; Yannis et al., 2005), establishing the behavioral basis for the time-safety trade-off modeled in this work. This directly addresses the weight of safety relative to travel time: it is not a fixed value but is captured by the heterogeneous value of safety (VoS) parameter, which varies across individuals based on their safety consciousness (Kavta et al., 2025).

To explain the heterogeneity in travelers' safety preferences, a small example is shown in Figure 7.1. For instance, Figure 7.1(a) shows a three-route network, and Figure 7.1(b) shows the features of each route, i.e., travel time and risk level. Route 1 is fast but risky, route 3 is slow but safe while route 2 lies between the two in terms of both travel time and risk. Route choice varies with individuals' safety preferences (Antoniou, 2014). For instance, safety-conscious travelers are likelier to choose the safer route 3, while less safety-conscious individuals prefer the faster route 1. Figure 7.1(c) illustrates the empirical distribution of users with heterogeneous safety preferences and their route choices, where some prefer riskier, faster routes, and others opt for safer, slower alternatives (Antoniou, 2014).

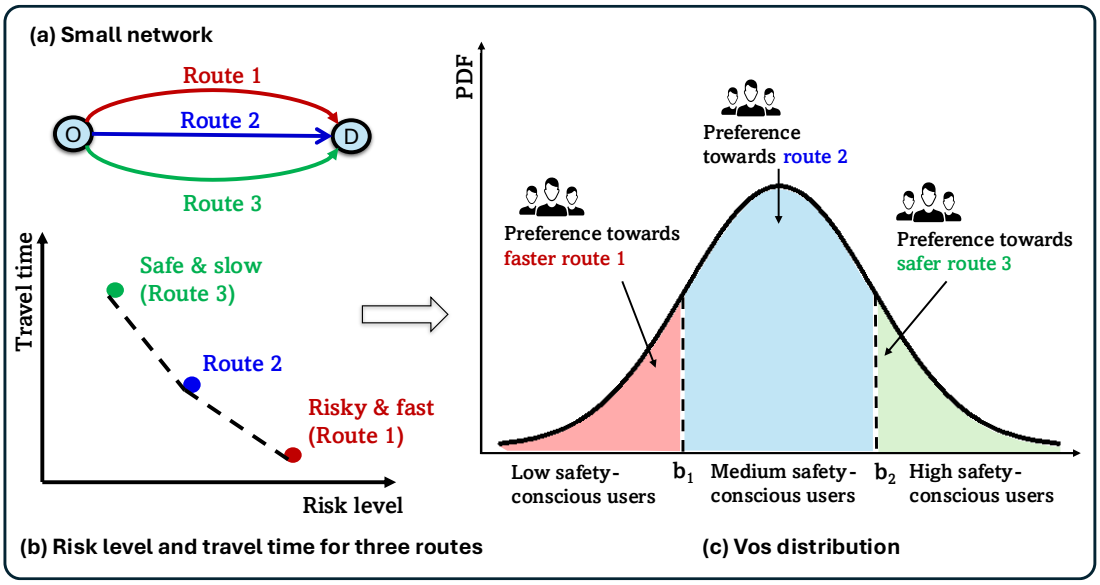

Figure 7.1. Continuous VoS distribution to represent heterogenous safety preferences

This heterogeneity in safety preferences can be effectively modeled in route choice using travelers' *value of safety* (VoS). VoS is defined as the additional time a traveler is willing to spend in exchange for enhanced safety (i.e., a unit reduction in risk) on a slower route (Kavta et al., 2025). VoS is measured in units of time per unit risk reduction, and reflects individual safety preferences in route choice behavior (Rizzi & Ortúzar, 2003; Yannis et al., 2005). VoS enables the conversion of safety into travel time units, thus incorporating both dimensions into the generalized travel cost. Prior research has modeled users' heterogeneity regarding the trade-off between expected safety and safety reliability by dividing users into discrete classes and assuming a crash risk cost (CRC) distribution on a route (Han et al., 2023; Huang et al., 2020). This approach assumes that users know the route's CRC distribution and have varying safety reliability requirements. For example, low safety-conscious individuals tend to select routes with lower expected CRC. In contrast, high safety-conscious users aim to choose routes with more reliable safety outcomes (i.e., lower CRC variance). However, this method does not explicitly address the heterogeneity in the time-safety trade-off, such as choosing the safest and fastest routes.

Additionally, this approach introduces two key challenges: First, it assumes that travelers can fully comprehend the variability in crash risk costs, a complex given the rarity of traffic crashes and the difficulty in accurately estimating CRC distributions for each route. This overlooks the cognitive burden on users who may struggle to incorporate such probabilistic information into their decision-making. Second, discretizing users into fixed classes raises the issue of determining an adequate number of segments, as each individual has unique safety preferences. To address these limitations, we propose using VoS as a subjective measure of safety preference. This measure can be easily captured through stated preference surveys, where individuals express how much value they place on safety in terms of additional travel time (Rizzi & Ortúzar, 2003; Yannis et al., 2005). Instead of imposing predefined classes, we treat VoS as a continuous variable to reflect individualized safety preferences. As illustrated in Figure 7.1(c) (Antoniou, 2014; Ghoul et al., 2023), this continuous VoS distribution allows for a more flexible modeling of route choice behavior, offering a more accurate representation of how travelers trade-off travel time and safety.

7.1.1 Contributions

This Chapter advances the understanding of the time-safety trade-off in transportation networks by integrating travelers' safety preferences in the traffic assignment model. Specifically, this makes the following contributions:

a) It proposes a traffic assignment framework that explicitly incorporates VoS to model the time-safety trade-off. By integrating safety considerations alongside travel time, the framework captures travelers' heterogenous safety preferences and willingness to accept additional travel time for safer routes. It highlights how these preferences shape route choice behavior and traffic flow patterns in real world scenarios.

b) This study introduces a continuous distribution for the value of safety, which better reflects the continuous nature of risk preference than traditional discrete-class models. By avoiding the arbitrary segmentation and oversimplification of discrete classes, this method more accurately and effectively captures heterogeneity in route choice behavior

7.2 Methodology

This section first explains the safety modeling of a route, followed by explaining travelers' heterogeneous trade-off between travel time and safety in their route choice decision making. Finally, the MP formulation for solving the continuous bicriteria TA problem is provided.

7.2.1 Notations

All the notations used in this Chapter are tabulated below unless otherwise specified.

Table 7.1. Notations

Symbol	Description
Sets:	
N	set of nodes
A	set of links (a)
R	set of origins (r)
S	set of destinations (s)
W	set of O-D pairs (w).
P_w	set of routes p between O-D pair w
Parameters/inputs	
$\widetilde{t_a}$	free flow travel time of link a
q_w	demand between O-D pair w
β	traveler's value of safety (VoS)
$f(.)$	probability density function (PDF) of VoS
$F(.)$	cumulative distribution function (CDF) of VoS
Variables	
β_p^w	VoS boundary corresponding to route p of O-D pair w
τ_p^w	VoS interval corresponding to route p of O-D pair w
f_p^w	flow on route p of O-D pair w
x_a	flow on link a
Others	
t_a	travel time of link a

δ_a^p	route-link incidence parameter
$ls_{lr}^{p,w}$	length share of local road on route p between O-D pair w
$ls_{cr}^{p,w}$	length share of collector road on route p between O-D pair w
l_p^w	total length of route p between O-D pair w
$id_{p,w}$	intersection density on route p between O-D pair w
G_p^w	generalized cost on route p of O-D pair w
T_p^w	time cost on route p of O-D pair w
R_p^w	Risk score of route p between O-D pair w

7.2.2 Modeling route safety

In this study, the safety level of a route is assessed based on its risk, where higher risk indicates lower safety. Routes with diverse roadway characteristics can exhibit varying levels of risk, influencing the route choices of different travelers. Specifically, routes vary in their composition of road functional classes, intersection density, and travel exposure (such as travel distance and time), all impacting travel safety. For instance, more uniform routes, with fewer speed variations due to consistent road functional classes, may offer higher safety levels. Additionally, routes with a greater proportion of separated opposing traffic and fewer intersections can reduce interactions between different travel modes, thereby enhancing safety.

The safety proxy variables were selected to align with the model's purpose of capturing safety perception in travelers' route choice. The chosen variables i.e., functional class, intersection density, travel time, and distance are both highly perceptible to travelers making route decisions and consistently available in network-wide datasets, ensuring model scalability (Dijkstra, 2013; Dijkstra et al., 2007; Sohrabi & Lord, 2022). While engineering variables like pavement condition or lane width improve site-specific crash prediction, they are often imperceptible to travelers and unavailable at a network scale, making them less suitable for this behavioral modeling context.

A key consideration in variable selection is the potential interdependence among route attributes like safety, travel time, and comfort, as they are often influenced by common road characteristics. To ensure methodological clarity, variable selection was guided by two principles. First, the data availability principle prioritized variables with readily accessible, network-wide data. Second, the dominance-based principle classified each variable according to the primary attribute it is most strongly documented to influence in the literature (Hao et al., 2025). For example, intersection density is included as a safety-perception variable due to its empirical link to crash risk, despite also correlating with travel time (Dijkstra, 2013). This approach allows for the explicit isolation of the time-safety trade-off, which is the core objective of this study. While some frameworks combine attributes such as safety, comfort and convenience into a composite score (Ehrgott et al., 2012; Wang et al., 2023), the chosen method provides a clear foundation for understanding the specific role of safety before integrating additional objectives in future multi-objective extensions.

7.2.2.1 Definition of different criteria

The selection of variables (criteria) for the safety proxy model comprising road functional class, travel time, distance, and intersection density is grounded in the requirements of a network-wide planning model. Theoretically, these variables serve as robust proxies for the primary determinants of safety perception: exposure and conflict risk. Travel time and distance provide direct measures of exposure (Amoh-Gyimah et al., 2017), while functional class and intersection density are well-established surrogates for complex risk factors like median types conflict points (Bagloee & Asadi, 2016; Sohrabi & Lord, 2022). Empirically these variables have been found to adequately proxy the number of road conflicts and crash risk (Dijkstra, 2013; Dijkstra et al., 2007). While site-specific models benefit from more granular data (e.g., lane

width, curvature), such data is rarely available consistently across an entire network. Therefore, this variable set prioritizes scalability and practical application while capturing the most significant sources of risk

i. Share of local roads on a route

The major function of local roads is to provide direct access to residential areas and commercial areas. These roads are not meant for through-traffic, and a higher percentage of local roads on a route may lead to more transitions from high-speed facilities to low-speed roads. Therefore, the proportion of this road type on a given route should be kept to a minimum. The ratio of length share ($ls_{lr}^{p,w}$) of local roads on a route is calculated as the length of local roads ($l_{lr}^{p,w}$) to the total length (l_p^w) of a route p between OD pair w (Equation (7.1)).

$$ls_{lr}^{p,w} = \frac{l_{lr}^{p,w}}{l_p^w}, \qquad \forall p \in P_w, w \in W \tag{7.1}$$

ii. Share of collector roads on a route

The collector roads have a higher crash risk than the highways and they should be used as little as possible. Therefore, the length of collector roads on a route should be minimized. The ratio of length share ($ls_{cr}^{p,w}$) of collector roads on a route is calculated as the length of collector roads ($l_{cr}^{p,w}$) to the total length (l_p^w) of a route p between OD pair w (Equation (7.2)).

$$ls_{cr}^{p,w} = \frac{l_{cr}^{p,w}}{l_p^w}, \qquad \forall p \in P_w, w \in W \tag{7.2}$$

iii. Total travel distance on a route

The total travel distance explains the exposure to crash risk, which is generally measured in terms of total vehicle kilometers traveled (VKT) (Amoh-Gyimah et al., 2017). The shorter the distance on a route, the lesser the exposure to crash risk.

Therefore, a lower risk score requires a smaller total distance traveled on a route. It is calculated by adding the length of all the links passing through a route, as shown in Equation (7.3).

$$l_p^w = \sum_{a \in A} \delta_a^p l_a, \qquad \forall p \in P_w, w \in W \tag{7.3}$$

iv. Density of intersections on a route

Intersections in a road network are hotspots for serious and fatal crashes (Alarifi et al., 2017). In the US, roughly one-quarter of deadly and one-half of serious crashes are attributed to intersections (FHWA, 2024). Thus, a route with a lower density of intersections will be safer than one with a higher density. To calculate the safety score for this criterion, the intersection density is calculated as the number of intersections (n_i^p) per kilometer on a routeas shown in Equation (7.4).

$$id_{p,w} = \frac{n_i^{p,w}}{l_p^w}, \qquad \forall p \in P_w, w \in W \tag{7.4}$$

i. Travel time on a route

Travel time serves as a proxy for measuring exposure, with routes featuring shorter travel times being less exposed to crash risk. The travel time on a route is measured as the sum of travel times on all the corresponding road segments of a route. For modeling convenience, we assume the risk score depends on the free flow travel time, which is calculated by dividing the length of the road segments by their speed limits. An alternative approach would be to consider congested travel times, which would significantly increase modeling complexity and is a topic for future research. The travel time on a route is shown in Equation (7.5).

$$\widetilde{T_p^w} = \sum_{a \in A} \delta_a^p \widetilde{t_a}, \qquad \forall p \in P_w, w \in W \tag{7.5}$$

7.2.2.2 Quantification of risk score of a route

For each route, the risk score is quantified based on the above five criteria by using the network topology data and applying Equations (7.6) and (7.7). To compare the scores of different routes, min-max normalization is carried out for each criterion, assigning a score of 0 to the best route and 1 to the worst route. The normalized score for any other route is calculated by subtracting the minimum criterion score from the score of the route in question and then dividing this value by the range between the maximum and minimum scores for that criterion as shown in Equation (7.6) (Dijkstra, 2013; Dijkstra et al., 2007).

$$score_c^{p,w} = \frac{y_c^{p,w} - \min_c\{y_c^{p,w}\}}{\max_c\{y_c^p\} - \min_c\{y_c^{p,w}\}}, \qquad \forall p \in P_w, w \in W \tag{7.6}$$

where $score_c^p$ is the normalized score for criterion c of route p and y_c^p is the score of a criterion c for route p. The total score is calculated by multiplying the normalized score by a weight factor and adding all the criteria to get the score indicating the risk level of a route, as shown in Equation (7.7).

$$R_p^w = \sum_{c=1}^{C} score_c^{p,w} \times \gamma_c, \qquad \forall p \in P_w, w \in W \tag{7.7}$$

where R_p^w is the risk score for route p, γ_c is the weight factor for the criterion c, and C is the number of total criteria. The sum of the weight factors for all criteria determines the risk score range. For example, if there are five criteria, each with a weight factor of one, the total weight is five. Consequently, the risk score for each route will range from 0 to 5.

Figure 7.2 illustrates the methodology outlined in Section 7.2.2 for assessing the safety levels of routes with diverse characteristics. For demonstration purposes, three routes

with distinct features are presented. The safety level of each route is computed based on Equation (7.7) using the criteria in Equations (7.1) – (7.5).

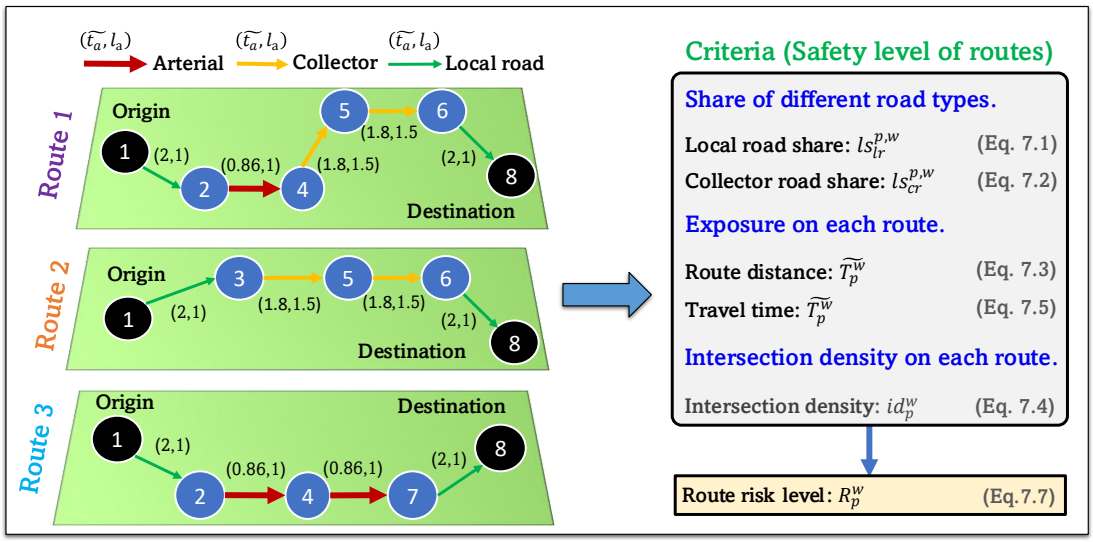

Figure 7.2: Methodology for calculating the safety level of routes based on different criteria

In Figure 7.2, the travel time and travel distance are presented on top of each link. Each route is characterized by five criteria: local road share, collector road share, travel time, travel distance, and intersection density.

Table 7.2. Normalized scores for each route

Criterion	Variable	Unit	Scores for each route			Normalized scores for each route		
			1	2	3	1	2	3
1	ls_{lr}^{p}	%	0.33	0.40	0.50	0.00	0.40	1.00
2	ls_{cr}^{p}	%	0.50	0.60	0.00	0.83	1.00	0.00
3	l_p	km	6	5	4	1.00	0.50	0.00
4	id_p	km^{-1}	0.67	0.60	0.75	0.44	0.00	1.00
5	$\tilde{T}_p$	min	8.46	7.60	5.71	1.00	0.69	0.00

Table 7.3. Weighted normalized scores for each route

Criterion	Variable	Unit	Weight	Weighted scores for each route		
				1	2	3
1	ls_{lr}^{p}	%	1.0	0.00	0.40	1.00
2	ls_{cr}^{p}	%	1.0	0.83	1.00	0.00
3	l_p	m	1.0	1.00	0.50	0.00
4	id_p	km^{-1}	1.0	0.44	0.00	1.00
5	$\tilde{T}_p$	min	1.0	1.00	0.69	0.00
			5.0	**3.28**	**2.59**	**2.00**

Based on these attributes, the calculation of risk scores is presented in Table 7.2 and Table 7.3. Table 7.2 details the risk score for each individual criterion, while Table 7.3

summarizes the total weighted risk score for each route. With equal weights assigned to all five criteria, the total risk score for any route ranges from 0 to 5. As shown in Table 7.3, Route 1 has the highest risk score of 3.28, whereas Route 3 has the lowest score of 2.0.

7.2.3 Efficient frontier for time-safety trade-off

This section explains the concept of efficient routes and efficient frontier in bicriteria route choice, which will be formally applied in Section 7.2.5 to explain the formulation of the continuous bicriteria traffic assignment model.

Definition 1 (efficient route). A route is called efficient if no other route offers a lower risk for a given travel time, and for a given risk score, no other route offers a shorter travel time. Formally, a route $p \in P_w$ is efficient if there exists no route $p' \in P_w$ and $p' \neq p$ such that.

$$\begin{aligned} T_{p'} < T_p \quad \text{and } R_{p'} \leq R_p \text{ or} \\ T_{p'} \leq T_p \quad \text{and } R_{p'} < R_p \end{aligned} \tag{7.8}$$

To illustrate this concept, consider a small network with three routes (Figure 7.3a), each characterized by different travel times and risk scores. Route 1 is the fastest but also the riskiest; Route 3 is the safest but the slowest; and Route 2 is both slower and riskier. It becomes evident that Route 2 is dominated by the other two and is therefore inefficient, whereas Routes 1 and 3 are both efficient. Specifically, Route 1 is efficient because no other route offers a shorter travel time for the same risk score, and Route 3 is efficient because no other route offers greater safety (a lower risk score) for the same travel time.

Figure 7.3b extends this concept to consider multiple routes. Any route lying outside the efficient frontier, represented by a dotted line, is considered inefficient, as a better route exists in terms of either travel time or risk score. Routes on the frontier represent optimal trade-offs where improving one criterion (e.g., reducing risk score) necessarily

involves a compromise in the other (e.g., increasing travel time). Identifying the efficient frontier is equivalent to finding minimum generalized cost routes for an appropriate set of VoS values.

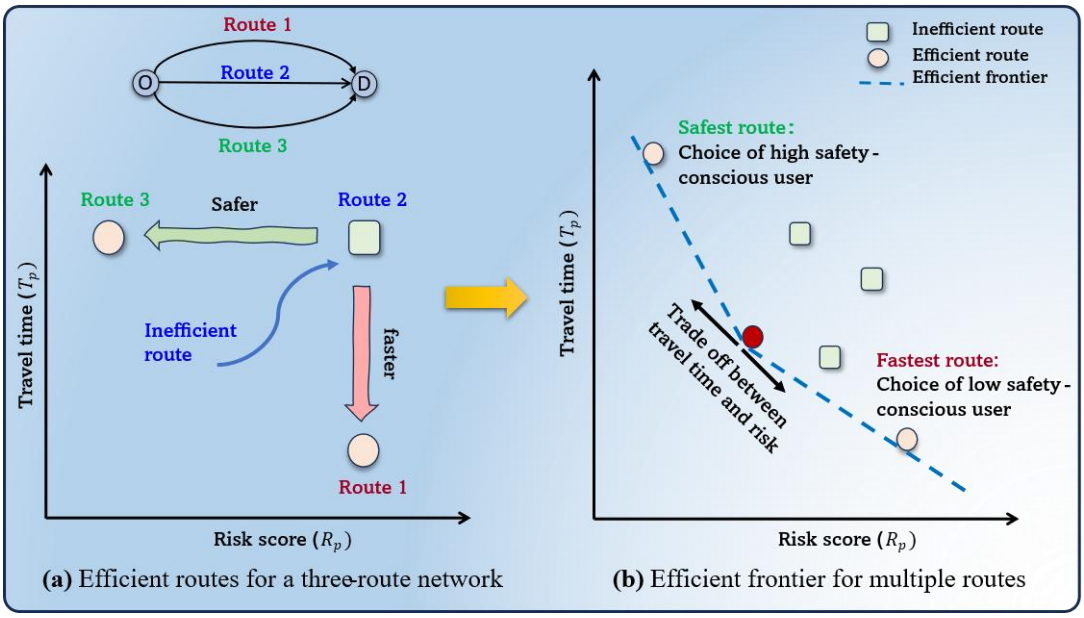

Figure 7.3. Efficient routes and efficient frontier for time-safety trade-off

Travelers can select routes on the efficient frontier by making a trade-off between travel time and safety based on their heterogeneous safety preferences (Intini et al., 2017; Noland, 2013). The heterogeneity in preferences is captured by each traveler's VoS, which determines how they balance these competing factors. For instance, travelers with a higher VoS (high safety-conscious) accept longer travel times to minimize risk, whereas travelers with a lower VoS (low safety-conscious) prioritize faster routes even at the cost of increased risk (Rizzi & Ortúzar, 2003; Yannis et al., 2005).

7.2.4 An illustrative example: Discrete vs continuous VoS distributions

We present an illustrative example in Figure 7.4, excluding congestion effects, to compare how discrete and continuous VoS distributions capture travelers' heterogeneous safety preferences. The focus is on highlighting the advantages of

employing a continuous VoS distribution, which more accurately reflects individual-specific safety preferences in route choice.

To explain this concept, Figure 7.4(a) shows a three-route example, where each route is characterized by different travel times and risk scores. In this illustrative example, the travel time and risk score values are exogenously assigned to clearly demonstrate the model's mechanics and enable a direct comparison between discrete and continuous distributions of the Value of Safety (VoS). The calculation procedure for risk scores is detailed in Figure 7.2. It is important to note that the generalized cost is expressed in units of travel time, as the risk score is multiplied by VoS to convert it into equivalent time units, thereby allowing for meaningful trade-offs on a common scale. Figure 7.4(b) shows a continuous VoS distribution with values ranging from 0 to 1. Figure 7.4(d) shows a discrete VoS distribution, where continuous distribution in Figure 7.4(b) is discretized into two classes: low safety-conscious (LS) with a VoS of 0.25 measured in $\frac{min}{risk\ reduction}$, and high safety-conscious (HS) with a VoS of 0.75. In the discrete class, travelers with a VoS between 0–0.5 (LS travelers) are represented by an average value of 0.25, while those with VoS between 0.50–1.0 (HS travelers) are represented by an average value of 0.75. This implies that all travelers within the same class have the same VoS value. In the discrete case (Figure 7.4(e)), generalized cost calculations reveal that LS travelers select route 1 (the fastest route), HS travelers choose route 3 (the safest route), and route 2 remains unused. In contrast, under the continuous VoS distribution (Figure 7.4(c)), travelers are divided into three classes: those with VoS values in the range [0–0.41) select route 1, those with VoS in the range [0.41–0.71) use route 2, and those with VoS in the range [0.71–1.0] prefer route 3, as shown in Figure 7.4(c). Figure 7.4(f) compares the two cases, highlighting the key difference: with

discrete VoS, only two routes (1 and 3) are used, while under continuous VoS, all three routes are utilized.

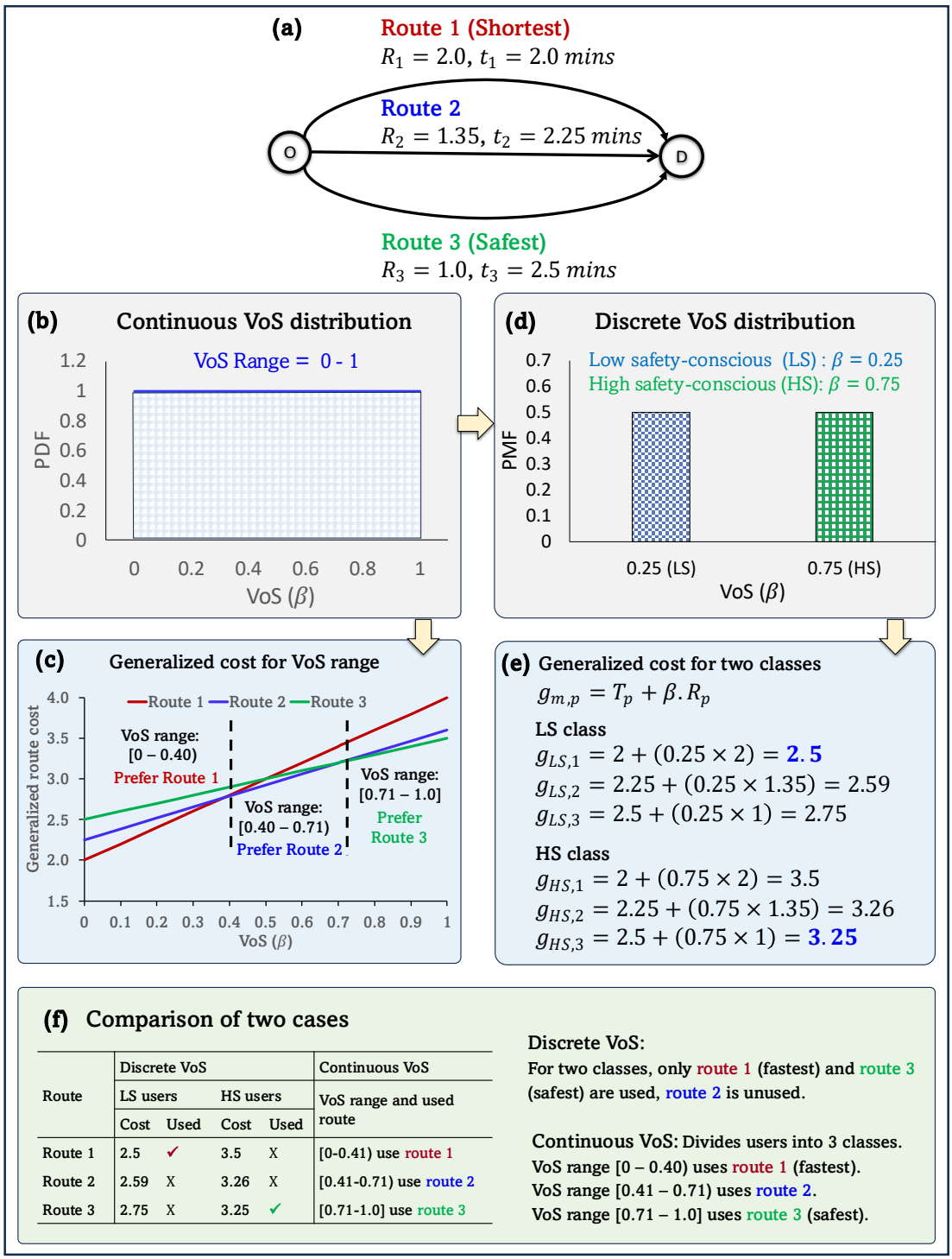

Route	Discrete VoS				Continuous VoS
	LS users		HS users		VoS range and used route
	Cost	Used	Cost	Used	
Route 1	2.5	✓	3.5	X	[0-0.41) use route 1
Route 2	2.59	X	3.26	X	[0.41-0.71) use route 2
Route 3	2.75	X	3.25	✓	[0.71-1.0] use route 3

Figure 7.4. An illustrative example comparing the discrete vs continuous VoS

This discrepancy arises because the discrete VoS approach groups users into rigid classes, each with identical VoS values for all individuals within a class. This

classification restricts model flexibility and oversimplifies heterogeneous preferences. In contrast, the continuous VoS distribution (Figure 7.4(d)) refines the model by representing safety preferences across a continuous spectrum, allowing each traveler to have a unique VoS. By capturing individualized safety preferences, this approach provides a more accurate and detailed depiction of safety-related route choice behavior.

7.2.5 Continuous VoS for time-safety trade-off

This chapter models the trade-off between travel time and safety (risk) by assuming that the generalized cost experienced by each traveler on a route is a linear combination of travel time and safety (risk score). This assumption offers modeling tractability and follows many studies in the literature that combine safety and travel time for different modeling purposes, such as the combination of travel time and safety in empirical route choice studies (Mouter et al., 2017), traffic assignment models (Han et al., 2023; Huang et al., 2020), and routing problems (Carmody & Sowers, 2019; Ghoul et al., 2023; Hoseinzadeh et al., 2020). Each traveler in the population is identified by a unique VoS, represented by a random variable β, which follows a continuous distribution across the population. The VoS parameter is central to capturing the time-safety trade-off and empirical evidence strongly supports the existence and quantifiability of this trade-off (Kavta et al., 2025; Yannis et al., 2005). To ensure behavioral realism, the model incorporates a continuous distribution of VoS across the population, reflecting the documented heterogeneity in safety preferences (Antoniou, 2014). The PDF and CDF of β are represented by $f(.)$ and $F(.)$, respectively. $f(.)$ is assumed to be measurable, almost everywhere, positive function with a compact support $\tau = \left[\underline{\beta}, \overline{\beta}\right]$ such that $\underline{\beta} < \overline{\beta}$. The CDF of β can be written as:

$$F(z) = P(\beta \leq z) \tag{7.9}$$

The generalized cost, G_p^w, for a traveler with VoS (β) traveling on route p is a linear combination of route travel time $\left(T_p^w = \sum_{a \in A} t_a(x_a)\delta_{ap}^w\right)$ and risk score $\left(R_p^w\right)$ given in Equation (7.10).

$$G_p^w = T_p^w + \beta . E_p^w \quad \forall p \in P_w, w \in W \tag{7.10}$$

In the continuous bicriteria traffic assignment problem, travelers minimize their generalized cost based on their unique VoS, where each traveler can be viewed as a distinct class within the continuous distribution function $f(.)$, leading to a theoretically infinite number of user classes. However, travelers are considered unique only if they select different routes, so the number of user classes between an O-D pair is constrained by the available routes. In practice, the number of routes considered is much smaller than the total number of available routes. This leads to the concepts of efficient routes and the efficient frontier introduced in Section 7.2.3.

Effectively, route $p \in P_w$ is considered efficient if it is used by at least one traveler with VoS, $\beta \in \tau$. An efficient route lies on the efficient frontier of two criteria for evaluating the generalized cost: travel time and safety. In the decreasing order of risk score, the line segments that join the efficient routes represent an efficient frontier.

This concept is elaborated using six routes between a single OD pair (Figure 7.5). In Figure 7.5(a), travel time is plotted on the y-axis and risk score on the x-axis. The distribution of VoS with a support $\tau = [\underline{\beta}, \overline{\beta}]$ is illustrated in Figure 7.5(b). Each route is associated with a travel time cost, T_p, and risk score, R_p. Within the support τ, the solid line in Figure 7.5(a) refers to the efficient frontier formed by the three efficient routes (routes 1,4, and 6) due to the generalized travel time cost minimization according to Equation (7.10). The slope of the line between two adjacent efficient routes represents the VoS threshold where route choice changes (Equation (7.11)).

$$\beta_p^w = \frac{(T_{p+1}^w - T_p^w)}{(E_p^w - E_{p+1}^w)} \tag{7.11}$$

In Figure 7.5(a), the slope of the line connecting routes 1 and 4 for a single OD pair is β_1. Thus, when VoS $\leq \beta_1$, the lowest generalized cost is experienced on route 1. As VoS exceeds β_1, route 4 will be the next minimum generalized cost route with VoS equal to β_4, unless VoS exceeds β_4. After VoS exceeds β_4, route 6 will be considered as the minimum generalized cost route. More specifically, a user will choose route 1 if his/her $\beta \in \left[\underline{\beta}, \beta_1\right)$, route 4 if $\beta \in [\beta_1, \beta_4)$, and route 6 if $\beta \in \left[\beta_4, \overline{\beta}\right]$. In Figure 7.5(b), three equal choice groups are illustrated in the PDF of VoS. The integral of each shaded area represents the flow on the selected efficient route.

To define efficient routes for each O-D pair w, the routes in P_w are ordered by decreasing risk score R_p^w. The support τ is divided into intervals equal to $|P_w|$, each defines the range of VoS for which a route minimizes generalized cost. These VoS boundaries can be written as:

$$\tau_p^w = \begin{cases} [\beta_{p-1}^w, \beta_p^w), & \text{if } p = 1, \ldots, |P_w| - 1 \\ [\beta_{p-1}^w, \beta_p^w], & \text{if } p = |P_w| \end{cases} \quad \forall\, w \in W \tag{7.12}$$

where $\beta_0^w = \underline{\beta}, \beta_{|P_w|}^w = \overline{\beta}, \beta_{p-1}^w \leq \beta_p^w,\ \forall\, p = 1, \ldots, |P_w|$

Once the VoS boundaries are determined, given O-D demand q_w, the VoS interval corresponding to each route can be used to determine the route flows by simply integrating the PDF of VoS within the interval.

$$f_p^w = q_w \int_{\beta_{p-1}^w}^{\beta_p^w} g(x)dx\,, \forall p = 1, \ldots, |P_w| \tag{7.13}$$

An efficient route satisfies $\beta_p^w > \beta_{p-1}^w$, which induces a flow $f_p^w > 0$, whereas an inefficient route has $\beta_p^w = \beta_{p-1}^w$, resulting in zero flow i.e., $f_p^w = 0$.

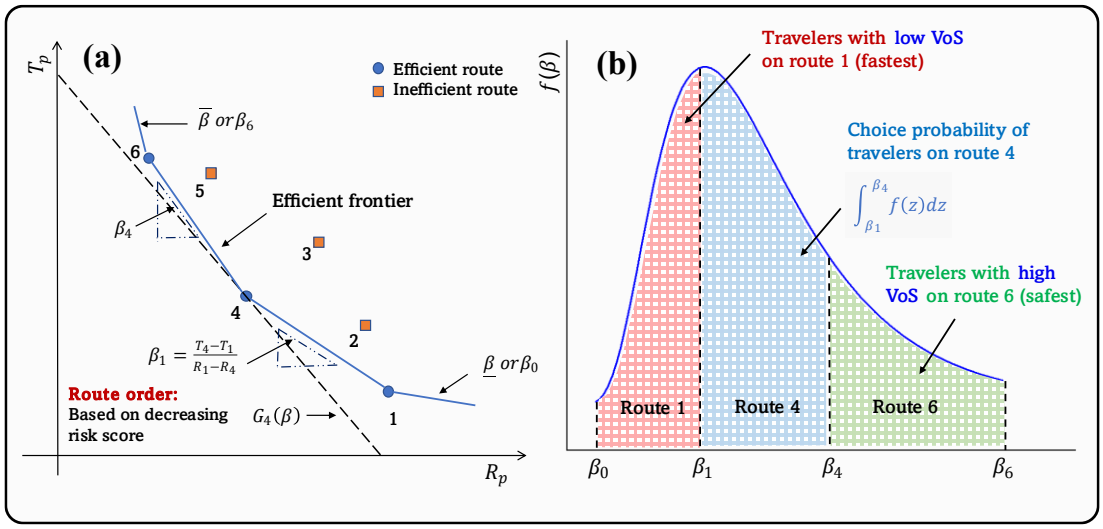

Figure 7.5. Illustration of (a) efficient frontier of time-safety trade-off, (b) PDF of VoS

While identifying efficient routes is straightforward with flow-independent travel times (Dial, 1979), the challenge arises when travel times depend on flow. A key assumption in this foundational model is that the travel time is flow-dependent while perceived safety of a link is flow-independent. Safety is determined by fixed link attributes (e.g., road type, intersection density) and does not change with traffic volume. This assumption is necessary to establish a tractable baseline model for analyzing safety-time trade-offs and is consistent with initial models in continuous bicriteria traffic assignment (Xie et al., 2021; Xu et al., 2024b). Due to the flow-dependent travel time, the VoS boundaries fluctuate based on assigned flows, and flow itself depends on these boundaries (Xie et al., 2021). The next section explains the formulation used to determine the VoS boundaries in case of flow-dependent travel times

7.2.6 Continuous bicriteria traffic assignment formulation

In the continuous bicriteria traffic assignment (C-BiTA) problem, the objective is to determine the set of efficient routes and their VoS boundaries for each O-D pair w. Two important points to note here: First, in the conventional TA problem, the efficient routes are effectively equal to the "used routes" by definition; second, the VoS boundaries are

consistent with the flows allocated to efficient routes. We use the C-BiTA formulation proposed by Marcotte (1998) and later adopted by Xie et al. (2021) for their solution algorithm development. The equilibrium conditions for C-BiTA for any O-D pair $w \in W$, and any route $p \in P_w$ which are an extension of Wardrop's first principle (Wardrop, 1952), can be stated as:

$$f_p^w > 0 \Rightarrow G_p^w(\beta) \leq G_l^w(\beta), \forall \beta \in \tau_p^w \neq \emptyset, \forall l \in P_w, l \neq p \tag{7.14}$$

This condition implies that each efficient route corresponds to a non-empty VoS interval, $\tau_p^w \neq \emptyset$. Thus, the VoS boundaries, $\beta_p^w \; \forall p = 1, \ldots\ldots, |P_w| - 1$, replace route flows as decision variables. The vector of VoS boundaries and the route flows are represented by $\boldsymbol{\beta}$ and $\mathbf{f}$. These VoS boundaries define the equal choice groups (ECGs), which become the primary decision variables. Furthermore, the traditional flow conservation conditions are replaced by simple box constraints that maintain the order of the boundaries (Figure 7.6).

Beckmann's transformation

Risk across all used routes

$$\min Z(\beta) = \sum_{a \in A} \int_{o}^{x_a} t_a(u)du + \sum_{w \in W} \sum_{p \in P_w} q_w . R_p^w . \int_{\beta_{p-1}^w}^{\beta_p^w} v.f(v)dv$$

Subject to:

Decision variables: VoS boundaries

$$\beta_p^w - \beta_{p-1}^w \geq 0, \qquad \forall w, p = 1, \ldots, |P_w|$$

Box constraints based on route order

$$x_a = \sum_{w \in W} \sum_{p \in P_w} \delta_{ap}^w q_w \int_{\beta_{p-1}^w}^{\beta_p^w} f(v)dv, \qquad \forall a \in A$$

Link flows

$$\beta_0^w = \underline{\beta}, \beta_{|P_w|}^w = \overline{\beta}, \qquad \forall w \in W$$

Bounds on VoS

Figure 7.6. Mathematical programming formulation

The objective function in this formulation (Figure 7.6) consists of two terms: the first term is the famous Beckman's transformation (Beckmann et al., 1956) widely used in

the standard TAP; the second term is the risk score incurred across all used routes. Notably, the order of routes is flow-independent since it relies on the risk score. This allows for the VoS constraints to be structured as shown in the first constraint in Figure 7.6.

Theorem 1 *(Equivalence)*. A solution to the MP (Figure 7.6), which is a vector of VoS boundaries $\boldsymbol{\beta}$ along with its corresponding path flow $\mathbf{f}$, satisfies the UE conditions in Equation (7.14).

Proof.

The lagrangian for the MP (Figure 7.6) can be expressed as follows:

$$L(\beta,\mu) = \sum_{a\in A}\int_{o}^{x_a} t_a(u)du + \sum_{w\in W}\sum_{p\epsilon P_w} q_w.R_p^w.\int_{\beta_{p-1}^w}^{\beta_p^w} v.f(v)dv - \mu_p^w(\beta_p^w - \beta_{p-1}^w) \tag{7.15}$$

where μ_p^w is the multiplier associated with constraint 1 in Figure 7.6. Accordingly, we can derive the KKT conditions as follows:

$$\frac{\partial L}{\partial \beta_p^w} = 0, \qquad \forall w, p = 1, \ldots\ldots, |P_w| \tag{7.16}$$

$$\mu_p^w \geq 0, \mu_p^w\left(\beta_p^w - \beta_{p-1}^w\right) = 0, \;\; \forall w, p = 1, \ldots\ldots, |P_w| \tag{7.17}$$

$$\frac{\partial L}{\partial \beta_p^w} = \sum_{a\in A}\frac{\partial \sum_{a\in A}\int_0^{x_a} t_a(v)dv}{\partial x_a} \times \frac{\partial x_a}{\beta_p^w} + \frac{\partial}{\partial \beta_p^w}\sum_{w\in W}\sum_{p\epsilon P_w} q_w.R_p^w.\int_{\beta_{p-1}^w}^{\beta_p^w} v.f(v)dv - \frac{\partial}{\partial \beta_p^w}\mu_p^w(\beta_p^w - \beta_{p-1}^w) \tag{7.18}$$

$$= q_w.f\left(\beta_p^w\right).\left(T_p^w - T_{p+1}^w\right) + q_w.f\left(\beta_p^w\right)\left(\beta_p^w R_p^w - \beta_p^w R_{p+1}^w\right) - \left(\mu_p^w - \mu_{p+1}^w\right) \tag{7.19}$$

$$= q_w . f(\beta_p^w).\left(T_p^w + \beta_p^w R_p - \left(T_{p+1}^w + \beta_p^w R_{p+1}\right)\right) - \left(\mu_p^w - \mu_{p+1}^w\right) \tag{7.20}$$

$$T_p^w + \beta_p^w R_p^w - \left(T_{p+1}^w + \beta_p^w R_{p+1}^w\right) = \frac{\left(\mu_p^w - \mu_{p+1}^w\right)}{q_w . f(\beta_p^w)} \tag{7.21}$$

Suppose $f_p^w > 0$, which implies that $\beta_p^w > \beta_{p-1}^w$, i.e., $\tau_p^w \neq \emptyset$. We shall show that $G_p^w(\beta) \leq G_l^w(\beta), \forall l \in P_w, l \neq p, \forall \beta \in \tau_p^w$. We first note that $\forall \beta \in \tau_p^w$. Equation (7.17) implies.

$$T_p^w + \beta R_p^w - \left(T_{p+1}^w + \beta R_{p+1}^w\right) \leq \frac{\left(\mu_p^w - \mu_{p+1}^w\right)}{q_w . f(\beta_p^w)} \tag{7.22}$$

Given $f_p^w > 0$, Equation (7.17) leads to $\mu_p^w = 0$. As $\mu_p^w \geq 0, \forall w, p$ we have.

$$T_p^w + \beta R_p^w \leq T_{p+1}^w + \beta R_{p+1}^w \rightarrow G_p^w(\beta) \leq G_{p+1}^w(\beta), \forall \beta \in \tau_p^w \tag{7.23}$$

By repeating the above steps, it can be shown that this relationship holds for any other path $l > p$, or $l < p$ (Xie et al., 2021).

$$G_p^w(\beta) \leq G_l^w(\beta)\ \forall \beta \in \tau_p^w \tag{7.24}$$

This completes the proof. □

Theorem 2 *(solution uniqueness in terms of link flows)*. Under the assumption that $t_a(.), \forall a \in A$ is positive, separable, continuously differentiable, and strictly increasing w.r.t x_a, the MP (Figure 7.6) has unique link flows $\mathbf{x}^*$.

Proof. It is straightforward to demonstrate that MP (Figure 7.6) is strictly convex w.r.t **x,** which guarantees the uniqueness of $\mathbf{x}^*$**.** □

Theorem 3 *(solution uniqueness in terms of VoS boundaries)*. For the solution to be unique in terms of VoS boundaries $\{\beta_p^{w*}, p = 1, \ldots, |P_w|\}$ and UE route flows $\{f_p^{w*}, p = 1, \ldots, |P_w|\}$, two conditions must be met: (1) $t_a(.), \forall a \in A$ is assumed to be a continuous, differentiable, and strictly increasing function of link flow, x_a, (2) every

route that connects an OD pair has a unique risk score i.e., $R_p^w \neq R_{p'}^w, \forall p, p' \in P_w, p \neq p', \forall w \in W$.

Proof. Since the link flow $\mathbf{x}^*$ is unique according to Theorem 2, the path travel times $\{T_p^*\}$ are also unique. For O-D pair w, the efficient frontier with unique T_p and R_p is also unique resulting in unique VoS boundaries $\{\beta_p^{w*}\}$. □.

7.2.7 Solution algorithm

This section presents the procedure for solving the MP formulation in Figure 7.6.

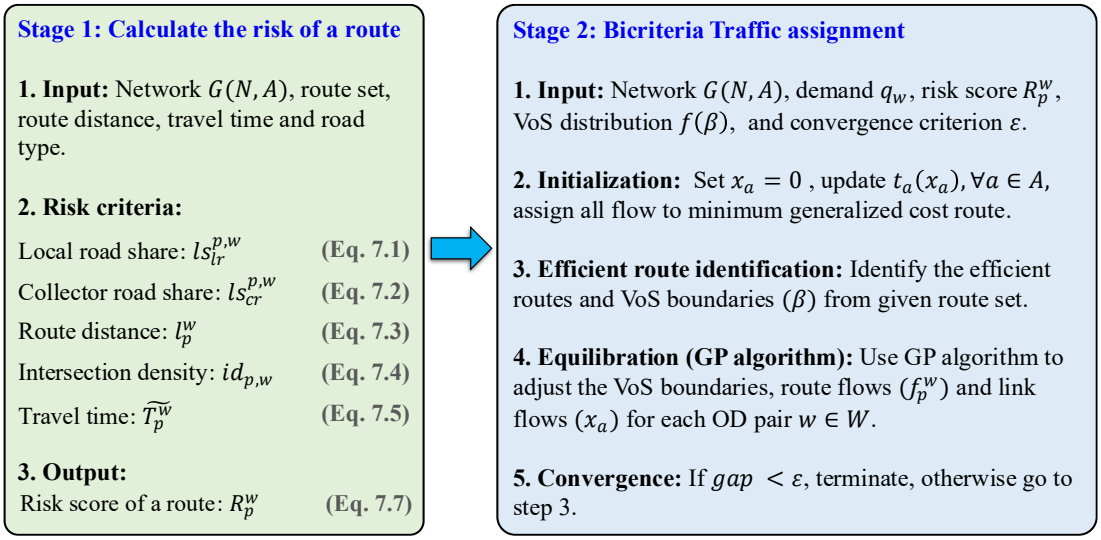

Figure 7.7. An overview of the two-stage solution algorithm

The procedure is divided into two stages. In the first stage, the algorithm calculates the risk scores for all the routes in a given route set between each OD pair using the methodology presented in Section 7.2.2. In the second stage, we use the path-based algorithm to solve the MP in Figure 7.6. We customize the single boundary adjustment algorithm proposed by Xie et al. (2021) for fixed demand C-BiTA and extended by Xu et al. (2024a) for elastic demand C-BiTA. The algorithm has three main steps: (1) After initialization, the algorithm identifies the efficient route set and their VoS boundaries from a given route set, (2) Second step finds the equilibrium solution using the gradient projection (GP) algorithm. It adjusts the VoS boundaries β_p^w for each OD pair and

updates the route and link flows accordingly, and (3) third step checks the convergence of the algorithm. An overview of the two-stage algorithm is provided in Figure 7.7.

7.3 Numerical experiments

This section presents results for two networks: a small three-route network to analyze user safety preferences, and the Winnipeg network to demonstrate real-world applicability.

7.3.1 A small network

This section uses a small network to understand the travelers' heterogeneous safety preferences in the C-BiTA model. As shown in Figure 7.8 and Table 7.4, the Braess network has 4 nodes, 6 links, and 3 routes. There is a single OD pair (1,4) with a total demand equal to 3000 veh/h. VoS (β) is assumed to follow a uniform distribution where $\underline{\beta} = 2$ and $\overline{\beta} = 20$, measured in $\frac{min}{risk\ reduction}$. The risk is calculated in terms of the risk score of each route.

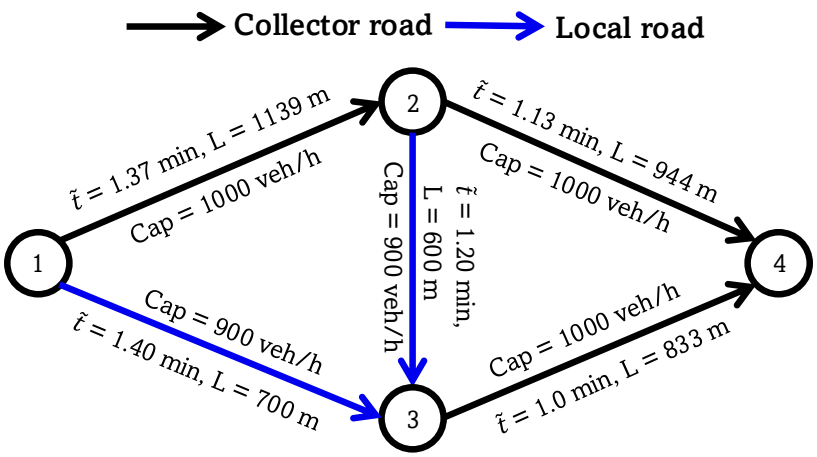

Figure 7.8. A small network example

The widely used BPR function is adopted (Equation (7.25)).

$$t_a = \tilde{t_a}\left(1 + 0.15\left(\frac{x_a}{Cap_a}\right)^4\right) \tag{7.25}$$

where $\widetilde{t_a}$ and Cap_a represent the free flow travel time and capacity of link a, respectively. Considering the uniform distribution, the PDF for VoS (β) is shown in Equation (7.26).

$$f(\beta) = \frac{1}{\overline{\beta} - \underline{\beta}}, \qquad \beta \in [\underline{\beta}, \overline{\beta}] \tag{7.26}$$

Table 7.4. Route characteristics of a small network

S.No	Route	Nodes	l_a (m)	$\widetilde{t_a}$ (min)
1	Route 1	1,2,3,4	2572	3.57
2	Route 2	1,3,4	1533	2.40
3	Route 3	1,2,4	2083	2.50

7.3.1.1 Calculation of risk score for each route

The risk score of each route is calculated following the procedure, following the procedure explained in Section 7.2.2 and the small numerical example in Figure 7.2.

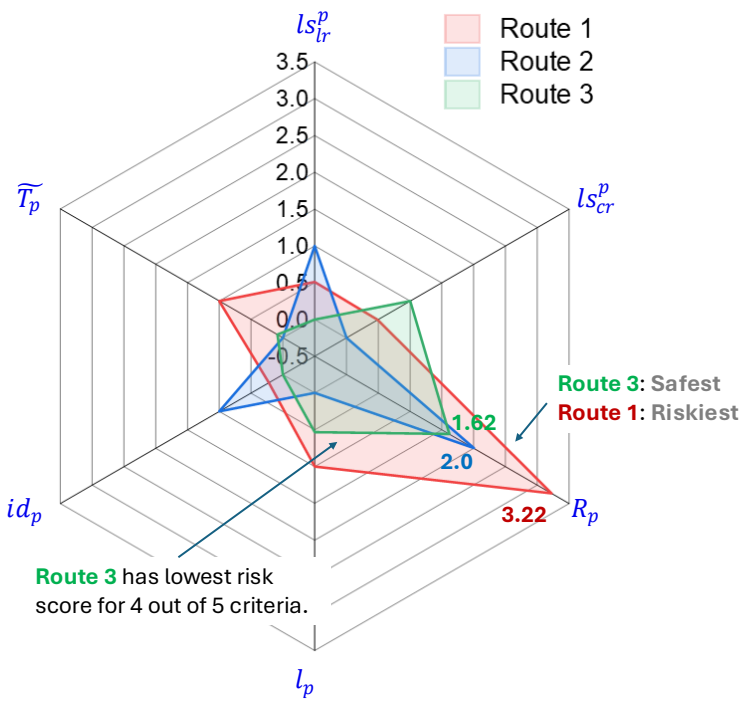

Figure 7.9. Illustration of risk score of routes for each criterion

Figure 7.9 presents a comparison of the risk scores of each criterion and the total risk score across the three routes. Route 1 has the highest risk score of 3.22 while route 3

has the lowest risk score of 1.62. Route 1, which has the highest overall risk score ($R_p = 3.22$), records the highest risk score for two criteria (i.e., l and $\tilde{T}$) and the second highest risk scores for the other three criteria (i.e., ls_{lr}, ls_{cr} and id) making it the riskiest route

7.3.1.2 Routes choices and equilibrium flows for heterogenous users

This section analyzes the route choice behavior of users with varying safety preferences in a small network where the three available routes differ in their risk scores. Route 1, with the highest risk score ($R_1 = 3.22$), is identified as the most dangerous. Route 3, with the smallest risk score ($R_3 = 1.62$), is deemed the safest. Assuming a uniform distribution for the VoS, the continuous bicriteria model is solved to determine the VoS boundaries and corresponding route flows. The resulting VoS boundaries are $\beta_1 = 2.0$ and $\beta_2 = 9.0$, which define the VoS intervals for each route as follows: $\tau_1 = [2.0,2.0]$, $\tau_2 = [2.0\,, 9.0]$ and $\tau_3 = [9.0, 20.0]$ (Figure 7.10).

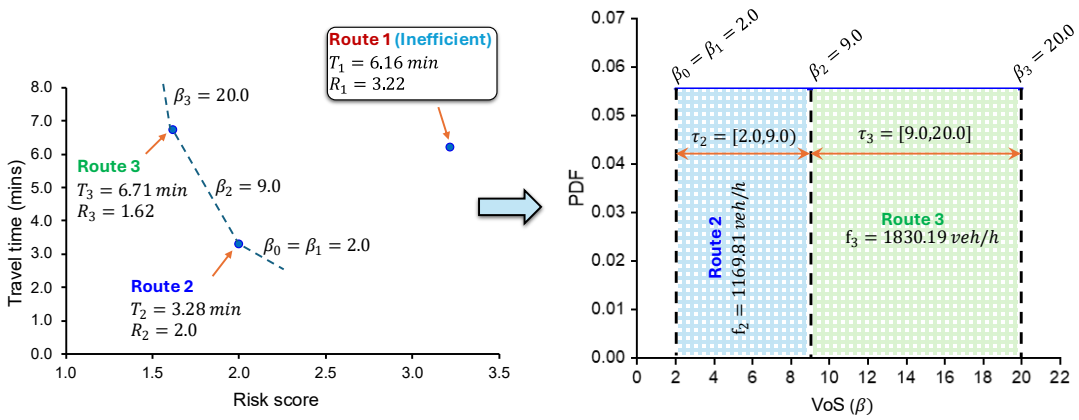

(a) Efficient routes with costs and VoS boundaries **(b)** VoS intervals and route flows

Figure 7.10. Illustration of route flows and VoS boundaries in traffic assignment

From the results shown in Figure 7.10, it is evident that route 1 is inefficient or dominated leading to $\beta_0 = \beta_1$ and resulting in $f_1 = 0$. In contrast, routes 2 and 3 are both efficient. Travelers with lower safety preferences, lying within the VoS interval τ_2, select route 2, which is faster ($T_2 = 3.28$ min) but less safe ($R_2 = 2.0$) compared to route 1. In contrast travelers with higher safety preferences, within the VoS interval

τ_3, opt for route 3 which is slower ($T_3 = 6.71$ min) but safer ($R_3 = 1.62$). The relationship between travelers' safety preferences and their route choices is clear: those who are more concerned about safety (with the highest VoS) are willing to tolerate slower routes in exchange for a lower risk score. On the other hand, travelers who are less concerned about safety prioritize faster routes, even at the cost of higher risk scores. This variation in safety sensitivity is reflected in the flow distribution across routes, as shown in Figure 7.10(b): route 2 carries 1169.8 veh/hr of flow, while route 3 carries 1830.2 veh/hr of flow.

7.3.1.3 Effect of the degree of users' safety heterogeneity on route choice

This section examines how varying degrees of safety preferences influence flow patterns.

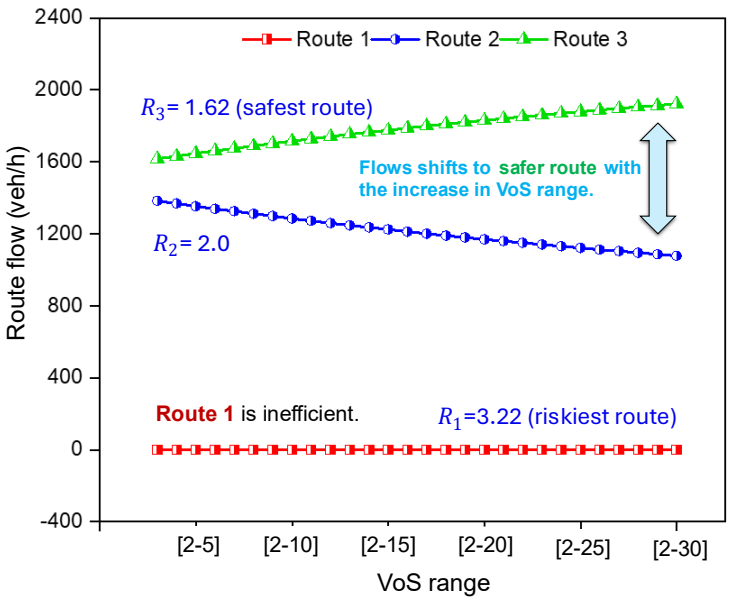

Figure 7.11. Effect of VoS range on route choice behavior

In Figure 7.11, the horizontal axis represents the VoS range, with the lower bound fixed at 2.0 and the upper bound gradually increases from 3.0 to 30.0. The broadening of the VoS range reflects an increasingly more diverse population in terms of safety sensitivity. As the upper bound of VoS increases, the proportion of more safety

conscious travelers in the population increases. This results in an increase in flow on route 3, the safest route, as more users prioritize safety over travel time. Conversely, the flow on route 2, which is less safe, decreases since fewer users are willing to choose a faster route with higher risk score. No flow is observed on route 1, as it remains inefficient and dominated in all cases.

These results highlight the importance of incorporating heterogeneous safety preferences of users into traffic assignment models. Neglecting this variability can result in less accurate estimation of route flows, especially in safety-critical contexts. By modeling the degree of users' safety heterogeneity, more practical and realistic traffic flow patterns can be obtained.

7.3.1.4 Comparison of flows between discrete and continuous VoS distributions

This section examines the differences in route flows between using a discrete versus continuous VoS distribution. In the discrete VoS approach, the population is divided into three classes, each representing a distinct level of safety preference. The corresponding VoS values and demands for each class are summarized in Table 7.5.

Table 7.5. Details of VoS and demands for three classes.

User Class Behavior	VoS (β)	Demand (veh/hr)
Class 1: Low VoS	2.0	1000.0
Class 2: Medium VoS	13.0	1000.0
Class 3: High VoS	20.0	1000.0

Figure 7.12(a) depicts the route flows for discrete VoS distribution, which is solved using the discrete multiclass traffic assignment formulation (Li et al., 2023; Yang & Huang, 2004). Travelers in class 1, characterized by a low VoS (less safety-conscious), all opt for route 2, which offers faster travel times despite its higher risk score. In contrast, travelers in class 3, who have a high VoS (more safety-conscious), exclusively use route 3, the safest route, as they prioritize safety over travel time. Travelers in class

2, with a medium VoS, split their choices between routes 2 and 3, with a higher proportion opting for route 2 due to its faster travel time while route 1 is inefficient.

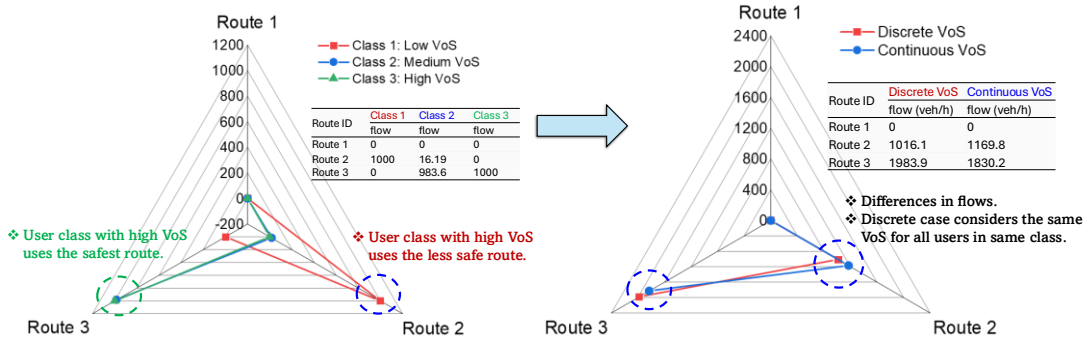

(a) Route flows for discrete VoS distribution **(b)** Discrete versus continuous

Figure 7.12. Comparison of flows between discrete and continuous VoS distributions

Figure 7.12(b) compares route flows under discrete and continuous VoS distributions, revealing noticeable differences even in the small network. For instance, the flow on route 2 is 1016.1 veh/h in the discrete VoS case, compared to 1169.8 veh/h in the continuous VoS case. Similarly, for route 3, the route flow is 1983.9 veh/h for the discrete case and 1830.2 veh/h for the continuous case. These differences arise from discretization errors in the discrete model, where a single average VoS value represents all users within each class. In larger, real-world networks, overlooking the distribution of individual VoS values could lead to substantial deviations in flow predictions. Therefore, considering continuous VoS distribution in bicriteria multiclass traffic assignment model gives more accurate and practical results, offering a better foundation for transportation planning and safety interventions.

7.3.2 Real world case study: Winnipeg network

This section demonstrates the proposed model and solution procedure using the Winnipeg network (Figure 7.13), a real-scale network comprising 2,535 links and 4,345 OD pairs, with a total demand of 54,459 trips. The working route set for the network is adopted from Bekhor et al. (2008). In total, 174,491 routes are considered across all

OD pairs, corresponding to an average of 40.1 routes for any OD pair. The maximum number of routes generated for any single OD pair is 50.

Figure 7.13. Winnipeg network showing the road functional class

Since the original network lacks route functional class information, which is necessary for calculating the risk level of each route in this study, we utilized Google Maps to classify roads, as illustrated in Figure 7.13. Roads are categorized into two types: arterials and non-arterials (collectors/local roads). Consequently, only four criteria are used to determine the risk score of each route. To make the risk score comparable to the travel time in real networks the weight factor for each criterion is set to 10, resulting in a risk score ranging from 0 to 40, where higher values indicate a higher risk level. The experimental settings for VoS (β) remain consistent with those in Section 7.3.1. The stopping criteria for algorithm convergence are set equal to 1e-12. Then the route-

based traffic assignment algorithm is tested on a PC with intel(R) Core (TM) i7-10700 CPU 2.9 GHz and 16 GB RAM using the Windows 10 operating system.

7.3.2.1 Equilibrium flows and route choices for heterogeneous users

We present results for two O-D pairs: O-D pair (31,3) which has three efficient routes and a destination within the CBD area, and O-D pair (91,102) with two efficient routes.

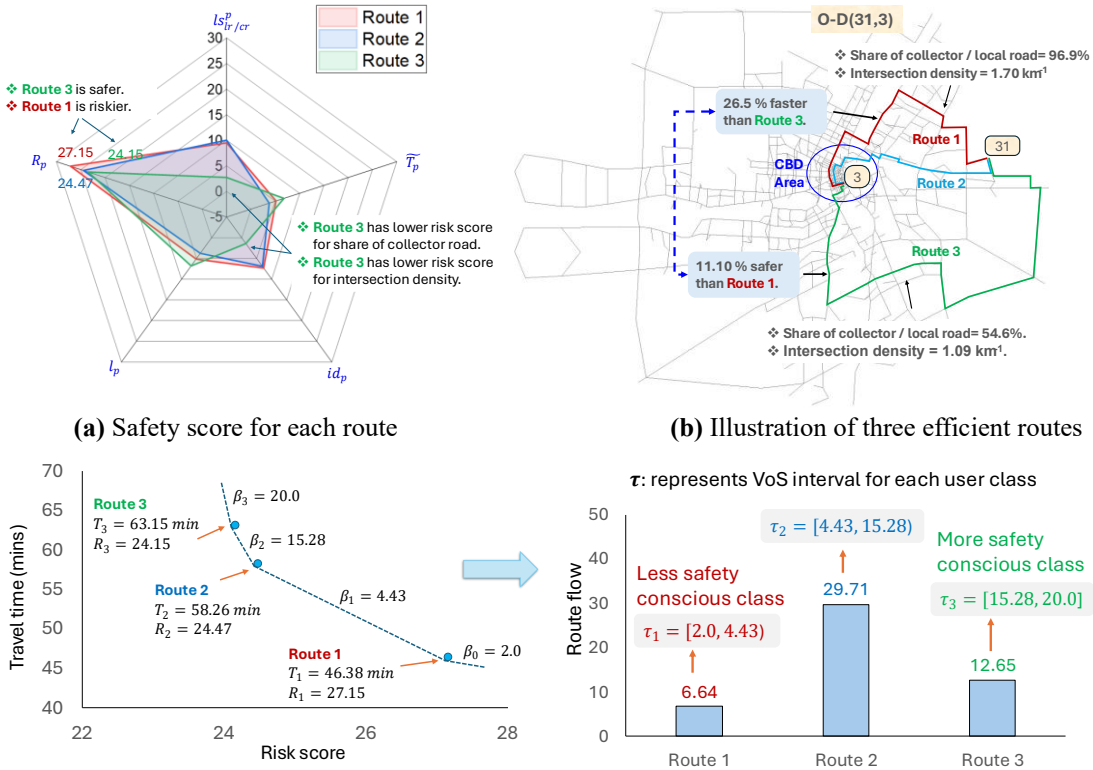

(a) Safety score for each route

(b) Illustration of three efficient routes

(c) Efficient frontier and VoS boundaries

(c) Route flows and VoS intervals

Figure 7.14. Efficient routes and route flows for heterogeneous users in OD pair (31,3)

For OD pair (31,3), Figure 7.14(a) shows the risk score calculations for the three routes. Route 1 is the riskiest ($R_p = 27.15$), while route 3 is the safest ($R_p = 24.15$). Route 3 has the lowest risk score for share of local/collector roads due to a 54.6% share of local/collector roads ($ls_{lr/cr}$) on this route while the remaining 45.6% is the share for arterials compared to 96.9% share of local/collector roads for route 1. Additionally, the intersection density (id) on route 3 is 1.09 km^{-1}, significantly lower than 1.70 km^{-1} on

route 1 resulting in a lower score of this criterion for route 3. While route 3 has the highest risk scores for the other 2 criteria ($\tilde{T} and\ l$), its overall risk score is the lowest.

Figure 7.14(b) shows the 3 chosen routes in the traffic assignment model. Route 1 is 26.5% faster than route 3 while route 3 is 11.10% safer than route 3 as shown in Figure 7.14(c). Thus, users with heterogeneous safety preferences make a trade-off between safety and travel time when selecting these routes. For example, users with lower VoS (less safety-conscious) choose route 1, which has a higher risk score but a shorter travel time ($R_1 = 27.15, T_1 = 46.38\ min$), while users with higher VoS choose route 3, which has a lower risk score and higher travel time ($R_3 = 24.15, T_3 = 63.15\ min$). Most users, however, select route 2 (Figure 7.14(d)), which offers a moderate risk score and medium travel time ($R_2 = 24.47, T_2 = 58.26\ min$). This highlights that users with higher VoS are willing to accept additional travel times in exchange for greater safety. The VoS intervals for the three user classes and the resulting route flows are depicted in Figure 7.14(d).

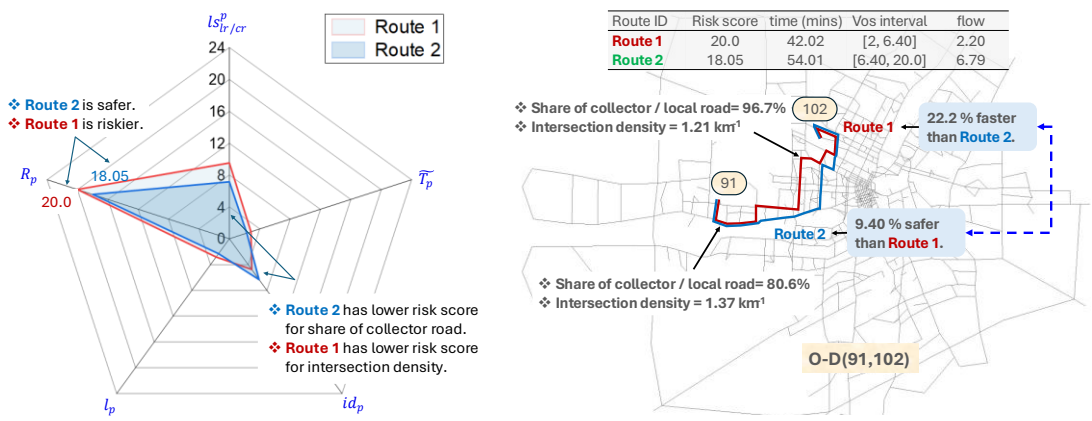

(a) Safety score for each route

(b) Illustration of two efficient routes

Figure 7.15. Efficient routes and route flows for heterogeneous users in OD pair (91,102)

Similarly, for OD pair (91,102), there are two efficient routes where route 1 is 22.2% faster than route 2, while route 2 is 9.40% safer than route 1. Figure 7.15(a) presents the risk score calculations for both routes. From Figure 7.15(b), we observe that users

with heterogeneous safety preferences choose routes differently. The less safety-conscious user class (VoS interval = 2–6.40) chooses route 1, which is faster. In contrast, the more safety-conscious user class chooses route 2, prioritizing safety over shorter travel time. These results show how flows are allocated in a road network based on travelers' varying safety preferences. This shows that more safety-conscious users are willing to accept longer travel times in exchange for increased safety.

Figure 7.16 illustrates the convergence performance of the path-based traffic assignment algorithm, which reaches the desired criterion for the Winnipeg network in under 60 seconds.

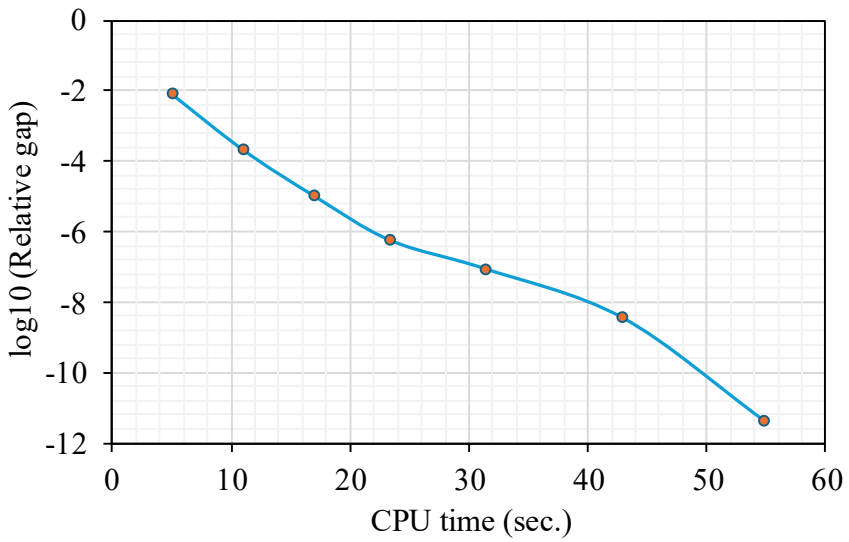

Figure 7.16. Convergence performance of the algorithm on the Winnipeg network

7.3.2.2 Reasonableness check of the model

To assess the reasonableness of our theoretical framework, we utilized a publicly available dataset of GPS trajectories from OpenStreetMap (OSM) for the Winnipeg network as a basis for model verification. The time-stamped traces provide useful insights into traffic flow, route popularity, and stop patterns. While the dataset does not constitute a full-scale empirical validation of the model, it offers valuable evidence to support the output of our traffic assignment results. We conducted a disaggregate

analysis by selecting OD pairs with the greatest GPS trajectory coverage and comparing the observed travel patterns with the model outputs. Specifically, OD pairs (3–31) and (91–102) were analyzed.

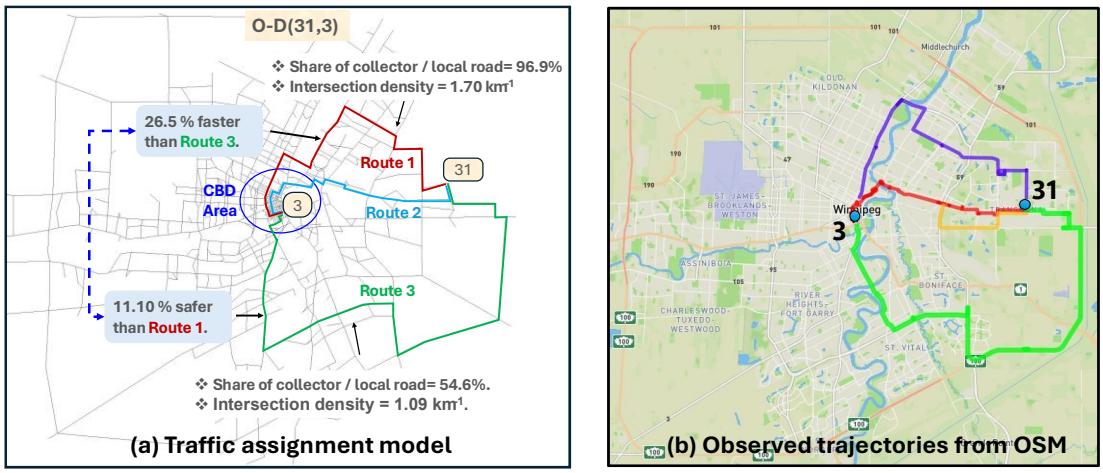

Figure 7.17. Reasonableness check using GPS trajectories for OD pair (31–3)

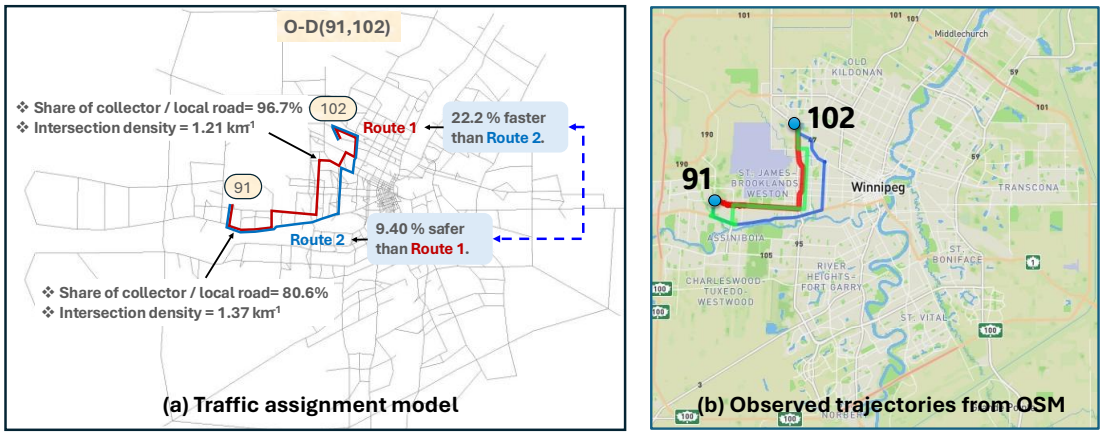

Figure 7.18. Reasonableness check using GPS trajectories for OD pair (91–102)

In Figure 7.17(b), for OD pair (3–31), the trajectories follow different routes that are broadly consistent with the model output in Figure 7.17(a). For example, the green trajectory follows a route with a lower proportion of local or collector roads and a smaller intersection density, criteria directly associated with safety in the proposed model. This suggests that travelers with different safety preferences may indeed select different routes. A similar consistency is observed between Figure 7.18(a) and Figure

7.18(b) for OD pair (91–102). Nevertheless, the precise motivations behind users' choices cannot be fully inferred from this data alone and would require additional information, such as stated preference surveys, to capture underlying behavioral drivers.

7.4 Implications for policy and practice

The proposed framework incorporates travelers' safety preferences into the traffic assignment model, offering valuable tools for traffic planners and policymakers to improve network safety. Unlike conventional traffic assignment models that assume travelers select routes based solely on travel time, this model accounts for safety as a critical factor in route choice. This is particularly relevant in the era of connected vehicles, where real time safety information will increasingly influence route choices. By incorporating travelers' heterogeneous safety preferences, the model allows planners to predict how safety concerns affect traffic flow patterns. This insight enables a systematic evaluation of traffic countermeasures and regulations by estimating their effects on route choices and identifying possible changes in flow patterns. Planners can thus develop safety improvement policies based on traveler behavior rather than relying solely on historical crash data or past experience. Moreover, the introduction of the VoS concept into the network equilibrium model provides a practical way to measure travelers' willingness to trade travel time for safety. Using SP surveys, policymakers can quantify VoS and use it to design safety policies that reflect the public's preferences.

The model also offers a framework to design targeted safety measures for vulnerable groups, those that are less concerned about safety. For instance, reckless or distracted driving behaviors, which significantly increase the crash risks (Gong & Fan, 2017; Islam & Mannering, 2006), can be addressed by implementing countermeasures on

routes used by such travelers. Effective measures include legislation and enforcement (Gitelman et al., 2012), raising awareness through safety campaigns and targeted education programs (such as educating young drivers about the risks of reckless driving) (Hoekstra & Wegman, 2011), and implementing traffic calming measures like speed humps to improve safety. By integrating individualized safety preferences into traffic assignment models, this study enables planners to provide safety related policies that address both behavioral and infrastructural aspects of safety more effectively.

7.4.1 Applicability in autonomous vehicle futures

Our current model, built around the heterogeneous VoS, remains highly relevant and adaptable in an era where AVs become the dominant mode. With vehicle connectivity providing real-time safety data, the reliance on user perception will diminish, aligning more closely with our foundational assumptions of informed route choices. One of the major anticipated benefits of AVs is the substantial improvement in transportation network safety, particularly through the reduction of crashes caused by human error (Hussain et al., 2021; Kockelman et al., 2016).

As AVs assume greater control over routing decisions, the assumptions underlying equilibrium principles in traffic assignment will also evolve. Equilibrium principles reflect individual route choice behavior, and many studies on multiclass traffic assignment have explored mixed environments of human-driven vehicles (HVs) and AVs. Some assume a unified user equilibrium (UE) principle (Liu & Song, 2019), while others differentiate by assigning system optimal (SO) principles to AVs (Bagloee et al., 2017), or stochastic user equilibrium (SUE) to HVs due to perception errors (Wang et al., 2021). Wang et al. (2020b) further modeled route choice across three vehicle types: private HVs, firm-operated AVs, and government-operated AVs, using SUE, Cournot-Nash (CN), and SO principles, respectively.

The key insight is that the heterogeneous VoS remains a foundational element for these adaptations. (1) In a mixed AV-HV environment with privately owned AVs, our model can be extended to reflect HVs choosing routes based on perceived safety and VoS, while AVs select routes using accurate safety data and owner-defined VoS preferences. (2) In a fully AV-dominated future, the VoS concept evolves but remains central. Privately owned AVs would follow a user equilibrium based on personalized VoS, while fleet-operated AVs could be guided by a centrally determined societal VoS, serving as a policy lever to achieve system optimality and reduce overall crash risk and travel time.

7.5 Conclusions

This Chapter models the trade-off between travel safety (measured as risk score) and travel time using the continuous bicriteria traffic assignment model. The model captures users' heterogeneous safety preferences through the value of safety (VoS), defined as the additional time an individual is willing to travel on a slower route to reduce risk. The risk score of a route is calculated by comparing several risk-related criteria of routes between each OD pair. The C-BiTA model allocates travelers to routes based on minimizing a generalized route cost, which is modeled as a linear combination of travel time and risk score. The effect of users' heterogeneous safety preferences on travelers' route choice behavior and network flow patterns was demonstrated using a small and real network example. The results showed that users with higher safety concerns (high VoS) are willing to accept longer travel times on safer routes. In comparison, users with lower safety concerns (low VoS) prioritize faster routes despite their higher associated risks.

CHAPTER 8 Conclusion and recommendations

8.1 Introduction

This research aims to enhance road network safety by proposing proactive safety improvement strategies, specifically through modeling travelers' safety behaviors and preferences on road networks. To achieve this, crash risk models, game theory, and network equilibrium approaches were integrated to address the challenges of creating a safer transportation system. Given that road crashes are a major global cause of fatalities and injuries, particularly affecting vulnerable road users in developing countries, this research emphasizes the importance of proactive safety improvement models.

The following objectives guided this research. Objective 1 examines the consistency of crash severity risk factors between statistical and interpretable ML models for motorcyclists in a developing country. Objective 2 aims to develop a framework to identify the safety-critical links in a road network proactively. Objectives 3-5 aim to model travelers' safety behaviors and preferences during several stages of the transportation planning process, specifically the car ownership, car type choices and traffic assignment step. A comprehensive review of the literature for each objective is presented in Chapter 2. The methodologies and findings are detailed in Chapters 3–7.

8.2 Summary of findings

Objective 1: Examining the consistency of risk factors between statistical ML models

Chapter 3 examined the consistency of crash severity risk factors between statistical models and ML methods using motorcycle crash data from Rawalpindi, Pakistan. The

analysis compared an MNL model with three ML models: random forest, naïve Bayes, and gradient-boosted trees. The RF model achieved the highest prediction accuracy (86.7%). The SHAP (SHapley Additive exPlanations) method, based on Shapley values from cooperative game theory, was applied to address the interpretability of ML models. Key findings revealed that risk factors identified by the RF model (e.g., distracted driving, collisions involving pedestrians or trucks, and female riders) were consistent with those identified by the MNL model. These results provide actionable insights for developing targeted safety countermeasures to improve motorcycle safety in Pakistan.

Objective 2: Develop a framework for proactive identification of safety-critical road links

In Chapter 4, a framework was developed to pinpoint safety-critical links in a road network. A cooperative game theory approach was employed, where road links act as players forming coalitions. The utility function of the cooperative game was quantified in the UE traffic assignment model using a flow-dependent safety evaluation metric. The solution of cooperative game was obtained using Shapley value, which calculates the average MC of links to network safety across all possible link coalitions, accounting for traffic interactions rather than considering only their MC to the grand coalition.

Numerical experiments demonstrated that the Shapley value approach offers a more comprehensive evaluation of link safety contributions than traditional marginal contribution methods. This framework provides transportation planners with a proactive tool to identify safety-critical links, prioritize interventions, and enhance network safety during the planning stage.

Objective 3: Modeling travelers' safety concerns in joint car ownership and car type choice

In Chapter 5, a joint car ownership and car type equilibrium choice model was proposed. The proposed discrete choice modeling-based equilibrium analysis framework integrates a dogit model to capture captivity effects in car ownership decisions and a nested logit model to account for similarities among car types. It explicitly incorporates users' concerns related to crash risk, security risk, and range anxiety. The framework was formulated as a mathematical programming problem, ensuring the solution's existence and uniqueness.

Numerical experiments on a toy network and a real-world case study revealed that reductions in travelers' risk perceptions toward AVs lead to significant increases in AV adoption, highlighting the critical role of public trust in transitioning to AV-dominated markets. By explicitly linking risk perceptions to long-term transportation planning, this model equips policymakers with a tool to design strategies that address behavioral barriers to AV adoption while balancing efficiency and safety objectives.

Objective 4: Modeling safety variability preferences and safety-conscious route choice sets in traffic assignment

Chapter 6 proposed an integrated network equilibrium framework that models safety-conscious class-specific route choice sets while simultaneously incorporating travelers' concerns about the reliability and unreliability of safety and travel time. Travelers were categorized into two classes, high safety-conscious and low safety-conscious, based on their safety requirements. The route choice set for each class was defined based on their safety score requirements, with the score of each route quantified by its roadway characteristics. The reliability and unreliability aspects of safety variability for

heterogeneous travelers were modeled using the α-reliable mean-excess concept, and a crash risk cost distribution represented their safety variability concerns.

The framework was formulated as a VI problem and solved using a two-stage algorithm. Numerical experiments demonstrated that highly safety-conscious travelers prioritize safer routes, influencing traffic flow patterns. This framework enables planners to consider heterogeneous safety preferences when designing safety-conscious transportation policies.

Objective 5: Modeling time-safety trade-off by considering continuous VoS in traffic assignment

In Chapter 7, a traffic assignment framework that models the time-safety trade-off for travelers with heterogeneous safety preferences was proposed. The value of safety (VoS) was introduced to capture these preferences, representing the additional travel time a traveler is willing to accept for improved safety. Unlike traditional approaches that categorize travelers into discrete classes, VoS was modeled as a continuous variable, allowing for a more refined representation of individual safety preferences. A bicriteria traffic assignment model incorporating this continuous VoS distribution was employed to determine route flows between origin-destination (OD) pairs based on both travel time and safety. Route safety was modeled in terms of risk, which was quantified by comparing routes between OD pairs based on various safety-related criteria. The proposed model was solved using a two-stage algorithm: the first stage evaluated route risk, while the second stage solved the bicriteria traffic assignment problem.

Numerical experiments on small-scale and real-world networks demonstrated how safety preferences influence route choices and subsequent flow patterns, showing that

high safety-conscious travelers prioritized safer routes, even at longer travel times. The framework provides planners with insights into how safety preferences shape route choices and traffic patterns, enabling the development of targeted safety improvement strategies.

8.3 Summary of research contributions

This research significantly contributes to the field of transportation network safety, both theoretically and practically. The proposed frameworks and models advance proactive safety planning by incorporating traveler safety behaviors and preferences into the planning process. The contributions of each objective are detailed below:

8.3.1 Consistency of risk factors between statistical and interpretable ML models

This part of the research contributes to the field by highlighting the consistency of crash severity risk factors between statistical and interpretable ML models. By making use of the Shapley value-based cooperative game theory, it interprets the output of ML models that are often criticized for their black-box nature. The findings revealed that although the statistical models and ML methods follow two streams of methodologies on prediction, the identified risk factors are reasonably consistent to a greater extent. Finally, according to the crash severity study's findings in Pakistan, this research has suggested appropriate policies and countermeasures to reduce motorcycle crash injuries. Analyzing the consistency between the two streams of methodologies will provide decision-makers with key insights that will help them initiate clear remedial measures to promote the safety of motorcyclists and pillion passengers in Pakistan.

8.3.2 Framework for identification of safety-critical road links

This study develops a framework that identifies the safety-critical links in road networks by integrating transportation safety analysis without network effect and

transportation network analysis without safety effect via the Shapley value from cooperative game theory. By accounting for cooperative interactions of links using a flow-dependent safety-evaluation metric, it enhances theoretical understanding of transportation network safety. From a practical perspective, this approach offers transportation safety planners a useful transportation network safety analysis framework to identify the most safety-critical links for investment strategy at the planning stage.

8.3.3 A joint car ownership and car type equilibrium choice model

This study contributes to the field by proposing an equilibrium analysis framework to model the joint car ownership and car type choice decisions based on endogenous travel disutility, considering the specific characteristics of each car type. The proposed framework explicitly considers travelers' risk perceptions related to safety (crash risk) and security issues of AVs, as well as the range anxiety associated with EVs, within the joint choice equilibrium model. This explicit focus provides insights into how these factors influence long-term decisions, including car ownership and car type preferences, which are often overlooked in existing models. By incorporating travelers' risk perceptions and demand-dependent disutility into long-term decision-making, the model provides a foundation for evaluating and developing safety-conscious transportation policies. The findings can guide policymakers in designing strategies to promote safer vehicle adoption (e.g., autonomous and electric vehicles) while addressing travelers' concerns about safety and security.

8.3.4 Modeling safety variability preferences and safety-conscious choice sets

This study develops a comprehensive network equilibrium framework that considers roadway characteristics and traffic conditions to model travelers' safety concerns in route choice. The proposed framework models and analyzes the effect of safety-based

class-specific route choice sets on equilibrium flow patterns. Moreover, it accounts for travelers' concerns about both the reliability and unreliability of safety and travel time variabilities, considering traveler classes with heterogeneous safety reliability preferences. It enables planners to explicitly incorporate travelers' safety preferences into the transportation planning process, allowing for the development of targeted safety improvement policies informed by travelers' behaviors.

8.3.5 Model time-safety trade-off by proposing travelers' value of safety

This study proposes a traffic assignment framework that explicitly incorporates travelers' value of safety (VoS) to model the trade-off between travel time and safety. By integrating safety considerations alongside travel time, the model captures travelers' heterogeneous safety preferences and their willingness to accept additional travel time in exchange for safer routes. This approach highlights how individual safety preferences influence route choice behavior and traffic flow patterns in real-world scenarios. A key contribution of this study is the introduction of a continuous distribution of VoS across the population, moving beyond the traditional use of discrete user classes. This continuous representation more accurately reflects the diverse nature of travelers' safety preferences, capturing subtle variations in route choices that discrete models may overlook. As a result, the framework provides policymakers with more precise insights into traveler behavior, enabling the development of targeted and effective safety policies. By focusing on traveler safety behaviors rather than relying solely on historical crash data or past experiences, the proposed framework empowers planners to design more informed and proactive safety improvement policies.

8.4 Research Limitations

Despite the contributions of this research to literature, several limitations must be acknowledged:

- Regarding the consistency analysis using motorcycle crash data, the study was limited to only one year of motorcycle crash data, and the dataset had underreported no-injury crashes. Underreporting of no-injury crashes is a universal issue in road crash data (Mannering & Bhat, 2014), which was also hard to avoid in the current study. Additionally, key variables such as helmet use were missing. Future studies should address these limitations by using more comprehensive datasets.
- The proposed critical link identification framework was tested only on a toy network, as the computational complexity of calculating the exact Shapley value increases exponentially with the number of links.
- The parameters and inputs used in the joint car ownership and car type choice model are illustrative and require calibration and validation with real-world data. In particular, the AV risk perception parameters should be calibrated using stated preference or revealed preference survey data. Moreover, the model only considers self-owned autonomous vehicles, excluding shared ones. Including shared mobility services in the model by incorporating specific utility functions is worth exploring.
- Regarding incorporating safety variability in the network equilibrium model, the link crash risk distribution was assumed to be normally distributed. However, validating the distribution parameters with empirical data is necessary to refine this assumption and calibrate it for different roadway types and traffic conditions.
- The time-safety trade-off model assumed flow-independent risk levels and a linear trade-off between time and safety. Risk levels vary with traffic conditions, and the

trade-off may be non-linear. The risk score is also based on predefined criteria; validating its relationship with actual crash data is necessary.

8.5 Future research directions

Based on the limitations identified, several directions for future research are proposed:

- In the motorcycle crash data, the challenges related to underreporting can be addressed by adopting several data sampling techniques, including over-sampling, under-sampling, and hybrid sampling (Bazarnovi & Mohammadian, 2024). Moreover, advanced statistical methods such as the mixed or random parameter logit can be employed to account for the issues of unobserved heterogeneity (Islam et al., 2014; Pervez et al., 2021).
- The proactive safety-critical link identification framework can be tested on real-world road networks. As the computational complexity of exact Shapley value calculation grows exponentially with the number of links, optimization techniques must be explored to enhance scalability. Approximation techniques such as Monte Carlo sampling have been widely used to estimate Shapley values in computationally demanding scenarios (Gnecco et al., 2021; Narayanam & Narahari, 2010; Touati et al., 2021). Moreover, recent advancements in ML could provide another promising direction. For example, supervised learning techniques could use a set of training pairs (e.g., input vectors of link-level crash probabilities and output vectors of Shapley values) to predict Shapley values for previously unseen scenarios. Doing so would make it possible to bypass solving the traffic assignment problem for each coalition evaluation, significantly reducing computational effort (Gückel & Fontaine, 2025). Furthermore, while this study utilizes the UE traffic assignment model to solve the utility function, future research could explore

quantifying the Shapley value within a stochastic traffic assignment model by incorporating user perception errors to capture more realistic user behaviors (Chen et al., 2012; Li et al., 2024).

- First, the current approach accounts for captivity at the car ownership choice level (upper level) using the dogit model for the joint car ownership and car type choice model. This framework can be extended to capture captivity for each mode type at the car type choice level (lower level) by replacing the nested logit model with the dogit nested logit model (Wang et al., 2024). Second, at the car type choice level, the basic model primarily examines travelers' preferences for self-owned human-driven and autonomous vehicles based on their risk perceptions. In this context, public transport is treated as a general mode. However, the model can be extended further to include other on-demand services such as ride-hailing and ridesharing and emerging public transportation options like customized buses. Last, the current analysis relies on hypothetical data to demonstrate the model's functionality as a proof-of-concept, but empirical validation is essential for credibility and practical application. Parameters can be calibrated using revealed preference data from traffic counts or stated preference surveys on user risk perceptions, enabling operationalization in specific contexts. Future research can therefore focus on integrating revealed preference data from AV pilot programs to test predictions of market shares. Building on similar theoretical foundations in AV literature (Xie & Liu, 2022; Zhang et al., 2020a), this empirical extension will position the model as a robust tool for long-term transportation planning
- To capture heterogeneous safety reliability preferences in the METE model, it would be valuable to model individual-specific safety preferences using a C-BiTA framework, which can theoretically accommodate infinite user classes (Xu et al.,

2024a). Additionally, incorporating more roadway characteristics can help better quantify the safety score of a route. From a computational perspective, developing more efficient algorithms for solving the bi-objective, non-additive generalized route cost problem would also be beneficial.

- In the time-safety trade-off model, it would be valuable to consider both travel time and safety as flow-dependent criteria. As travelers gravitate towards safer routes, increased volumes on those links could potentially alter their risk profiles, a phenomenon analogous to congestion effects on travel time. Developing an equilibrium model with flow-dependent safety risk represents the most important direction for future work. Tackling this challenge would require solving a complex fixed-point problem, advancing the methodological frontier of multi-criteria traffic assignment. Additionally, this study assumes a linear trade-off between travel time and safety. In reality, the relationship may not be strictly linear. Exploring non-linear utility forms or incorporating interaction effects could yield a more behaviorally realistic representation of traveler decision-making. The main challenge lies in identifying appropriate non-linear forms, which would require extensive empirical calibration. We see this as an important direction for future research. Finally, while VoS is assumed to follow a uniform distribution in numerical experiments, future research could investigate alternative distributions and empirically evaluate their suitability.
- Moreover, safety behaviors can be incorporated into other choice dimensions such as location and trip choices, within network equilibrium models.

REFERENCES

Abdel-Aty, M., Kitamura, R., & Jovanis, P. P. (1995). Exploring route choice behavior using geographic information system-based alternative routes and hypothetical travel time information input. *Transportation Research Record*(1493).

Abdel-Aty, M., Lee, J., Siddiqui, C., & Choi, K. (2013). Geographical unit based analysis in the context of transportation safety planning. *Transportation Research Part A: Policy and Practice, 49*, 62-75. doi:https://doi.org/10.1016/j.tra.2013.01.030

Abdel-Aty, M. A., & Abdelwahab, H. T. (2004). Predicting injury severity levels in traffic crashes: a modeling comparison. *Journal of Transportation Engineering, 130*(2), 204-210.

Adeel, M., Yeh, A. G., & Zhang, F. (2016). Towards an inclusive public transport system in Pakistan. *Transport and Communications Bulletin for Asia and the Pacific*.

Agyemang, W., Adanu, E. K., & Jones, S. (2021). Understanding the factors that are associated with motorcycle crash severity in rural and urban areas of Ghana. *Journal of Advanced Transportation, 2021*(1), 6336517.

Ahmed, A. (2007). National Road Safety Plan 2007-2012. *Islamabad: National Road Safety Secretariat, Ministry of Communications*.

Ahmed, A., Khan, B. A., Khurshid, M. B., Khan, M. B., & Waheed, A. (2016). Estimating national road crash fatalities using aggregate data. *International Journal of Injury Control and Safety Promotion, 23*(3), 249-254.

Al-Ahmadi, H. M., Jamal, A., Ahmed, T., Rahman, M. T., Reza, I., & Farooq, D. (2021). Calibrating the highway safety manual predictive models for multilane rural highway segments in Saudi Arabia. *Arabian Journal for Science and Engineering, 46*(11), 11471-11485. doi:10.1007/s13369-021-05944-6

Alarifi, S. A., Abdel-Aty, M. A., Lee, J., & Park, J. (2017). Crash modeling for intersections and segments along corridors: A Bayesian multilevel joint model with random parameters. *Analytic Methods in Accident Research, 16*, 48-59. doi:https://doi.org/10.1016/j.amar.2017.08.002

Alberini, A., & Santoboni, G. (2025). Ownership and use of electric vehicles in the Washington, DC, metro area. *Travel Behaviour and Society, 39*, 100945. doi:https://doi.org/10.1016/j.tbs.2024.100945

Ali, Y., Haque, M. M., & Mannering, F. (2023). Assessing traffic conflict/crash relationships with extreme value theory: Recent developments and future directions for connected and autonomous vehicle and highway safety research. *Analytic Methods in Accident Research, 39*, 100276. doi:https://doi.org/10.1016/j.amar.2023.100276

Aljanahi, A., Rhodes, A., & Metcalfe, A. V. (1999). Speed, speed limits and road traffic accidents under free flow conditions. *Accident Analysis & Prevention, 31*(1-2), 161-168.

Amirgholy, M., Golshani, N., Schneider, C., Gonzales, E. J., & Gao, H. O. (2017). An advanced traveler navigation system adapted to route choice preferences of the individual users. *International Journal of Transportation Science and Technology, 6*(4), 240-254.

Amoh-Gyimah, R., Saberi, M., & Sarvi, M. (2017). The effect of variations in spatial units on unobserved heterogeneity in macroscopic crash models. *Analytic Methods in Accident Research, 13*, 28-51. doi:https://doi.org/10.1016/j.amar.2016.11.001

Anderson, J., & Hernandez, S. (2017). Roadway classifications and the accident injury severities of heavy-vehicle drivers. *Analytic Methods in Accident Research, 15*, 17-28. doi:https://doi.org/10.1016/j.amar.2017.04.002

Anderson, J. M., Nidhi, K., Stanley, K. D., Sorensen, P., Samaras, C., & Oluwatola, O. A. (2014). *Autonomous vehicle technology: A guide for policymakers*: Rand Corporation.

Andersson, H., & Treich, N. (2011). The value of a statistical life. In: *A Handbook of Transport Economics*: Edward Elgar Publishing.

Antoniou, C. (2014). A stated-preference study of the willingness-to-pay to reduce traffic risk in urban vs. rural roads. *European Transport Research Review, 6*(1), 31-42.

Anvari, M. B., Tavakoli Kashani, A., & Rabieyan, R. (2017). Identifying the most important factors in the at-fault probability of motorcyclists by data mining, based on classification tree models. *International Journal of Civil Engineering, 15*(4), 653-662.

Arvin, R., Khattak, A. J., Kamrani, M., & Rio-Torres, J. (2020). Safety evaluation of connected and automated vehicles in mixed traffic with conventional vehicles at intersections. *Journal of Intelligent Transportation Systems, 25*(2), 170-187.

Bagloee, S. A., & Asadi, M. (2016). Crash analysis at intersections in the CBD: A survival analysis model. *Transportation Research Part A: Policy and Practice, 94*, 558-572. doi:https://doi.org/10.1016/j.tra.2016.10.019

Bagloee, S. A., Sarvi, M., Patriksson, M., & Rajabifard, A. (2017). A mixed user-equilibrium and system-optimal traffic flow for connected vehicles stated as a complementarity problem. *Computer-Aided Civil and Infrastructure Engineering, 32*(7), 562-580.

Bahat, O., & Bekhor, S. (2016). Incorporating ridesharing in the static traffic assignment model. *Networks and Spatial Economics, 16*(4), 1125-1149. doi:10.1007/s11067-015-9313-7

Bansal, P., & Kockelman, K. M. (2017). Forecasting Americans' long-term adoption of connected and autonomous vehicle technologies. *Transportation Research Part A: Policy and Practice, 95*, 49-63.

Bates, J., Polak, J., Jones, P., & Cook, A. (2001). The valuation of reliability for personal travel. *Transportation Research Part E: Logistics and Transportation Review, 37*(2), 191-229. doi:https://doi.org/10.1016/S1366-5545(00)00011-9

Batool, Z., & Carsten, O. (2017). Self-reported dimensions of aberrant behaviours among drivers in Pakistan. *Transportation Research Part F: Traffic Psychology and Behaviour, 47*, 176-186. doi:https://doi.org/10.1016/j.trf.2017.04.017

Bazarnovi, S., & Mohammadian, A. (2024). *Addressing imbalanced data in predicting injury severity after traffic crashes: A comparative analysis of machine learning models*. Paper presented at the Procedia Computer Science, The 15th International Conference on Ambient Systems, Networks and Technologies (ANT), Hasselt, Belgium. https://www.sciencedirect.com/science/article/pii/S1877050924012304

Beckmann, M. J., McGuire, C. B., & Winsten, C. B. (1956). *Studies in the Economics of Transportation*: Rand Corporation.

Behnood, A., & Mannering, F. (2019). Time-of-day variations and temporal instability of factors affecting injury severities in large-truck crashes. *Analytic Methods in Accident Research, 23*, 100102. doi:https://doi.org/10.1016/j.amar.2019.100102

Bekhor, S., Toledo, T., & Prashker, J. N. (2008). Effects of choice set size and route choice models on path-based traffic assignment. *Transportmetrica, 4*(2), 117-133.

Belgiawan, P. F., Schmöcker, J.-D., Abou-Zeid, M., & Fujii, S. (2017). Analysis of car type preferences among students based on seemingly unrelated regression. *Transportation Research Record, 2666*(1), 85-93. doi:10.3141/2666-10

Belgiawan, P. F., Schmöcker, J.-D., Abou-Zeid, M., Walker, J., Lee, T.-C., Ettema, D. F., & Fujii, S. (2014). Car ownership motivations among undergraduate students in China, Indonesia, Japan, Lebanon, Netherlands, Taiwan, and USA. *Transportation, 41*(6), 1227-1244. doi:10.1007/s11116-014-9548-z

Bellman, R. (1958). On a routing problem. *Quarterly of Applied Mathematics, 16*(1), 87-90.

Ben-Akiva, M. E., & Lerman, S. R. (1985). *Discrete choice analysis: theory and application to travel demand* (Vol. 9): MIT press.

Berkeley, N., Jarvis, D., & Jones, A. (2018). Analysing the take up of battery electric vehicles: An investigation of barriers amongst drivers in the UK. *Transportation Research Part D: Transport and Environment, 63*, 466-481.

Bjørnskau, T., Nævestad, T.-O., & Akhtar, J. (2012). Traffic safety among motorcyclists in Norway: A study of subgroups and risk factors. *Accident Analysis & Prevention, 49*, 50-57. doi:https://doi.org/10.1016/j.aap.2011.09.051

Bonera, M., Barabino, B., & Maternini, G. (2022). A straightforward framework for road network screening to lombardy region (Italy). *Sustainability, 14*(19). doi:10.3390/su141912424

Bonera, M., Barabino, B., Yannis, G., & Maternini, G. (2024). Network-wide road crash risk screening: A new framework. *Accident Analysis & Prevention, 199*, 107502.

Breiman, L. (2001). Random forests. *Machine Learning, 45*(1), 5-32.

Cai, Q., Abdel-Aty, M., Sun, Y., Lee, J., & Yuan, J. (2019). Applying a deep learning approach for transportation safety planning by using high-resolution transportation and land use data. *Transportation Research Part A: Policy and Practice, 127*, 71-85.

Carmody, D. R., & Sowers, R. B. (2019). Tradeoffs between safety and time: A routing view. *Transportation Research Part C: Emerging Technologies, 108*, 357-377. doi:https://doi.org/10.1016/j.trc.2019.09.020

Castellà, J., & Pérez, J. (2004). Sensitivity to punishment and sensitivity to reward and traffic violations. *Accident Analysis & Prevention, 36*(6), 947-952.

Chandra, S. (2014). Safety-based path finding in urban areas for older drivers and bicyclists. *Transportation Research Part C: Emerging Technologies, 48*, 143-157.

Chang, F., Xu, P., Zhou, H., Lee, J., & Huang, H. (2019). Identifying motorcycle high-risk traffic scenarios through interactive analysis of driver behavior and traffic characteristics. *Transportation Research Part F: Traffic Psychology and Behaviour, 62*, 844-854. doi:https://doi.org/10.1016/j.trf.2019.03.010

Chapman, R. (1973). The concept of exposure. *Accident Analysis & Prevention, 5*(2), 95-110.

Chatterjee, K., & and McDonald, M. (1999). The network safety effects of dynamic route guidance. *ITS Journal - Intelligent Transportation Systems Journal, 4*(3-4), 258-260. doi:10.1080/10248079908903751

Chen, A., Pravinvongvuth, S., Xu, X., Ryu, S., & Chootinan, P. (2012). Examining the scaling effect and overlapping problem in logit-based stochastic user equilibrium models. *Transportation Research Part A: Policy and Practice, 46*(8), 1343-1358. doi:https://doi.org/10.1016/j.tra.2012.04.003

Chen, A., & Zhou, Z. (2010). The α-reliable mean-excess traffic equilibrium model with stochastic travel times. *Transportation Research Part B: Methodological, 44*(4), 493-513.

Chen, A., Zhou, Z., & Lam, W. H. K. (2011). Modeling stochastic perception error in the mean-excess traffic equilibrium model. *Transportation Research Part B: Methodological, 45*(10), 1619-1640. doi:https://doi.org/10.1016/j.trb.2011.05.028

Chen, J., Li, K., Tang, Z., Bilal, K., Yu, S., Weng, C., & Li, K. (2016). A parallel random forest algorithm for big data in a spark cloud computing environment. *IEEE Transactions on Parallel and Distributed Systems, 28*(4), 919-933.

Chen, P., Tong, R., Yu, B., & Wang, Y. (2020). Reliable shortest path finding in stochastic time-dependent road network with spatial-temporal link correlations: A case study from Beijing. *Expert Systems with Applications, 147*, 113192. doi:https://doi.org/10.1016/j.eswa.2020.113192

Chen, S., Wang, H., & Meng, Q. (2019). Designing autonomous vehicle incentive program with uncertain vehicle purchase price. *Transportation Research Part C: Emerging Technologies, 103*, 226-245.

Chen, Z., & Lym, Y. (2021). The influence of built environment on distracted driving related crashes in Ohio. *Transport Policy, 101*, 34-45. doi:https://doi.org/10.1016/j.tranpol.2020.11.011

Cheng, W., Gill, G. S., Sakrani, T., Dasu, M., & Zhou, J. (2017). Predicting motorcycle crash injury severity using weather data and alternative Bayesian multivariate crash frequency models. *Accident Analysis & Prevention, 108*, 172-180.

Cherry, C. R., & Adelakun, A. A. (2012). Truck driver perceptions and preferences: Congestion and conflict, managed lanes, and tolls. *Transport Policy, 24*, 1-9. doi:https://doi.org/10.1016/j.tranpol.2012.07.012

Chipman, M. L., MacGregor, C. G., Smiley, A. M., & Lee-Gosselin, M. (1992). Time vs. distance as measures of exposure in driving surveys. *Accident Analysis & Prevention, 24*(6), 679-684. doi:https://doi.org/10.1016/0001-4575(92)90021-A

Choi, J. K., & Ji, Y. G. (2015). Investigating the importance of trust on adopting an autonomous vehicle. *International Journal of Human-Computer Interaction, 31*(10), 692-702.

Christoforou, Z., Cohen, S., & Karlaftis, M. G. (2011). Identifying crash type propensity using real-time traffic data on freeways. *Journal of Safety Research, 42*(1), 43-50. doi:https://doi.org/10.1016/j.jsr.2011.01.001

Chu, Y.-L. (2016). Automobile ownership model that incorporates captivity and proximate covariance. *Transportation Research Record, 2563*(1), 80-87.

Clarke, D. D., Ward, P., Bartle, C., & Truman, W. (2007). The role of motorcyclist and other driver behaviour in two types of serious accident in the UK. *Accident Analysis & Prevention, 39*(5), 974-981.

Cunto, F. J., & Ferreira, S. (2017). An analysis of the injury severity of motorcycle crashes in Brazil using mixed ordered response models. *Journal of Transportation Safety & Security, 9*(sup1), 33-46.

Damani, J., & Vedagiri, P. (2021). Safety of motorised two wheelers in mixed traffic conditions: literature review of risk factors. *Journal of Traffic and Transportation Engineering (English edition)*.

Das, S., Dzinyela, R., Liu, J., Dadashova, B., & Silvestri-Dobrovolny, C. (2025). Understanding patterns of factor influences in motorcycle crashes with fixed objects. *Journal of Transportation Safety & Security, 17*(5), 483-509. doi:10.1080/19439962.2024.2429077

Deery, H. A. (1999). Hazard and risk perception among young novice drivers. *Journal of Safety Research, 30*(4), 225-236.

Delen, D., Sharda, R., & Bessonov, M. (2006). Identifying significant predictors of injury severity in traffic accidents using a series of artificial neural networks. *Accident Analysis & Prevention, 38*(3), 434-444.

Dial, R. B. (1979). A model and algorithm for multicriteria route-mode choice. *Transportation Research Part B: Methodological, 13(4)*, 311-316.

Dial, R. B. (1996). Bicriterion traffic assignment: Basic theory and elementary algorithms. *Transportation Science, 30*(2), 93-111.

Dijkstra, A. (2013). Assessing the safety of routes in a regional network. *Transportation Research Part C: Emerging Technologies, 32*, 103-115. doi:https://doi.org/10.1016/j.trc.2012.10.008

Dijkstra, A., Drolenga, H., & van Maarseveen, M. (2007). Method for assessing safety of routes in a road network. *Transportation Research Record, 2019*(1), 82-90. doi:10.3141/2019-11

Domingos, P., & Pazzani, M. (1997). On the optimality of the simple Bayesian classifier under zero-one loss. *Machine Learning, 29*(2), 103-130.

Dong, C., Wang, H., Ni, D., Liu, Y., & Chen, Q. (2020). Impact evaluation of cyber-attacks on traffic flow of connected and automated vehicles. *IEEE Access, 8*, 86824-86835. doi:10.1109/ACCESS.2020.2993254

Dong, J., Liu, C., & Lin, Z. (2014). Charging infrastructure planning for promoting battery electric vehicles: An activity-based approach using multiday travel data. *Transportation Research Part C: Emerging Technologies, 38*, 44-55.

Dong, S., Khattak, A., Ullah, I., Zhou, J., & Hussain, A. (2022). Predicting and Analyzing Road Traffic Injury Severity Using Boosting-Based Ensemble Learning Models with SHAPley Additive exPlanations. *International Journal of Environmental Research and Public Health, 19*(5). doi:10.3390/ijerph19052925

Ehrgott, M., Wang, J. Y. T., Raith, A., & van Houtte, C. (2012). A bi-objective cyclist route choice model. *Transportation Research Part A: Policy and Practice, 46*(4), 652-663. doi:https://doi.org/10.1016/j.tra.2011.11.015

Elliot, M., Baughan, C., Broughton, J., Chinn, B., Grayson, G., Knowles, J., & Simpson, H. (2003). Motorcycle safety: A scoping study. TRL report TRL581. *Bracknell Forest, UK: Department of Transport, Road Safety Division*.

Elvik, R. (2002). Optimal speed limits: Limits of optimality models. *Transportation Research Record, 1818*(1), 32-38.

Elvik, R. (2010). Why some road safety problems are more difficult to solve than others. *Accident Analysis & Prevention, 42*(4), 1089-1096.

Elvik, R., Christensen, P., & Amundsen, A. H. (2004). *Speed and road accidents: An evaluation of the power model*: Transportøkonomisk Institutt.

Elvik, R., Erke, A., & Christensen, P. (2009). Elementary units of exposure. *Transportation Research Record, 2103*(1), 25-31. doi:10.3141/2103-04

Fagnant, D. J., & Kockelman, K. (2015). Preparing a nation for autonomous vehicles: Opportunities, barriers and policy recommendations. *Transportation Research Part A: Policy and Practice, 77*, 167-181. doi:https://doi.org/10.1016/j.tra.2015.04.003

Farid, A., & Ksaibati, K. (2021). Modeling severities of motorcycle crashes using random parameters. *Journal of Traffic and Transportation Engineering (English edition), 8*(2), 225-236.

FHWA. (2024). About intersection safety. Retrieved from https://highways.dot.gov/safety/intersection-safety/about

Forkenbrock, D. J., & Foster, N. S. J. (1997). Accident cost saving and highway attributes. *Transportation, 24*(1), 79-100. doi:10.1023/A:1017978227554

Friedman, J. H. (2002). Stochastic gradient boosting. *Computational Statistics & Data Analysis, 38*(4), 367-378.

Gaundry, M. J. I., & Dagenais, M. G. (1979). The dogit model. *Transportation Research Part B: Methodological, 13*(2), 105-111. doi:https://doi.org/10.1016/0191-2615(79)90028-6

Geedipally, S. R., Turner, P. A., & Patil, S. (2011). Analysis of motorcycle crashes in Texas with multinomial logit model. *Transportation Research Record, 2265*(1), 62-69.

Gendreau, M., Ghiani, G., & Guerriero, E. (2015). Time-dependent routing problems: A review. *Computers & Operations Research, 64*, 189-197.

Ghoul, T., Sayed, T., & Fu, C. (2023). Real-time safest route identification: Examining the trade-off between safest and fastest routes. *Analytic Methods in Accident Research, 39*, 100277.

Giannaros, A., Karras, A., Theodorakopoulos, L., Karras, C., Kranias, P., Schizas, N., . . . Tsolis, D. (2023). Autonomous vehicles: Sophisticated attacks, safety issues, challenges, open topics, blockchain, and future directions. *Journal of Cybersecurity and Privacy, 3*(3), 493-543. doi:10.3390/jcp3030025

Gitelman, V., Hendel, L., Carmel, R., & Bekhor, S. (2012). An examination of the national road-safety programs in the ten world's leading countries in road safety. *European Transport Research Review, 4*(4), 175-188.

Gkartzonikas, C., & Gkritza, K. (2019). What have we learned? A review of stated preference and choice studies on autonomous vehicles. *Transportation Research Part C: Emerging Technologies, 98*, 323-337.

Gnecco, G., Hadas, Y., & Sanguineti, M. (2021). Public transport transfers assessment via transferable utility games and Shapley value approximation. *Transportmetrica A: Transport Science, 17*(4), 540-565.

Gnecco, G., Hadas, Y., & Sanguineti, M. (2022). A game-theoretic approach for reliability evaluation of public transportation transfers with stochastic features. *EURO Journal on Transportation and Logistics, 11*, 100090.

Gong, L., & Fan, W. D. (2017). Modeling single-vehicle run-off-road crash severity in rural areas: Accounting for unobserved heterogeneity and age difference. *Accident Analysis & Prevention, 101*, 124-134. doi:https://doi.org/10.1016/j.aap.2017.02.014

Granié, M.-A., Devif, J., Moreau, N., & Delannoy, S. (2025). Gender differences in drivers' road risks and gender equality policies: A gender paradox? Comparative analysis of 39

countries. *IATSS Research, 49*(3), 291-304. doi:https://doi.org/10.1016/j.iatssr.2025.06.004

Gu, Y., & Chen, A. (2023). Modeling mode choice of customized bus services with loyalty subscription schemes in multi-modal transportation networks. *Transportation Research Part C: Emerging Technologies, 147*, 104012.

Gu, Y., Chen, A., & Xu, X. (2023). Measurement and ranking of important link combinations in the analysis of transportation network vulnerability envelope buffers under multiple-link disruptions. *Transportation Research Part B: Methodological, 167*, 118-144. doi:https://doi.org/10.1016/j.trb.2022.11.013

Gückel, J., & Fontaine, P. (2025). *Fast Shapley value approximation in routing problems through machine learning models.* Paper presented at the The 12th Triennial Symposium on Transportation Analysis Conference (TRISTAN XII), Okinawa, Japan.

Gupta, M., Pawar, N. M., Velaga, N. R., & Mishra, S. (2022). Modeling distraction tendency of motorized two-wheeler drivers in time pressure situations. *Safety Science, 154*, 105820. doi:https://doi.org/10.1016/j.ssci.2022.105820

Guria, J., & Leung, J. (2004). An evaluation of a supplementary road safety package. *Accident Analysis & Prevention, 36*(5), 893-904. doi:https://doi.org/10.1016/j.aap.2003.09.005

Haboucha, C. J., Ishaq, R., & Shiftan, Y. (2017). User preferences regarding autonomous vehicles. *Transportation Research Part C: Emerging Technologies, 78*, 37-49.

Hadas, Y., Gnecco, G., & Sanguineti, M. (2017). An approach to transportation network analysis via transferable utility games. *Transportation Research Part B: Methodological, 105*, 120-143.

Hamadneh, J., Duleba, S., & Esztergár-Kiss, D. (2022). Stakeholder viewpoints analysis of the autonomous vehicle industry by using multi-actors multi-criteria analysis. *Transport Policy, 126*, 65-84. doi:https://doi.org/10.1016/j.tranpol.2022.07.005

Han, C., Xu, G., Pervez, A., Gao, F., Huang, H., Pei, X., & Zhang, Y. (2023). Modeling traveler's speed-route joint choice behavior with heterogeneous safety concern. *Analytic Methods in Accident Research, 37*, 100253.

Hao, W., Liu, F., Han, C., Pervez, A., Wang, K., Chen, J., & Tang, J. (2025). Do motorists select safe routes over efficient routes? An empirical study using travel trajectory data. *Accident Analysis & Prevention, 218*, 108090. doi:https://doi.org/10.1016/j.aap.2025.108090

Haque, M. B., Choudhury, C., Hess, S., & Sourd, R. C. d. (2019). Modelling residential mobility decision and its impact on car ownership and travel mode. *Travel Behaviour and Society, 17*, 104-119. doi:https://doi.org/10.1016/j.tbs.2019.07.005

Haque, M. M., & Chin, H. C. (2010). Right-angle crash vulnerability of motorcycles at signalized intersections: Mixed logit analysis. *Transportation Research Record, 2194*(1), 82-90.

Haque, M. M., Chin, H. C., & Debnath, A. K. (2013). Sustainable, safe, smart—three key elements of Singapore's evolving transport policies. *Transport Policy, 27*, 20-31. doi:https://doi.org/10.1016/j.tranpol.2012.11.017

Haque, M. M., Chin, H. C., & Huang, H. (2009). Modeling fault among motorcyclists involved in crashes. *Accident Analysis & Prevention, 41*(2), 327-335. doi:https://doi.org/10.1016/j.aap.2008.12.010

Hastie, T., Tibshirani, R., & Friedman, J. (2009). *The elements of statistical learning: data mining, inference, and prediction*: Springer Science & Business Media.

Hauer, E. (1982). Traffic conflicts and exposure. *Accident Analysis & Prevention, 14*(5), 359-364.

Hauer, E. (2009). Speed and safety. *Transportation Research Record, 2103*(1), 10-17. doi:10.3141/2103-02

Hensher, D. A., Rose, J. M., de Dios Ortuzar, J., & Rizzi, L. I. (2009). Estimating the willingness to pay and value of risk reduction for car occupants in the road environment. *Transportation Research Part A: Policy and Practice, 43*(7), 692-707.

Hess, S., Fowler, M., Adler, T., & Bahreinian, A. (2012). A joint model for vehicle type and fuel type choice: evidence from a cross-nested logit study. *Transportation, 39*(3), 593-625. doi:10.1007/s11116-011-9366-5

Hoekstra, T., & Wegman, F. (2011). Improving the effectiveness of road safety campaigns: Current and new practices. *IATSS Research, 34*(2), 80-86. doi:https://doi.org/10.1016/j.iatssr.2011.01.003

Hoseinzadeh, N., Arvin, R., Khattak, A. J., & Han, L. D. (2020). Integrating safety and mobility for pathfinding using big data generated by connected vehicles. *Journal of Intelligent Transportation Systems, 24*(4), 404-420.

Høye, A. K., & Hesjevoll, I. S. (2020). Traffic volume and crashes and how crash and road characteristics affect their relationship – A meta-analysis. *Accident Analysis & Prevention, 145*, 105668. doi:https://doi.org/10.1016/j.aap.2020.105668

Huang, H., & Abdel-Aty, M. (2010). Multilevel data and Bayesian analysis in traffic safety. *Accident Analysis & Prevention, 42*(6), 1556-1565.

Huang, H., Han, C., Xu, G., Jiang, M., Wong, S., & Haque, M. M. (2020). Incorporating safety reliability into route choice model: Heterogeneous crash risk aversions. *Analytic Methods in Accident Research, 25*, 100112.

Hulse, L. M., Xie, H., & Galea, E. R. (2018). Perceptions of autonomous vehicles: Relationships with road users, risk, gender and age. *Safety Science, 102*, 1-13.

Hussain, Q., Alhajyaseen, W. K., Adnan, M., Almallah, M., Almukdad, A., & Alqaradawi, M. (2021). Autonomous vehicles between anticipation and apprehension: Investigations through safety and security perceptions. *Transport Policy, 110*, 440-451.

Ijaz, M., Zahid, M., & Jamal, A. (2021). A comparative study of machine learning classifiers for injury severity prediction of crashes involving three-wheeled motorized rickshaw. *Accident Analysis & Prevention, 154*, 106094.

Intini, P., Colonna, P., Berloco, N., & Ranieri, V. (2017). *Measuring trade-offs between risk and travel time based on experimental speed data.* Paper presented at the Advances in Human Aspects of Transportation, Cham.

Islam, S., Jones, S. L., & Dye, D. (2014). Comprehensive analysis of single- and multi-vehicle large truck at-fault crashes on rural and urban roadways in Alabama. *Accident Analysis & Prevention, 67*, 148-158. doi:https://doi.org/10.1016/j.aap.2014.02.014

Islam, S., & Mannering, F. (2006). Driver aging and its effect on male and female single-vehicle accident injuries: Some additional evidence. *Journal of Safety Research, 37*(3), 267-276. doi:https://doi.org/10.1016/j.jsr.2006.04.003

Jabbari, P., Auld, J., & MacKenzie, D. (2022). How do perceptions of safety and car ownership importance affect autonomous vehicle adoption? *Travel Behaviour and Society, 28*, 128-140. doi:https://doi.org/10.1016/j.tbs.2022.02.002

Jafari, M., Starewich, M., Hossain, A., Barua, S., Alnawmasi, N., Ye, X., & Das, S. (2025). Assessing motorcyclist injury severity on curved road segments with temporal dynamics and unobserved heterogeneity. *Scientific Reports, 15*(1), 13110. doi:10.1038/s41598-025-97972-7

Jamson, S., & Chorlton, K. (2009). The changing nature of motorcycling: Patterns of use and rider characteristics. *Transportation Research Part F: Traffic Psychology and Behaviour, 12*(4), 335-346.

Jardim, A. S., Quartulli, A. M., & Casley, S. V. (2013). *A study of public acceptance of autonomous cars.* Retrieved from https://digital.wpi.edu/concern/student_works/pz50gw37k?locale=en

Jenn, A., Springel, K., & Gopal, A. R. (2018). Effectiveness of electric vehicle incentives in the United States. *Energy Policy, 119*, 349-356. doi:https://doi.org/10.1016/j.enpol.2018.04.065

Jiang, N., & Xie, C. (2014). Computing and analyzing mixed equilibrium network flows with gasoline and electric vehicles. *Computer-Aided Civil and Infrastructure Engineering, 29*(8), 626-641.

Jiang, N., Xie, C., Duthie, J. C., & Waller, S. T. (2014). A network equilibrium analysis on destination, route and parking choices with mixed gasoline and electric vehicular flows. *EURO Journal on Transportation and Logistics, 3*, 55-92.

Jones-Lee, M. W., Hammerton, M., & Philips, P. R. (1985). The value of safety: Results of a national sample survey. *The Economic Journal, 95*(377), 49-72.

Jones, S., Gurupackiam, S., & Walsh, J. (2013). Factors influencing the severity of crashes caused by motorcyclists: analysis of data from Alabama. *Journal of Transportation Engineering, 139*(9), 949-956.

Kadeha, C., Haule, H., Ali, M. S., Alluri, P., & Ponnaluri, R. (2021). Modeling wrong-way driving (WWD) crash severity on arterials in Florida. *Accident Analysis & Prevention, 151*, 105963.

Kanitpong, K., Boontob, N., & Tanaboriboon, Y. (2008). Helmet Use and Effectiveness in Reducing the Severity of Head Injuries in Thailand. *Transportation Research Record, 2048*(1), 66-76. doi:10.3141/2048-09

Karlsson, S. (2020). Utilization of battery-electric vehicles in two-car households: Empirical insights from Gothenburg Sweden. *Transportation Research Part C: Emerging Technologies, 120*, 102818. doi:https://doi.org/10.1016/j.trc.2020.102818

Kashani, A. T., Mahsa, J., Azizi, B. M., & and Dabirinejad, S. (2020). Factors affecting the accident size of motorcycle-involved crashes: a structural equation modeling approach. *International Journal of Injury Control and Safety Promotion, 28*(1), 16-21. doi:10.1080/17457300.2020.1833041

Kashifi, M. T. (2024). Robust spatiotemporal crash risk prediction with gated recurrent convolution network and interpretable insights from SHapley additive explanations. *Engineering Applications of Artificial Intelligence, 127*, 107379.

Kavta, K., Azadeh, S. S., Maknoon, Y., Wang, Y., & Homem de Almeida Correia, G. (2025). Estimating the value of safety against road crashes: A stated preference experiment on route choice of food delivery riders. *Transportation Research Part C: Emerging Technologies, 179*, 105272. doi:https://doi.org/10.1016/j.trc.2025.105272

Kazmierska, J., & Malicki, J. (2008). Application of the Naïve Bayesian Classifier to optimize treatment decisions. *Radiotherapy and Oncology, 86*(2), 211-216.

Kenesei, Z., Ásványi, K., Kökény, L., Jászberényi, M., Miskolczi, M., Gyulavári, T., & Syahrivar, J. (2022). Trust and perceived risk: How different manifestations affect the adoption of autonomous vehicles. *Transportation Research Part A: Policy and Practice, 164*, 379-393. doi:https://doi.org/10.1016/j.tra.2022.08.022

Khan, U. R., Bhatti, J. A., Shamim, M. S., Zia, N., Razzak, J. A., & Jooma, R. (2015). Clothing-related motorcycle injuries in Pakistan: findings from a surveillance study. *International Journal of Injury Control and Safety Promotion, 22*(4), 308-313.

Kidando, E., Moses, R., Ozguven, E. E., & Sando, T. (2019). Incorporating travel time reliability in predicting the likelihood of severe crashes on arterial highways using non-parametric random-effect regression. *Journal of Traffic and Transportation Engineering (English edition), 6*(5), 470-481.

Kim, J., Tanaka, H. S., & Schmöcker, J.-D. (2020). Joint car ownership and car type preference model considering engagement in online activities and environmental concern. *Transportation Research Part F: Traffic Psychology and Behaviour, 68*, 293-305. doi:https://doi.org/10.1016/j.trf.2019.11.012

Kingsbury, H. (2016). *Incorporating road safety into vehicle routing*. Retrieved from https://static1.squarespace.com/static/5591f57ee4b07952c1a4d8bd/t/56c18c308259b5cdaf93f27a/1455524916322/Kingsbury%2C+Hamish+-+Paper+17+-+Incorporating+Road+Safety+into+Vehicle+Routing.pdf

Kitali, A. E., Kidando, E., Alluri, P., Sando, T., & Salum, J. H. (2020). Modeling severity of motorcycle crashes with Dirichlet process priors. *Journal of Transportation Safety & Security*, 1-22.

Kockelman, K. M., Avery, P., Bansal, P., Boyles, S. D., Bujanovic, P., Choudhary, T., . . . Helsel, J. (2016). *Implications of connected and automated vehicles on the safety and operations of roadway networks: A final report, University of Texas Center for*

Transportation Research. Retrieved from http://library.ctr.utexas.edu/ctr-publications/0-6849-1.pdf

Kolarova, V., Steck, F., & Bahamonde-Birke, F. J. (2019). Assessing the effect of autonomous driving on value of travel time savings: A comparison between current and future preferences. *Transportation Research Part A: Policy and Practice, 129*, 155-169.

Kong, X., Zhang, Y., Eisele, W. L., & Xiao, X. (2022). Using an interpretable machine learning framework to understand the relationship of mobility and reliability indices on truck drivers' route choices. *IEEE Transactions on Intelligent Transportation Systems, 23*(8), 13419-13428. doi:10.1109/TITS.2021.3124221

Kurmankhojayev, D., Li, G., & Chen, A. (2024). Link criticality index: Refinement, framework extension, and a case study. *Reliability Engineering & System Safety, 243*, 109889. doi:https://doi.org/10.1016/j.ress.2023.109889

Kweon, Y.-J., & Lim, I.-K. (2014). *Development of safety performance functions for multilane highway and freeway segments maintained by the Virginia Department of Transportation*. Retrieved from https://vtrc.virginia.gov/media/vtrc/vtrc-pdf/vtrc-pdf/14-R14.pdf

Lam, W. H. K., Shao, H., & Sumalee, A. (2008). Modeling impacts of adverse weather conditions on a road network with uncertainties in demand and supply. *Transportation Research Part B: Methodological, 42*(10), 890-910. doi:https://doi.org/10.1016/j.trb.2008.02.004

Lamotte, R., de Palma, A., & Geroliminis, N. (2017). On the use of reservation-based autonomous vehicles for demand management. *Transportation Research Part B: Methodological, 99*, 205-227. doi:https://doi.org/10.1016/j.trb.2017.01.003

Leurent, F. (1993). Cost versus time equilibrium over a network. *European Journal of Operational Research, 71*(2), 205-221.

Li, G., Chen, A., Ryu, S., Kitthamkesorn, S., & Xu, X. (2024). Modeling elasticity, similarity, stochasticity, and congestion in a network equilibrium framework using a paired combinatorial weibit choice model. *Transportation Research Part B: Methodological, 179*, 102870. doi:https://doi.org/10.1016/j.trb.2023.102870

Li, J., Fang, S., Guo, J., Fu, T., & Qiu, M. (2021). A Motorcyclist-Injury Severity Analysis: A Comparison of Single-, Two-, and Multi-Vehicle Crashes Using Latent Class Ordered Probit Model. *Accident Analysis & Prevention, 151*, 105953. doi:https://doi.org/10.1016/j.aap.2020.105953

Li, M.-s., & Huang, H.-l. (2019). Road-safety recognition and network equilibrium with perceived route-choice sets. *Transportation Safety and Environment, 1*(2), 126-134.

Li, Z., Li, G., Xu, Z., & Chen, A. (2023). Multiclass bi-criteria traffic assignment without class-specific variables: An alternative formulation and a subgradient projection algorithm. *Transportation Research Part E: Logistics and Transportation Review, 176*, 103210.

Li, Z., Liu, P., Wang, W., & Xu, C. (2012). Using support vector machine models for crash injury severity analysis. *Accident Analysis & Prevention, 45*, 478-486.

Li, Z., Wang, W., Liu, P., Bigham, J. M., & Ragland, D. R. (2013). Using Geographically Weighted Poisson Regression for county-level crash modeling in California. *Safety Science, 58*, 89-97. doi:https://doi.org/10.1016/j.ssci.2013.04.005

Lim, S. H., & Chi, J. (2013). Are cell phone laws in the U.S. effective in reducing fatal crashes involving young drivers? *Transport Policy, 27*, 158-163. doi:https://doi.org/10.1016/j.tranpol.2013.01.011

Lin, D.-Y., & Leong, P. W. (2014). An N-path user equilibrium for transportation networks. *Applied Mathematical Modelling, 38*(2), 667-682.

Lin, H.-Z., & Wei, J. (2019). Optimal transport network design for both traffic safety and risk equity considerations. *Journal of Cleaner Production, 218*, 738-745. doi:https://doi.org/10.1016/j.jclepro.2019.02.070

Litman, T. (2017). *Autonomous vehicle implementation predictions, Victoria Transport Policy Institute Victoria, Canada*. Retrieved from https://www.vtpi.org/avip.pdf

Liu, K., Gao, S., Qiu, P., Liu, X., Yan, B., & Lu, F. (2017). Road2vec: Measuring traffic interactions in urban road system from massive travel routes. *ISPRS International Journal of Geo-Information, 6*(11), 321.

Liu, Z., & Song, Z. (2019). Strategic planning of dedicated autonomous vehicle lanes and autonomous vehicle/toll lanes in transportation networks. *Transportation Research Part C: Emerging Technologies, 106*, 381-403. doi:https://doi.org/10.1016/j.trc.2019.07.022

Lo, H. K., & Chen, A. (2000). Traffic equilibrium problem with route-specific costs: formulation and algorithms. *Transportation Research Part B: Methodological, 34*(6), 493-513.

Lo, H. K., Luo, X., & Siu, B. W. (2006). Degradable transport network: travel time budget of travelers with heterogeneous risk aversion. *Transportation Research Part B: Methodological, 40*(9), 792-806.

Lord, D. (2002). Application of accident prediction models for computation of accident risk on transportation networks. *Transportation Research Record, 1784*(1), 17-26. doi:10.3141/1784-03

Lovegrove, G. R., & Sayed, T. (2006). Using macrolevel collision prediction models in road safety planning applications. *Transportation Research Record, 1950*(1), 73-82.

Lundberg, S., & Lee, S.-I. (2017). *A unified approach to interpreting model predictions.* Paper presented at the In Proceedings of the 31st Conference on Neural Information Processing Systems (NIPS 2017),, Long Beach, CA, USA.

Lv, Y., Duan, Y., Kang, W., Li, Z., & Wang, F. Y. (2015). Traffic flow prediction with big data: A deep learning approach. *IEEE Transactions on Intelligent Transportation Systems, 16*(2), 865-873. doi:10.1109/TITS.2014.2345663

Ma, R., & Zhang, M. (2019). *Routing traffic for community health: The case with safety-conscious travelers*. Retrieved from https://rosap.ntl.bts.gov/view/dot/62859

Ma, Z., Mei, G., & Cuomo, S. (2021). An analytic framework using deep learning for prediction of traffic accident injury severity based on contributing factors. *Accident Analysis & Prevention, 160*, 106322.

Machin, M. A., & Sankey, K. S. (2008). Relationships between young drivers' personality characteristics, risk perceptions, and driving behaviour. *Accident Analysis & Prevention, 40*(2), 541-547.

Machina, M., & Viscusi, K. (2013). *Handbook of the Economics of Risk and Uncertainty*: Elsevier: Amsterdam, The Netherlands.

Mahmud, A., Agnimitra, S., & and Gayah, V. V. (2024). Crash classification based on manner of collision: a comparative analysis. *Transportation Letters, 16*(3), 207-217. doi:10.1080/19427867.2023.2175419

Manan, M. M. A., Várhelyi, A., Çelik, A. K., & Hashim, H. H. (2018). Road characteristics and environment factors associated with motorcycle fatal crashes in Malaysia. *IATSS Research, 42*(4), 207-220.

Mannering, F., Bhat, C. R., Shankar, V., & Abdel-Aty, M. (2020). Big data, traditional data and the tradeoffs between prediction and causality in highway-safety analysis. *Analytic Methods in Accident Research, 25*, 100113. doi:https://doi.org/10.1016/j.amar.2020.100113

Mannering, F. L., & Bhat, C. R. (2014). Analytic methods in accident research: Methodological frontier and future directions. *Analytic Methods in Accident Research, 1*, 1-22.

Manski, C. F., & McFadden, D. (1981). *Structural analysis of discrete data with econometric applications*: MIT press Cambridge, MA.

Manski, C. F., & Sherman, L. (1980). An empirical analysis of household choice among motor vehicles. *Transportation Research Part A: General, 14*(5), 349-366. doi:https://doi.org/10.1016/0191-2607(80)90054-0

Mansoor, U., Jamal, A., Su, J., Sze, N. N., & Chen, A. (2023). Investigating the risk factors of motorcycle crash injury severity in Pakistan: Insights and policy recommendations. *Transport Policy, 139*, 21-38. doi:https://doi.org/10.1016/j.tranpol.2023.05.013

Mansoor, U., Ratrout, N. T., Rahman, S. M., & Assi, K. (2020). Crash severity prediction using two-layer ensemble machine learning model for proactive emergency management. *IEEE Access, 8*, 210750-210762. doi:10.1109/ACCESS.2020.3040165

Marcotte, P. (1998). Reformulations of a bicriterion equilibrium model. In: *Reformulation: Nonsmooth, Piecewise Smooth, Semismooth and Smoothing Methods* (pp. 269-291): Springer.

May, M., Tranter, P. J., & Warn, J. R. (2008). Towards a holistic framework for road safety in Australia. *Journal of Transport Geography, 16*(6), 395-405. doi:https://doi.org/10.1016/j.jtrangeo.2008.04.004

McKenna, F. P., & Horswill, M. S. (2006). Risk taking from the participant's perspective: The case of driving and accident risk. *Health Psychology, 25*(2), 163.

Meng, Q., & Liu, Z. (2011). Trial-and-error method for congestion pricing scheme under side-constrained probit-based stochastic user equilibrium conditions. *Transportation, 38*(5), 819-843. doi:10.1007/s11116-011-9346-9

Mfinanga, D. A. (2014). Implication of pedestrians′ stated preference of certain attributes of crosswalks. *Transport Policy, 32*, 156-164. doi:https://doi.org/10.1016/j.tranpol.2014.01.011

Miranda-Moreno, L. F., Fu, L., Ukkusuri, S., & Lord, D. (2009). How to incorporate accident severity and vehicle occupancy into the hot spot identification process? *Transportation Research Record, 2102*(1), 53-60. doi:10.3141/2102-07

MOC. (2018). National Road Safety Strategy 2018-2030. . *Ministry of Communications, Government of Pakistan. Accessed on: December 24, 2021. URL:* Retrieved from http://www.roadsafetypakistan.pk/download/Pakistan-National-Road-Safety-Strategy-2018-2030.pdf.

Mon, E. E., Jomnonkwao, S., Khampirat, B., Satiennam, T., & Ratanavaraha, V. (2019). Estimating the willingness to pay and the value of fatality risk reduction for car drivers in Myanmar. *Case Studies on Transport Policy, 7*(2), 301-309.

Moody, J., Bailey, N., & Zhao, J. (2020). Public perceptions of autonomous vehicle safety: An international comparison. *Safety Science, 121*, 634-650. doi:https://doi.org/10.1016/j.ssci.2019.07.022

Morando, M. M., Tian, Q., Truong, L. T., & Vu, H. L. (2018). Studying the safety impact of autonomous vehicles using simulation-based surrogate safety measures. *Journal of Advanced Transportation, 2018*(1), 6135183.

Mouter, N., van Cranenburgh, S., & van Wee, B. (2017). Do individuals have different preferences as consumer and citizen? The trade-off between travel time and safety. *Transportation Research Part A: Policy and Practice, 106*, 333-349. doi:https://doi.org/10.1016/j.tra.2017.10.003

Nagurney, A. (2000). A multiclass, multicriteria traffic network equilibrium model. *Mathematical and Computer Modelling, 32*(3-4), 393-411.

Nagurney, A., & Dong, J. (2002). A multiclass, multicriteria traffic network equilibrium model with elastic demand. *Transportation Research Part B: Methodological, 36*(5), 445-469.

Narayanam, R., & Narahari, Y. (2010). A Shapley value-based approach to discover influential nodes in social networks. *IEEE Transactions on Automation Science and Engineering, 8*(1), 130-147.

Nazari, F., Noruzoliaee, M., & Mohammadian, A. K. (2018). Shared versus private mobility: Modeling public interest in autonomous vehicles accounting for latent attitudes. *Transportation Research Part C: Emerging Technologies, 97*, 456-477.

Nguyen-Phuoc, D. Q., Nguyen, H. A., De Gruyter, C., Su, D. N., & Nguyen, V. H. (2019). Exploring the prevalence and factors associated with self-reported traffic crashes among app-based motorcycle taxis in Vietnam. *Transport Policy, 81*, 68-74. doi:https://doi.org/10.1016/j.tranpol.2019.06.006

NHTSA. (2008). *National motor vehicle crash causation survey: Report to congress*. Retrieved from https://crashstats.nhtsa.dot.gov/Api/Public/ViewPublication/811059

Niu, C., Jian, S., Nair, D., & Dixit, V. (2023). Pre-disaster resilient road network investment strategy with uncertainty quantification. *IEEE Transactions on Intelligent Transportation Systems, 24*(7), 6849-6864. doi:10.1109/TITS.2023.3264471

Noland, R. B. (2013). From theory to practice in road safety policy: Understanding risk versus mobility. *Research in Transportation Economics, 43*(1), 71-84.

Noruzoliaee, M., Zou, B., & Liu, Y. (2018). Roads in transition: Integrated modeling of a manufacturer-traveler-infrastructure system in a mixed autonomous/human driving environment. *Transportation Research Part C: Emerging Technologies, 90*, 307-333.

O'donnell, C., & Connor, D. (1996). Predicting the severity of motor vehicle accident injuries using models of ordered multiple choice. *Accident Analysis & Prevention, 28*(6), 739-753.

Ortúzar, J., & Willumsen, L. G. (2011). *Modelling Transport*: John wiley & sons.

Ozonder, G., & Miller, E. J. (2021). Longitudinal microeconomic and machine learning models of skeletal activity generation. *Travel Behaviour and Society, 23*, 40-64.

Pai, C.-W., & Saleh, W. (2007). An analysis of motorcyclist injury severity under various traffic control measures at three-legged junctions in the UK. *Safety Science, 45*(8), 832-847.

Palmer, K. (2015). Driverless cars will shave '£265' off insurance premiums in five years. Retrieved from https://www.telegraph.co.uk/finance/personalfinance/insurance/motorinsurance/11623218/Driverless-cars-will-shave-265-off-insurance-premiums-in-five-years.html

Panagiotopoulos, I., & Dimitrakopoulos, G. (2018). An empirical investigation on consumers' intentions towards autonomous driving. *Transportation Research Part C: Emerging Technologies, 95*, 773-784.

Papadoulis, A., Quddus, M., & Imprialou, M. (2019). Evaluating the safety impact of connected and autonomous vehicles on motorways. *Accident Analysis & Prevention, 124*, 12-22.

Papu Carrone, A., Monteiro, M. M., & Rich, J. (2021). Modelling car ownership dynamics based on irregularly spaced panel data. *Travel Behaviour and Society, 25*, 223-232. doi:https://doi.org/10.1016/j.tbs.2021.07.008

Parkinson, S., Ward, P., Wilson, K., & Miller, J. (2017). Cyber threats facing autonomous and connected vehicles: Future challenges. *IEEE Transactions on Intelligent Transportation Systems, 18*(11), 2898-2915. doi:10.1109/TITS.2017.2665968

Passacantando, M., Gnecco, G., Hadas, Y., & Sanguineti, M. (2021a). Braess' paradox: A cooperative game-theoretic point of view. *Networks, 78*(3), 264-283.

Passacantando, M., Gnecco, G., Hadas, Y., & Sanguineti, M. (2021b). *On Braess' paradox and average quality of service in transportation network cooperative games.* Paper presented at the Optimization and Decision Science: ODS, Virtual Conference, November 19, 2020.

PBS. (2015). Pakistan Statistical Year Book Pakistan Bureau of Statistics.

PBS. (2017). Provisional Summary Results of 6th Population and Housing Census, Pakistan Bureau of Statistics, Islamabad. In: Government of Pakistan Islamabad, Pakistan.

Pei, X., Wong, S., & Sze, N.-N. (2012). The roles of exposure and speed in road safety analysis. *Accident Analysis & Prevention, 48*, 464-471.

Pervaz, S., Bhowmik, T., & Eluru, N. (2024). An integrated multi-resolution framework for jointly estimating crash type and crash severity. *Analytic Methods in Accident Research, 42*, 100321. doi:https://doi.org/10.1016/j.amar.2024.100321

Pervez, A., Lee, J., & Huang, H. (2021). Identifying factors contributing to the motorcycle crash severity in Pakistan. *Journal of Advanced Transportation, 2021*.

Petit, J., & Shladover, S. E. (2015). Potential cyberattacks on automated vehicles. *IEEE Transactions on Intelligent Transportation Systems, 16*(2), 546-556. doi:10.1109/TITS.2014.2342271

Pour-Rouholamin, M., Jalayer, M., & Zhou, H. (2017). Modelling single-vehicle, single-rider motorcycle crash injury severity: an ordinal logistic regression approach. *International Journal of Urban Sciences, 21*(3), 344-363. doi:10.1080/12265934.2017.1311801

Prakash, A. A., Seshadri, R., & Srinivasan, K. K. (2018). A consistent reliability-based user-equilibrium problem with risk-averse users and endogenous travel time correlations:

Formulation and solution algorithm. *Transportation Research Part B: Methodological, 114*, 171-198. doi:https://doi.org/10.1016/j.trb.2018.06.003
Prakash, A. A., & Srinivasan, K. K. (2015). Optimal Reliability Path Problem on Networks with Random and Correlated Link Travel Times: Bilevel Formulation and Solution Procedure. *Transportation Research Record, 2497*(1), 54-62. doi:10.3141/2497-06
Quddus, M. A., Noland, R. B., & Chin, H. C. (2002). An analysis of motorcycle injury and vehicle damage severity using ordered probit models. *Journal of Safety Research, 33*(4), 445-462.
Radin Umar, R. (2006). Motorcycle safety programmes in Malaysia: how effective are they? *International Journal of Injury Control and Safety Promotion, 13*(2), 71-79.
Rahman, M. H., Zafri, N. M., Akter, T., & Pervaz, S. (2021). Identification of factors influencing severity of motorcycle crashes in Dhaka, Bangladesh using binary logistic regression model. *International Journal of Injury Control and Safety Promotion*, 1-12.
Ratanavaraha, V., & Jomnonkwao, S. (2013). Community participation and behavioral changes of helmet use in Thailand. *Transport Policy, 25*, 111-118. doi:https://doi.org/10.1016/j.tranpol.2012.11.002
Rescue 1122. (2016). Consolidated Report of Road Traffic Emergencies. Punjab Emergency Service, Pakistan.
Rezapour, M., Farid, A., Nazneen, S., & Ksaibati, K. (2021). Using machine leaning techniques for evaluation of motorcycle injury severity. *IATSS Research, 45*(3), 277-285. doi:https://doi.org/10.1016/j.iatssr.2020.07.004
Rezapour, M., Molan, A. M., & Ksaibati, K. (2020a). Analyzing injury severity of motorcycle at-fault crashes using machine learning techniques, decision tree and logistic regression models. *International Journal of Transportation Science and Technology, 9*(2), 89-99.
Rezapour, M., Nazneen, S., & Ksaibati, K. (2020b). Application of deep learning techniques in predicting motorcycle crash severity. *Engineering Reports, 2*(7), e12175.
Rizzi, L. I., & Ortúzar, J. d. D. (2003). Stated preference in the valuation of interurban road safety. *Accident Analysis & Prevention, 35*(1), 9-22.
Robbins, C., & Fotios, S. (2020). Motorcycle safety after-dark: The factors associated with greater risk of road-traffic collisions. *Accident Analysis & Prevention, 146*, 105731.
Rudin, C. (2019). Stop explaining black box machine learning models for high stakes decisions and use interpretable models instead. *Nature Machine Intelligence, 1*(5), 206-215.
Salvarani, C. P., Colli, B. O., & Júnior, C. G. C. (2009). Impact of a program for the prevention of traffic accidents in a Southern Brazilian city: a model for implementation in a developing country. *Surgical Neurology, 72*(1), 6-13. doi:https://doi.org/10.1016/j.surneu.2007.10.008
Santos, K., Dias, J. P., & Amado, C. (2022). A literature review of machine learning algorithms for crash injury severity prediction. *Journal of Safety Research, 80*, 254-269. doi:https://doi.org/10.1016/j.jsr.2021.12.007
Savolainen, P., & Mannering, F. (2007). Probabilistic models of motorcyclists' injury severities in single-and multi-vehicle crashes. *Accident Analysis & Prevention, 39*(5), 955-963.
Schneider, W. H., & Savolainen, P. T. (2011). Comparison of severity of motorcyclist injury by crash types. *Transportation Research Record, 2265*(1), 70-80.
Schoettle, B., & Sivak, M. (2014). *Public opinion about self-driving vehicles in China, India, Japan, the US, the UK, and Australia*. Retrieved from https://deepblue.lib.umich.edu/handle/2027.42/109433
Shaheed, M. S., & Gkritza, K. (2014). A latent class analysis of single-vehicle motorcycle crash severity outcomes. *Analytic Methods in Accident Research, 2*, 30-38.
Shalev-Shwartz, S., & Ben-David, S. (2014). *Understanding Machine Learning: From Theory to Algorithms*: Cambridge university press.
Shamim, S., Razzak, J. A., Jooma, R., & Khan, U. (2011). Initial results of Pakistan's first road traffic injury surveillance project. *International Journal of Injury Control and Safety Promotion, 18*(3), 213-217.
Shankar, V., & Mannering, F. (1996). An exploratory multinomial logit analysis of single-vehicle motorcycle accident severity. *Journal of Safety Research, 27*(3), 183-194.

Shao, H., Lam, W. H., Meng, Q., & Tam, M. L. (2006). Demand-driven traffic assignment problem based on travel time reliability. *Transportation Research Record, 1985*(1), 220-230.

Shapley, L. S. (1953). A value for N-person games. In: H. W. Kuhn, Tucker, A.W. (Ed.), *Contributions to the Theory of Games* (Vol. 2, pp. 307-318). Princeton, New Jersey: Princeton University Press.

Sharifi, M. S., & Shabaniverki, H. (2016). Modeling crash delays in a route choice behavior model for two way road networks. *Journal of Geotechnical and Transportation Engineering, 2*(1).

She, Z.-Y., Qing Sun, Ma, J.-J., & Xie, B.-C. (2017). What are the barriers to widespread adoption of battery electric vehicles? A survey of public perception in Tianjin, China. *Transport Policy, 56*, 29-40. doi:https://doi.org/10.1016/j.tranpol.2017.03.001

Sheffi, Y. (1985). *Urban Transportation Networks: Equilibrium Analysis with Mathematical Programming Methods*: Prentice-Hall, Englewood Cliffs, NJ.

Silva, P. B., Andrade, M., & Ferreira, S. (2020). Machine learning applied to road safety modeling: A systematic literature review. *Journal of Traffic and Transportation Engineering (English edition), 7*(6), 775-790. doi:https://doi.org/10.1016/j.jtte.2020.07.004

Simons-Morton, B. G., Bingham, C. R., Falk, E. B., Li, K., Pradhan, A. K., Ouimet, M. C., . . . Shope, J. T. (2014). Experimental effects of injunctive norms on simulated risky driving among teenage males. *Health Psychology, 33*(7), 616.

Singh, H., Kavianipour, M., Ghamami, M., & Zockaie, A. (2023). Adoption of autonomous and electric vehicles in private and shared mobility systems. *Transportation Research Part D: Transport and Environment, 115*, 103561. doi:https://doi.org/10.1016/j.trd.2022.103561

Sivasankaran, S. K., Rangam, H., & Balasubramanian, V. (2021). Investigation of factors contributing to injury severity in single vehicle motorcycle crashes in India. *International Journal of Injury Control and Safety Promotion, 28*(2), 243-254.

Sohrabi, S., Khodadadi, A., Mousavi, S. M., Dadashova, B., & Lord, D. (2021). Quantifying the automated vehicle safety performance: A scoping review of the literature, evaluation of methods, and directions for future research. *Accident Analysis & Prevention, 152*, 106003. doi:https://doi.org/10.1016/j.aap.2021.106003

Sohrabi, S., & Lord, D. (2022). Navigating to safety: Necessity, requirements, and barriers to considering safety in route finding. *Transportation Research Part C: Emerging Technologies, 137*, 103542. doi:https://doi.org/10.1016/j.trc.2021.103542

Solomon, D. H. (1974). *Accidents on main rural highways: related to speed, driver, and vehicle*: US Department of Transportation, Federal Highway Administration.

Srinivasan, K. K., Prakash, A. A., & Seshadri, R. (2014). Finding most reliable paths on networks with correlated and shifted log–normal travel times. *Transportation Research Part B: Methodological, 66*, 110-128. doi:https://doi.org/10.1016/j.trb.2013.10.011

Starkey, P., Batool, Z., Younis, E. M. W., Rehman, A. U., & Ali, M. S. (2021). Motorcycle three-wheelers in Pakistan: Low-cost rural transport services, crucial for women's mobility. *Transportation Research Interdisciplinary Perspectives, 12*, 100479.

Stipancic, J., Miranda-Moreno, L., Saunier, N., & Labbe, A. (2019). Network screening for large urban road networks: Using GPS data and surrogate measures to model crash frequency and severity. *Accident Analysis & Prevention, 125*, 290-301. doi:https://doi.org/10.1016/j.aap.2019.02.016

Sze, N. N., & Wong, S. C. (2007). Diagnostic analysis of the logistic model for pedestrian injury severity in traffic crashes. *Accident Analysis & Prevention, 39*(6), 1267-1278. doi:https://doi.org/10.1016/j.aap.2007.03.017

Tahfim, S. A.-S., & Yan, C. (2021). Analysis of severe injuries in crashes involving large trucks using K-prototypes clustering-based GBDT model. *Safety, 7*(2), 32.

Tan, H., Chen, A., & Xu, X. (2024). Equilibria for joint congestion game with destination and route choices. *IEEE Transactions on Intelligent Transportation Systems*, 1-11. doi:10.1109/TITS.2024.3449450

Touati, S., Radjef, M. S., & Sais, L. (2021). A bayesian monte carlo method for computing the Shapley value: Application to weighted voting and bin packing games. *Computers & Operations Research, 125*, 105094. doi:https://doi.org/10.1016/j.cor.2020.105094

Truong, L. T., & Currie, G. (2019). Macroscopic road safety impacts of public transport: A case study of Melbourne, Australia. *Accident Analysis & Prevention, 132*, 105270. doi:https://doi.org/10.1016/j.aap.2019.105270

Valeri, E., & Danielis, R. (2015). Simulating the market penetration of cars with alternative fuelpowertrain technologies in Italy. *Transport Policy, 37*, 44-56.

van Wee, B., & Rietveld, P. (2013). Using value of statistical life for the ex ante evaluation of transport policy options: A discussion based on ethical theory. *Transportation, 40*(2), 295-314. doi:10.1007/s11116-012-9425-6

Von Neumann, J., & Morgenstern, O. (1944). *Theory of Games and Economic Behaviour*: Princeton University Press.

Wadud, Z. (2017). Fully automated vehicles: A cost of ownership analysis to inform early adoption. *Transportation Research Part A: Policy and Practice, 101*, 163-176.

Wahab, L., & Jiang, H. (2019a). A comparative study on machine learning based algorithms for prediction of motorcycle crash severity. *PLoS One, 14*(4), e0214966.

Wahab, L., & Jiang, H. (2019b). A multinomial logit analysis of factors associated with severity of motorcycle crashes in Ghana. *Traffic Injury Prevention, 20*(5), 521-527.

Wali, B., Khattak, A. J., Bozdogan, H., & Kamrani, M. (2018). How is driving volatility related to intersection safety? A Bayesian heterogeneity-based analysis of instrumented vehicles data. *Transportation Research Part C: Emerging Technologies, 92*, 504-524.

Wallace, C., Courage, K., Hadi, M., & Gan, A. (1998). *TRANSYT-7F User's Guide*: University of Florida, Gainesville, Florida.

Wang, C., Quddus, M., & Ison, S. (2013). A spatio-temporal analysis of the impact of congestion on traffic safety on major roads in the UK. *Transportmetrica A: Transport Science, 9*(2), 124-148. doi:10.1080/18128602.2010.538871

Wang, C., Quddus, M. A., & Ison, S. G. (2011). Predicting accident frequency at their severity levels and its application in site ranking using a two-stage mixed multivariate model. *Accident Analysis & Prevention, 43*(6), 1979-1990. doi:https://doi.org/10.1016/j.aap.2011.05.016

Wang, G., Chen, A., Kitthamkesorn, S., Ryu, S., Qi, H., Song, Z., & Song, J. (2020a). A multi-modal network equilibrium model with captive mode choice and path size logit route choice. *Transportation Research Part A: Policy and Practice, 136*, 293-317.

Wang, G., Qi, H., Xu, H., & Ryu, S. (2020b). A mixed behaviour equilibrium model with mode choice and its application to the endogenous demand of automated vehicles. *Journal of Management Science and Engineering, 5*(4), 227-248. doi:https://doi.org/10.1016/j.jmse.2020.05.003

Wang, G., Song, D., Qi, H., Zhou, J., & He, Z. (2024). A multi-modal network equilibrium model considering captive travelers and mode correlation. *Transportation*, 1-34. doi:10.1007/s11116-024-10475-8

Wang, J., Lu, L., Peeta, S., & He, Z. (2021). Optimal toll design problems under mixed traffic flow of human-driven vehicles and connected and autonomous vehicles. *Transportation Research Part C: Emerging Technologies, 125*, 102952. doi:https://doi.org/10.1016/j.trc.2020.102952

Wang, J. Y., Wu, Z., Kang, Y., Brown, E., Wen, M., Rushton, C., & Ehrgott, M. (2023). Walking school bus line routing for efficiency, health and walkability: A multi-objective optimisation approach. *Journal of Multi-Criteria Decision Analysis, 30*(3-4), 109-131.

Wang, X., Khattak, A. J., Liu, J., Masghati-Amoli, G., & Son, S. (2015). What is the level of volatility in instantaneous driving decisions? *Transportation Research Part C: Emerging Technologies, 58*, 413-427.

Wardrop, J. G. (1952). Road paper. some theoretical aspects of road traffic research. *Proceedings of the Institution of Civil Engineers, 1*(3), 325-362.

Waseem, M., Ahmed, A., & Saeed, T. U. (2019). Factors affecting motorcyclists' injury severities: An empirical assessment using random parameters logit model with heterogeneity in means and variances. *Accident Analysis & Prevention, 123*, 12-19.

Washington, S. P., Karlaftis, M. G., & Mannering, F. (2003). *Statistical and econometric methods for transportation data analysis*: Chapman and Hall/CRC.

WHO. (2023). *Global status report on road safety*. Retrieved from https://www.who.int/teams/social-determinants-of-health/safety-and-mobility/global-status-report-on-road-safety-2023

Wong, S., Sze, N.-N., & Li, Y.-C. (2007). Contributory factors to traffic crashes at signalized intersections in Hong Kong. *Accident Analysis & Prevention, 39*(6), 1107-1113.

Wundersitz, L. (2019). Driver distraction and inattention in fatal and injury crashes: Findings from in-depth road crash data. *Traffic Injury Prevention, 20*(7), 696-701.

Xie, C., Wu, X., & Boyles, S. (2019). Traffic equilibrium with a continuously distributed bound on travel weights: The rise of range anxiety and mental account. *Annals of Operations Research, 273*, 279-310.

Xie, J., Wang, Q., & Nie, Y. M. (2021). An efficient algorithm for continuous bi-criteria traffic assignment,https://www.researchgate.net/profile/Jun_Xie:18/publication/352931588:An_efficient_algorithm_for_continuous_bi-criteria_traffic_assignment.

Xie, T., & Liu, Y. (2022). Impact of connected and autonomous vehicle technology on market penetration and route choices. *Transportation Research Part C: Emerging Technologies, 139*, 103646.

Xu, G., Liu, W., & Yang, H. (2018a). A reliability-based assignment method for railway networks with heterogeneous passengers. *Transportation Research Part C: Emerging Technologies, 93*, 501-524.

Xu, X., Chen, A., & Cheng, L. (2015). Reformulating environmentally constrained traffic equilibrium via a smooth gap function. *International Journal of Sustainable Transportation, 9*(6), 419-430.

Xu, X., Chen, A., Lo, H. K., & Yang, C. (2018b). Modeling the impacts of speed limits on uncertain road networks. *Transportmetrica A Transport Science, 14*(1), 66-88. doi:https://doi.org/10.1080/23249935.2017.1317879

Xu, X., Chen, A., Zhou, Z., & Cheng, L. (2014). A multi-class mean-excess traffic equilibrium model with elastic demand. *Journal of Advanced Transportation, 48*(3), 203-222.

Xu, Z., Chen, A., Li, G., Li, Z., & Liu, X. (2024a). Elastic-demand bi-criteria traffic assignment under the continuously distributed value of time: A two-stage gradient projection algorithm with graphical interpretations. *Transportation Research Part E: Logistics and Transportation Review, 183*, 103425.

Xu, Z., Chen, A., & Liu, X. (2023). Time and toll trade-off with heterogeneous users: A continuous time surplus maximization bi-objective user equilibrium model. *Transportation Research Part B: Methodological, 173*, 31-58.

Xu, Z., Peng, Y., Li, G., Chen, A., & Liu, X. (2024b). Range-constrained traffic assignment for electric vehicles under heterogeneous range anxiety. *Transportation Research Part C: Emerging Technologies, 158*, 104419. doi:https://doi.org/10.1016/j.trc.2023.104419

Yamai, Y., & Yoshiba, T. (2002). On the validity of value-at-risk: comparative analyses with expected shortfall. *Monetary and Economic Studies, 20*(1), 57-85.

Yang, C., Chen, M., & Yuan, Q. (2021). The application of XGBoost and SHAP to examining the factors in freight truck-related crashes: an exploratory analysis. *Accident Analysis & Prevention, 158*, 106153.

Yang, H., & Huang, H.-J. (2004). The multi-class, multi-criteria traffic network equilibrium and systems optimum problem. *Transportation Research Part B: Methodological, 38*(1), 1-15.

Yannis, G., Kanellopoulou, A., Aggeloussi, K., & Tsamboulas, D. (2005). Modelling driver choices towards accident risk reduction. *Safety Science, 43*(3), 173-186.

Yasmin, S., & Eluru, N. (2018). A joint econometric framework for modeling crash counts by severity. *Transportmetrica A: Transport Science, 14*(3), 230-255. doi:10.1080/23249935.2017.1369469

Zeng, Q., Qianfang, W., Fangzhou, W., & and Sze, N. N. (2022). Revisiting spatial correlation in crash injury severity: a Bayesian generalized ordered probit model with Leroux conditional autoregressive prior. *Transportmetrica A: Transport Science, 18*(3), 1084-1102. doi:10.1080/23249935.2021.1922536

Zhang, F., Lu, J., & Hu, X. (2020a). Traffic equilibrium for mixed traffic flows of human-driven vehicles and connected and autonomous vehicles in transportation networks under tradable credit scheme. *Journal of Advanced Transportation, 2020*, 1-18.

Zhang, J., Li, Z., Pu, Z., & Xu, C. (2018). Comparing prediction performance for crash injury severity among various machine learning and statistical methods. *IEEE Access, 6*, 60079-60087. doi:10.1109/ACCESS.2018.2874979

Zhang, T., Niu, C., Nair, D. J., Robson, E. N., & Dixit, V. (2023). Transportation resilience optimization from an economic perspective at the pre-event stage. *Sustainability Analytics and Modeling, 3*, 100027. doi:https://doi.org/10.1016/j.samod.2023.100027

Zhang, W., Zhao, Y., Cao, X. J., Lu, D., & Chai, Y. (2020b). Nonlinear effect of accessibility on car ownership in Beijing: pedestrian-scale neighborhood planning. *Transportation Research Part D: Transport and Environment, 86*, 102445.

Zhao, S., Liu, L., & Zhao, P. (2023). Traffic assignment in urban transportation network problem with emission constraints in China: a cooperative game theory. *Environmental Science and Pollution Research, 30*(26), 69274-69288. doi:10.1007/s11356-023-27108-9

Zhao, X., Yan, X., Yu, A., & Van Hentenryck, P. (2020). Prediction and behavioral analysis of travel mode choice: A comparison of machine learning and logit models. *Travel Behaviour and Society, 20*, 22-35.

Zhou, W., Cleaver, C. J., Dunant, C. F., Allwood, J. M., & Lin, J. (2023). Cost, range anxiety and future electricity supply: A review of how today's technology trends may influence the future uptake of BEVs. *Renewable and Sustainable Energy Reviews, 173*, 113074.

Zhu, J.-s., Lam, W. H., Chen, A., & Lo, H. K. (2009). Modeling the effects of turn delay uncertainties on route choice behavior in signalized road networks. *Transportation Research Record, 2091*(1), 1-11.

Zimmerman, K., Deepani, J., Bertha, M., & and Guerrero, A. (2015). Road Traffic Injury on Rural Roads in Tanzania: Measuring the Effectiveness of a Road Safety Program. *Traffic Injury Prevention, 16*(5), 456-460. doi:10.1080/15389588.2014.973491

APPENDIX

Results of the SHAP method applied to the GBT model are illustrated in Figures A1, Figure A2, and Figure A3 for minor injury, severe injury, and fatal injury crashes respectively. These results are similar to the RF model to a greater extent.

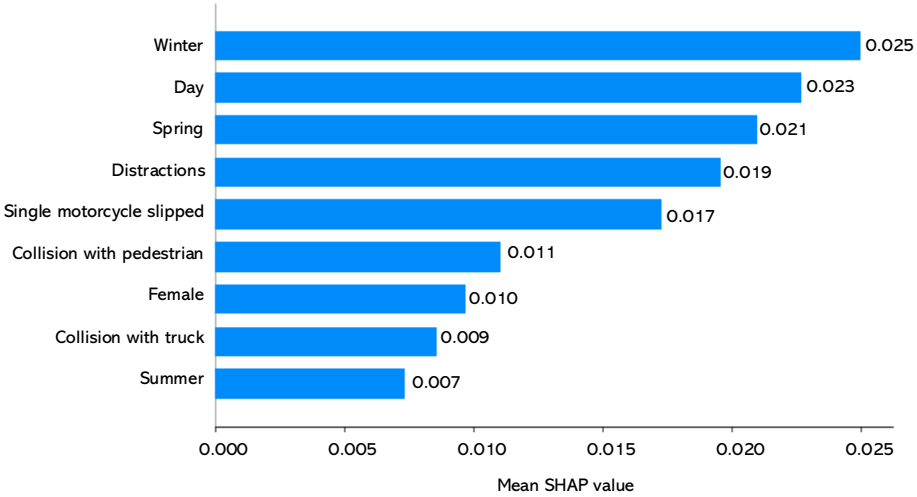

(a) SHAP feature importance for minor injury crash

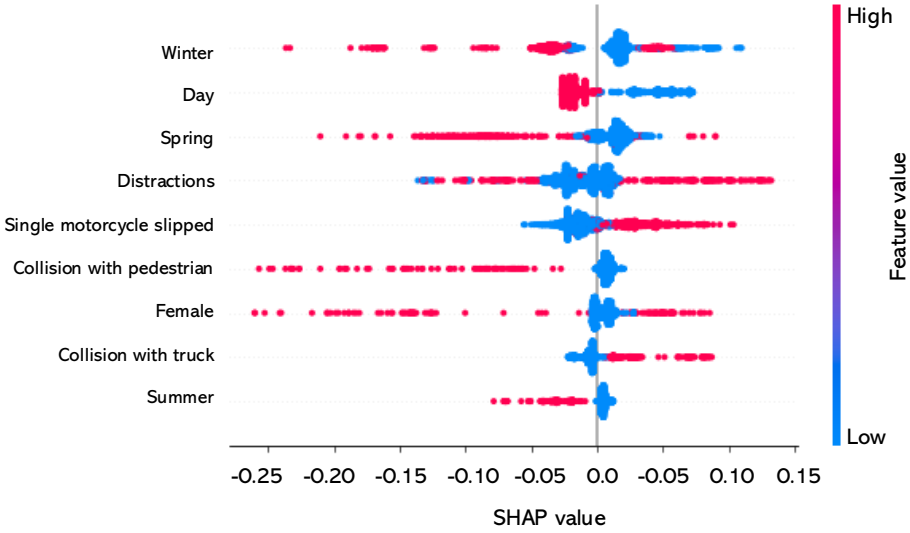

(b) SHAP summary plot for minor injury crash

Figure A1. Interpretations of the GBT model using SHAP method for minor injury crash

From Figure A3, we notice that influencing factors such as distractions, collisions with pedestrians/trucks, and the female motorcyclists involved in motorcycle crashes significantly increase the chance of crashes resulting in fatalities. Similarly, teenage

motorcyclists, female motorcyclists, and collisions with trucks (SHAP are significant positive contributors to severe injury crashes (Figure A2).

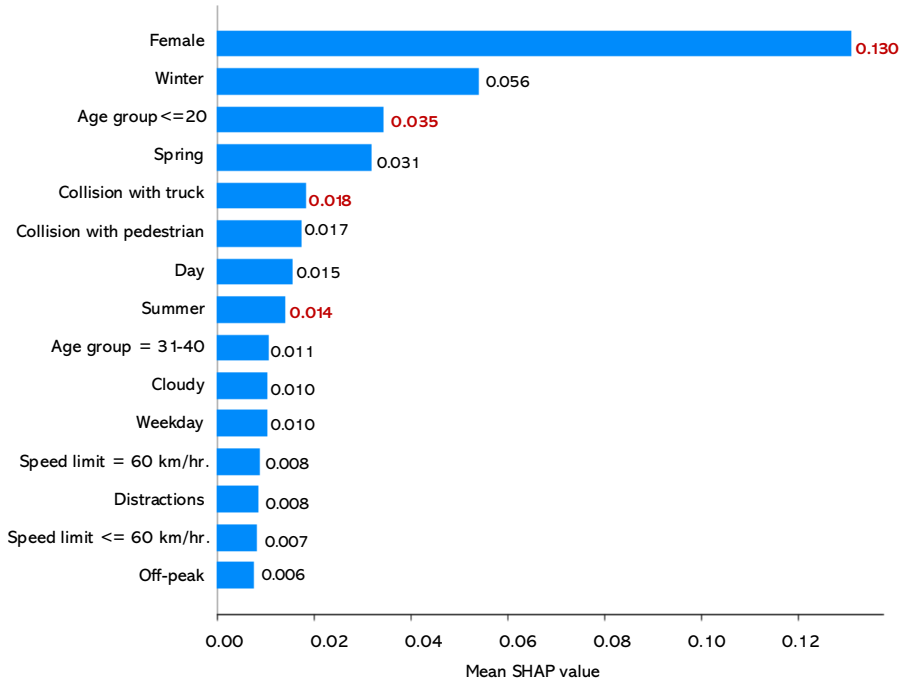

(a) SHAP feature importance for severe injury crash

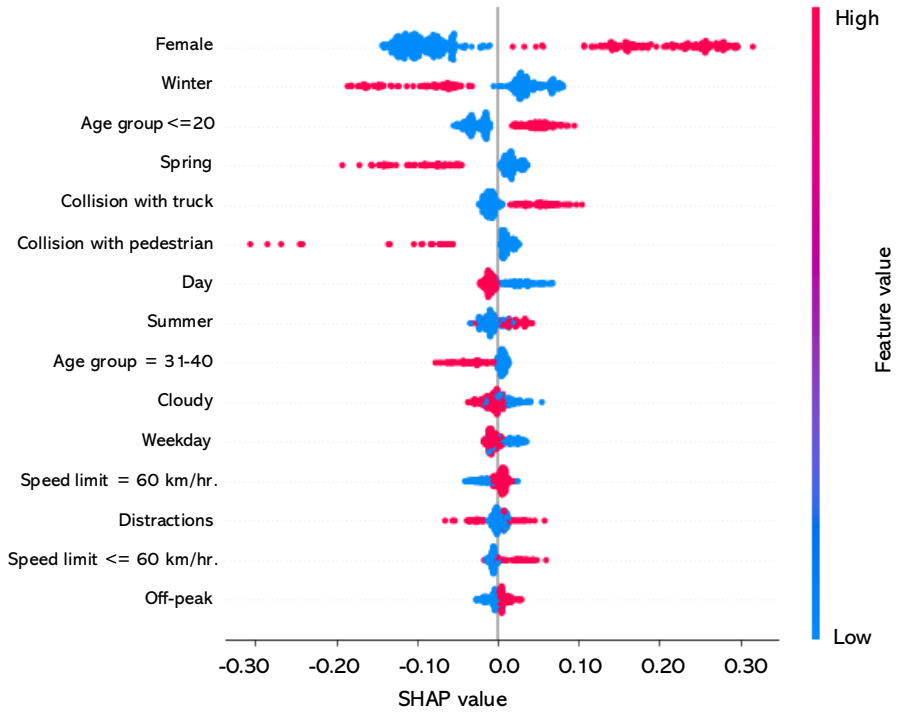

(b) SHAP summary plot for severe injury crash

Figure A2. Interpretations of the GBT model using SHAP method for severe injury crash

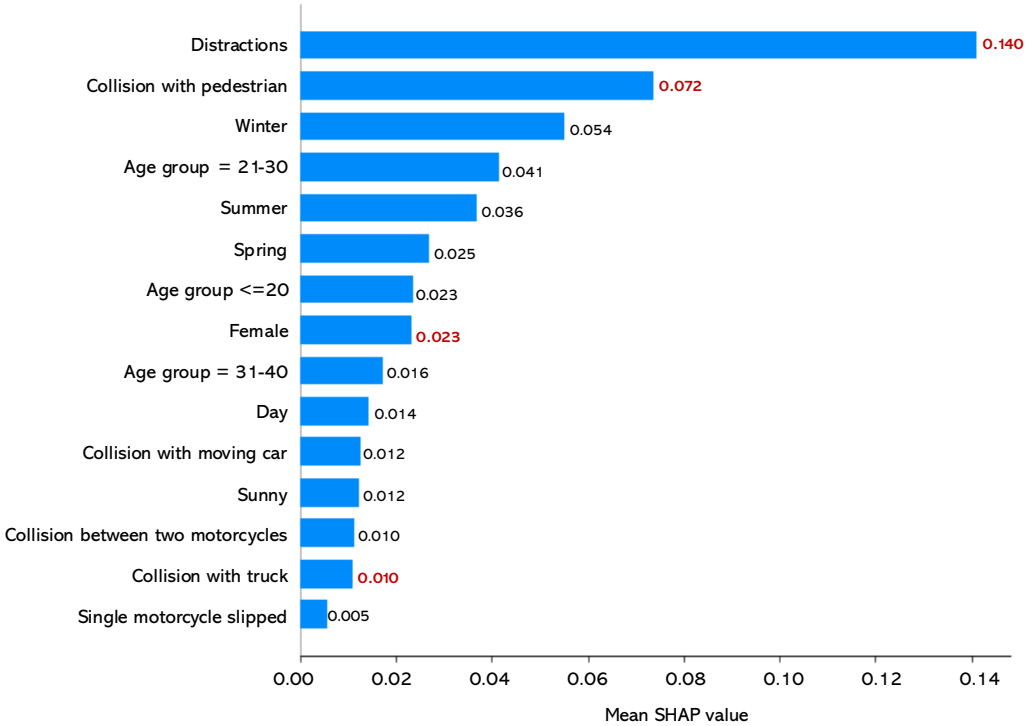

(a) SHAP feature importance for fatal injury crash

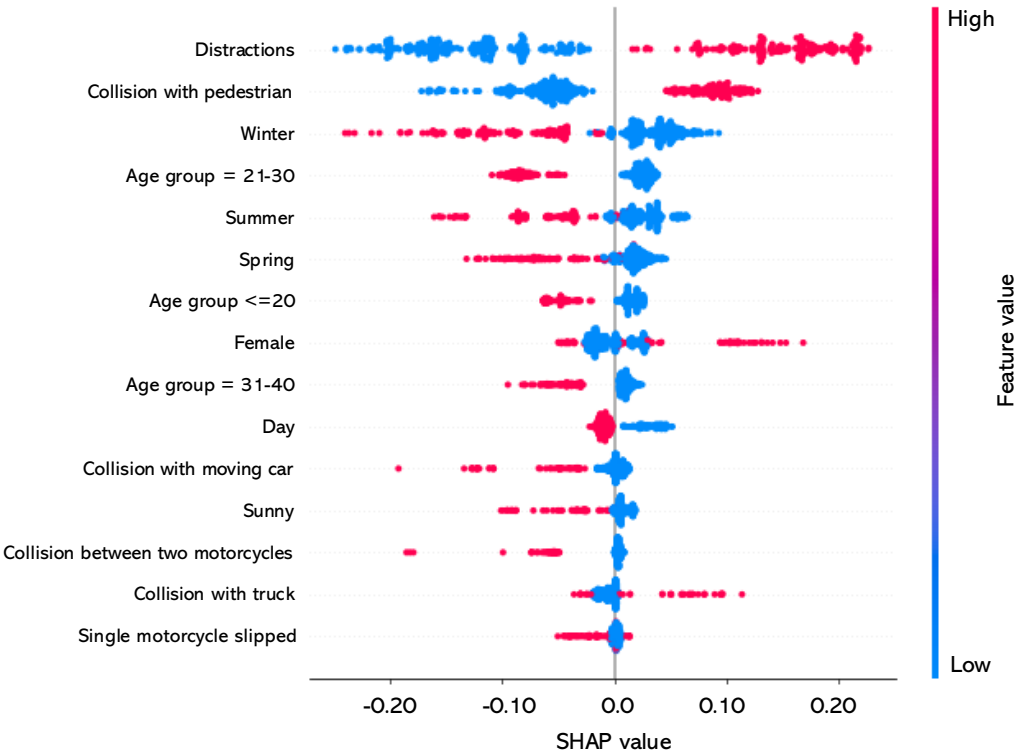

(b) SHAP summary plot for fatal injury crash

Figure A3. Interpretations of the GBT model using SHAP method for fatal injury crash

Table A1. Consistency analysis of risk factors between the MNL and GBT models

Variables	**Minor Injury**		**Severe Injury**		**Fatal Injury**	
	MNL	GBT (SHAP)	MNL	GBT (SHAP)	MNL	GBT (SHAP)
Lighting Condition						
Day	-0.429***	-(0.023)	-0.432*	-(0.015)	-0.484***	-(0.014)
Weather						
Cloudy	-0.309**	IS	-0.528***	-(0.010)	-0.303*	IS
Season						
Winter	-0.838***	-(0.025)	-0.906***	-(0.056)	-1.385***	-(0.054)
Summer	-0.423***	-(0.007)	IS	+(0.014)	-0.869**	-(0.036)
Spring	-1.029***	-(0.021)	-0.898***	-(0.031)	-1.088***	-(0.025)
Gender						
Female	-0.902***	-(0.010)	**+1.86*****	**+(0.130)**	**+0.188*****	**+(0.023)**
Age group						
Age (≤20 yr)	IS	IS	**+0.600*****	**+(0.035)**	-1.307***	-(0.023)
Age (21–30 yr)	IS	IS	IS	IS	-1.564***	-(0.041)
Age (31–40 yr)	IS	IS	IS	-(0.011)	-1.101**	-(0.016)
Vehicle/Object Involved						
Collision with truck/van	+0.385*	IS	**+0.579****	**+(0.018)**	**+0.482****	**+(0.010)**
Collision with pedestrian	-1.331***	-(0.011)	IS	-(0.017)	**+1.187*****	**+(0.072)**
Motorcyclist Behavior						
Distractions	+0.464*	+(0.019)	**+0.363****	IS	**+1.779*****	**+(0.140)**
Speed Limit						
60 km/h.	IS	IS	**+0.305***	**+(0.008)**	IS	IS

Notes: *, **, and *** represent statistical significance at 10%, 5%, and 1% levels, respectively. +: Positive effect, -: Negative effect IS: insignificant; numbers in parentheses indicate SHAP feature importance; numbers without parenthesis are MNL coefficients.